

**School of Chemistry
Cardiff University**



**Novel Expanded Ring N-Heterocyclic
Carbenes; Coordination and Application in
Catalysis**

Katharine R. Sampford

**A thesis submitted to Cardiff University
in accordance with the requirements for the degree of
Doctor of Philosophy**

May 2013

Acknowledgements

Firstly I would like to thank my supervisors: Prof Kingsley Cavell for his expert guidance and support over the last few years and for giving me this opportunity, Dr Damien Murphy for his advice and knowledge regarding the EPR side of my PhD, and Dr Paul Newman (Woody) for the constant guidance and understanding in the lab and for having the patience to help me. A huge thank you has to go to the technical staff at Cardiff University; with particular thanks to Robyn for his patience with mass spectrometry including the testing of some very sensitive samples, Dr Rob Jenkins for his help with NMR and keeping those machines online, and Dr Benson Kariuki for his excellent handling of sensitive materials; as without them the work reported in this thesis would not have been possible. A great thank you has to go to Dr Emma Carter for her understanding and patience with me when it came to analysing EPR spectra, and Dr Jamie Platts for his support with the computational aspects which I have come across. I would also like to thank everyone past and present who have been in Lab 2.84, Tracey H for her help with paramagnetic complexes early on, Jay and Wei for their continuous guidance and friendships throughout my PhD, and Becky for keeping me sane and for letting me know when it was time for tea. I'd also like to thank everyone in the inorganic department for making my time during my PhD so enjoyable, so a huge thanks goes to Steve, Owen, Stacey, Thomas, Tracy N, Brendan, Ollie, Emily, Jenn, and Andy. A group of friends who have been especially important over this time and who have shown me the great outdoors are Tim, Flo, Alex, Cathy, and Emma, I really appreciated the distractions guys. Possibly most importantly my friends and family in Devon who have supported and encouraged me, loved and believed in me, and whom have always been there. So I would like to send my endless thanks to my Mum Caroline, Dad Keith, Brother Tom, Sister in Law Laura, and last but no means least my best friend in the world Kirsty. Without you all this thesis would not have been possible, thank you all. Finally I would like to give an enormous thanks to Shaun, who over the last 7 years has always been there through the good times and the bad. He has picked me up when things get tough, always made me smile, and understood my odd ways. He has also been there to explain computational chemistry to me along with many other aspects of chemistry. Most importantly he has always believed in me and for this I will always be grateful.

Abstract

The work presented in this thesis is concerned with the synthesis, characterisation, and application in catalysis of mono- and bis-expanded ring (including bicyclic) N-heterocyclic carbenes (NHCs) with emphasis on their coordination to palladium, silver, rhodium, gold, copper, and nickel.

Chapter two provides the synthesis and characterisation of a series of bis-expanded ring NHC precursors along with the attempted synthesis of mixed 5- and 6-membered types. The attempted coordination of the bis-NHC precursors to palladium did not produce the desired complexes rather a rearrangement occurred to give nitrogen coordinated species through elimination of the linking group between the two heterocycles.

Chapter three explores the synthesis and characterisation of a range of novel alkylated bicyclic NHC precursors including the dimethyl, diethyl, and diisopropyl derivatives, and their coordination to rhodium(I). The increased steric demand ($iPr > Et > Me$) of the exocyclic substituent leads to a larger NCN angle across the series. The rhodium complexes exist as a mixture of two isomers (*syn*-alkene and *syn*-chloride) in a 2:1 ratio resulting from restricted rotation about the Rh-C_{NHC} bond. The complexes are active for the transfer hydrogenation of ketones with conversions up to 37 %.

Chapter four discusses the coordination chemistry of monocyclic expanded-ring and bicyclic NHCs with copper(I). The expanded ring NHC copper(I) complexes of the type [Cu(NHC)X] show typical C_{carbene}-Cu-X bond angles of around 180 °. However, the related complex of the mesityl bicyclic NHC shows an apparent non covalent interaction between the metal and the mesityl ring causing a deviation of the C_{carbene}-Cu-X bond away from linearity. The catalytic activity of the expanded ring copper(I) halide complexes for hydrosilylation was explored but were shown to be inactive.

Chapter five concerns gold(I) complexes of expanded-ring and bicyclic NHCs. A small crystallographic library of complexes enabled the percentage buried volumes to be determined. As expected, these were large for the aromatic substituted expanded ring complexes of type [Au(NHC)X] but appreciably smaller (more akin to the common 5-membered NHCs) for the bicyclic systems and the alkylated expanded ring systems. The catalytic activity of the complexes in the hydration of alkynes was explored with

conversions of up to 100 % being observed. Selectivities were noticeably better than those reported for the [Au(6-DIPP)Cl] and [Au(7-DIPP)Cl] with values of around 30:70.

Chapter six moves into the coordination and characterisation of a series of highly sensitive expanded ring nickel(I) complexes. Due to the paramagnetic nature of these compounds analysis using EPR was achieved. This showed that the nickel(I) complexes all exhibited orthorhombic g values.

Table of Contents

Chapter 1: Introduction.....	1
1.1: What is a Carbene?.....	1
1.2: First Carbene Complexes.....	1
1.3: Schrock and Fischer Carbenes.....	3
1.4: N-Heterocyclic Carbenes.....	4
1.4.1: History of the Free NHC.....	5
1.4.2: Inductive Effects.....	7
1.4.3: Mesomeric Effects.....	8
1.4.4: Steric Effects.....	9
1.5: Ligand Design.....	10
1.5.1: Synthetic Route to Expanded Ring NHCs.....	11
1.5.2: Synthesis of Bis-NHCs.....	17
1.6: Complexation of NHCs.....	18
1.6.1: Coordination of 5-Membered NHCs.....	18
1.6.2: Coordination of Expanded Ring NHCs.....	19
1.6.2.1: Coordination of Expanded Ring NHCs to Ruthenium, Rhodium, and Iridium.....	20
1.6.2.2: Coordination of Expanded Ring NHCs to Palladium and Nickel.....	23
1.6.2.3: Coordination of Expanded Ring NHCs to Coinage Metals, Silver, Gold, and Copper.....	25
1.6.3: Coordination of Bis-NHCs.....	26
1.7: Catalytic Properties of NHCs.....	29
1.8: Aims of Thesis.....	32
1.9: References.....	33

Chapter 2: Synthesis and Attempted Coordination of Novel Bis-N-Heterocyclic Carbenes.....	39
2.1: Introduction.....	39
2.2: Results and Discussion.....	43
2.2.1: Initial Attempted Synthesis of Bis-NHCs.....	43
2.2.2: Attempted Synthesis of Mixed 5- and 6-Membered NHCs.....	50
2.2.3: Successful Synthesis and Characterisation of Bis-NHC precursors.	54
2.2.4: Attempted Coordination of the Bis-NHCs.....	62
2.3: Conclusions.....	68
2.4: Experimental.....	69
2.4.1: General Remarks.....	69
2.4.2: Experimental Data for the Initial Synthesis of Bis-NHC Precursors.....	70
2.4.3: Experimental Data for the Initial Synthesis of Mixed Ring Size Bis-NHC precursors.....	76
2.4.4: Experimental Data for the Synthesis of Bis-NHC Precursors.....	80
2.4.5: Experimental Data for the Attempted Complexes of Bis-NHCs.....	85
2.5: References.....	87
Chapter 3: Synthesis of Novel Bicyclic N-Heterocyclic Carbenes and Their Coordination to Rhodium.....	91
3.1: Introduction.....	91
3.2: Results and Discussion.....	93
3.2.1: Synthesis and Characterisation of Alkylated Bicyclic NHC Ligands.....	93
3.2.2: Coordination of Aliphatic Bicyclic NHC Precursors to Rhodium..	102
3.2.3: Catalysis.....	108
3.2.3.1: Catalytic Activity of Rhodium Bicyclic NHC Complexes.....	110
3.3: Conclusions.....	113
3.4: Experimental.....	114

3.4.1: General Remarks.....	114
3.4.2: Experimental Data for Aliphatic Bicyclic NHC Precursors.....	115
3.4.3: Experimental Data for Aliphatic Bicyclic NHC Rhodium Complexes.....	119
3.4.4: General Procedure for Transfer Hydrogenation.....	122
3.5: References.....	123
Chapter 4: Coordination of Expanded Ring N-Heterocyclic Carbenes to Copper(I).....	126
4.1: Introduction.....	126
4.2: Results and Discussion.....	126
4.2.1: Synthetic Route to Copper(I) Complexes.....	127
4.2.2: Copper(I) Complexes with Monocyclic Expanded Ring NHC Ligands.....	130
4.2.2.1: Synthesis and Characterisation of Compounds with the General Formula [Cu(NHC)X], Where X = I or Br.....	130
4.2.2.2: Synthesis and Characterisation of Compounds with the General Formula [Cu(NHC)OH].....	133
4.2.3: Synthesis and Characterisation of Copper(I) Complexes with Bicyclic Expanded Ring NHC Ligands.....	136
4.2.4: Attempted Formation of Other Copper(I) Complexes.....	142
4.2.4.1: The Attempted Synthesis and Characterisation of Expanded Ring Copper(I) Complexes.....	142
4.2.4.2: The Attempted Synthesis and Characterisation of Bicyclic Copper(I) Complexes.....	147
4.2.5: Catalysis.....	149
4.2.5.1: Catalytic Activity of Expanded Ring Copper(I) Complexes..	150
4.3: Conclusions.....	152
4.4: Experimental.....	154
4.4.1: General Remarks.....	154
4.4.2: Experimental Data for Copper(I) Complexes.....	156

4.4.3: Experimental Data for the Attempted Synthesis of Copper(I) Complexes.....	163
4.4.4: General Procedure for Hydrosilylation of Ketones.....	167
4.5: References.....	168
Chapter 5: Synthesis and Coordination of Expanded Ring N-Heterocyclic Carbenes to Gold(I).....	171
5.1: Introduction.....	171
5.2: Results and Discussion.....	172
5.2.1: General Synthesis of Gold(I) Complexes.....	173
5.2.2: The Synthesis of Expanded Ring NHC Gold(I) Complexes.....	173
5.2.2.1: The Characterisation of Aromatic Expanded Ring NHC Gold(I) Complexes.....	175
5.2.2.2: The Characterisation of Alkylated Expanded Ring NHC Gold(I) Complexes.....	181
5.2.3: The Synthesis and Characterisation of Bicyclic NHC Gold(I) Complexes.....	185
5.2.4: Catalysis.....	189
5.2.4.1: Catalytic Activity of Expanded Ring Gold(I) Complexes.....	191
5.3: Conclusions.....	193
5.4: Experimental.....	195
5.4.1: General Remarks.....	195
5.4.2: Experimental Data for Expanded Ring Gold(I) Complexes.....	197
5.4.3: Experimental Data for Bicyclic Gold(I) Complexes.....	203
5.4.4: General Procedure for the Hydration of Alkynes.....	206
5.5: References.....	207

Chapter 6: Coordination of Expanded Ring N-Heterocyclic Carbenes to Nickel(I).....	210
6.1: Introduction.....	210
6.2: Results and Discussion.....	210
6.2.1: Synthesis of Nickel(I) Complexes.....	211
6.2.2: Characterisation of Nickel(I) Complexes.....	213
6.2.3: EPR Studies.....	223
6.2.3.1: Background to EPR.....	223
6.2.3.2: Basic Principles of EPR.....	224
6.2.3.3: Multi-Electron Systems.....	226
6.2.3.4: EPR Studies of Nickel(I) Complexes.....	228
6.3: Conclusions.....	232
6.4: Experimental.....	234
6.4.1: General Remarks.....	234
6.4.2: Experimental Data for Nickel(I) Complexes.....	236
6.5: References.....	239

Chapter 1: Introduction

1.1: What is a Carbene?

A carbene is a molecule which contains at least one carbon atom which is divalent in nature. Carbenes have a set of unpaired electrons in their valence shell along with four other electrons, which leads to a total of six valence electrons. It is the two unpaired electrons in the valence shell which cause the reactivity of these molecules. The carbene itself is linked to two adjacent species by covalent bonds. Due to their unshared electrons it is possible for carbenes to have two main ground states, these are singlet, where two non bonding electrons occupy the σ -orbital with opposite spins, and the triplet ground state, where one electron is occupying the σ -orbital and one electron is occupying the $p\pi$ -orbital with the same spins, as shown in Figure 1.

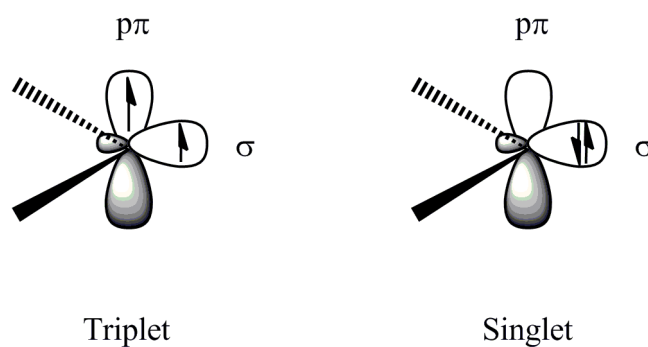
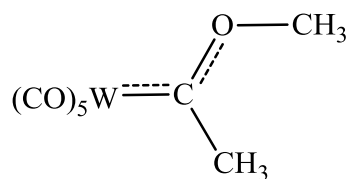


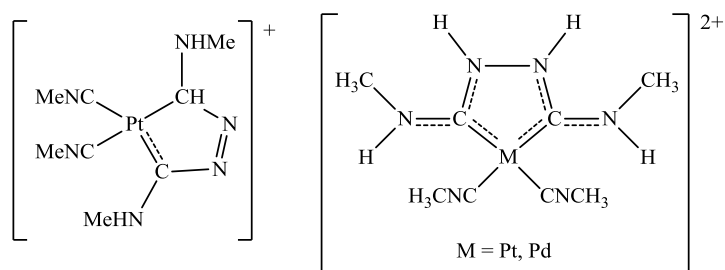
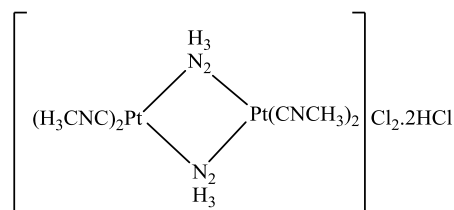
Figure 1: Two possible ground states of carbenes.

1.2: First Carbene Complexes

The first documented carbene metal complex was the tungsten carbonyl carbene complex reported by Fischer in 1964 as shown in Figure 2.¹

**Fischer 1964****Figure 2:** First documented metal carbene complex.

It was not until six years later that Fischer's successors reported another recognised carbene metal complex. These were complexes of a coordinated isocyanide moiety to platinum as reported by Shaw *et al.*² After the publication by Shaw, the reports of established carbene metal complexes were more frequent with Balch³ and Enemark⁴ reporting the coordination of isocyanide carbene moieties to platinum and palladium, Figure 3.

**Shaw 1970****Balch 1970****Enemark 1971****Figure 3:** Subsequent established metal carbene complexes.

1.3: Schrock and Fischer Carbenes

Metal-bound carbenes can be classed as Schrock and Fischer carbenes. There are two main differences between Fischer type carbenes and Schrock type carbenes. The first is whether they are π -acceptor or π -donor ligands. Fischer carbenes are π -acceptors and Schrock carbenes are π -donors. The second main difference is in the type of metal they favour, with Schrock type carbenes favouring high oxidation state metals such as titanium(V) and tantalum(V), and Fischer carbenes favouring low oxidation state metals such as iron(0), molybdenum(0), and chromium(0). The bonding to metals for each is very different with the Fischer carbenes bonding in a σ -type electron donation from the lone pair of the carbene to the empty d-orbital of the metal with subsequent π -backbonding, Figure 4. The Schrock carbenes are described by a different bonding approach due to the nucleophilicity of the carbene moiety and is viewed as a coupling between a triplet metal and a triplet carbene, Figure 4.

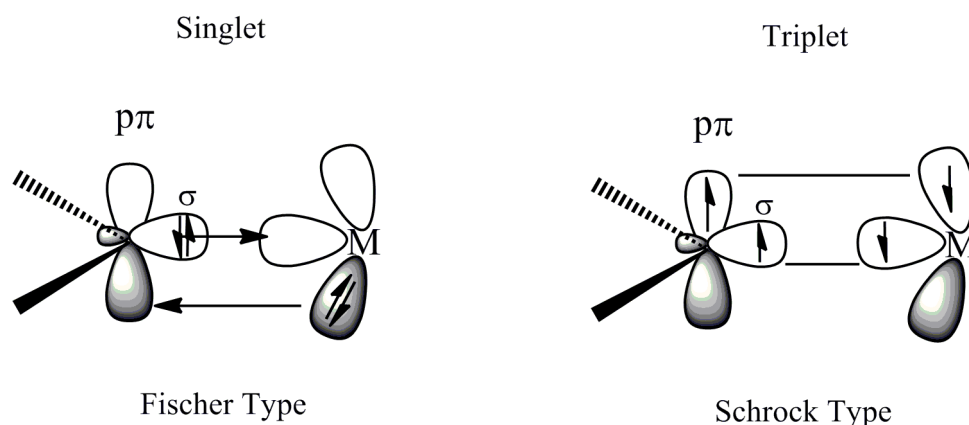
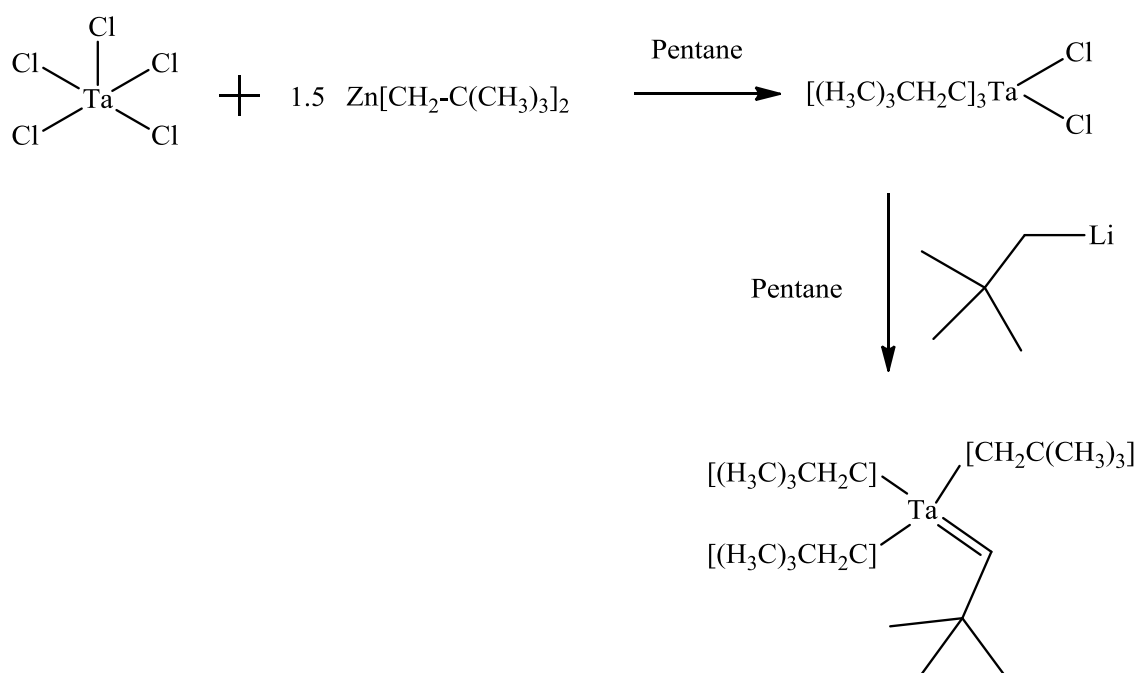


Figure 4: Bonding of Fischer and Schrock type carbenes.

An example of a Fischer type carbene with coordination to tungsten is shown in Figure 2, and the Schrock type carbene with coordination to tantalum is shown in Scheme 1.

The reaction of TaCl_5 and one and a half mole equivalents of $\text{Zn}[\text{CH}_2\text{-C}(\text{CH}_3)_3]_2$ yields the $\text{Ta}[\text{CH}_2\text{C}(\text{CH}_3)_3]_3\text{Cl}_2$. This was then reacted with two mole equivalents of neopentyllithium in pentane yielding two moles of lithium chloride, one mole of neopentane, and $\text{Ta}[\text{CH}_2\text{C}(\text{CH}_3)_3]_3[\text{CHC}(\text{CH}_3)_3]$, as reported by Schrock.⁵ This compound was isolated as a orange crystalline compound and reported to be thermally stable.

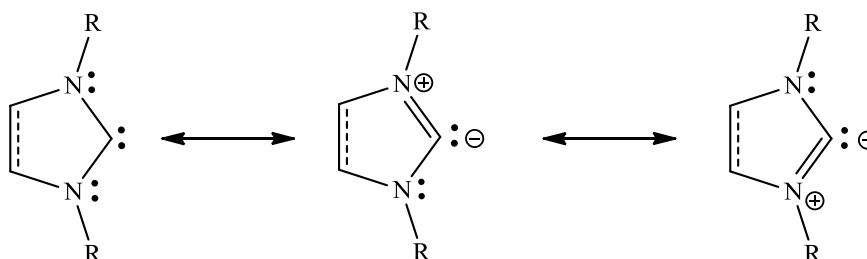


Scheme 1: Synthesis of the first Schrock carbene, 1974.⁵

1.4: N-Heterocyclic Carbenes

There are three types of carbenes, (X, X), which is bent, (Z, Z), which is linear, and the (X, Z), which is quasi-linear. N-heterocyclic carbenes are classed as (X, X) carbenes due to their bent geometries. They are bent due to the impact of the heterocyclic ring, which the carbene centre forms part of. The N-C bonds within the heterocycle can form

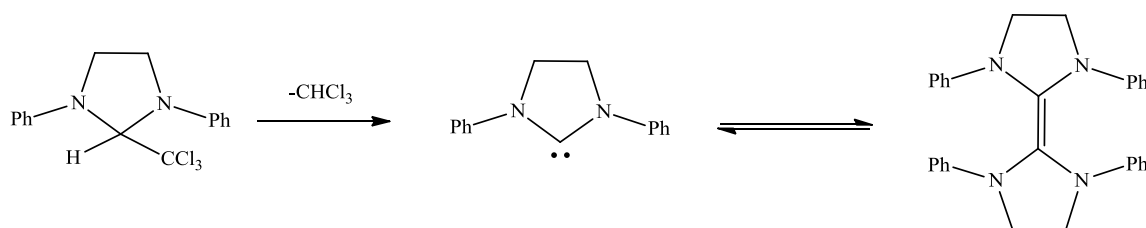
a partial double bond due to the interaction of the π -electrons on the nitrogen atoms with the empty $p\pi$ -orbital on the carbene. This interaction forms a four electron-three centre π -system within the heterocycle, and can therefore form three resonance structures, Scheme 2.



Scheme 2: Resonance structures of N-heterocyclic carbenes.

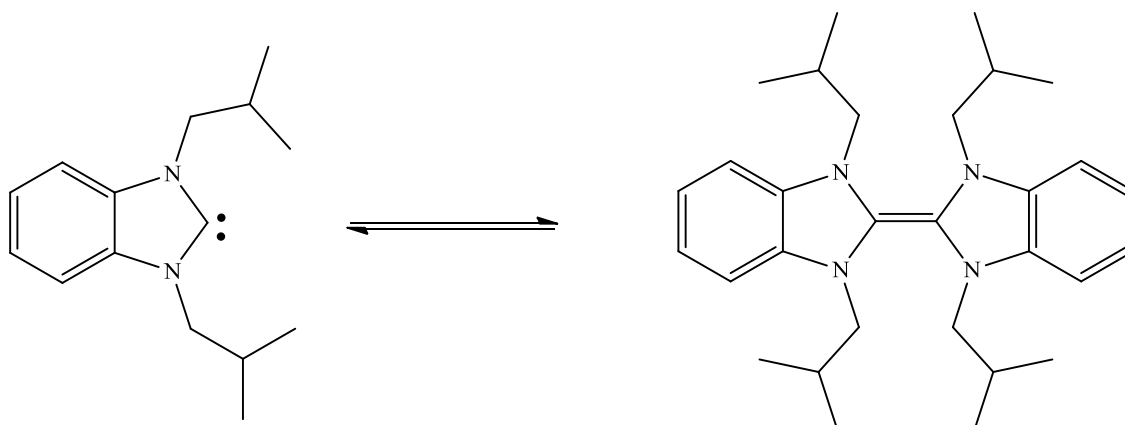
1.4.1: History of the Free NHC

In between the discovery of the Schrock and Fischer carbenes Wanzlick⁶ and Ofele⁷⁻⁹ reported the first coordination of an NHC to mercury,⁶ chromium,^{7,8} and palladium.⁹ Once Wanzlick had established this mercury NHC complex, his aims moved towards the isolation of the free carbene, however he never achieved his goal instead he managed to establish the basis for the synthesis of the free carbene along with a postulated equilibrium between the carbene and the dimeric species, Scheme 3.



Scheme 3: The attempted first isolation of the free carbene species.¹⁰

Although Wanzlick had postulated the equilibrium between the free carbene and the dimer there was no conclusive evidence reported until that of Hahn and co-workers in 2000¹¹ and until this time the idea postulated by Wanzlick¹⁰ was controversial for nearly 40 years.¹²⁻¹⁴ Hahn and co-workers showed that Wanzlick's postulated equilibrium was indeed the process occurring. Hahn demonstrated this theory using a dibenzotetraazafulvalene NHC as exhibited in Scheme 4.

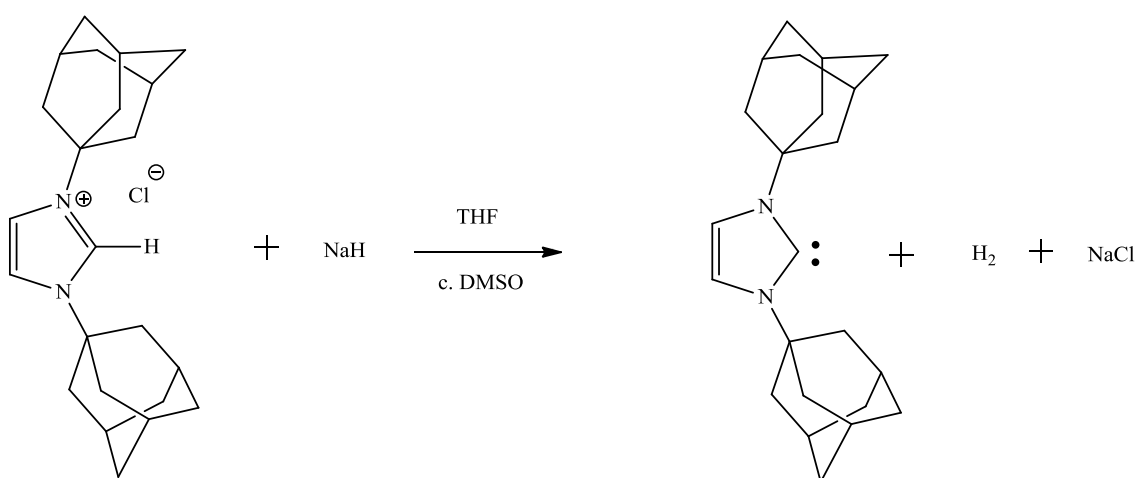


Scheme 4: First evidence of the Wanzlick rearrangement.¹¹

N-heterocyclic carbenes are known to dimerise as shown in Scheme 4. It was not until 2004 when Alder and co-workers¹⁵ established a connection between ring size, and whether or not it is cyclic or acyclic and the potential to dimerise. It is believed, through computational studies, that the larger the ring size, 7 and above, and acyclic NHCs, the less stable the monomeric species. This is in part due to the increased NCN angle and loss of conjugation through twisting of the N-C_{carbene} bonds. The comparison between acyclic and cyclic compounds was made using the same N-substituents and it was found that the dimer of the acyclic derivative was more stable by 100 kJ mol⁻¹.¹⁵

Twenty nine years after Wanzlick had first attempted to isolate a free carbene species Arduengo and co-workers established the synthesis, structure, and characterisation of the first crystalline free N-heterocyclic carbene.¹⁶ The synthesis of this free carbene

was carried out using the NHC precursor, which was reacted with sodium hydride in THF using a catalytic amount of DMSO, in turn forming the free carbene species, Scheme 5. The NHC precursor used contained adamantyl N-substituents, to provide both steric and electronic stabilization, including a π -donation into the carbene p-orbital by the electron rich π -system (N-C=C-N). This π -donation leads to a delocalised effect around the imidazole ring, and it is this delocalisation which can aid stabilisation of the nucleophilic carbenes as reported by Wanzlick in 1962.¹⁰



Scheme 5: Synthesis of the first crystalline free carbene.¹⁶

1.4.2: Inductive Effects

Inductive effects are described as a transmission of charge through a series of atoms in a specific compound by electrostatic induction, they have an effect on the σ - $p\pi$ separation due to the nature of the substituents. This is where in the NHCs a large σ - $p\pi$ separation is observed as shown in Figure 5. This large separation is due to the electron withdrawing nature of the amine substituents, stabilising the σ -non bonding orbital through inductive effects. This stabilisation occurs by increasing the s-type character of the orbital. When the substituents are electron withdrawing the carbene favours the

singlet state, and when the substituents are electron donating the σ - π separation is smaller in turn favouring the triplet state,¹⁷ Figure 5.

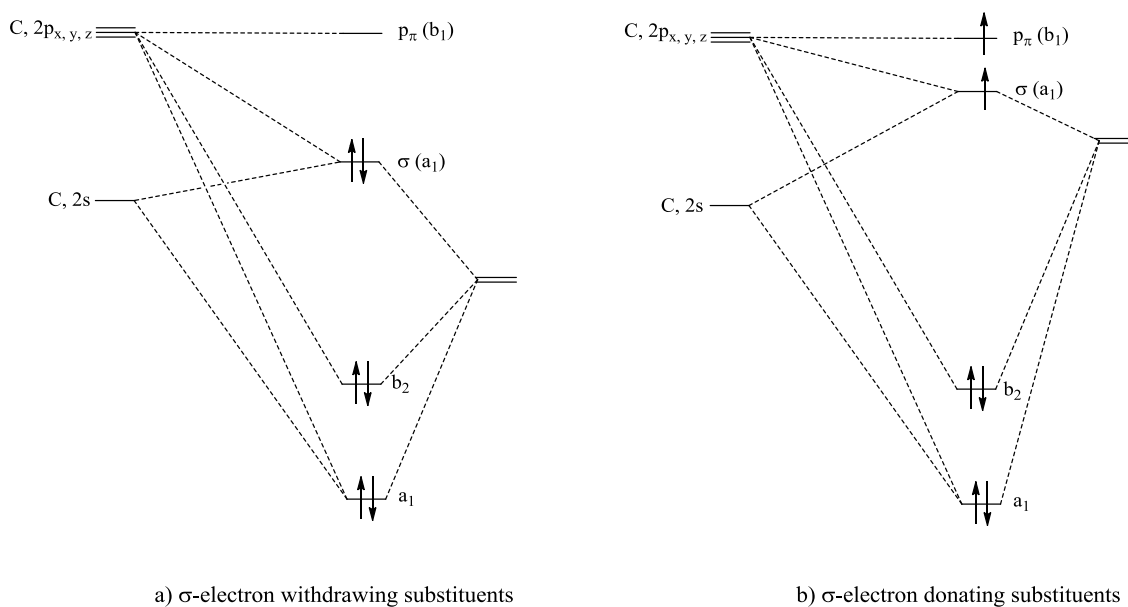


Figure 5: Perturbation orbital diagram showing the difference between electron donating and electron withdrawing inductive effects.

1.4.3: Mesomeric Effects

The mesomeric effect is also known as the resonance effect, and as shown in Scheme 2 N-heterocyclic carbenes are able to resonate between three structures. The mesomeric effect is dependent upon the properties possessed by the N-substituents. If the N-substituents are electron withdrawing in nature then the mesomeric effect will be negative and when the N-substituents are electron releasing groups the mesomeric effect is positive.

The singlet carbene in this case is stabilised by two properties, mesomeric effects and inductive effects as described in Section 1.4.2. The stabilisation through mesomeric

effects is apparent due to the donation of electron density from the nitrogens to the empty $p\pi$ orbital on the carbene thus raising the energy of the $p\pi$ orbital and increasing the σ - $p\pi$ gap, Figure 6.

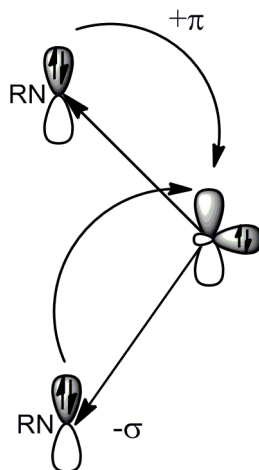


Figure 6: Mesomeric and inductive effects in N-heterocyclic carbenes.

1.4.4: Steric Effects

N-heterocyclic carbenes have the potential for attachment of any N-substituent, this includes extremely sterically hindered N-substituents like 2,6-diisopropylphenyl (DIPP). These can have huge effects on the coordination abilities of the NHCs, with steric hindrance so large that it results in no complexation.^{18,19} The steric bulk for a particular ligand is measured by calculation of the percentage buried volume, Figure 7, as first conceptualised by Cavallo²⁰ and Nolan,²¹ and is an alternative to the Tolman's cone angle, which is used for phosphines. NHC steric bulk cannot be defined using Tolman's cone angle as a NHC is an sp^2 hybridised donor containing two substituents and is usually planar, whereas the PR_3 ligands are sp^3 hybridised and contain three substituents in a conical formation. The percentage buried volume is defined as "the percentage of the volume occupied by ligand atoms in a sphere centred on the metal

(% V_{Bur})".²² The volume of the sphere must represent the area around the metal that should be occupied by the different ligands once coordination has occurred.

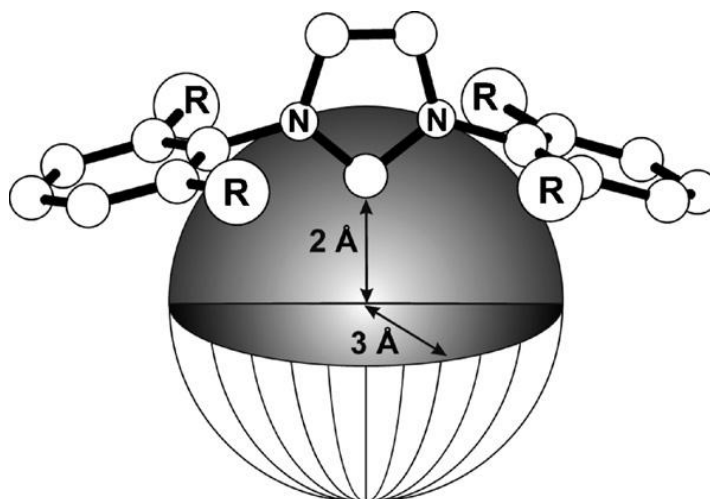


Figure 7: Percentage buried volume diagram showing the sphere dimensions.²²

The sphere dimensions, shown in Figure 7, use a standard metal-carbene bond length of 2 Å, with the radius of the sphere, which is centred on the metal being 3 Å. These were originally found by optimising the geometries using density functional theory (DFT).²¹

1.5: Ligand Design

Over the years there has been an extensive amount of research carried out on NHCs, including synthesis, coordination, and applications. Due to the widespread knowledge of the variety of synthetic routes it would not be effective to discuss all of the known synthetic routes and resultant compounds here, however, Figure 8 shows the structures of the most widely used NHC systems.²³

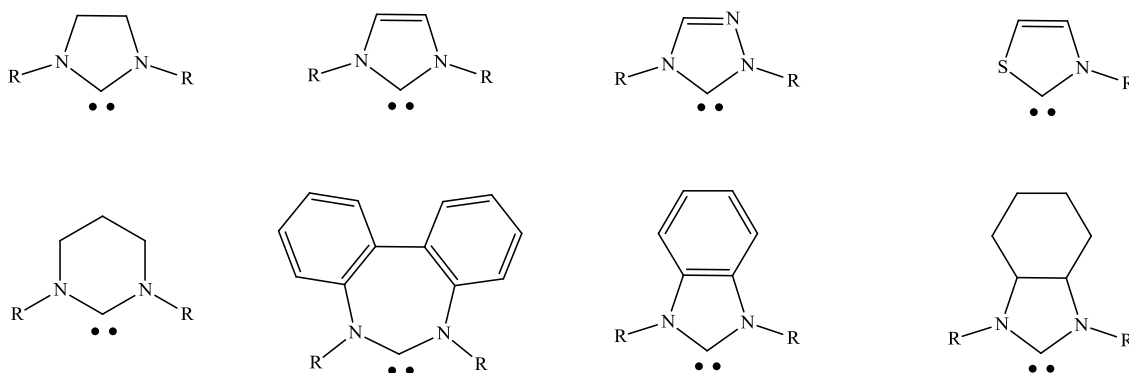
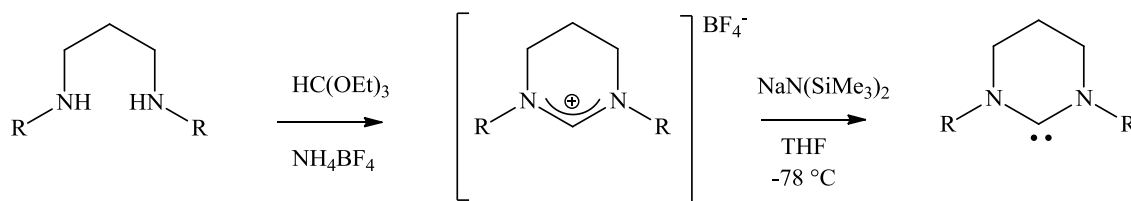


Figure 8: Most commonly used NHCs.

Out of these most common NHCs, the 5-membered saturated and unsaturated NHCs have been the most reported by far, this is due to the ease of synthesis and the versatility of functionality, with the possibility to tune the sterics and electronic properties through changing R groups and backbone functionality. Since 5-membered ring NHCs have been so extensively researched with many excellent reviews covering various aspects of the area,²⁴⁻²⁹ the remaining discussions in this chapter will concentrate on expanded ring, bicyclic, and bis-NHCs.

1.5.1: Synthetic Route to Expanded Ring NHCs

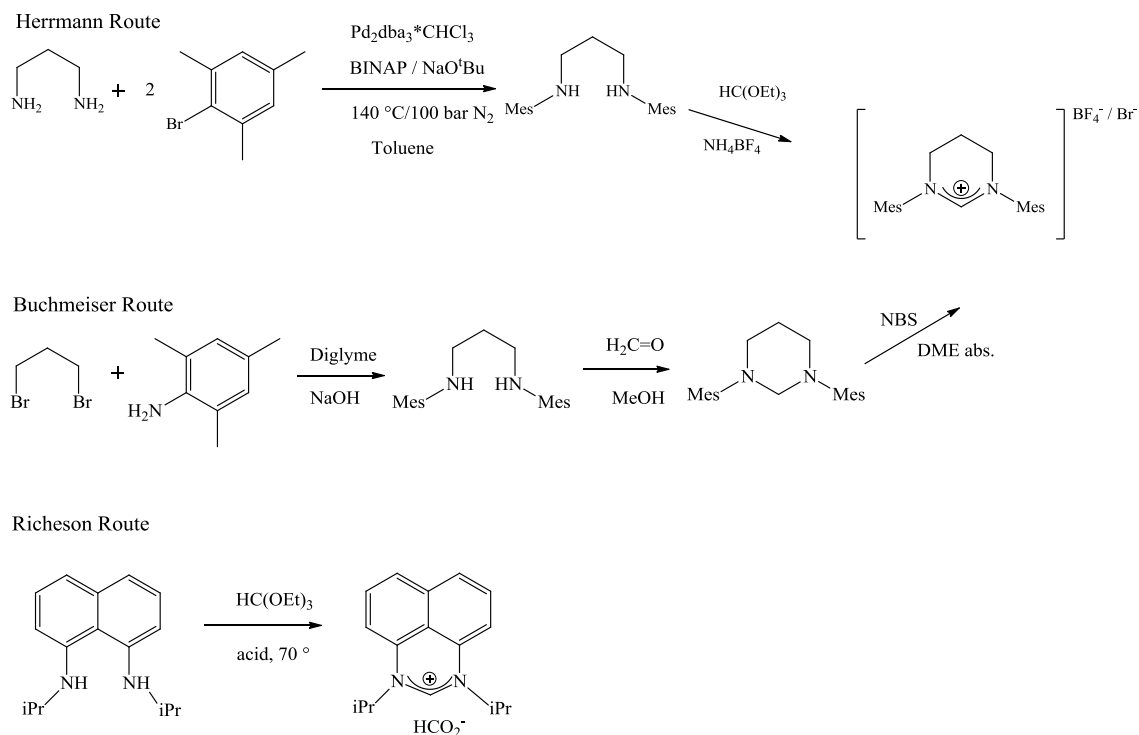
In more recent years research has moved towards expanded ring NHCs and it has been found that there are two main ways to synthesise expanded ring NHCs. These are the diamine route and the amidine route. The diamine route was the first route to be established and this was reported initially by Alder *et al.* in 1999 forming the 6-*i*Pr·BF₄,³⁰ Scheme 6, the reaction proceeds with an amination subsequently followed by the ring closure of a substituted diamino species.



Scheme 6: First synthesis of expanded ring NHC.³⁰

The discovery of an expanded ring NHC sparked an interest in the research field and led to Richeson,³¹ Herrmann,³² and Buchmeiser³³ all synthesising 6-membered NHCs through similar procedures to that first reported by Alder *et al.*³⁰ as shown in Scheme 7. A series of 6-membered NHCs comparisons have now been made. It was at this stage that the observation of increased NCN bond angles and in turn basicity was found. The 6-membered NHCs have much larger NCN bond angles than their 5-membered counterparts with values in the region of 120 °. Parallel with this increase in angle there is an increase in basicity of the carbene, which has been calculated to have a pK_a value in DMSO of 27.1,³⁴ which again is a considerable increase from its 5-membered counterpart which has a calculated value of 22.3 in DMSO.³⁴

This knowledge and understanding of the increase in NCN bond angle and basicity led to the discovery of a series of 7-membered NHCs by Stahl³⁵ and Cavell.³⁶ The route initially employed to synthesise these 7-membered NHC derivatives, 7-adamantyl,³⁵ and 7-cyclohexyl,³⁶ Figure 9, was the diamine route reported for the 6-membered NHCs.



Scheme 7: Different analogues of the initial route proposed by Alder.

The increase in NCN bond angle and basicity was again observed for the 7-membered salts with values of around 126° . This increase was due to the torsional strain of the heterocycle. Cavell and co-workers also synthesised a diester tartrate derivative, which exhibited an NCN bond angle larger than any reported thus far, with a value of 135.9° .

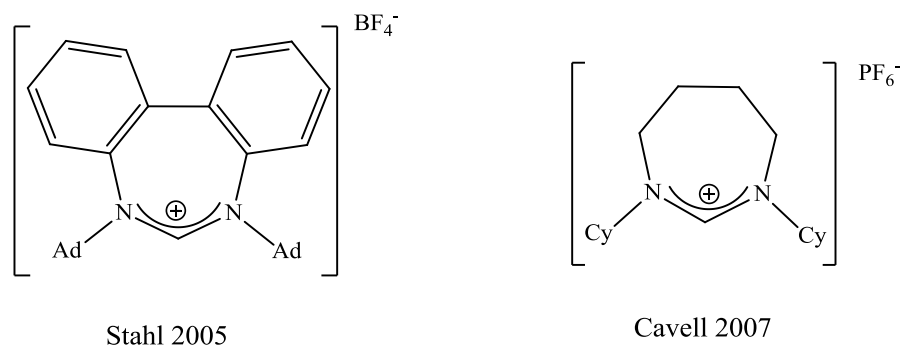


Figure 9: 7-Membered amidinium salts synthesised by Stahl and Cavell.^{35,36}

The diamine route was also used for the production of a series of bicyclic NHCs, as reported by Wilhelm³⁷ and Newman³⁸ some examples of which are shown in Figure 10. It was unclear in the beginning how these compounds would behave since they contained fused 6- and 7-membered rings. From the compounds synthesised it was beginning to show that these NHCs had basicity of somewhere between that of a 5-membered NHC and an expanded ring NHC.

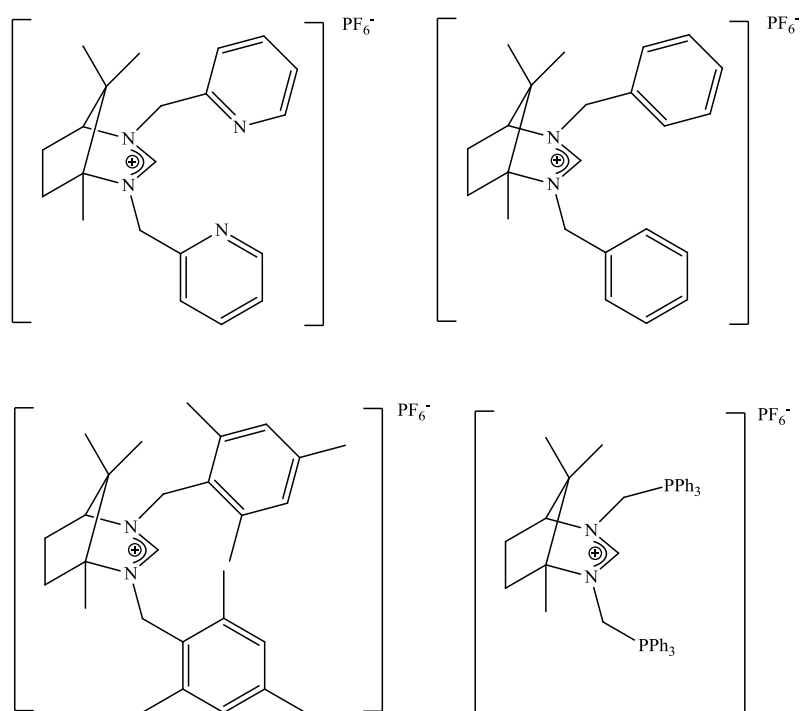
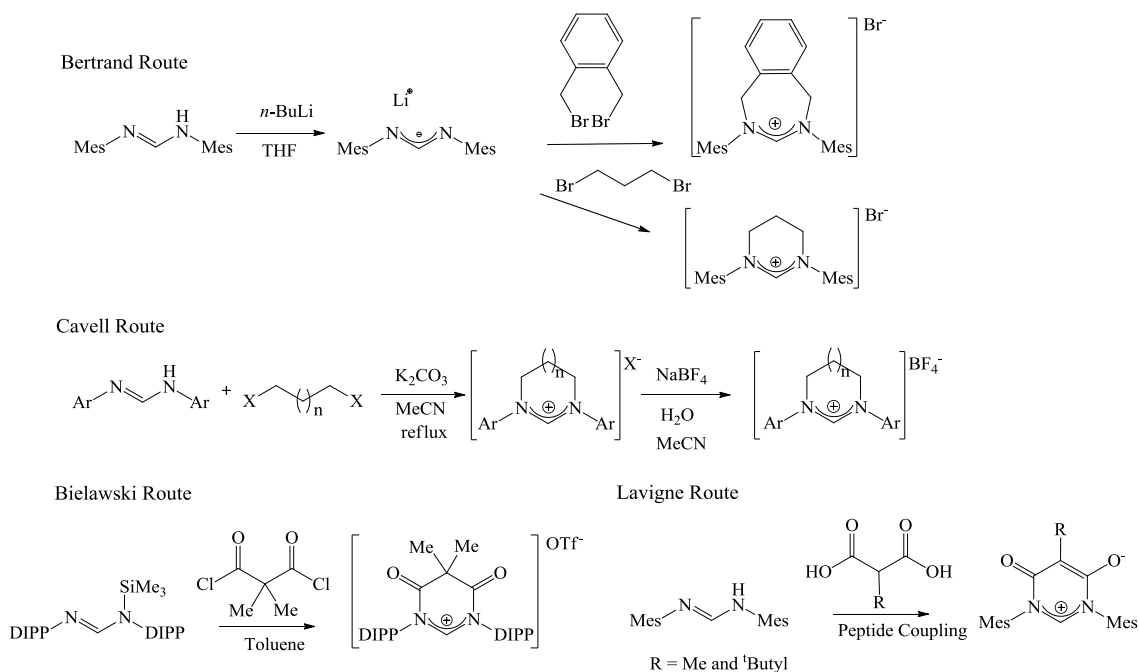


Figure 10: A selection of bicyclic NHC precursors synthesised by Wilhelm and Newman.³⁷⁻³⁹

Although the routes reported by Herrmann, Buchmeiser, Alder, and Richeson had been successful, the research area would benefit from a pathway which was higher yielding and employed sufficiently more gentle conditions, which did not use pressure, a catalyst or high temperatures. This led to the second most commonly used synthetic route to expanded ring NHCs, the amidine route, which is where a formamidine is formed

analogously to that by Cotton^{40,41} and subsequently ring closed in a "click" type reaction. This route has been employed by Bertrand,⁴² Cavell,^{43,44} Lavigne,^{45,46} and Bielawski⁴⁷ to synthesise a series of expanded ring NHCs as shown in Scheme 8.



Scheme 8: Amidinium route to expanded ring NHC precursor salt.⁴²⁻⁴⁷

This led to a cleaner, higher yielding, and generally milder route to expanded ring carbenes, with excellent yields of up to 90 % being achieved without the use of high pressure or a catalyst. It also led to a major breakthrough in this area of research with the development of the first 8-membered NHC by Cavell and co-workers in 2011, Figure 11.¹⁹ The salts exhibited greater NCN bond angles than the previous 6- and 7-membered derivatives of up to 5 ° larger.

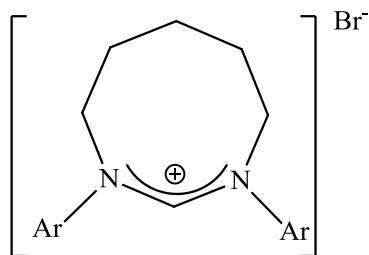


Figure 11: The first example of 8-membered NHC precursor salt.¹⁹

As noted earlier the bond angle increases as you increase the size of the N-heterocyclic carbene ring and there is an increase in basicity of the carbene. This has been observed in the cases reported thus far and is apparent when attempting to form the free carbene. This is because the larger the ring the stronger the base which is required to deprotonate the NHC, as exhibited with the 5-membered NHCs requiring a base such as potassium carbonate,⁴⁸ whereas the 6-membered NHCs require a base like potassium tertiary butoxide,⁴⁹ and the 7- and 8-membered NHCs require bases such as KHMDS^{18,19,36,43,44} or as strong as lithium diisopropylamide (LDA).³⁶ This is shown in Figure 12 with the scale exhibiting the relationship between NHC ring size and basicity, where the bicyclic NHCs fall in the middle between the 5-membered and the 6-membered derivatives.

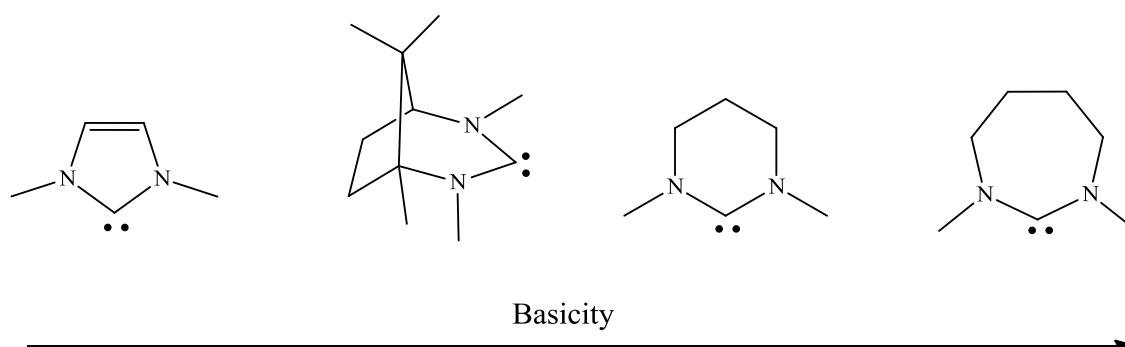


Figure 12: How the basicity changes through different NHC architectures.

1.5.2: Synthesis of Bis-NHCs

The interest in bis-NHCs grew due to the ability to functionalise and tune the electronic, steric, chiral, and orientational properties, and also with the stability of resultant complexes which will be explained further in Chapter 2.

There are two main types of bis-NHCs, those that are chelating bis-NHCs and bis-NHCs which are bridging. In this section we will concentrate on the synthesis of chelating bis-NHCs, this will solely be about 5-membered NHCs as there are no reports on chelating expanded ring bis-NHCs. There has been a substantial number of reports synthesising chelating bis-NHCs, Figure 13 shows just a snapshot of what has been reported in the last few decades.

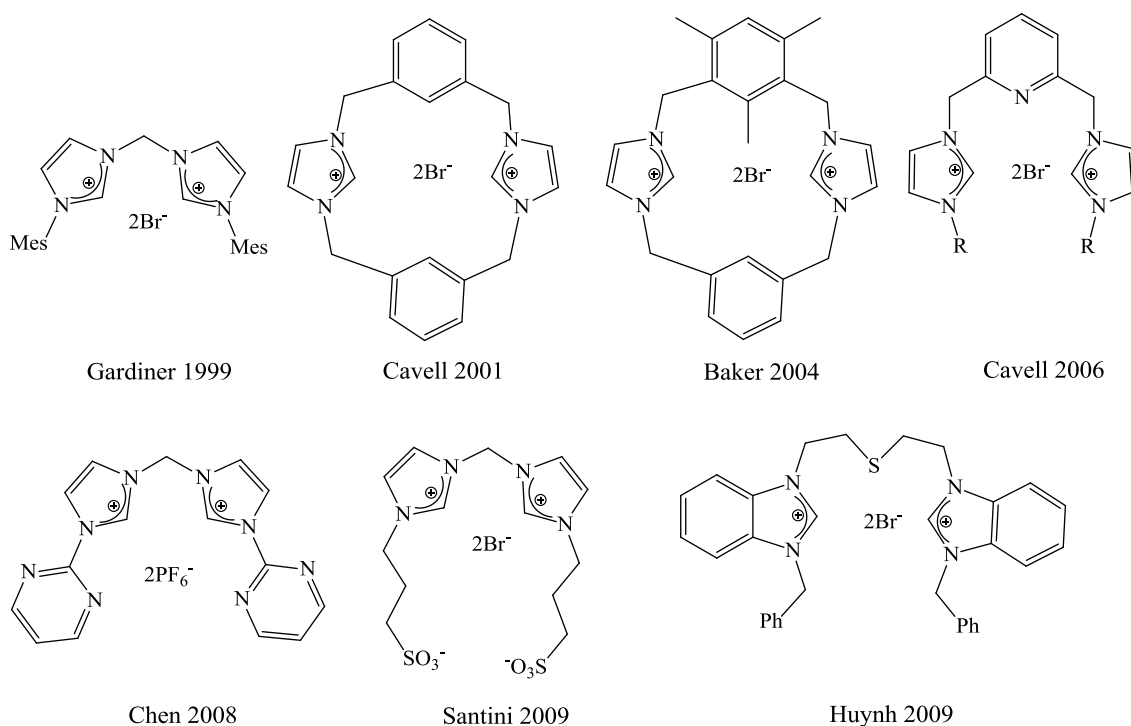


Figure 13: A snapshot of synthesised bis-chelating NHC amidinium salts.⁵⁰⁻⁵⁶

As exhibited in Figure 13 many different architectures of chelating bis-NHCs have been reported going from large cyclophane systems reported by Cavell⁵⁶ and Baker,⁵⁰ to simple alkylated systems reported by Gardiner.⁵⁴ There has been many synthetic routes reported⁵⁷⁻⁶¹ but the main ones are based around the use of commercially available imidazolium precursors, which are then reacted with a linker group to form the bis-carbene, which was reported by Vargas *et al.* in 2003.⁵⁷ The other main route is very similar to that by Vargas, except here the mono-NHC is synthesised to allow functionality and then reacted with a linker to form the bis-NHC, this route was reported by Bessel *et al.* in 2010.⁵⁸ The synthetic detail of these two routes will be discussed further in Chapter 2 of this thesis.

1.6: Complexation of NHCs

1.6.1: Coordination of 5-Membered NHCs

As mentioned in Section 1.5, 5-membered NHCs have been extensively researched with many successful coordinations being accomplished. It has been reported that a substantial number of the transition metals and several of the s, p, and f block elements have been coordinated to 5-membered NHCs,^{28,29,62-64} with a concentration on the late transition metals.^{23,65,66} Since they have been so extensively reported as with the synthetic routes the procedures will not be discussed here. However, Figure 14 shows a selection of complexes of 5-membered NHCs coordinated to a range of transition metals.

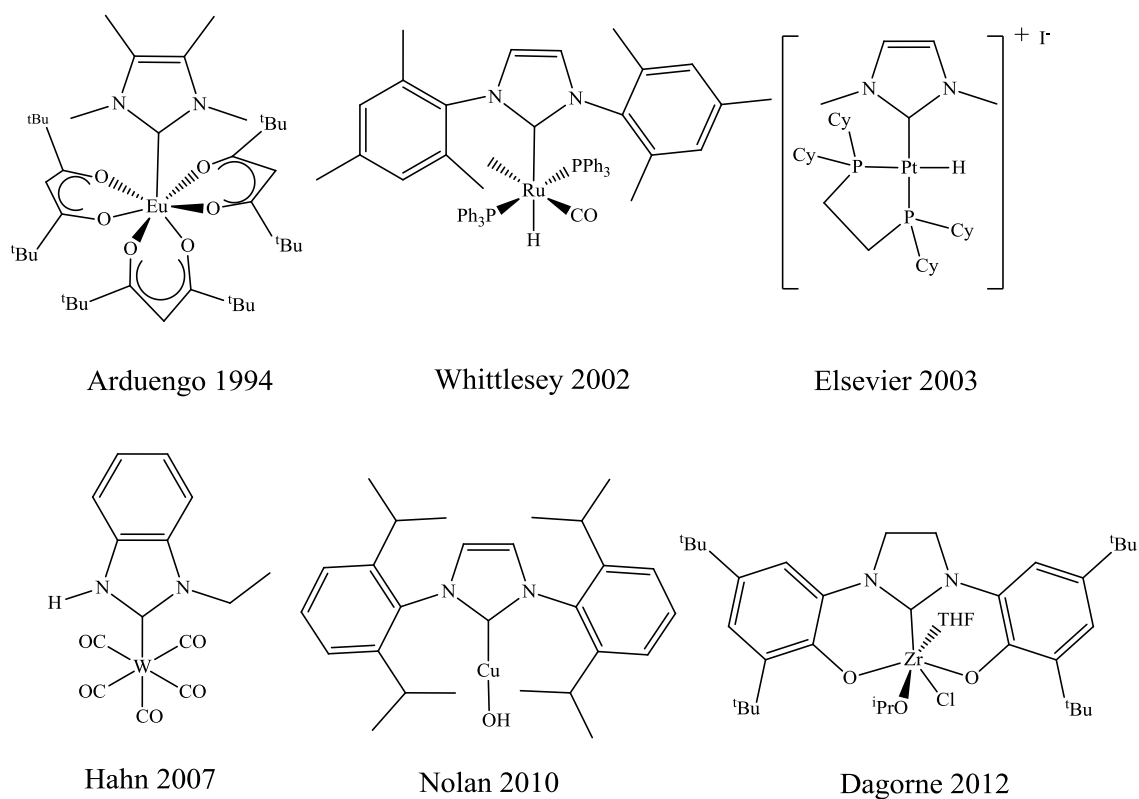


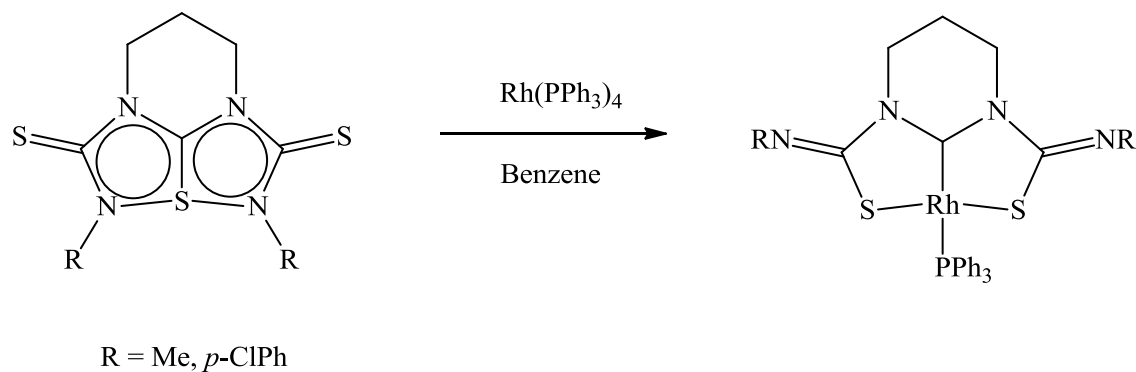
Figure 14: A selection of complexes, exhibiting the range of transition metal coordinations with NHCs.^{63,67-71}

1.6.2: Coordination of Expanded Ring NHCs

Complexes of expanded ring NHCs are relatively unknown in comparison to their 5-membered counterparts. The recent developments involving coordination of these types of ligand architectures is predominantly directed to the late transition metals (Rh, Ir, Pt, Pd, Ag, Cu, Ru, Ni, and Au), and in this section we will briefly discuss these complexes.

The first example of the coordination of expanded ring NHCs was to rhodium and this was carried out by Iwasaki and co-workers in 1996,⁷² three years previous to Alder³⁰ publishing the first isolation of a 6-membered NHC. This was achieved by reacting

tetraazathiapentalene compounds, which contain a hypervalent sulphur atom, with the corresponding metal precursor to form the novel metal carbene complexes, Scheme 9.

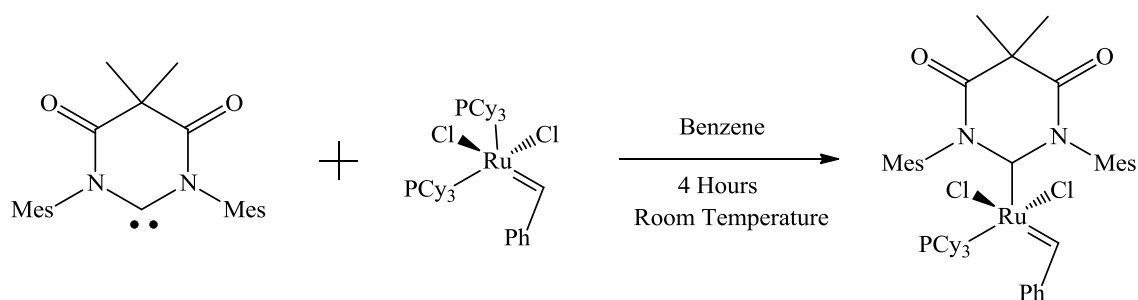


Scheme 9: Synthesis of the first 6-membered NHC transition metal complex.⁷²

After it had been found that expanded ring complexes could be synthesised, coordination to different metals was reported. As mentioned earlier this was mainly with the late transition metals.

1.6.2.1: Coordination of Expanded Ring NHCs to Ruthenium, Rhodium, and Iridium

Bielewaski and co-workers synthesised a 6-membered NHC complex employing a ruthenium metal centre from the $[\text{PhCH}=\text{Ru}(\text{PCy}_3)_2\text{Cl}_2]$ precursor, Scheme 10. This complex was originally based upon the Hoveyda-Grubbs type catalyst, which have been shown to have high catalytic activity.⁷³



Scheme 10: Synthesis of Bielewski ruthenium complex.

A series of different ruthenium complexes containing an expanded ring moiety have also been synthesised by Whittlesey,⁷⁴ Figure 15. These complexes were produced from a reaction between the free carbene and the corresponding ruthenium precursor, which in turn contain a carbonyl moiety. This carbonyl moiety in the complex exhibits a considerably lower C=O stretching frequency than that of its 5-membered counterpart.⁷⁵ This decrease in carbonyl stretching frequency can be attributed to the σ -donor capacity of the expanded ring NHC ligand.

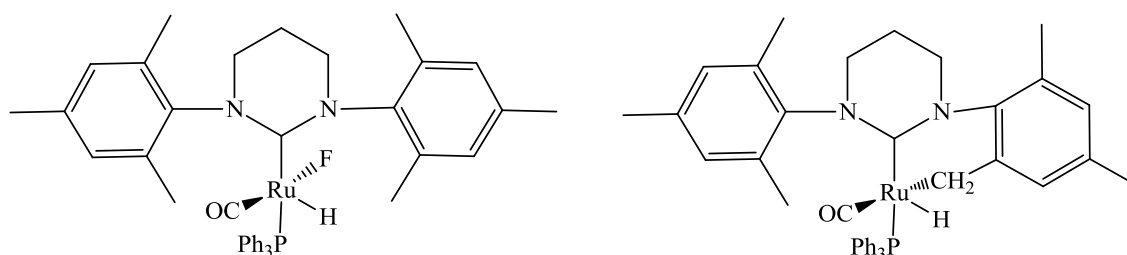


Figure 15: Whittlesey's ruthenium complexes exhibiting low carbonyl frequencies.⁷⁴

The observation of low carbonyl stretching frequencies is not just limited to ruthenium complexes, it has been found in several rhodium complexes synthesised by Newman,³⁸ Richeson,³¹ and Cavell^{19,76} as shown in Figure 16. These are not, however, the only

types of rhodium complexes which have been synthesised as Buchmeiser,³³ Richeson,³¹ Cavell,^{19,76} and Newman³⁸ have synthesised rhodium and iridium complexes of general formula $[M(\text{NHC})(\text{COD})\text{Cl}]$, where $M = \text{Rh}$ or Ir , Figure 16. These complexes are all synthesised in a very similar fashion with the *in situ* formation of the free carbene followed by coordination using the corresponding precursor. This included the coordination to rhodium and iridium of the novel 8-membered NHC as synthesised by Cavell via the amidinium route mentioned in Section 1.5.1.¹⁹ These 8-membered rhodium complexes, containing a carbonyl moiety, continue the trend observed with large ring NHCs with a decrease in carbonyl frequency, and these 8-membered derivatives have the lowest carbonyl frequency values to date due to their extensive σ -donor abilities.

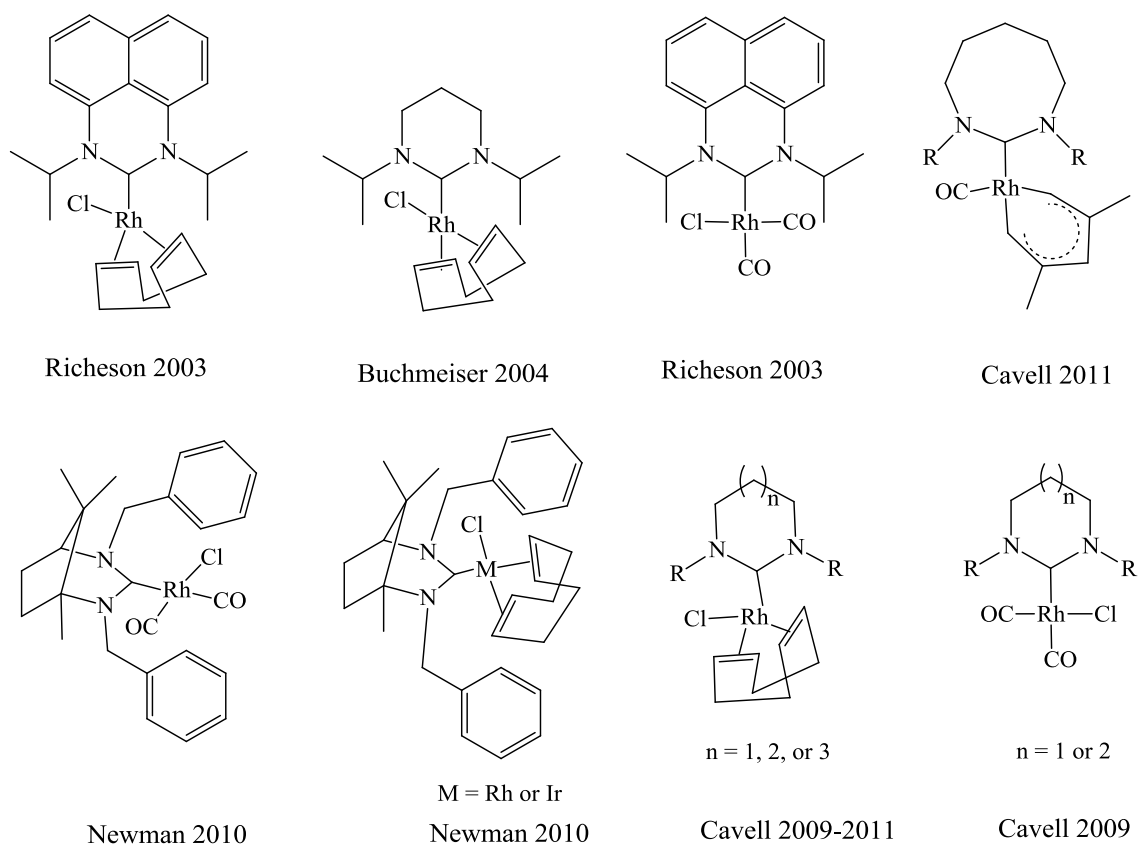


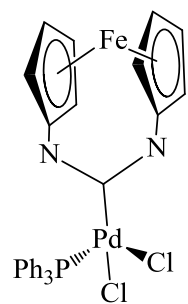
Figure 16: A few examples of low frequency rhodium carbonyl complexes of general formula $[M(\text{NHC})(\text{COD})\text{Cl}]$, where $M = \text{Rh}$ or Ir .^{19,31,33,38,76}

Wilhelm has shown that the free carbene can be formed of these bicyclic systems due to the entrapment using CS₂.³⁷ This discovery led Newman to synthesise a series of bicyclic NHCs and their complexes as shown in Figure 16.

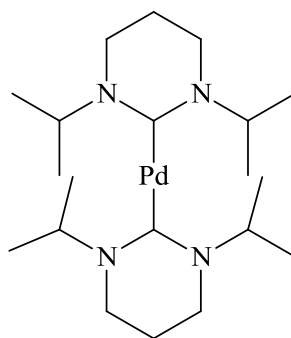
1.6.2.2: Coordination of Expanded Ring NHCs to Palladium and Nickel

Following an initial report by Buchmeiser³³ describing the formation of group ten 6-membered ring NHC complexes, using Pd(MeCN)₂Cl₂ as the metal palladium precursor, Figure 17, Stahl and co-workers³⁵ synthesised a series of 7-membered NHC palladium complexes by the reaction of the free carbene with the corresponding palladium precursor, Figure 17. This route appeared to be more efficient than that of the transmetallation as Herrmann and co-workers have shown the latter route does not always yield the palladium complex.³² This failure to coordinate through the transmetallation route was based upon the σ -donor abilities of the NHC causing very strong NHC-Ag bonds, and therefore not yielding the corresponding palladium complexes. Siemeling⁷⁷ and Cavell⁷⁸ have also synthesised novel expanded ring palladium complexes as shown in Figure 17.

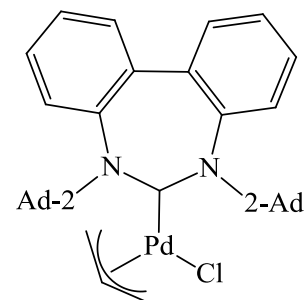
A series of expanded ring complexes containing a nickel centre have also been reported with some interesting outcomes, such as a series of nickel complexes that can undergo C-H activation of one of the N-substituents as shown by Whittlesey and co-workers,⁷⁹ Figure 18, this will be discussed further in Chapter 6 of this thesis. Cavell and Whittlesey have also shown that expanded rings up to the size of 8-membered, have been successful in the formation of nickel(I) species as shown in Figure 18.^{79,80} Newman has also shown how nickel can coordinate to expanded ring NHCs where the NHC employed here was of bicyclic architecture. These latter nickel complexes are very reactive in the presence of chloroform, they produce the nickel chloride adduct as shown in Figure 18.



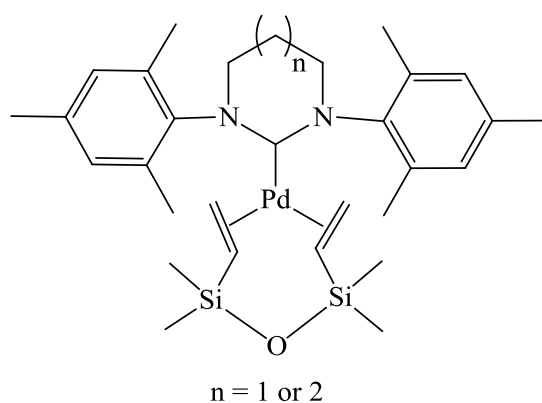
Siemeling 2012



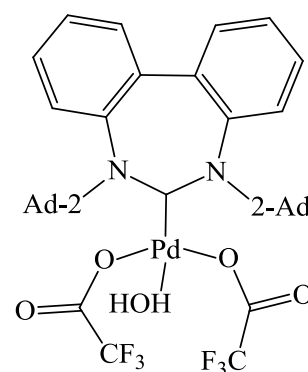
Buchmeiser 2004



Stahl 2005



Cavell 2011



Stahl 2006

Figure 17: A select few palladium complexes which have been synthesised.^{33,35,77,78}

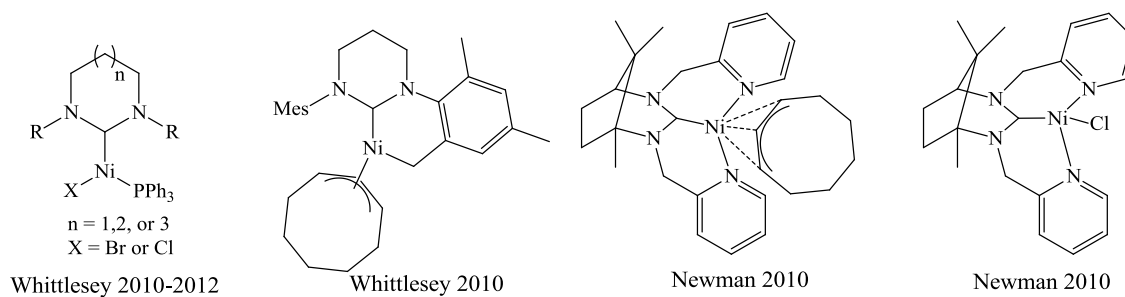


Figure 18: Expanded ring NHC nickel complexes.^{38,79,80}

1.6.2.3: Coordination of Expanded Ring NHCs to Coinage Metals, Silver, Gold, and Copper

NHC complexes of silver are well known,^{19,32,33,43,81,82} however gold and copper are relatively unexplored in comparison. Silver complexes are versatile due to their stability to air and their requirement of no adverse reaction conditions to synthesise such complexes. The first expanded ring silver complexes were synthesised by Buchmeiser³³ and Herrmann³² independently as shown in Figure 19. A range of expanded ring NHCs was then synthesised by Cavell,^{19,43} a selection of which are shown in Figure 19. It is usual that silver complexes are starting complexes for transmetallation to other metal centres. These have led to Nechaev and co-workers^{83,84} synthesising copper(I) and copper(II) complexes, and McQuade and co-workers⁸⁵ have also reported copper(I) expanded ring NHCs, Figure 19. Most recently Newman has reported the first bicyclic expanded ring NHC copper complex, which employs phosphine moieties on the N-substituents, Figure 19. These bicyclic systems appear to behave somewhere between that of the 5-membered NHCs and the 6-membered NHCs, this is apparent due to their NCN bond angles which are half way between the size of the two rings mentioned. A number of gold(I) complexes have been synthesised recently with Bielawski and co-workers employing a 7-membered NHC architecture⁸⁶ and Dunsford employing sterically demanding N-substituents such as diisopropylphenyl (DIPP) and mesityl (Mes),⁸⁷ as shown in Figure 19. These sterically demanding gold(I) complexes exhibit the largest percentage buried volumes to date, this will be discussed further in later chapters of this thesis.

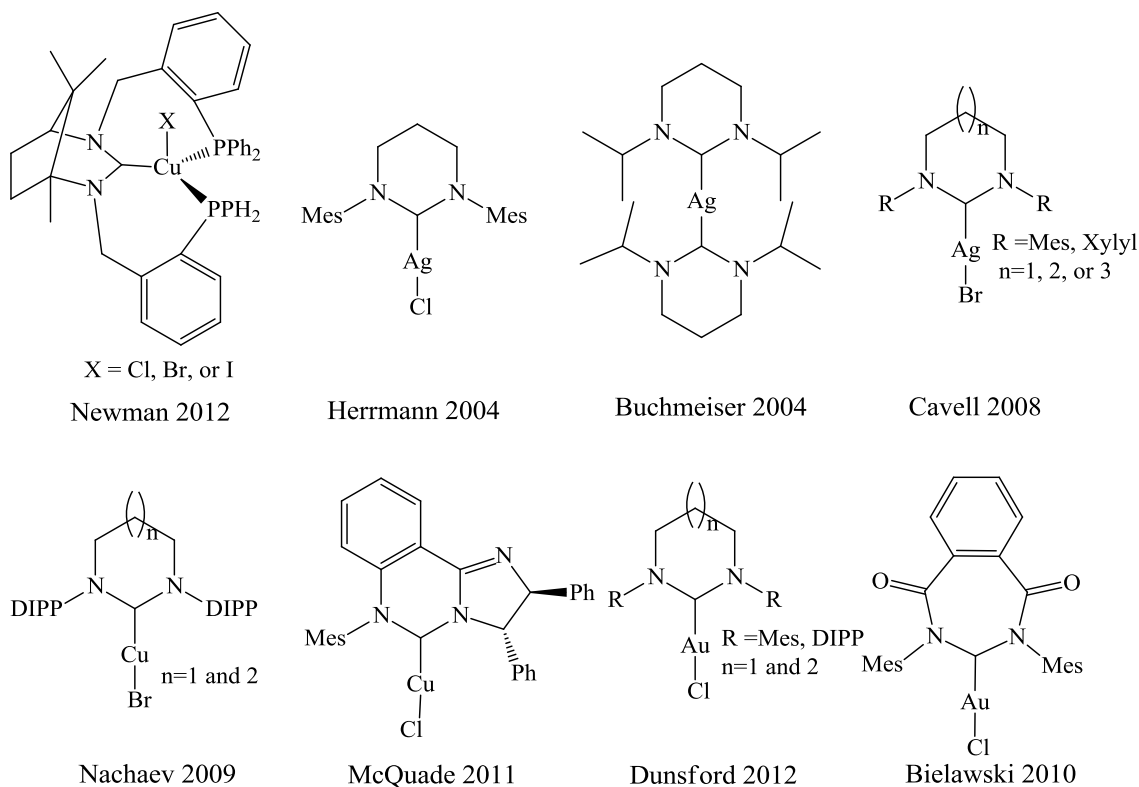


Figure 19: Silver, copper, and gold complexes.^{19,32,33,43,83-87}

1.6.3: Coordination of Bis-NHCs

The bis-NHCs are not as widely published as those of the mono 5-membered NHCs, however; they are still extensively researched in comparison to the expanded ring systems and the bicyclic systems. In this section the discussion will provide an overview of the assortment of coordination abilities of chelating bis-NHCs and bridging bis-NHCs. The synthetic routes to complexes of bis-NHCs are very similar to that of the mono-NHCs with either a transmetallation process or an *in situ* production of the free carbene followed by a subsequent reaction with the corresponding metal precursor. The feature which decides whether the bis-NHC is going to chelate or bridge is the linking group between the two carbenes. If this is a small alkyl linker then the bis-NHC is more likely to chelate, whereas when this is longer it may preferably bridge. When

the linking groups are aromatic moieties, the more bulky they are more likely the bis-NHC will bridge. The discussion will start with the coordination of chelating bis-carbenes and their versatility to complex to a range of different metals, Figure 20.

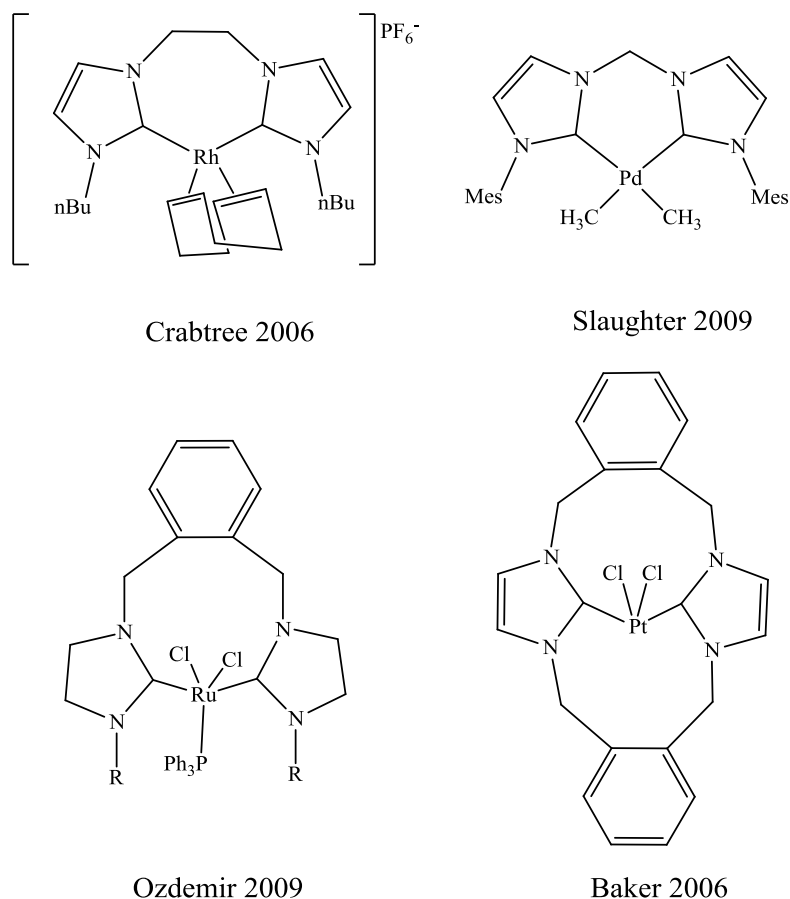


Figure 20: A range of chelating bis-NHC complexes showing the versatility of metals.⁸⁸⁻⁹¹

As can be observed by the structures in Figure 20, the chelate angle is very dependent on the linking group between the two NHCs. When this is a small linker such as a methyl or ethyl moiety then the coordination area is much more compact, whereas when the linker is for instance a meta-xylylene moiety the coordination sphere is much larger.

The other type of bis-NHCs which have been reported are bridging types, of which a selection are shown in Figure 21.

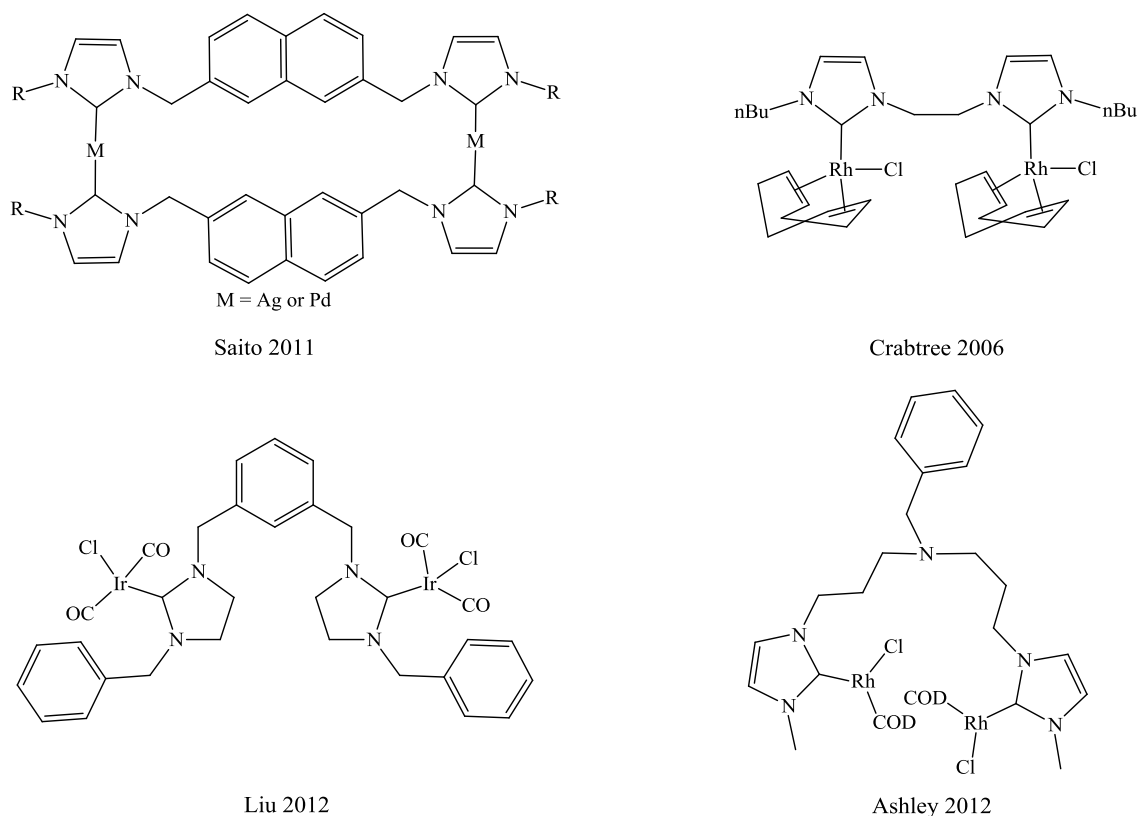
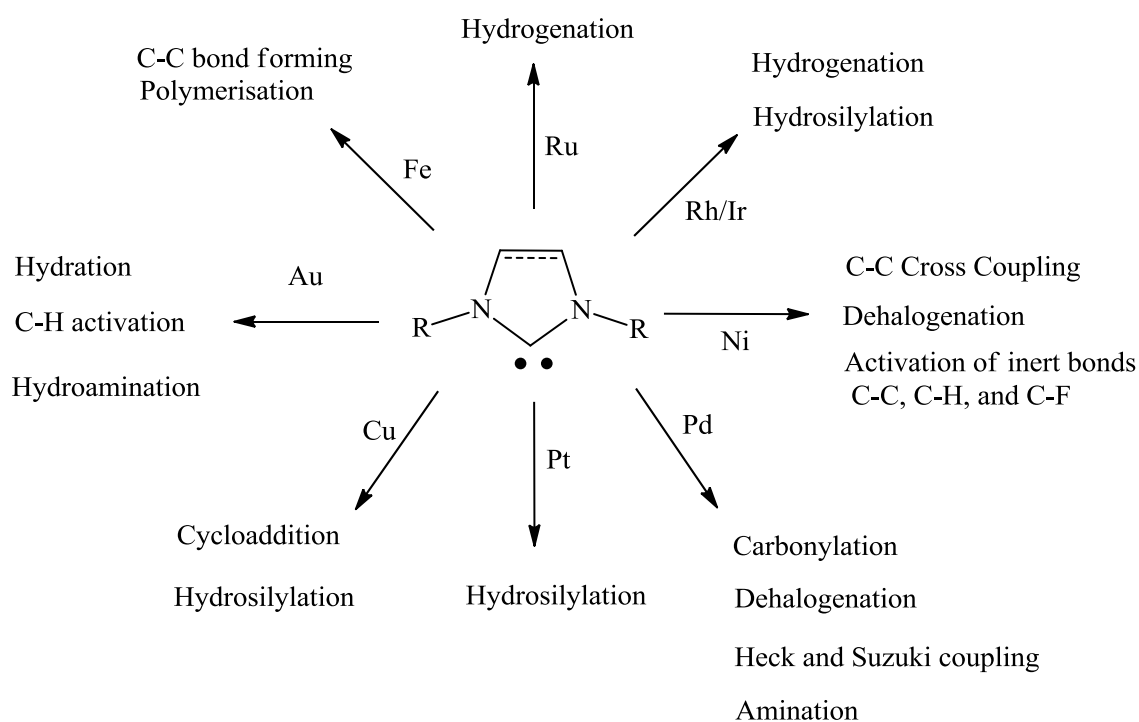


Figure 21: A selection of bridging bis-NHC complexes.^{88,92-94}

As exhibited in Figures 20 and 21 there is a significant range of bis-NHC which have been reported in recent years. This is due to the ability, which these complexes possess, to be fine tuned to specific applications for example by altering the linking group, the backbone functionality, or the metal centre the complex can be altered very simply to be used for different catalytic processes. These functionalities and applications will be discussed further in subsequent chapters of this thesis. As stated previously bis-expanded ring NHC ligands and complexes thereof are not known.

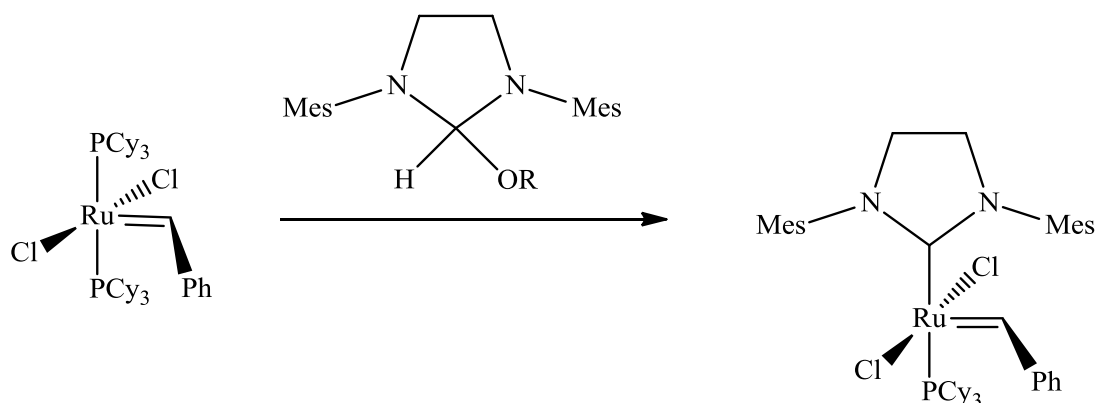
1.7: Catalytic Properties of NHCs

In previous sections it has been discussed how a large range of NHC complexes of varying architectures have been synthesised over the years. Many of these complexes have been successfully employed as catalysts, which have been shown to have promising potential. In this section the discussion will concentrate on how the metal NHC complexes have been used for catalysis in recent years as discussions of earlier results are covered in excellent reviews on the topic.^{24,26-28,95,96} The catalytic applications vary depending mainly on the metal which is employed, this is shown in Scheme 11 where a series of common transformations using 5-membered NHCs as ligands are shown.²³



Scheme 11: A series of transformations exhibiting the versatility of 5-membered NHCs in catalysis.^{23,97}

The most well known example of the use of NHC ligands in catalysis, is the 2nd generation Grubbs metathesis catalyst, which is derived from the 1st generation catalyst by substituting one phosphine ligand with an NHC ligand, Scheme 12. It was this development in the world of catalysis that helped earn Grubbs a share in the Nobel Prize for Chemistry in 2005.



Scheme 12: Synthesis of 2nd generation Grubbs catalyst.⁹⁸

It is not just 5-membered ring NHCs that have shown to be effective in homogenous catalysis, with expanded ring NHCs and bicyclic NHCs also showing promising outcomes in several different transformations, Figure 22. For example these large ring ligand systems have been used for hydrogenation with conversions exceeding 99 %.^{44,99,100} In addition, cross coupling employing palladium as the metal showed conversions of up to 100 %, ^{33,78,101} ruthenium catalysed olefin metathesis with conversions of 96 %, ^{102,103} hydrosilylation where the catalyst is copper based show 100 % conversions,^{49,104} aerobic oxidative cyclisation with conversions exceeding 90 %, ¹⁰⁵ hydroformylation of alkenes with excellent yield of 100 %, ¹⁰⁶ polymerisation reactions employing rhodium NHCs as the catalyst show yields of up to 90 %, ¹⁰⁷ and hydrations of alkynes are the most recently reported expansion to the uses of expanded ring NHC in catalysis, and the reports are excellent with conversions of 100 %.⁸⁷

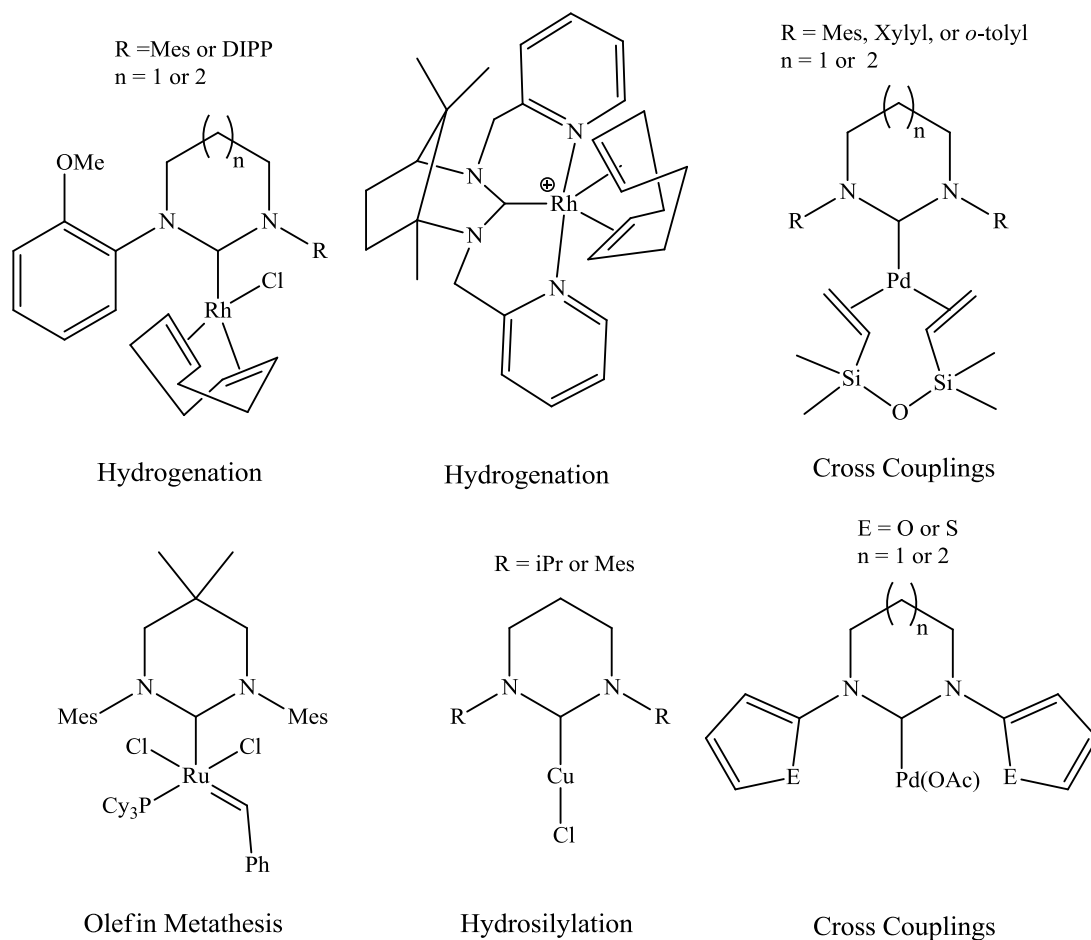


Figure 22: A few of the expanded ring and bicyclic ring catalysts and their applications.^{44,49,78,87,99-102,104}

The expanded ring and bicyclic ring NHCs have not just shown high conversions but they also employ low catalyst loadings as low as 0.001 mol % with promising results. However, conversions greater than 95 % were observed when catalyst loadings of 0.01 % were employed.⁹⁹ 7-Membered NHC systems have been shown to exceed the catalytic activity of their 5- and 6-membered counterparts in reactions such as hydrosilylations, where turnover frequencies have been fivefold greater, and the percentage yield has increased from 61 % to 100 %, when employing the 7-membered catalyst instead of the 6-membered analogues.⁷⁸ However, this increase in activity is only apparent up until a certain ring size when the conversion starts to decrease. At the

8-membered ring stage catalytic performances are less efficient than that of the 6- and 7-membered analogues.^{18,19} More in depth catalytic information such as how the catalytic cycle proceeds can be found in subsequent chapters of this thesis.

1.8: Aims of Thesis

It is apparent from the discussions in this chapter that the bis-NHCs, expanded ring NHCs, and bicyclic NHCs have been shown to successfully coordinate and have also been shown to have promising catalytic properties and interesting features, such as increased basicity and larger NCN bond angles, and large steric demand around the metal centre, in comparison to their 5-membered counterparts. One aspect of this thesis concentrates on the synthesis of a series of bis-NHC and attempted coordination to silver and palladium. In other chapters the synthesis, coordination, and application of a series of novel rhodium, copper, and gold fused 6- and 7-membered bicyclic NHCs; and the synthesis and application, including catalysis and EPR studies, of a series of expanded ring copper, gold, and nickel complexes is described.

1.9: References

- 1 Fischer, E. O.; Maasböl, A. *Angew. Chem. Int. Ed.* **1964**, 3, 8, 580-581.
- 2 Rouschias, G.; Shaw, B. L. *J. Chem. Soc. D Chem. Comm.* **1970**, 183-183.
- 3 Burke, A.; Balch, A. L.; Enemark, J. H. *J. Am. Chem. Soc.* **1970**, 92, 8, 2555-2557.
- 4 Butler, W. M.; Enemark, J. H. *Inorg. Chem.* **1971**, 10, 11, 2416-2419.
- 5 Schrock, R. R. *J. Am. Chem. Soc.* **1974**, 96, 21, 6796-6797.
- 6 Wanzlick, H. -W.; Schönherr, H. -J. *Angew. Chem. Int. Ed.* **1968**, 7, 2, 141-142.
- 7 Öfele, K. *J. Organomet. Chem.* **1968**, 12, P42-43.
- 8 Öfele, K.; Herberhold, M. *Angew. Chem. Int. Ed.* **1970**, 9, 9, 739-740.
- 9 Öfele, K. *J. Organomet. Chem.* **1970**, 22, C9-11.
- 10 Ing, D. R.; Wanzlick, H. -W. *Angew. Chem. Int. Ed.* **1962**, 1, 2, 75-80.
- 11 Hahn, F. E.; Wittenbecher, L.; Le Van, D.; Fröhlich, R. *Angew. Chem. Int. Ed.* **2000**, 39, 3, 541-544.
- 12 Liu, Y.; Lemal, D. M. *Tett. Lett.* **2000**, 41, 5, 599-602.
- 13 Winberg, H. E.; Carnahan, J. E.; Coffman, D. F.; Brown, M. *J. Am. Chem. Soc.* **1965**, 87, 9, 2055-2056.
- 14 Cardin, D. J.; Doyle, M. J.; Lappert, M. F. *J. Chem. Soc. Chem. Comm.* **1972**, 927-928.
- 15 Alder, R. W.; Blake, M. E.; Chaker, L.; Harvey, J. N.; Paolini, F.; Schütz, J. *Angew. Chem. Int. Ed.* **2004**, 43, 44, 5896-5911.
- 16 Arduengo, A. J.; Harlow, R. L.; Kline, M. *J. Am. Chem. Soc.* **1991**, 113, 1, 361-363.
- 17 Baird, N. C.; Taylor, K. F. *J. Am. Chem. Soc.* **1978**, 100, 5, 1333-1338.
- 18 Lu, W. Y. *PhD Thesis* **2012**
- 19 Lu, W. Y.; Cavell, K. J.; Wixey, J. S.; Kariuki, B. *Organometallics* **2011**, 30, 5649-5655.
- 20 Poater, A.; Cosenza, B.; Correa, A.; Giudice, S.; Ragone, F.; Scarano, V.; Cavallo, L. *Eur. J. Inorg. Chem.* **2009**, 13, 1759-1766.
- 21 Hillier, A. C.; Sommer, W. J.; Yong, B. S.; Petersen, J. L.; Cavallo, L.; Nolan, S.

- P. Organometallics* **2003**, 22, 21, 4322-4326.
- 22 Díez-González, S.; Nolan, S. P. *Coord. Chem. Rev.* **2007**, 251, 874-883.
- 23 Díez-González, S.; Marion, N.; Nolan, S. P. *Chem. Rev.* **2009**, 109, 8, 3612-3676.
- 24 Normand, A. T.; Cavell, K. J. *Eur. J. Inorg Chem.* **2008**, 18, 2781-2800.
- 25 Cavell, K. J.; McGuinness, D. S. *Coord. Chem. Revs.* **2004**, 248, 671-681.
- 26 Fortman, G. C.; Nolan, S. P. *Chem. Soc. Revs.* **2011**, 40, 5151-5169.
- 27 Wang, F.; Liu, L. -L.; Wang, W.; Li, S.; Shi, M. *Coord. Chem. Revs.* **2012**, 256, 804-853.
- 28 Herrmann, W. A.; Köcher, C. *Angew. Chem. Int. Ed.* **1997**, 36, 20, 2162-2187.
- 29 Hahn, F. E.; Jahnke, M. C. *Angew. Chem. Int. Ed.* **2008**, 47, 17, 3122-3172.
- 30 Alder, R. W.; Blake, M. E.; Bortolotti, C.; Bufali, S.; Butts, C. P.; Linehan, E.; Oliva, J. M.; Orpen, A. G.; Quayle, M. J. *Chem. Comm.* **1999**, 241-242.
- 31 Bazinet, P.; Yap, G. P. A.; Richeson, D. S. *J. Am. Chem. Soc.* **2003**, 125, 44, 13314-13315.
- 32 Herrmann, W. A.; Schneider, S. K.; Öfele, K.; Sakamoto, M.; Herdtweck, E. *J. Organomet. Chem.* **2004**, 689, 15, 2441-2449.
- 33 Mag, M. M.; Wurst, K.; Ongania, K. -H.; Buchmeiser, M. R. *Chem. Eur. J.* **2004**, 10, 5, 1256-1266.
- 34 Magill, A. M.; Cavell, K. J.; Yates, B. F. *J. Am. Chem. Soc.* **2004**, 126, 28, 8717-8724.
- 35 Scarborough, C. C.; Grady, M. J. W.; Guzei, L. A.; Ghandi, B. A.; Bunel, E. E.; Stahl, S. S. *Angew. Chem. Int. Ed.* **2005**, 44, 33, 5269-5272.
- 36 Iglesias, M.; Beetstra, D. J.; Stasch, A.; Horton, P. N.; Hursthouse, M. B.; Coles, S. J.; Cavell, K. J.; Dervisi, A.; Fallis, I. A. *Organometallics* **2007**, 26, 19, 4800-4809.
- 37 Reddy, P. V. G.; Tabassum, S.; Blanrue, A.; Wilhelm, R. *Chem. Comm.* **2009**, 5910-5912.
- 38 Newman, P. D.; Cavell, K. J.; Kariuki, B. M. *Organometallics* **2010**, 29, 12, 2724-2734.
- 39 Newman, P. D.; Cavell, K. J.; Kariuki, B. M. *Chem. Comm.* **2012**, 48, 6511-6513.
- 40 Cotton, F. A.; Haefner, S. C.; Matonic, J. H.; Wang, X.; Murillo, C. A. *Polyhedron* **1997**, 16, 3, 541-550.

- 41 Cotton, F. A.; Lei, P.; Murillo, C. A.; Wang, L. -S. *Inorganica Chimica Acta* **2003**, 349, 165-172.
- 42 Jazzar, R.; Liang, H.; Donnadieu, B.; Bertrand, G. *J. Organomet. Chem.* **2006**, 691, 14, 3201-3205.
- 43 Iglesias, M.; Beetstra, D. J.; Knight, J. C.; Ooi, L. -L.; Stasch, A.; Coles, S.; Male, L.; Hursthouse, M. B.; Cavell, K. J.; Dervisi, A.; Fallis, I. A. *Organometallics* **2008**, 27, 13, 3279-3289.
- 44 Binobaid, A.; Iglesias, M.; Beetstra, D. J.; Kariuki, B.; Dervisi, A.; Fallis, I. A.; Cavell, K. J. *Dalton Trans.* **2009**, 7099-7112.
- 45 César, V.; Lugan, N.; Lavigne, G. *J. Am. Chem. Soc.* **2008**, 130, 34, 11286-11287.
- 46 César, V.; Lugan, N.; Lavigne, G. *Eur. J. Inorg. Chem.* **2009**, 3, 361-365.
- 47 Hudnall, t. W.; Bielawski, C. W. *J. Am. Chem. Soc.* **2009**, 131, 44, 16039-16041.
- 48 Berding, J.; van Dijkman, T. F.; Lutz, M.; Spek, A. L.; Bouwman, E. *Dalton Trans.* **2009**, 6948-6955.
- 49 Dunsford, J. J. *PhD Thesis* **2012**.
- 50 Baker, M. V.; Bosnich, M. J.; Brown, D. H.; Byrne, L. T.; Hesler, V. J.; Skelton, B. W.; White, A. H.; Williams, C. C. *J. Org. Chem.* **2004**, 69, 22, 7640-7652.
- 51 Nielsen, D. J.; Cavell, K. J.; Skelton, B. W.; White, A. H. *Inorganica Chimica Acta* **2006**, 359, 6, 1855-1869.
- 52 Papini, G.; Pellei, M.; Lobbia, G. G.; Burini, A.; Santini, C. *Dalton Trans.* **2009**, 6985-6990.
- 53 Ye, J.; Chen, W.; Wang, D. *Dalton Trans.* **2008**, 4015-4022.
- 54 Gardiner, M. G.; Herrmann, W. A.; Reisinger, C. -P.; Schwarz, J.; Spiegler, M. *J. Organomet. Chem.* **1999**, 572, 2, 239-247.
- 55 Huynh, H. V.; Yuan, D.; Han, Y. *Dalton Trans.* **2009**, 7262-7268.
- 56 Magil, A. M.; McGuinness, D. S.; Cavell, K. J.; Britovsek, G. J. P.; Gibson, V. C.; White, A. J. P.; Williams, D. J.; White, A. H.; Skelton, B. W. *J. Organomet. Chem.* **2001**, 617-618, 546-560.
- 57 Vargas, V. C.; Rubio, R. J.; Hollis, T. K.; Salcido, M. E. *Org. Lett.* **2003**, 5, 25, 4847-4849.
- 58 Bessel, M.; Rominger, F.; Straub, B. F. *Synthesis* **2010**, 9, 1459-1466.
- 59 Marshall, C.; Ward, M. F.; Skakle, J. M. S. *Synthesis* **2006**, 6, 1040-1044.

- 60 Dyson, G.; Frison, J. -C.; Whitwood, A. C.; Douthwaite, R. E. *Dalton Trans.* **2009**, 7141-7151.
- 61 Alcalde, E.; Ceder, R. M.; López, C.; Mesquida, N.; Muller, G.; Rodríguez, S. *Dalton Trans.* **2007**, 2696-2706.
- 62 Bourissou, D.; Guerret, O.; Gabbaï, F. P.; Bertrand, F. *Chem Rev.* **2000**, 100, 1, 39-92.
- 63 Arduengo, A. J.; Tamm, M.; McLain, S. J.; Calabrese, J. C.; Davidson, F.; Marshall, W. J. *J. Am. Chem. Soc.* **1994**, 116, 17, 7927-7928.
- 64 Kuhn, N.; Al-Sheikh, A. *Coord. Chem. Rev.* **2005**, 249, 829-857.
- 65 Weskamp, T.; Böhm, V. P. W.; Herrmann, W. A. *J. Organomet. Chem.* **2000**, 600, 12-22.
- 66 Crudden, C. M.; Allen, D. P. *Coord. Chem. Rev.* **2004**, 248, 2247-2273.
- 67 Jazzar, R. F. R.; Macgregor, S. A.; Mahon, M. F.; Richards, S. P.; Whittlesey, M. K. *J. Am. Chem. Soc.* **2002**, 124, 18, 4944-4945.
- 68 Duin, M. A.; Clement, N. D.; Cavell, K. J.; Elsevier, C. J. *Chem. Comm.* **2003**, 400-401.
- 69 Meier, N.; Hahn, F. E.; Pape, T.; Siering, C.; Waldvogel, S. R. *Eur. J. Inorg. Chem.* **2007**, 9, 1210-1214.
- 70 Fortman, G. C.; Slawin, A. M. Z.; Nolan, S. P. *Organometallics* **2010**, 29, 17, 3966-3972.
- 71 Romain, C.; Heinrich, B.; Laponnaz, S. B.; Dagonne, S. *Chem. Comm.* **2012**, 48, 2213-2215.
- 72 Iwasaki, F.; Yasui, M.; Yoshida, S.; Nishiyama, H.; Shimamoto, S.; Matsumura, N. *Bull. Chem. Soc. Jpn.* **1996**, 69, 10, 2759-2770.
- 73 Garber, S. B.; Kingsbury, J. S.; Gray, B. L.; Hoveyda, A. H. *J. Am. Chem. Soc.* **2000**, 122, 34, 8168-8179.
- 74 Armstrong, R.; Ecott, C.; Mas-Marzá, E.; Page, M. J.; Mahon, M. F.; Whittlesey, M. K. *Organometallics* **2010**, 29, 4, 991-997.
- 75 Reade, S. P.; Mahon, M. F.; Whittlesey, M. K. *J. Am. Chem. Soc.* **2009**, 131, 5, 1847-1861.
- 76 Iglesias, M.; Beetstra, D. J.; Kariuki, B.; Cavell, K. J.; Dervisi, A.; Fallis, I. A. *Eur. J. Inorg. Chem.* **2009**, 1913-1919.

- 77 Siemeling, U.; Färber, C.; Bruhn, C.; Fürmeier, S.; Schulz, T.; Kurlemann, M.; Tripp, S. *Eur. J. Inorg. Chem.* **2012**, 1413-1422.
- 78 Dunsford, J. J.; Cavell, K. J. *Dalton Trans.* **2011**, 40, 9131-9135.
- 79 Davies, C. J. E.; Page, M. J.; Ellil, C. E.; Mahon, M. F.; Whittlesey, M. K. *Chem. Comm.* **2010**, 46, 5151-5153.
- 80 Page, M. J.; Lu, W. Y.; Poulten, R. C.; Carter, E.; Algarra, A. G.; Kariuki, B. M.; Macgregor, S. A.; Mahon, M. F.; Cavell, K. J.; Murphy, D. M.; Whittlesey, M. K. *Chem. Eur. J.* **2012**, In Press.
- 81 Maishal, T. K.; Basset, J. -M.; Boualleg, M.; Copéret, C.; Veyre, L.; Thieuleux, C. *Dalton Trans.* **2009**, 6959-6959.
- 82 Raynal, M.; Liu, X.; Pattacini, R.; Vallée, C.; Olivier-Bourbigou, H.; Braunstein, P. *Dalton Trans.* **2009**, 7288-7293.
- 83 Kolychev, E. L.; Portnyagin, I. V.; Shuntikov, V. V.; Khrustalev, V. N.; Nechaev, M. S. *J. Organomet. Chem.* **2009**, 694, 15, 2454-2462.
- 84 Kolychev, E. L.; Shuntikov, V. V.; Khrustalev, V. N.; Bush, A. A.; Nechaev, M. S. *Dalton Trans.* **2011**, 40, 3074-3076.
- 85 Park, J. K.; Lackey, H. H.; Ondrusek, B. A.; McQuade, D. T. *J. Am. Chem. Soc.* **2011**, 133, 8, 2410-2413.
- 86 Moerdyk, J. P.; Bielawski, C. W. *Organometallics* **2011**, 30, 8, 2278-2284.
- 87 Dunsford, J. J.; Cavell, K. J.; Kariuki, B. M. *Organometallics* **2012**, 31, 4118-4121.
- 88 Crabtree, R. H. *J. Organomet. Chem.* **2006**, 691, 14, 3146-3150.
- 89 Özdemir, I.; Demir, S.; Gürbuz, N.; Çetinkaya, B.; Toupet, L.; Bruneau, C.; Dixneuf, P. H. *Eur. J. Inorg. Chem.* **2009**, 13, 1942-1949.
- 90 Subramaniam, S. S.; Slaughter, L. M. *Dalton Trans.* **2009**, 6930-6933.
- 91 Baker, M. V.; Brown, D. H.; Simpson, P. V.; Skelton, B. W.; White, A. H.; Williams, C. C. *J. Organomet. Chem.* **2006**, 691, 26, 5845-5855.
- 92 Ashley, J. M.; Farnaby, J. H.; Hazari, N.; Kim, K. E.; Luzik Jr, E. D.; Meehan, R. E.; Meyer, E. B.; Schley, N. D.; Schmeier, T. J.; Taylor, A. N. *Inorganica Chimica Acta* **2012**, 380, 399-410.
- 93 Saito, S.; Saika, M.; Yamasaki, R.; Azumaya, I.; Masu, H. *Organometallics* **2011**, 30, 6, 1366-1373.

- 94 Kuo, H. -Y.; Liu, Y. -H.; Peng, S. -M.; Liu, S. -T. *Organometallics* **2012**, 31, 20, 7248-7255.
- 95 Sommer, W. J.; Weck, M. *Coord. Chem. Revs.* **2007**, 251, 860-873.
- 96 Mata, J. A.; Poyatos, M.; Peris, E. *Coord. Chem. Revs.* **2007**, 251, 841-859.
- 97 Herrmann, W. A. *Angew. Chem. Int. Ed.* **2002**, 8, 1290-1309.
- 98 Scholl, M.; Ding, S.; Lee, C. W.; Grubbs, R. H. *Org. Lett.* **1999**, 1, 6, 953-956.
- 99 Binonaid, A.; Iglesias, M.; Beetstra, D.; Dervisi, A.; Fallis, I.; Cavell, K. J. *Eur. J. Inorg. Chem.* **2010**, 34, 5426-5431.
- 100 Newman, P. D.; Cavell, K. J.; Hallett, A. J.; Kariuki, B. M. *Dalton Trans.* **2011**, 40, 8807
- 101 Özdemir, I.; Gürbüz, N.; Gök, Y.; Çetinkaya, B. *Heteroatom Chem.* **2008**, 19, 1, 82-86.
- 102 Yun, J.; Marinez, E. R.; Grubbs, R. H. *Organometallics* **2004**, 23, 18, 4172-4173.
- 103 Yang, L.; Mayr, M.; Wurst, K.; Buchmeiser, M. R. *Chem. Eur. J.* **2004**, 10, 22, 5761-5770.
- 104 Bantu, B.; Wang, D.; Wurst, K.; Buchmeiser, M. R. *Tetrahedron* **2005**, 61, 51, 12145-12152.
- 105 Scarborough, C. C.; Bergant, A.; Sazama, G. T.; Guzei, L. A.; Spencer, L. C.; Stahl, S. S. *Tetrahedron* **2009**, 65, 26, 5084-5092.
- 106 Bortenschlager, M.; Mayr, M.; Nuyken, O.; Buchmeiser, M. R. *J. Mol. Cat. A: Chemical* **2005**, 233, 67-71.
- 107 Zhang, Y.; Wang, D.; Wurst, K.; Buchmeiser, M. R. *J. Organomet. Chem.* **2005**, 690, 5728-5735.

2: Synthesis and Attempted Coordination of Novel Bis-N-Heterocyclic Carbenes

2.1: Introduction

The synthesis and attempted coordination of bis-N-heterocyclic carbenes to palladium and silver has provided the basis of this chapter. Over the years the main uses of azolium salts has been for carbene precursors¹ and to date the N-heterocyclic carbene work has predominantly concentrated on 5-membered,²⁻⁴ and to a less extent 6-membered derivatives.⁵⁻⁷ More recently studies have included novel 7-membered⁵⁻⁸ and most recently 8-membered NHC precursors as shown in Figure 1.⁹ Chelating bis-NHCs have focused exclusively on 5-membered rings as shown in Chapter 1,¹⁰⁻¹² no expanded ring bis-NHCs have been reported.

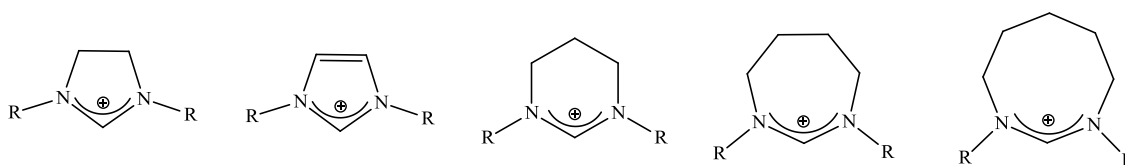


Figure 1: Series of NHC precursors from 5-membered saturated and unsaturated, through 6- and 7-membered to 8-membered.

The interest in bis-chelating NHCs arose due to the stability of the metal complexes which are formed using these precursors, and the ability to fine tune the topological properties such as sterics, fluxionality, chirality, and the size of the bite angle. The areas which can be fine tuned are shown in Figure 2, with the wingtips (R_1) allowing the steric properties to be altered, the linker groups (R_2) enabling the orientation of the rings

in the planes, and the backbone of the NHC (R_3) allowing the electronic properties of the ring to be fine tuned.

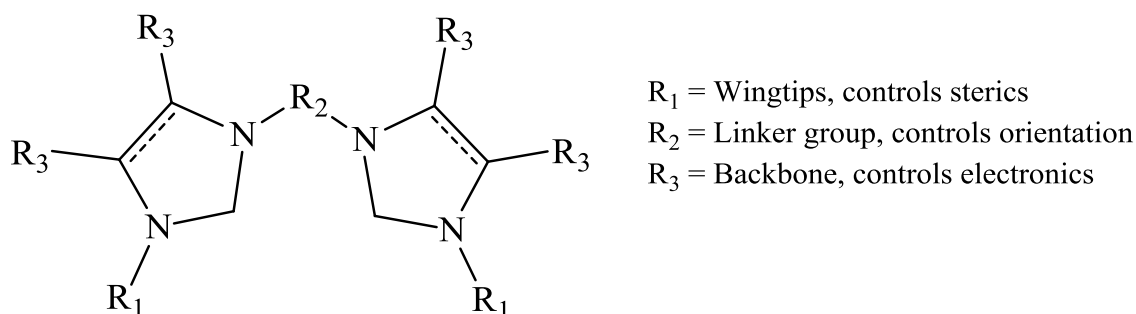
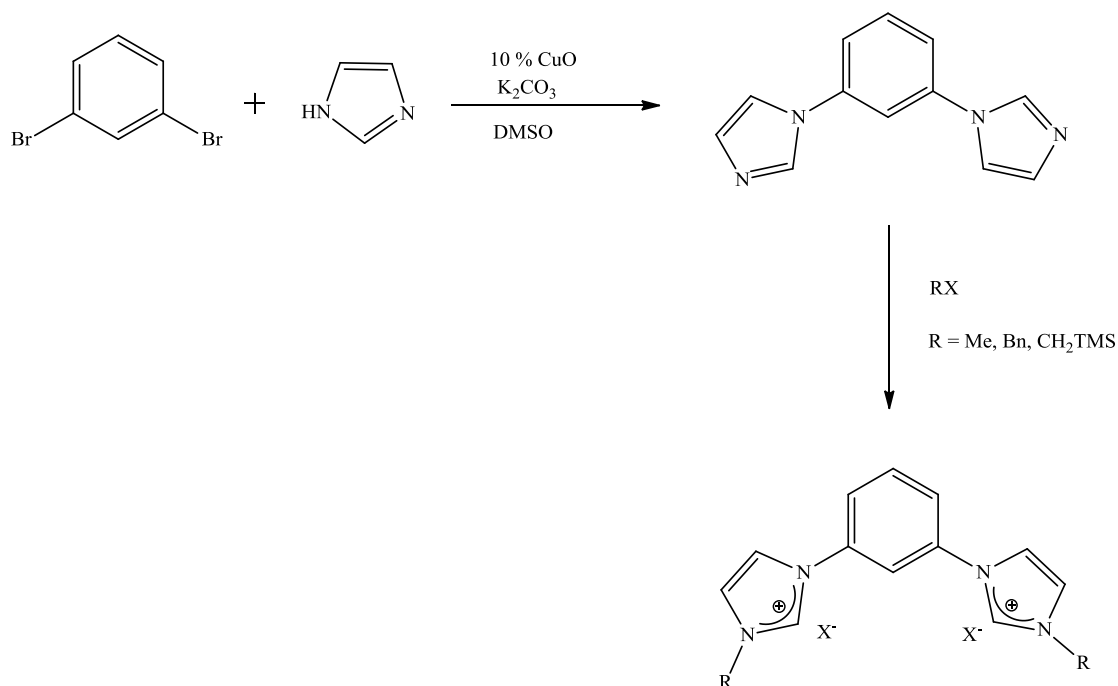


Figure 2: Fine tuning abilities of the bis-NHC precursors.¹³

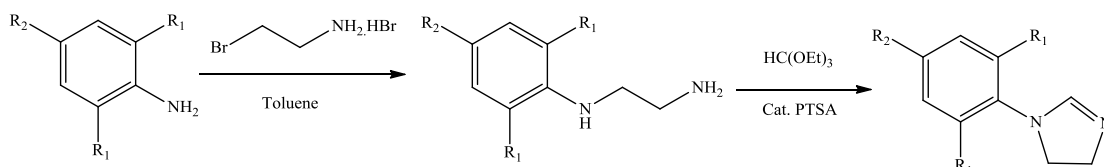
Another reason for the interest into bis-NHCs is the catalytic properties, due to the strong $M-C_{\text{carbene}}$ bond, and the added stability from the chelating effects in most cases enables the catalytic process to be harsher as there is less chance of catalyst degradation.

There have been many different routes in which bis-NHCs have been synthesised.¹⁴⁻¹⁸ There are two main routes to the synthesis of these compounds, the first is through a route using a premade NHC source such as imidazole and then reacting it with a linker to form the bis-N-heterocyclic carbenes in yields of 77 % as shown in Scheme 1.¹⁴

The second route is by synthesising a mono NHC precursor and then reacting it with a linking fragment to form the bis-NHC salt. The mono NHC fragment is synthesised by either starting with an aromatic amine and reacting it with a haloethyl amine followed by a ring closure using triethylorthoformate as shown in Scheme 2.¹⁹ This can then be simply converted to the bis-N-heterocyclic carbene as Bessel showed by reacting it with dibromopropane, this reaction occurs in a yield of 90-92 %.

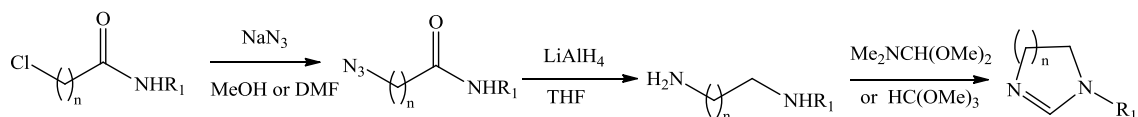


Scheme 1: Synthesis of 5-membered bis-NHC precursors by Vargas *et al.*¹⁴



Scheme 2: Synthesis of bis-NHC precursors by Bessel *et al.*¹⁹

An alternative route to synthesise the mono NHC is by reacting ω -chloroalkanoyl chlorides with sodium azide, followed by a reduction of the azide using lithium aluminium hydride and then a ring closure using trimethylorthoformate, as shown in Scheme 3, which yields the mono carbene in 65-99 %.²⁰



Scheme 3: Synthesis of bis-NHC precursors by Kotschy *et al.*²⁰

As discussed in Chapter 1, expanded ring N-heterocyclic carbenes are synthesised in a different way to that of 5-membered NHCs especially the unsymmetrical derivatives.²¹⁻²³ Due to these synthetic differences the routes to the NHCs in this chapter will be a combination of both the expanded ring routes and the 5-membered NHC routes.

The coordination of the chelating bis-5-membered NHCs to metals such as palladium and silver as discussed in Chapter 1, have been successful as shown by Gardiner *et al.*^{24,25} and Cavell *et al.*²⁶ as shown in Figure 3. Coordination of chelating bis-5-membered NHCs to other metals such as rhodium,^{13,17} nickel,²⁷ ruthenium,¹³ and platinum²⁸ have also shown great success in forming the desired complexes.

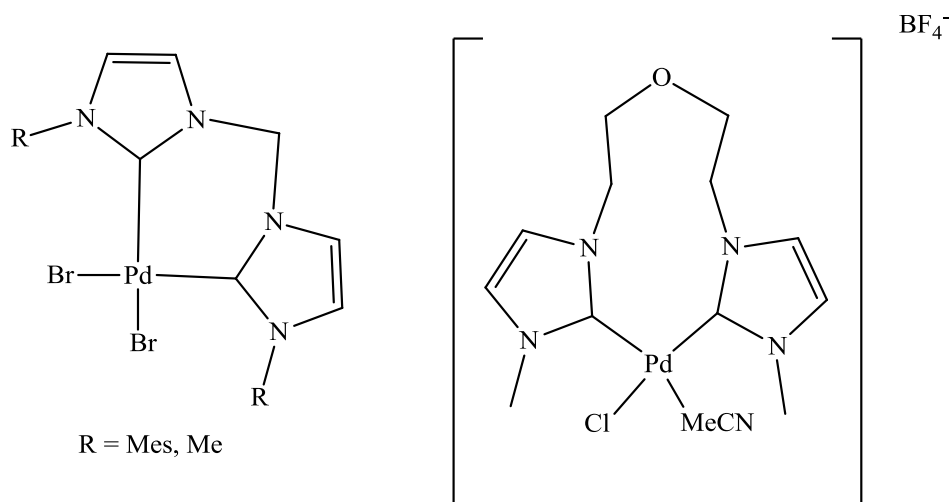
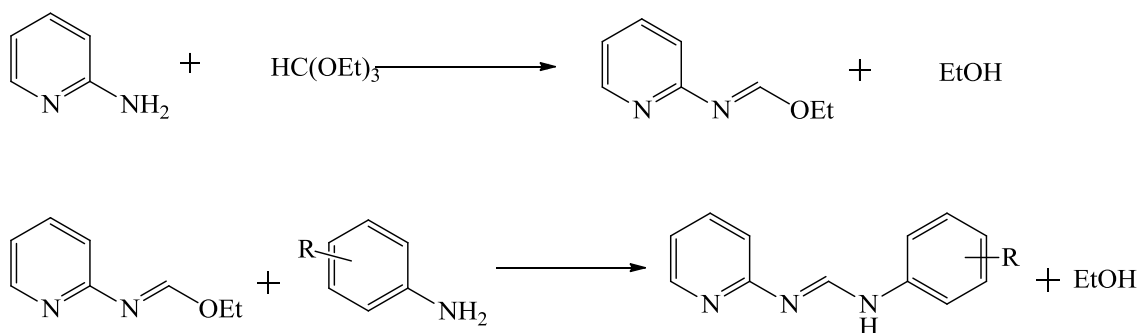


Figure 3: Examples of reported chelating bis-NHCs coordinating to palladium.^{25,26}

2.2: Results and Discussion

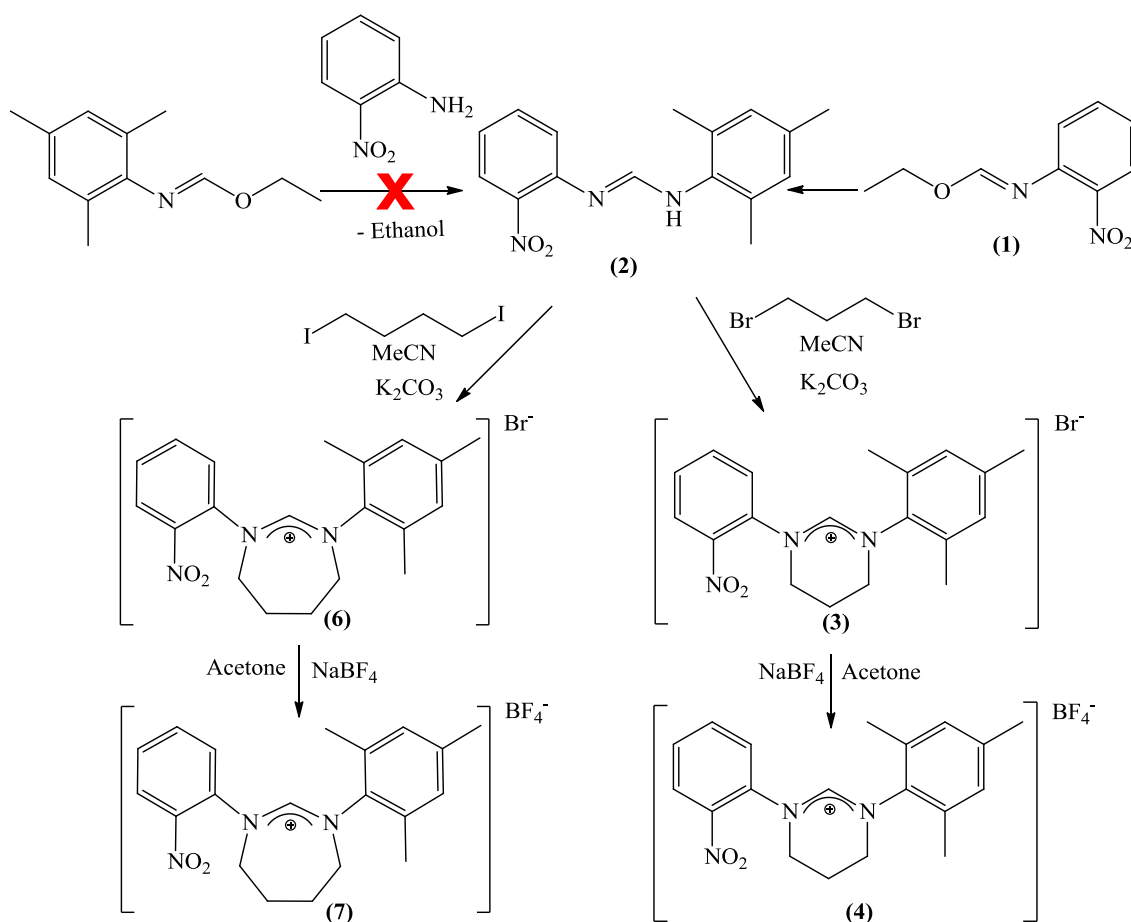
2.2.1: Initial Attempted Synthesis of Bis-NHCs

Over recent years many symmetrical and unsymmetrical imidazolium salts have been synthesised^{21,29} and used in homogenous catalysis, such as transfer hydrogenations,³⁰⁻³² Mizoroki-Heck couplings,³³ C-H activations,³⁴ and hydrosilylations.³⁵⁻³⁸ In more recent years there has been success with the synthesis of expanded ring carbenes,^{23,39} their coordination, and finally their catalytic properties.^{5,40} Such reactions as in hydrosilylation⁶ and C-C cross couplings have been investigated.⁴¹ There has been intensive work on the synthesis of 5-membered bis-N-heterocyclic carbenes,¹⁴⁻¹⁸ their complexes, and their uses in catalysis.^{13,24-28} NHCs show good yields and excellent catalytic outcomes with low catalyst loadings, *i.e.* 0.0002 mol % for Heck reactions, 0.002 mol % for Suzuki couplings both using bis-5-membered NHCs,²⁸ 0.005 mol % for hydrosilylations using mono 5-membered NHCs,³⁷ and even expanded ring systems have shown low loadings of 0.001 mol % for transfer hydrogenations.⁴² Using the knowledge we have of the expanded ring NHCs and the breakthroughs made with the catalytic studies of the 5-membered bis-NHCs the aim was to synthesise, coordinate, and gather catalytic knowledge of the expanded ring bis-NHCs.



Scheme 4: Synthetic route to unsymmetrical NHCs.²³

The initial synthesis of the bis-NHC was carried out using the approach employed by Cotton *et al.* as shown in Scheme 4.²³ During the second step of the synthesis problems occurred as shown in Scheme 5, this was presumably due to the nitroaniline not being sufficiently nucleophilic to generate the predicted formamidine. To overcome this problem the reaction was carried out again, employing nitroaniline and triethyl orthoformate, which were reacted to produce the desired alternative formamidine. This reaction was successful in the formation of compound **2** as shown in Scheme 5, as demonstrated by ¹H NMR with the amidine NCHN peak occurring at 7.80 ppm.



Scheme 5: Failed and successful route to expanded ring NHCs **7** and **4**.

Now the formamidine had been successfully synthesised and fully characterised the ring closure was completed using a similar method to that by Cavell *et al.* except this reaction was refluxed for 5 days, Scheme 5, as opposed to sixteen hours for the standard 6-membered NHCs.⁴⁰ After recrystallisation from DCM and diethyl ether, the proton NMR spectrum of **3** showed a large shift of 1.50 ppm in the proton adjacent to the nitro group, also the appearance of the N-heterocyclic carbene ring backbone at 3.80 ppm and 2.60 ppm. The mass spectrum also indicated that compound **3** had been synthesised due to the presence of the molecular ion at 324.1712 amu, which had a calculated value of 324.1712 amu. The counter-ion was then converted to tetrafluoroborate, as shown in the crystal structure in Figure 4 as the solubility is better and the subsequent reactions cleaner for the tetrafluoroborate salts. The important factor found from the crystal structure data, as shown in Table 1, was that the N(1)-C(1)-N(2) angle was comparable to that of the symmetrical 6-membered NHC (124.4(2) °).^{40,43}

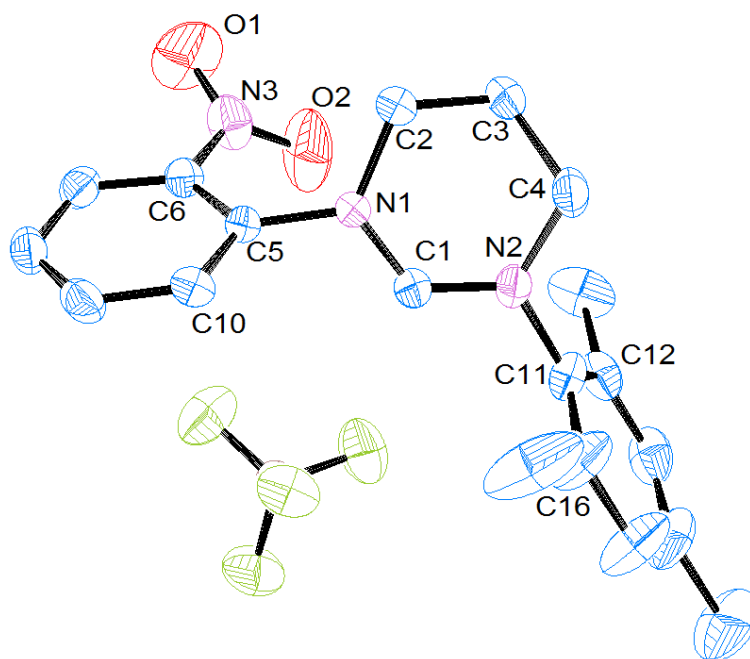


Figure 4: ORTEP ellipsoid plots at 50 % probability of the molecular structure of 1-(2-nitrophenyl)-3-(2,4,6-trimethylphenyl)-3,4,5,6-tetrahydropyrimidin-1-ium tetrafluoroborate (**4**).

Table 1: Selected bond lengths (Å) and angles (°) for 1-(2-nitrophenyl)-3-(2,4,6-trimethylphenyl)-3,4,5,6-tetrahydropyrimidin-1-ium tetrafluoroborate (**4**).

Lengths (Å)		Angles (°)	
C(1)-N(1)	1.314(3)	N(1)-C(1)-N(2)	124.4(2)
C(1)-N(2)	1.311(3)	C(1)-N(1)-C(2)	121.24(18)
C(2)-C(3)	1.514(3)	C(1)-N(1)-C(5)	119.00(18)
N(1)-C(2)	1.484(3)	C(1)-N(2)-C(11)	118.6(2)
C(3)-C(4)	1.516(3)	C(1)-N(2)-C(4)	120.72(19)
N(2)-C(4)	1.470(3)	C(5)-N(1)-C(2)	119.67(17)
N(1)-C(5)	1.431(3)	C(11)-N(2)-C(4)	120.66(18)
N(2)-C(11)	1.452(3)	N(2)-C(4)-C(3)	109.46(19)
C(5)-C(6)	1.396(3)	N(1)-C(2)-C(3)	109.71(19)
C(6)-N(3)	1.456(3)	C(2)-C(3)-C(4)	110.4(2)
N(3)-O(2)	1.218(3)	N(1)-C(5)-C(6)	122.7(2)
		C(5)-C(6)-N(3)	121.1(2)
		C(6)-N(3)-O(2)	118.0(2)

To form the second NHC moiety on **4**, the reduction of the nitro group was required. This reduction was carried out by hydrogenation over a palladium on carbon catalyst to produce the amino derivative **5**, as shown in Figure 5, as shown by mass spectrometry with the molecular ion appearing at 294.1983 amu, which had a calculated value of 294.1970 amu. To produce the second formamidine the reaction as shown in Scheme 5 was carried out using **5**.

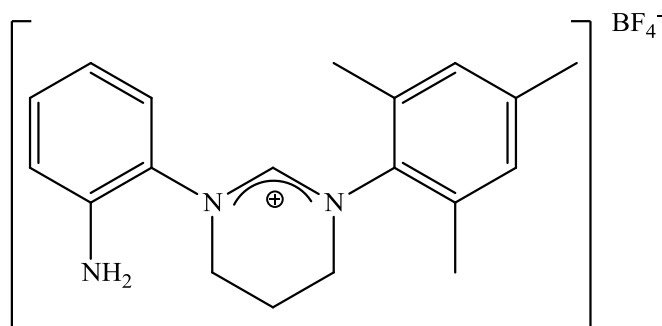


Figure 5: Structure of **5**.

The ideal synthesis to form the second carbene moiety was to react the amine with one equivalent of formamidate; this reaction was attempted several times, each time altering the conditions. The outcome of each of these reactions was an incomprehensible ^1H NMR spectrum. After several attempts to analyse the proton NMR spectrum the conclusion was that the newly reduced amine group was not reactive enough to displace the ethanol from the formamidate completely and therefore was giving multiple products.

The seven membered analogue of this compound was also synthesised by the route of Cavell *et al.* by ring closing N^7 -(2-nitrophenyl)- N -(2,4,6-trimethylphenyl)imidofornamide with 1,4-diiodobutane and potassium carbonate in acetonitrile as shown in Scheme 5.⁴⁰ This reaction, in a similar fashion to the 6-membered analogue, was refluxed for sixteen days yielding **6** in quantitative yield. The ^1H NMR spectrum of **6** shows the NCHN peak upfield of the formamidine at 7.55 ppm, this shift in peaks combined with the crystal structure of the tetrafluoroborate salt, shown in Figure 6 and Table 2 respectively; and the mass spectrometry data (molecular ion at 338.1875 amu, which has a calculated value of 338.1869 amu) indicates that the compound was successfully synthesised. The NCHN angle, Table 2, is 126.3(2) $^\circ$, which is comparable with literature values for NHC salts having an average NCHN bond angle of about 127.4 $^\circ$.^{8,40,44}

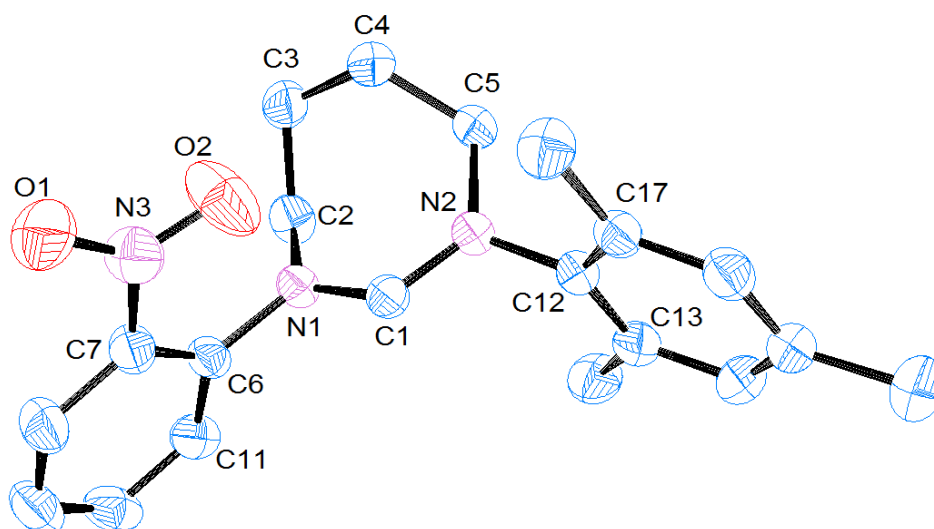


Figure 6: ORTEP ellipsoid plots at 50 % probability of the molecular structure of 1-(2-nitrophenyl)-3-(2,4,6-trimethylphenyl)-3,4,5,6,7-tetrahydropyrimidin-1-ium tetrafluoroborate (**7**), hydrogens and the counter-ion have been omitted for clarity.

Compound **6** was further reacted with sodium tetrafluoroborate to convert the counter-ion from bromide to tetrafluoroborate as the solubility is better and subsequent reactions cleaner. This was a relatively high yielding reaction with formation of **7** in a 69 % yield; the ^1H NMR spectrum shows a slight shift in the NCHN proton from 7.55 ppm in the bromide salt to 7.40 ppm in the tetrafluoroborate salt. Following counter-ion exchange to **7**, the reduction of the nitro group was carried out. This reaction was carried out in the same manner as the 6-membered analogue using a palladium on carbon catalyst in a solution of methanol under a hydrogen atmosphere. The outcome of this procedure however was not the same; the ^1H NMR spectrum showed that the reduction had failed and only starting material was recovered. This procedure was carried out again and left for a substantially longer time, the outcome was still the same, no reaction had occurred.

Table 2: Selected bond lengths (Å) and angles (°) for 1-(2-nitrophenyl)-3-(2,4,6-trimethylphenyl)-3,4,5,6,7-tetrahydropyrimidin-1-ium tetrafluoroborate (**7**).

Lengths (Å)		Angles (°)	
N(2)-C(1)	1.311(3)	N(2)-C(1)-N(1)	126.3(2)
N(1)-C(1)	1.319(3)	C(1)-N(1)-C(2)	122.58(19)
N(1)-C(2)	1.485(3)	N(1)-C(2)-C(3)	112.5(2)
C(2)-C(3)	1.516(4)	C(2)-C(3)-C(4)	112.7(2)
C(3)-C(4)	1.529(4)	C(4)-C(5)-N(2)	112.71(19)
C(4)-C(5)	1.520(3)	C(5)-N(2)-C(1)	126.12(18)
N(2)-C(5)	1.496(3)	C(5)-N(2)-C(12)	116.83(17)
N(2)-C(12)	1.455(3)	C(1)-N(2)-C(12)	117.05(18)
N(1)-C(6)	1.440(3)	C(1)-N(1)-C(6)	118.48(18)
C(6)-C(7)	1.387(3)	C(2)-N(1)-C(6)	118.36(17)
C(7)-N(3)	1.473(3)	C(11)-C(6)-C(7)	118.1(2)
N(3)-O(1)	1.218(3)	C(6)-C(7)-N(3)	122.7(2)
N(3)-O(2)	1.216(3)	C(7)-N(3)-O(1)	118.4(2)
		C(7)-N(3)-O(2)	118.9(2)
		O(1)-N(3)-O(2)	122.8(2)

Due to the insufficient reactivity and the lack of efficiency which occurred with the 6-membered amino NHC and the 7-membered nitro NHC respectively, this synthetic route to bis-N-heterocyclic carbenes was halted and modified to overcome these problems.

2.2.2: Attempted Synthesis of Mixed 5- and 6-Membered NHCs

As the initial route to the bis-NHC was not efficient, the aim was to have a pre-made amidinium salt and react it with a second moiety producing a bis-NHC. To achieve this, initially imidazole was reacted with bromoethylamine to produce 1-ethylamineimidazolium as shown in Figure 7. Analysis of the reaction was carried out and results showed that in addition to the desired product **A**, side reactions forming **B** and **C** occurred. The three products formed could be due to, the formation of the target imidazolium, **A** Figure 7, self cyclisations of the bromoethylamine, **B** Figure 7, and the 1:2 product where the bromoethylamine has reacted with both nitrogens on the imidazole, **C** Figure 7.

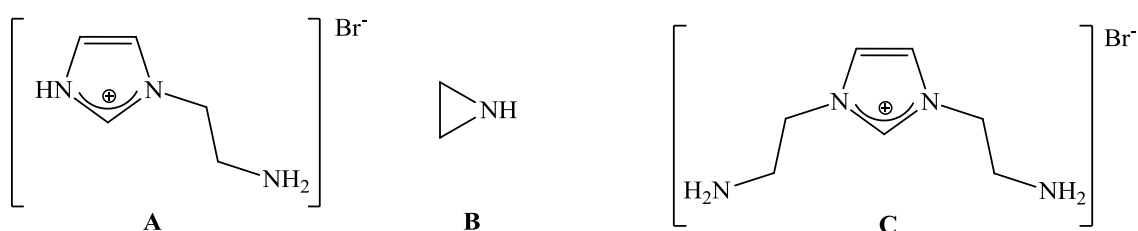


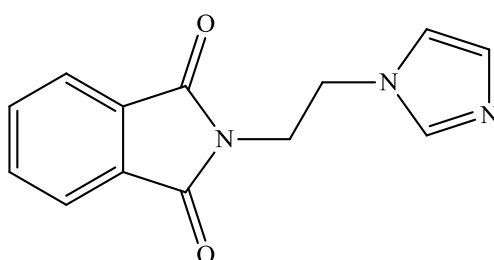
Figure 7: Possible products of the reaction of bromoethylamine and imidazole.

To hinder the production of the self cyclisation product, the bromoethylamine was substituted by N-(2-bromoethyl)phthalimide, which can easily be synthesised from potassium phthalimide and ethylene dibromide in acetone as shown by Drake *et al.*⁴⁵ Once the phthalimide protecting group had been synthesised (**8**) it was then reacted with imidazole and potassium bromide as first shown by Popkov *et al.*⁴⁶ this was successfully carried out in yield of 78 %, as shown in Figure 8. Although the synthesis of **9** was successful, the ¹H NMR spectrum showed two products.

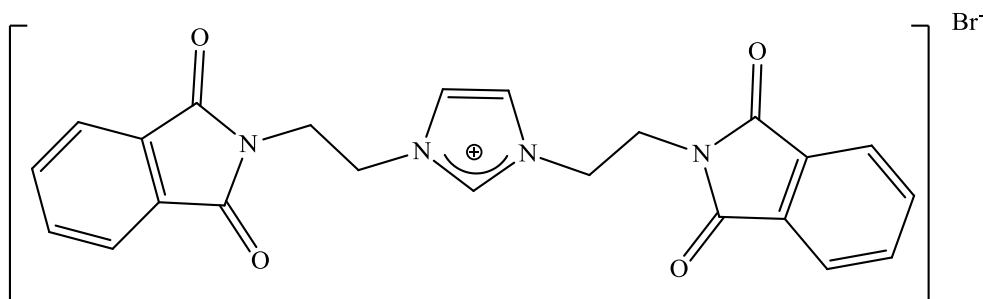
After several failed attempts at isolating the two products it was clear that the by-product was the bis-phthalimide product, where two phthalimides had reacted with one

imidazole forming **10** shown in Figure 8. The molecular ion found in the mass spectrum at 415.14 amu, which has a calculated value of 415.27 amu, confirms that the compound is **10**.

This by-product was then synthesised purposefully by altering the stoichiometry of the reaction to one equivalent of imidazole to four equivalents of N-(2-bromoethyl)phthalimide. By changing the stoichiometry to favour the formation of the bis-phthalimide, **10** was successfully synthesised in 54 % yield.



(9)



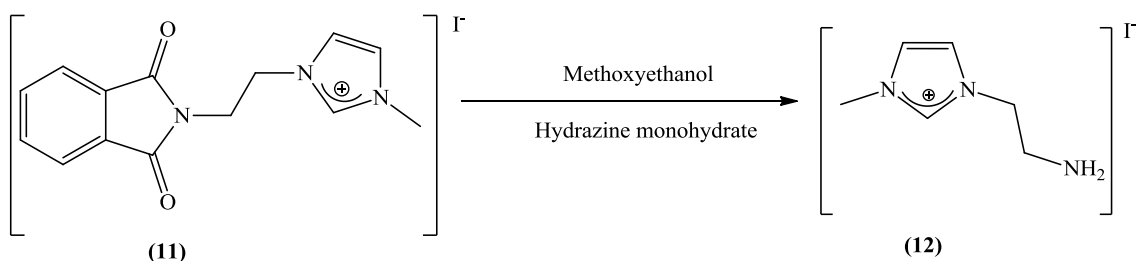
(10)

Figure 8: 9 and 10.

Following the formation of **9**, in 77 % yield, the unreacted nitrogen on the imidazole moiety was then reacted with methyl iodide, forming the methyl adduct, **11**, in an excellent yield of 91 %. The ^1H NMR spectrum of **11** shows a peak at 3.75 ppm, which

is not present in the ^1H NMR spectrum of **9**, indicating the presence of the methyl groups and that the reaction was successful. Due to the commercial availability of methyl imidazole, the process of synthesising the methylated species from methyl iodide and the imidazole compound was unnecessary and therefore this reaction pathway could be cut short by one step. Methyl imidazole was then reacted with N-(2-bromoethyl)phthalimide resulting in **11** in a yield of 60 %. The yield of the reaction was not as high as the previous route but the speed at which the product was synthesised was much more efficient. These compounds have previously been synthesised through an alternative route by Harjani *et al.*⁴⁷

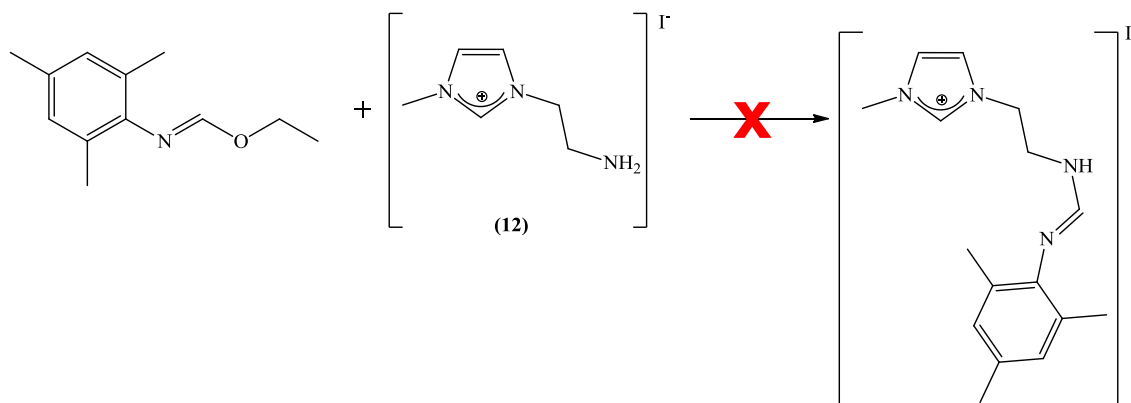
Since the methyl adduct of the protected mono carbene had been successfully synthesised the aim was then to deprotect the phthalimide group resulting in the production of a reactive amine, which can then be used to create the second NHC moiety. The methylated mono NHC, **11**, was dissolved in methoxyethanol and reacted at reflux with hydrazine monohydrate over a five hour period as shown in Scheme 6. The resulting yellow oil, **12**, was found to be pure by ^1H NMR spectrum.



Scheme 6: Synthesis of compound **12**.

The amine had now been de-protected enabling the second NHC moiety to be synthesised. The pathway which was attempted was analogous to the route that failed due to lack of reactivity from the amine in the six and seven membered ring mentioned in section 2.2.1. This pathway was to react the mesityl formamidate with **12**, as shown in Scheme 7, to synthesis the unsymmetrical formamidines.²³ This route was unsuccessful, the ^1H NMR spectrum showed a large mixture of products, causing the spectrum to be very complex and incomprehensible. The reaction was attempted for a

second time with a slight vacuum attached to the reaction vessel to remove any ethanol which would be produced in the process. This was left for several hours at which stage, the ^1H NMR spectrum, as previously noted showed multiple products. The mass spectrum analysis was collected and this was also inconclusive as several peaks were observed and none of them were the expected molecular ion.



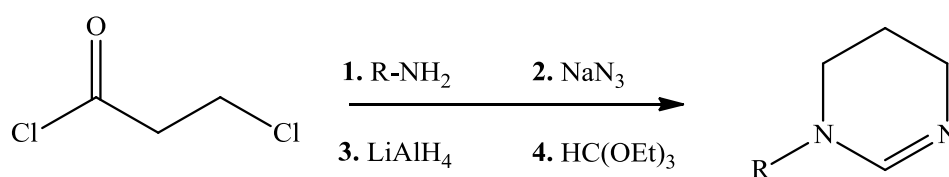
Scheme 7: Unsuccessful synthesis of mixed 5- and 6-membered NHC salts.

Due to the complexity of the ^1H NMR spectrum and mass spectrum of the reaction between **12** and the mesityl formamdate this route to mixed 5- and 6-bis-NHCs was not further pursued.

Since it has been found that none of the bis-6-membered NHC, bis-7-membered NHC, or the mixed 5- and 6-bis-NHCs have been successful, a new pathway to bis-NHCs was required.

2.2.3: Successful Synthesis and Characterisation of Bis-NHC Precursors

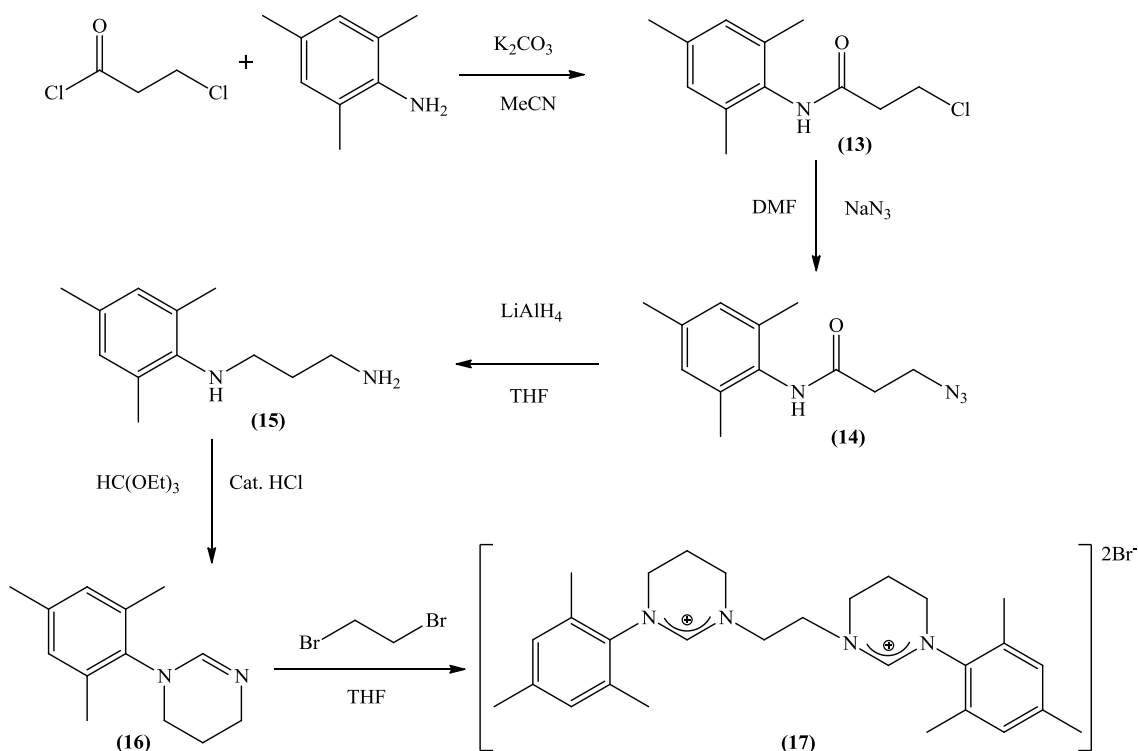
Due to the unsuccessful previous attempts at synthesising a novel bis-NHC ligand a new route was proposed. The aim was to start with a chloroalkanoyl chloride and a series of nitrogen donors followed by a ring closure to give the tetrahydropyrimidine as shown in Scheme 8, this route is analogous to that used by Kotschy *et al.*²⁰



Scheme 8: Proposed route to tetrahydropyrimidine salts.²⁰

The first step of this synthesis was to react 3-chloropropionylchloride with mesitylaniline to yield the N-(3'-chloropropionyl)mesitylamine, **13**, in 71 %. This was then reacted with sodium azide to gain the second nitrogen moiety, **14**; the carbonyl was then reduced using lithium aluminium hydride to give the diamine, **15**. The diamine was then ring closed using triethyl orthoformate to yield the target tetrahydropyrimidine, **16**, analogously to that by Kotschy *et al.*²⁰ as shown in Scheme 9. This tetrahydropyrimidine had a very similar structure to imidazole, therefore it was thought that the reactivity would be similar. This idea was tested by reacting two equivalents of the tetrahydropyrimidine with one equivalent of dihaloalkane to produce the alkane linked bis-NHC. This reaction was carried out in a pressure tube at 90 °C using 1,2-dibromoethane. The reaction was successful and yielded 1,1'-di-(2,4,6-trimethylphenyl)-3,3'-ethylene-di-(3,4,5,6-tetrahydropyrimidin-1-ium bisbromide, **17**, in 39 % yield as shown in Scheme 9. The reaction was very clean providing a simple ¹H NMR spectrum, showing that the NCHN peak had shifted significantly downfield from 7.10 ppm in the tetrahydropyrimidine to 9.35 ppm in the bis-NHC. The other

notable shift was of the NHC backbone, this was a shift of 0.65 ppm from 3.40 ppm to 4.05 ppm for the NCH₂ protons and a shift of 0.25 ppm for the NCH₂CH₂ protons.



Scheme 9: Synthetic route to bis-6-NHC salts.²⁰

Although this synthesis was successful the synthetic pathway was not ideal, due to the number of synthetic steps required, and the nature of the reagents used. These factors were limiting the scale on which the reactions could be carried out and the overall yield of the final product. Therefore the synthetic route was altered so there were fewer synthetic steps and the reagents used were not prohibiting in any way. The new synthetic route involved reacting mesitylaniline with 3-bromopropylamine in toluene for five days yielding **15**. The success in the production of the diamine, **15**, enabled the ring closure using triethylorthoformate to produce the tetrahydropyrimidinium salt of **16**, compound **18**. The ¹H NMR and mass spectra were obtained and the NCHN peak appears at 7.85 ppm in the ¹H NMR spectrum and the molecular ion is apparent at

203.1541, which has a calculated value of 203.1548 amu. Single crystals suitable for X-ray diffraction were grown by vapour diffusion of diethyl ether into a solution of **18** in acetonitrile, the structure and data are shown in Figure 9 and Table 3 respectively.

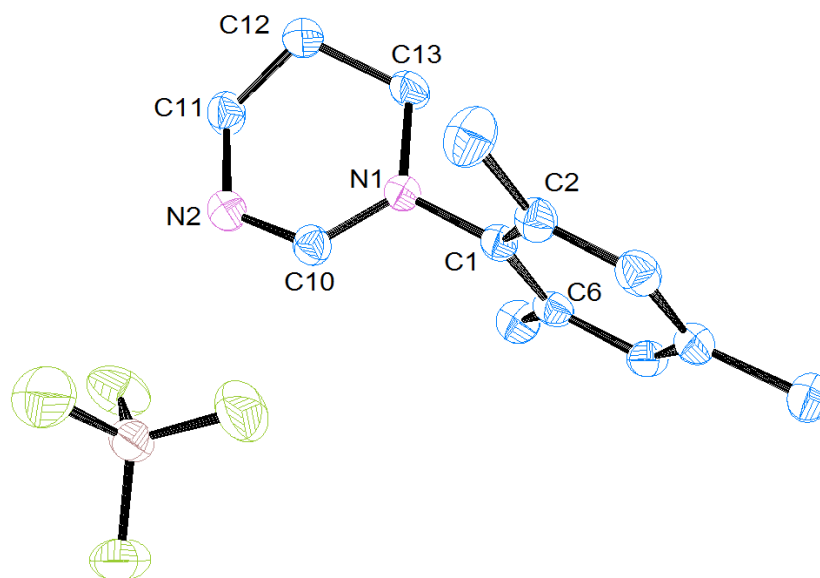


Figure 9: ORTEP ellipsoid plots at 50 % probability of the molecular structure of 1-(2,4,6-trimethylphenyl)-3,4,5,6-tetrahydropyrimidin-1-ium tetrafluoroborate (**18**).

As is evident from the X-ray diffraction data the N(1)-C(10)-N(2) angle is 123.8(2) °, this value for a 6-membered NHC salt is in accordance with the other data that has been reported in recent years.^{8,40,48}

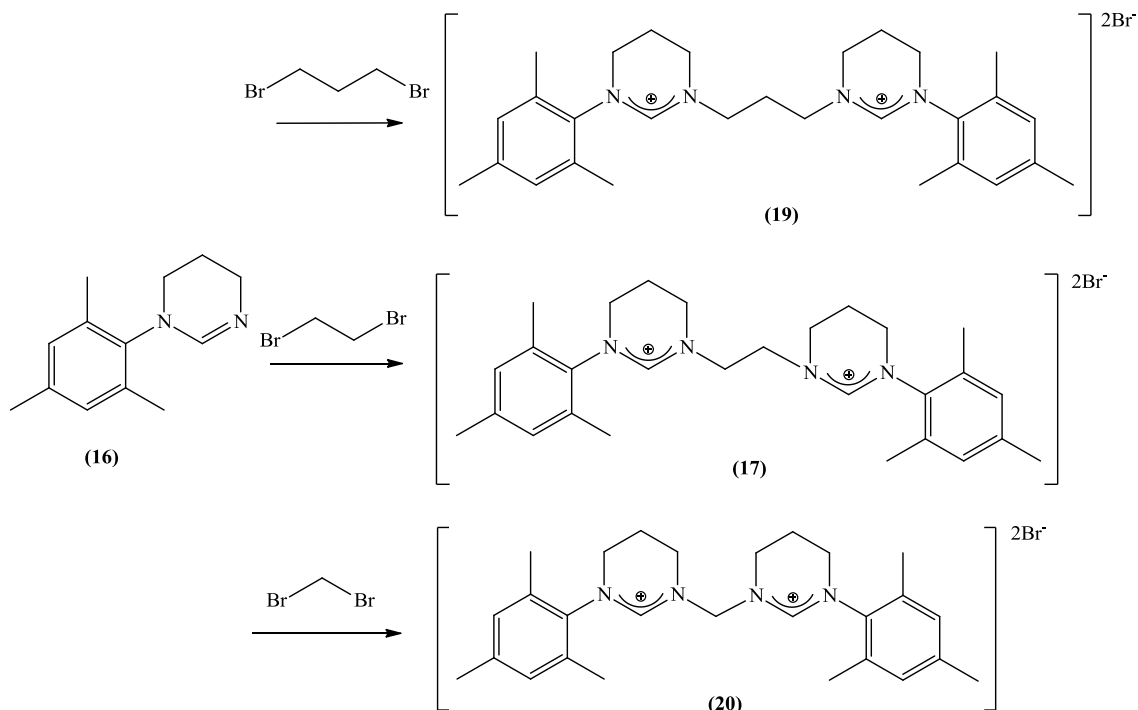
The tetrahydropyrimidinium salt, **18**, was now accessible in fewer steps than before. The bis-6-NHC was previously synthesised by reacting the tetrahydropyrimidine (see Scheme 9) with a dihaloalkane. To get to the tetrahydropyrimidine, **18** needs to be deprotonated. This deprotonation was carried out under an inert atmosphere, to prohibit any re-protonation, using potassium tertiary butoxide in THF. This reaction was very quick and efficient in producing the required tetrahydropyrimidine (**16**) in a yield of 83 %. The ¹H NMR spectrum analysis was not that dissimilar from that of **18**, but this was to be expected, the observed difference was with the NCHN proton, this had shifted

upfield from 7.85 ppm in **18** to 7.10 ppm in **16**, resulting in a total shift of 0.75 ppm, which confirmed the formation of the compound. Since the tetrahydropyrimidine had now been effectively synthesised the production of the bis-N-heterocyclic carbenes could be completed, in the manner previously mentioned in Scheme 9.

Table 3: Selected bond lengths (Å) and angles (°) for 1-(2,4,6-trimethylphenyl)-3,4,5,6-tetrahydropyrimidin-1-ium tetrafluoroborate (**18**).

Lengths (Å)		Angles (°)	
C(6)-C(1)	1.397(3)	C(6)-C(1)-C(2)	122.8(2)
C(1)-C(2)	1.401(3)	C(6)-C(1)-N(1)	118.6(2)
C(1)-N(1)	1.447(3)	C(2)-C(1)-N(1)	118.6(2)
N(1)-C(10)	1.314(3)	C(1)-N(1)-C(10)	119.3(2)
N(1)-C(13)	1.478(3)	C(1)-N(1)-C(13)	119.38(19)
C(10)-N(2)	1.311(3)	N(1)-C(10)-N(2)	123.8(2)
N(2)-C(11)	1.462(3)	N(1)-C(13)-C(12)	109.2(2)
C(11)-C(12)	1.513(4)	C(10)-N(2)-C(11)	121.6(2)
C(12)-C(13)	1.524(4)	N(2)-C(11)-C(12)	108.9(2)
		C(11)-C(12)-C(13)	109.8(2)

The assembly of the bis-6-NHC precursor salts were carried out resulting in the production of four potential novel ligands. Three of these were synthesised as shown in Scheme 10, which is the same as the route planned in Scheme 9, where the tetrahydropyrimidine (compound **16**) was reacted with dibromopropane, dibromoethane, and dibromomethane to yield compounds **19**, **17**, and **20** respectively.



Scheme 10: Production of novel bis-6-NHC salts.

The yields of the reactions in Scheme 10 were low, being on average 15 %. Despite the yields being poor, the overall time the reactions took to complete and the ease of the reactions are more satisfactory than that of the previously mentioned route using sodium azide and lithium aluminium hydride (Scheme 9). The ^1H NMR and $^{13}\text{C}\{^1\text{H}\}$ NMR spectra of these compounds were obtained, and due to the shift in the proton NMR spectra from 7.10 ppm in **16** to 8.70 ppm, 9.35 ppm, and 9.25 ppm in **19**, **17**, and **20**, respectively, it was confirmed that the compounds had been successfully synthesised. The carbon-13 NMR spectra show peaks at 154 ppm, 155 ppm, and 155 ppm for **19**, **17**, and **20** respectively, assigned to the NCHN peak, which is in accordance with the recent literature for 6-membered NHCs.^{39,48} Single crystals of **17** and **20** were grown by vapour diffusion of diethyl ether into a solution of the compounds in CH_2Cl_2 , as shown in Figure 10 and 11 for compounds **17** and **20** respectively, enabling the NCN angles to be calculated. The angles are shown in Table 4 for compound **17** and Table 5 for **20**, and are $124.7(12)^\circ$ and $123.2(12)^\circ$ for **17** and $124.6(7)^\circ$ and $123.9(8)^\circ$ for **20**.

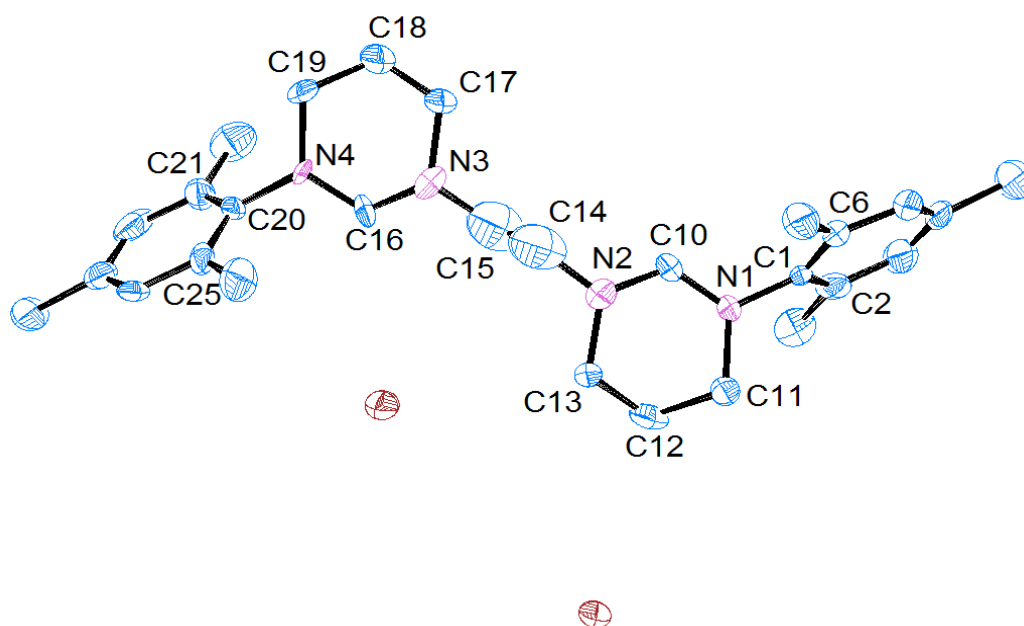


Figure 10: ORTEP ellipsoid plots at 50 % probability of the molecular structure of 1,1'-di-(2,4,6-trimethylphenyl)-3,3'-ethylene-di-(3,4,5,6-tetrahydropyrimidin-1-ium bisbromide (**17**).

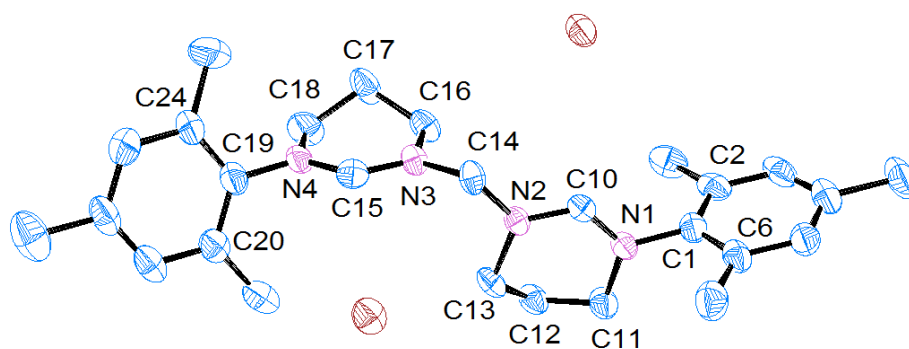


Figure 11: ORTEP ellipsoid plots at 50 % probability of the molecular structure of 1,1'-di-(2,4,6-trimethylphenyl)-3,3'-methylene-di-(3,4,5,6-tetrahydropyrimidin-1-ium bisbromide (**20**).

Table 4: Selected bond lengths (Å) and angles (°) for 1,1'-di-(2,4,6-trimethylphenyl)-3,3'-ethylene-di-(3,4,5,6-tetrahydropyrimidin-1-ium bisbromide (**17**)).

Lengths (Å)		Angles (°)	
N(1)-C(10)	1.308(15)	N(1)-C(10)-N(2)	124.7(12)
N(1)-C(11)	1.493(14)	N(3)-C(16)-N(4)	123.2(12)
N(1)-C(1)	1.445(14)	C(10)-N(1)-C(1)	121.5(9)
C(1)-C(2)	1.390(16)	C(10)-N(1)-C(11)	119.3(10)
C(1)-C(6)	1.380(16)	N(1)-C(11)-C(12)	107.9(10)
C(11)-C(12)	1.513(16)	C(11)-C(12)-C(13)	109.9(10)
C(12)-C(13)	1.507(16)	N(2)-C(13)-C(12)	110.6(10)
N(2)-C(13)	1.456(15)	C(10)-N(2)-C(13)	120.9(11)
N(2)-C(10)	1.333(16)	C(10)-N(2)-C(14)	124.1(12)
N(2)-C(14)	1.492(9)	C(14)-N(2)-C(13)	113.6(11)
C(14)-C(15)	1.440(10)	N(2)-C(14)-C(15)	107.7(12)
N(3)-C(15)	1.495(10)	C(14)-C(15)-N(3)	105.9(12)
N(3)-C(16)	1.296(16)	C(15)-N(3)-C(17)	118.5(12)
N(3)-C(17)	1.498(16)	C(15)-N(3)-C(16)	118.2(12)
N(4)-C(16)	1.320(15)	N(3)-C(17)-C(18)	109.2(12)
N(4)-C(19)	1.474(14)	N(3)-C(16)-N(4)	123.2(12)
N(4)-C(20)	1.435(15)	C(17)-C(18)-C(19)	111.0(14)
C(17)-C(18)	1.46(2)	C(18)-C(19)-N(4)	109.0(10)
C(18)-C(19)	1.512(18)	C(19)-N(4)-C(16)	120.7(10)
C(20)-C(25)	1.383(17)	C(19)-N(4)-C(20)	119.8(9)
C(20)-C(21)	1.423(18)	C(16)-N(4)-C(20)	119.4(10)

Table 5: Selected bond lengths (Å) and angles (°) for 1,1'-di-(2,4,6-trimethylphenyl)-3,3'-methylene-di-(3,4,5,6-tetrahydropyrimidin-1-ium bisbromide (**20**).

Lengths (Å)		Angles (°)	
C(1)-N(1)	1.444(10)	C(2)-C(1)-C(6)	123.8(8)
N(1)-C(10)	1.300(10)	C(2)-C(1)-N(1)	119.3(8)
N(1)-C(11)	1.458(10)	C(6)-C(1)-N(1)	116.9(8)
C(1)-C(2)	1.385(12)	C(1)-N(1)-C(10)	119.3(6)
C(1)-C(6)	1.419(12)	C(1)-N(1)-C(11)	121.8(7)
C(10)-N(2)	1.319(10)	N(1)-C(10)-N(2)	124.6(7)
N(2)-C(13)	1.462(10)	N(1)-C(11)-C(12)	110.8(7)
N(2)-C(14)	1.464(10)	C(11)-C(12)-C(13)	110.7(7)
C(11)-C(12)	1.491(12)	C(12)-C(13)-N(2)	108.6(6)
C(12)-C(13)	1.526(12)	C(10)-N(2)-C(14)	120.0(6)
C(14)-N(3)	1.452(10)	C(13)-N(2)-C(14)	119.6(6)
N(3)-C(15)	1.331(10)	N(2)-C(14)-N(3)	110.4(6)
N(3)-C(16)	1.457(10)	C(14)-N(3)-C(15)	119.2(7)
C(15)-N(4)	1.297(10)	C(14)-N(3)-C(16)	118.9(6)
N(4)-C(18)	1.470(11)	N(3)-C(16)-C(17)	109.1(7)
N(4)-C(19)	1.444(11)	N(3)-C(15)-N(4)	123.9(8)
C(16)-C(17)	1.520(12)	C(16)-C(17)-C(18)	109.5(7)
C(17)-C(18)	1.521(12)	C(17)-C(18)-N(4)	108.6(7)
C(19)-C(20)	1.390(12)	C(15)-N(3)-C(16)	121.9(7)
C(19)-C(24)	1.399(14)	C(15)-N(4)-C(18)	120.6(7)
		C(15)-N(4)-C(19)	118.4(7)
		C(18)-N(4)-C(19)	120.9(7)
		N(4)-C(19)-C(20)	120.0(8)
		N(4)-C(19)-C(24)	118.7(8)
		C(20)-C(19)-C(24)	121.3(9)

The fourth novel bis-NHC salt that was synthesised was the aromatic derivative, **21** shown in Figure 12, from the reaction of **16**, with *m*-xylene dichloride in DMF. The proton NMR spectrum showed the NCHN peak at 9.45 ppm, which is very similar to that of **19**, **17**, and **20**. The mass spectrum analysis was also collected and this shows an ion peak at 543.3277 amu, which has a calculated value of 543.3255 amu, this is due to $[M^+ + Cl^-]$, concluding that the compound shown in Figure 12 was synthesised.

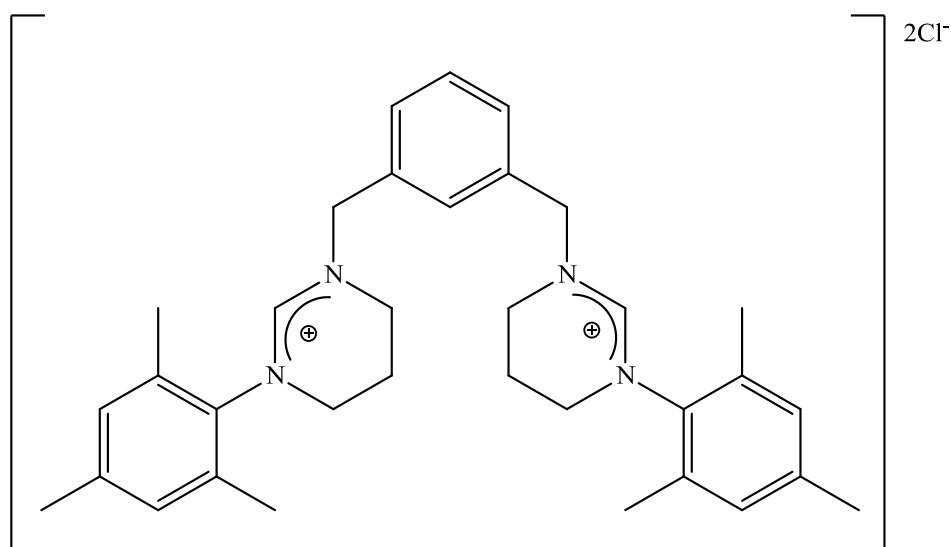
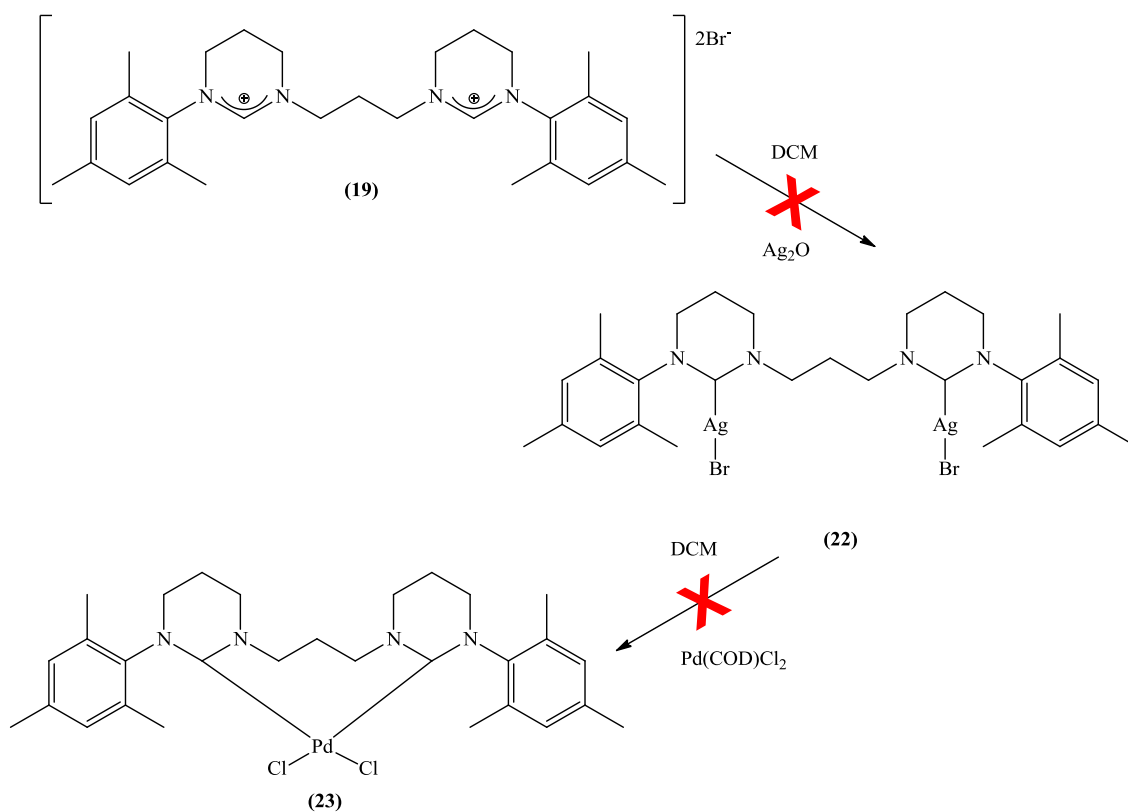


Figure 12: Structure of **21**.

2.2.4: Attempted Coordination of the Bis-NHCs

Due to the success of the coordination of the 5-membered bis-NHCs to palladium by the groups of Herrmann,⁴⁹ Alcade,¹⁸ and Baker²⁸ it seemed reasonable to try to coordinate our bis-NHC compounds in a similar manner. This was initially via production of the silver(I) complex, **22**, by reacting the bis-NHC with one equivalent of silver(I) oxide in DCM, as shown in Scheme 11, and then producing the palladium complex, **23**, from the transmetallation of the silver complex with palladium.



Scheme 11: Initial synthesis to bis-NHC palladium complexes.

This route was attempted and proved to be unsuccessful, due to the opening of the ring, with formation of **24**, as shown in Figure 13. This was evident in the proton NMR spectrum where the aldehyde hydrogen peaks appeared at 8.30 ppm and 7.90 ppm, which was too far upfield for the NCHN proton of the salt precursor which appears at 8.70 ppm. There appeared to be two aldehyde hydrogen peaks in the proton NMR, this was due to the way in which both rings had opened. The first ring would have the carbonyl on the nitrogen closest to the aromatic group and the other ring would have opened with the carbonyl being present on the nitrogen closest to the alkyl linker, in turn making this compound unsymmetrical, hence the aldehyde hydrogen peaks are inequivalent as shown in Figure 13. The mass spectrum was obtained and this supported the proposal that the rings had indeed opened by showing a molecular ion peak at 481.35 amu, which had a calculated value of 481.33 amu. Due to the ring opening of the carbene forming **24**, transmetalation could not be carried out.⁵⁰⁻⁵⁴

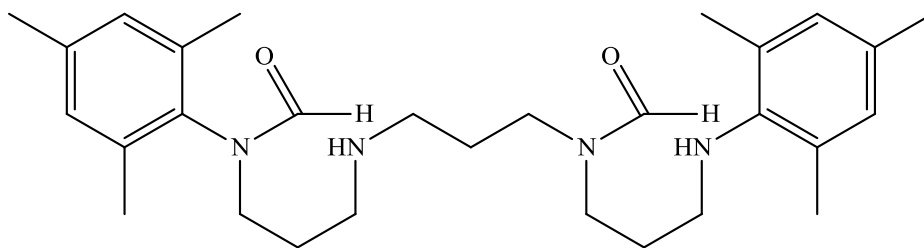
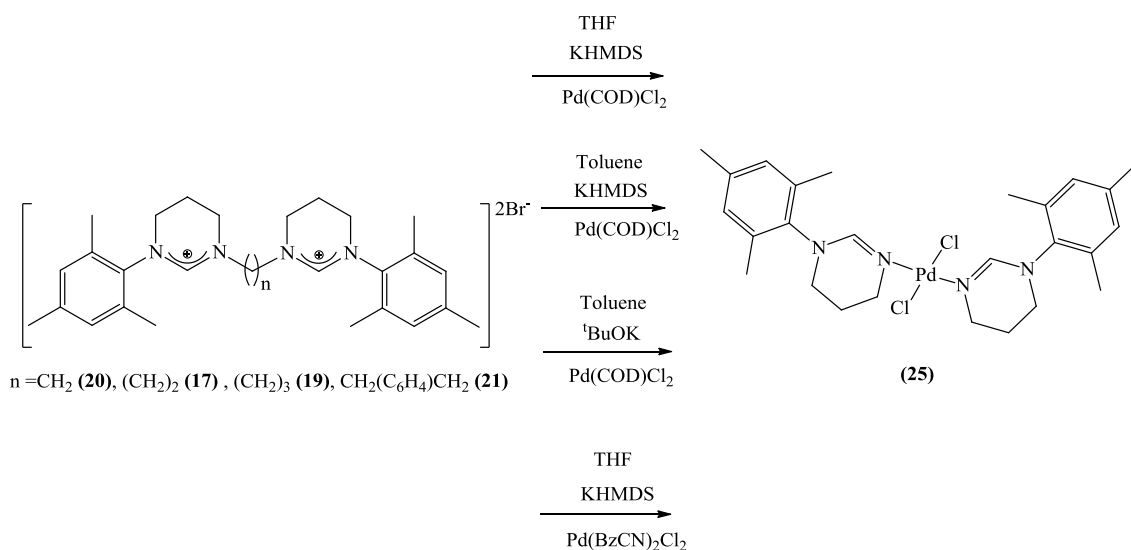


Figure 13: Ring opened bis-NHC salt (**24**).⁵⁰⁻⁵⁴

A new route was needed as the water, which was produced as a result of the silver oxide reaction with the salt, was causing the salt to hydrolyse and in turn forming the ring opened product, **24**. The new route proposed was to perform the reaction in the absence of air and moisture, as the carbene is sensitive to water, and by carrying out the procedure under an inert atmosphere it would reduce the possibility that the ring opening would occur. The pathway which was attempted was the free carbene route as proposed by Cavell *et al.*⁴⁰ This involves the reaction of the salt with potassium bistrimethylsilylamide to deprotonate the salt and produce the free carbene, which can then be reacted with the palladium to form the target complex. This reaction was carried out under an inert atmosphere, however after several attempts, with alterations to the solvent (THF and toluene), the palladium precursor [Pd(1,5-COD)Cl₂] and [Pd(PhCN)₂Cl₂], the base (potassium tertiary butoxide and potassium bistrimethylsilylamide) and the bis-salt which was reacted as shown in Scheme 12, the outcome remained the same. The anticipated complexation had not occurred, the proton NMR spectrum was extremely complex, showing multiple, but very similar products.



Scheme 12: Attempted coordination of bis-NHCs to palladium.

The crystal structure of **25** showed why the reactions had been unsuccessful. During the reaction the base was not simply deprotonating the expected site but causing cleavage of the alkyl linker groups as shown in the crystal structure of **25**, Figure 14. This has also been reported by Mao *et al.*^{55,56} Once the structure of the compound had been determined the proton NMR spectrum was analysed and confirmed that there has been loss of the alkyl linker groups. This palladium species (**25**) appears to be the major product in the proton NMR spectrum. The mass spectrum is consistent with the data, with the ion peak at 587.19 amu, which has a calculated value of 587.20 amu, being representative of $[\text{M}^+ - \text{Cl}^- + \text{MeCN}]$; *i.e.* a complex in which the palladium is coordinating directly to the pyrimidine nitrogens. As the NHC precursor was altered, using varying linkers, there did not appear to be much variation in product formation in the proton NMR spectra, with **25** being the major product in all cases, with a yield of 53 %.

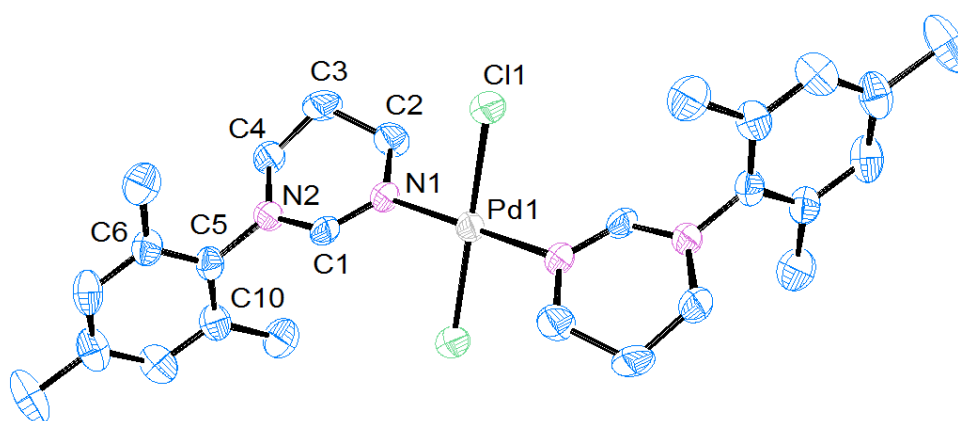


Figure 14: ORTEP ellipsoid plots at 50 % probability of the molecular structure of bis-[1-(2,4,6-trimethylphenyl)-3,4,5,6-tetrahydropyrimidine] dichloropalladium (**25**).

Due to the potassium bistrimethylsilylamide deprotonating at the alkyl linker rather than at the carbene as expected, a different synthetic route was attempted. This was to use palladium acetate instead of potassium bistrimethylsilylamide and palladium cyclooctadiene dichloride. In an effort to promote deprotonation at the NCHN carbon rather than inducing decomposition, $[\text{Pd}(\text{OAc})_2]$ was employed as both metal source and base. However, after heating the palladium acetate and compound **20** in DMSO for a few hours it was clear that the formation of **25** (Figure 14) was still occurring. It appears the same reactivity is occurring as in reactions with strong base, this is clear even though only a proton NMR was collected, as the spectrum was in complete accordance with that of **25**. The same reaction was carried out using **21**, the route employed was analogous to that of **20**, however the outcome was inconclusive as the proton NMR spectrum was extremely complex. It is believed that the same process may be occurring as reported by Mao *et al.* *i.e.* deprotonation at the aromatic NCH_2 linker groups has occurred as previously reported with this type of system.⁵⁵ Reactions with other metals were also attempted using the free carbene route. The metals attempted were iridium and silver; however the outcomes were very similar in that they produced extremely complex proton NMR spectra. This phenomenon is unique to expanded ring carbenes as 5-membered derivatives have successfully been coordinated

to palladium as shown by Cavell²⁶ and Gardiner,²⁴ to silver as shown by Cavell,²⁶ and to rhodium and platinum as shown by Baker.²⁸

Table 6: Selected bond lengths (Å) and angles (°) for bis-[1-(2,4,6-trimethylphenyl)-3,4,5,6-tetrahydropyrimidine] dichloropalladium (**25**).

Lengths (Å)		Angles (°)	
C(6)-C(5)	1.396(9)	C(6)-C(5)-N(2)	118.6(6)
C(5)-C(10)	1.388(10)	C(10)-C(5)-N(2)	119.9(6)
C(5)-N(2)	1.444(8)	C(6)-C(5)-C(10)	121.5(6)
N(2)-C(1)	1.330(8)	C(5)-N(2)-C(1)	120.3(6)
N(2)-C(4)	1.477(9)	C(5)-N(2)-C(4)	117.7(5)
C(1)-N(1)	1.299(8)	N(2)-C(1)-N(1)	125.7(7)
C(4)-C(3)	1.507(10)	N(2)-C(4)-C(3)	108.1(6)
C(3)-C(2)	1.507(11)	C(1)-N(2)-C(4)	121.5(5)
C(2)-N(1)	1.473(9)	C(1)-N(1)-C(2)	118.5(6)
N(1)-Pd(1)	2.017(6)	C(1)-N(1)-Pd(1)	120.8(5)
Pd(1)-Cl(1)	2.3078(18)	C(2)-N(1)-Pd(1)	120.7(4)
		C(4)-C(3)-C(2)	111.2(7)
		C(3)-C(2)-N(1)	110.1(6)
		N(1)-Pd(1)-Cl(1)	91.34(17)

Since the deprotonation was occurring at the nitrogens rather than the carbenes, these reaction routes were not pursued further. Numerous attempts at complex synthesis proved unsuccessful and due to time constraints this aspect of this research was not further pursued.

2.3: Conclusions

The overall aim of this section was to synthesise a series of bis-NHC salts, coordinate them to metals and then carry out the relevant catalysis using these complexes. The successful synthesis of bis-NHCs was achieved after several routes were attempted. This included the use of nitro groups as a way to introduce the second carbene moiety and the use of imidazole as an initial building block and a successful route which used tetrahydropyrimidine in a similar way to that employed with imidazole to form the bis-NHCs. The synthesis of the tetrahydropyrimidine was achieved by two different routes, however the first route attempted was less efficient and was limited in scale. Therefore, the second route, which started initially by reacting 2,4,6-trimethylaniline and 3-bromopropylamine hydrobromide gave the best results. This enabled the production of three novel bis-NHCs from the reaction of the tetrahydropyrimidine with the appropriate dihaloalkane to produce compounds **17**, **19**, and **20**. A fourth bis-NHC precursor was synthesised by a slightly different route; instead of reacting the tetrahydropyrimidine with the dihaloalkane it was reacted with *m*-xylene dichloride to produce the novel bis-NHC precursor with an aromatic linker compound **21**.

Coordination of these compounds was attempted, however none of the reactions produced the desired complexes. This was due to the loss of the linker groups between the two NHC salt moieties, and palladium dichloride coordinated in its place, producing **25**. When the bis-NHC precursor salts were reacted with silver(I) oxide, the product formed was the hydrolysed ring opened compound. The ring opened compound, **24**, was due to the water produced during the reaction with silver(I) oxide, reacting with the carbene and forming the formamides at both the carbene rings. This formamide production was observed in the proton NMR and mass spectra.

2.4: Experimental

2.4.1: General Remarks

All air sensitive experiments were carried out using standard Schlenk techniques, under an atmosphere of argon or in a MBRAUN M72 glove box (N₂ atmosphere with > 0.1 ppm O₂ and H₂O) unless otherwise stated. Glassware was dried overnight in an oven at 120 °C and flame dried prior to use. Toluene, pentane, and DCM of analytical grade were freshly collected from a MBRAUN sps 800 solvent purification system, THF was dried in a still over calcium hydride and DMSO was dried over molecular sieves. All other solvents were used as purchased.

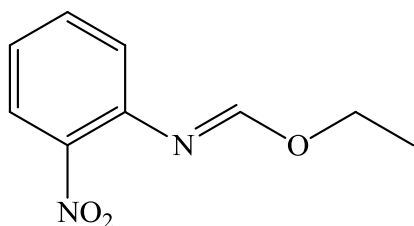
All NMR solvents used were purchased from Goss Scientific Ltd, and distilled from the appropriate drying agents under N₂ prior to use, following standard literature methods.⁵⁷ All NMR spectra were obtained from a Bruker Avance AMX 400 or 500 MHz and referenced to SiMe₄ and coupling constants *J* are expressed in Hertz as positive values regardless of their real individual signs. Mass spectrometry data was recorded HRMS were obtained on a Waters Q-ToF micromass spectrometer and are reported as *m/z* (relative intensity) by the department of chemistry, Cardiff University.

All the X-ray Crystal structures were obtained on a Bruker Nonius Kappa CCD diffractometer using graphite mono-chromated Mo KR radiation ($\lambda(\text{Mo KR}) = 0.71073 \text{ \AA}$). An Oxford Cryosystems cooling apparatus was attached to the instrument, and all data were collected at 150 K. Data collection and cell refinement were carried out by Dr Benson Kariuki, using COLLECT⁵⁸ and HKL SCALEPACK.⁵⁹ Data reduction was applied using HKL DENZO and SCALEPACK.⁵⁹ The structures were solved using direct methods (Sir92)⁶⁰ and refined with SHELX-97.⁶¹ Absorption corrections were performed using SORTAV.⁶²

All compounds **8** and **13-16** were synthesised by known procedures^{20,45} all other reagents were used as purchased.

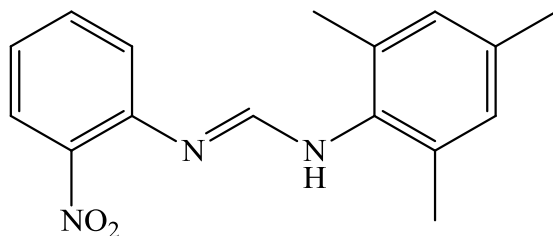
2.4.2: Experimental Data for the Initial Synthesis of Bis-NHC Precursors

Synthesis of ethyl-(2-nitrophenyl)imidoformate (1)



2-nitroaniline (6.91 g, 50 mmol, 1 eq), triethylorthoformate (50 ml, excess) and 1 drop of 2M HCl were placed in a flask and heated and at approximately 110 °C, ethanol began to distil. When 95 % of the theoretical amount of ethanol (5.75 ml) had been collected, the flask was allowed to cool slowly. The excess of triethylorthoformate was removed by vacuum distillation (95 °C). Upon further heating a viscous yellow liquid, ethyl-(2-nitrophenyl)imidoformate, was distilled at (120 °C), yield (5.22 g, 53.8 %). ¹H NMR (CDCl₃, 250 MHz, 298 K): δ 7.70 (1 H, dd, CH_{Ar}, ⁴J_{HH} = 1.5 Hz, ³J_{HH} = 7.4 Hz), δ 7.60 (1 H, s, NCHO), δ 7.35 (1 H, td, CH_{Ar}, ⁴J_{HH} = 1.5 Hz, ³J_{HH} = 7.4 Hz), δ 7.10 (1 H, td, CH_{Ar}, ⁴J_{HH} = 1.3 Hz, ³J_{HH} = 7.7 Hz) δ 6.85 (1 H, dd, CH_{Ar}, ⁴J_{HH} = 1.3 Hz, ³J_{HH} = 7.7 Hz), δ 4.20 (2 H, q, CH₂, ³J_{HH} = 7.1 Hz), δ 1.25 (3 H, t, CH₃, ³J_{HH} = 7.1 Hz).

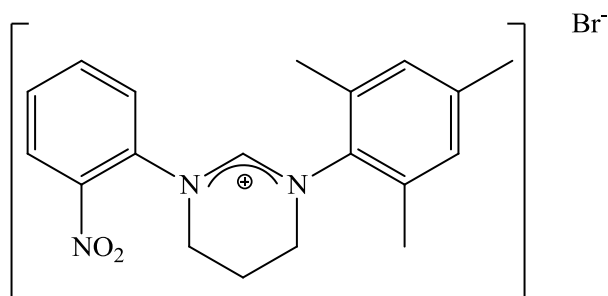
Synthesis of N'-(2-nitrophenyl)-N-(2,4,6-trimethylphenyl)imidoformamide (2)



Ethyl-(2-nitrophenyl)imidoformate (1.00 g, 5.16 mmol, 1 eq) was placed in an acid free flask containing 2,4,6-trimethylaniline (0.72 ml, 5.16 mmol, 1 eq) and heated to 80 °C for 24 hours. The crude product was washed in cold hexanes (20 ml) and dried under high vacuum. This yielded N'-(2-nitrophenyl)-N-(2,4,6-trimethylphenyl)imidoformamide as a bright yellow solid (0.93 g, 63.8 %). ¹H NMR (CDCl₃, 400 MHz, 298 K): δ 8.15 (1 H, d, CH_{Ar}, ³J_{HH} = 8.1 Hz), δ

7.95 (1 H, m, CH_{Ar}), δ 7.80 (1 H, s, NCHN), δ 7.50 (1 H, m, CH_{Ar}), δ 6.95 (1 H, t, CH_{Ar}, ³J_{HH} = 8.1 Hz), δ 6.80 (2 H, s, CH_{Ar}), δ 2.25 (3 H, s, CH₃), δ 2.10 (6 H, s, CH₃).

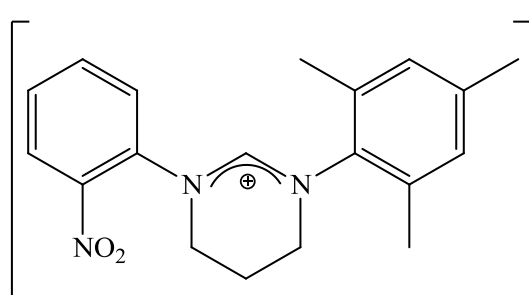
Synthesis of 1-(2-nitrophenyl)-3-(2,4,6-trimethylphenyl)-3,4,5,6-tetrahydropyrimidin-1-ium bromide (3)



Br⁻ N'-(2-nitrophenyl)-N-(2,4,6-trimethylphenyl)imidoforamide (0.64 g, 2.26 mmol, 1 eq), 1,3-dibromopropane (0.25 ml, 2.49 mmol, 1.1 eq), potassium carbonate (0.16 g, 1.13 mmol, 0.5 eq) in acetonitrile (50

ml) were placed in a flask and heated to reflux for 5 days. The reaction mixture was then left to cool to room temperature, the base was removed by filtration and the solvent was removed by evaporation. The crude product was then recrystallised from DCM and diethyl ether to yield 1-(2-nitrophenyl)-3-(2,4,6-trimethylphenyl)-3,4,5,6-tetrahydropyrimidin-1-ium bromide as a pale yellow solid (0.24 g, 32.8 %). ¹H NMR (CDCl₃, 125 MHz, 298 K): δ 8.95 (1 H, d, CH_{Ar}, ³J_{HH} = 7.3 Hz), δ 8.10 (1 H, d, CH_{Ar}, ³J_{HH} = 7.8 Hz), δ 7.80 (1 H, t, CH_{Ar}, ³J_{HH} = 7.3 Hz), δ 7.70 (1 H, s, NCHN), δ 7.60 (1 H, t, CH_{Ar}, ³J_{HH} = 7.8 Hz), δ 6.85 (2 H, s, CH_{Ar}), δ 4.00 (4 H, m, NCH₂, broad) δ 2.60 (2 H, m, NCH₂CH₂, broad), δ 2.35 (6 H, m, CH₃, broad), δ 2.20 (3 H, s, CH₃). ¹³C{¹H} NMR (CDCl₃, 125 MHz, 298 K): δ 153.0 (NCHN), δ 140.0 (CH_{Ar}), δ 135.5 (CH_{Ar}), δ 133.5 (CH_{Ar}), δ 131.0 (CH_{Ar}), δ 124.5 (CH_{Ar}), δ 48.5 (NCH₂), δ 46.0 (NCH₂), δ 20.5 (CH₃), δ 18.0 (NCH₂CH₂), δ 14.0 (CH₃). MS(ES) *m/z*: [M⁺] 324.1712 (C₁₉H₂₂N₃O₂ requires 324.1712), [M⁺ + H] 325.1757 (C₁₉H₂₃N₃O₂ requires 325.1757).

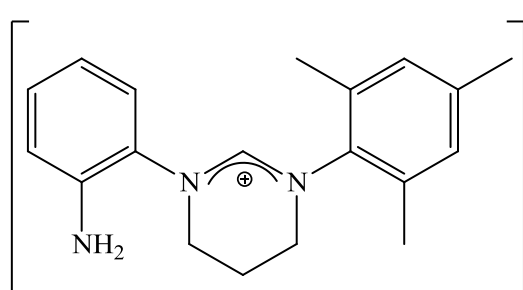
Synthesis of 1-(2-nitrophenyl)-3-(2,4,6-trimethylphenyl)-3,4,5,6-tetrahydropyrimidin-1-ium tetrafluoroborate (4)

BF₄⁻

1-(2-nitrophenyl)-3-(2,4,6-trimethylphenyl)-3,4,5,6-tetrahydropyrimidin-1-ium bromide (1.00 g, 3.09 mmol, 1 eq) in acetone (20 ml), and a solution of sodium tetrafluoroborate (0.51 g, 4.63 mmol,

1.5 eq) in water (10 ml) were placed in a flask and stirred at room temperature for 30 minutes. The organic solvent was then removed in *vacuo* producing the crude product as an oil. The oil was then dissolved in DCM and any remaining precipitates were removed by filtration. On addition of diethyl ether a precipitate was formed, this precipitate was then filtered and dried in *vacuo*. The crude product was then purified by column chromatography on silica gel with a mixture of DCM:methanol (98:2) as the mobile phase, yielding 1-(2-nitrophenyl)-3-(2,4,6-trimethylphenyl)-3,4,5,6-tetrahydropyrimidin-1-ium tetrafluoroborate as a brown solid (0.40 g, 40.0 %). ¹H NMR (CDCl₃, 250 MHz, 298 K): δ 8.25 (1 H, d, CH_{Ar}, ³J_{HH} = 7.3 Hz) δ 8.15 (1 H, dd, CH_{Ar}, ⁴J_{HH} = 1.4 Hz, ³J_{HH} = 8.0 Hz), δ 7.80 (1 H, td, CH_{Ar}, ⁴J_{HH} = 1.4 Hz, ³J_{HH} = 8.0 Hz), δ 7.65 (1 H, t, CH_{Ar}, ³J_{HH} = 7.3 Hz), δ 7.60 (1 H, s, NCHN), δ 6.85 (2 H, s, CH_{Ar}), δ 4.05 (2 H, m, NCH₂, broad), δ 3.85 (2 H, m, NCH₂, broad), δ 2.55 (2 H, m, NCH₂CH₂), δ 2.30 (6 H, s, CH₃), δ 2.20 (3 H, s, CH₃). ¹³C{¹H} NMR (CDCl₃, 125 MHz, 298 K): δ 154.0 (NCHN), δ 144.0 (C_{Ar}), δ 140.5 (NC_{Ar}), δ 136.0 (CH_{Ar}), δ 134.5 (CH_{Ar}), δ 132.0 (CH_{Ar}), δ 130.0 (CH_{Ar}), δ 126.5 (CH_{Ar}), δ 48.5 (NCH₂), δ 46.0 (NCH₂), δ 21.0 (CH₃), δ 18.5 (NCH₂CH₂), δ 16.5 (CH₃). MS(ES) *m/z*: [M⁺] 324.1698 (C₁₉H₂₂N₃O₂ requires 324.1712), [M⁺ + H] 325.1826 (C₁₉H₂₃N₃O₂ requires 325.1712).

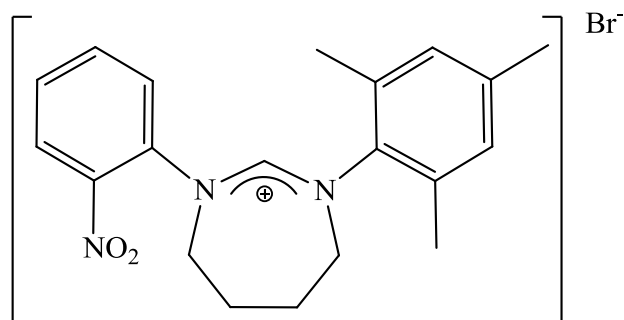
Synthesis of 1-(2-(aminophenyl)-3-(2,4,6-trimethylphenyl)-3,4,5,6-tetrahydropyrimidin-1-ium tetrafluoroborate (5)

BF₄⁻

1-(2-(aminophenyl)-3-(2,4,6-trimethylphenyl)-3,4,5,6-tetrahydropyrimidin-1-ium tetrafluoroborate (0.32 g, 0.99 mmol, 1 eq) in methanol (20 ml) was placed in a Schlenk, to which a spatula of

palladium on carbon (10 %) was added and 1 atm pressure of hydrogen was bubbled through the reaction for 1 hour. The hydrogen was removed and the Schlenk was flushed with nitrogen for 10 minutes. The palladium was then filtered and the filtrate was evaporated. The crude product was triturated in diethyl ether to yield 1-(2-(aminophenyl)-3-(2,4,6-trimethylphenyl)-3,4,5,6-tetrahydropyrimidin-1-ium tetrafluoroborate as a purply brown semicrystalline solid (0.23 g, 79.2 %). ¹H NMR (CDCl₃, 400 MHz, 298 K): δ 7.55 (1 H, s, NCHN), δ 7.15 (1 H, m, CH_{Ar}), δ 6.95 (1 H, m, CH_{Ar}), δ 6.90 (2 H, m, CH_{Ar}), δ 6.70 (1 H, m, CH_{Ar}), δ 6.65 (1 H, m, CH_{Ar}), δ 4.05 (2 H, m, NCH₂, broad), δ 3.80 (2 H, m, NCH₂, broad), δ 2.45 (2 H, m, NCH₂CH₂, broad), δ 2.25 (3 H, m, CH₃), δ 2.20 (6 H, m, CH₃). ¹³C{¹H} NMR (CDCl₃, 125 MHz, 298 K): δ 154.0 (NCHN), δ 144.0 (C_{Ar}), δ 139.5 (C_{Ar}), δ 136.5 (C_{Ar}), δ 134.0 (CH_{Ar}), δ 130.5 (CH_{Ar}), δ 129.5 (CH_{Ar}), δ 128.0 (CH_{Ar}), δ 126.0 (CH_{Ar}), δ 46.5 (NCH₂), δ 46.0 (NCH₂), δ 21.0 (CH₃), δ 19.5 (NCH₂CH₂), δ 17.0 (CH₃). MS(AP) *m/z*: [M⁺] 294.1983 (C₁₉H₂₄N₃ requires 294.1970).

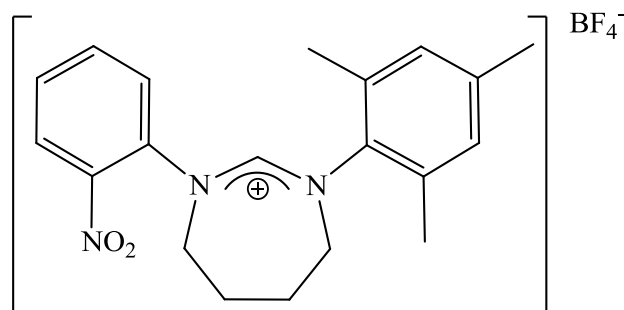
Synthesis of 1-(2-nitrophenyl)-3-(2,4,6-trimethylphenyl)-3,4,5,6,7-tetrahydropyrimidin-1-ium bromide (6)



N^2 -(2-nitrophenyl)- N -(2,4,6-trimethylphenyl)imidiformamide (3.00 g, 0.01 moles, 1 eq), 1,1-diodobutane (1.54 ml, 0.01 moles, 1.1 eq), potassium carbonate (0.73 g, 5.30 mmol, 0.5 eq) in acetonitrile

(300 ml) were placed in a flask and heated to reflux for 16 days. The reaction mixture was then left to cool to room temperature, the base was removed by filtration and the solvent was removed by evaporation. The remaining solid was then redissolved in DCM (50 ml) and refiltered to ensure no base was remaining. The dried crude product was then recrystallised from DCM and diethyl ether to yield 1-(2-nitrophenyl)-3-(2,4,6-trimethylphenyl)-3,4,5,6,7-tetrahydropyrimidin-1-ium bromide as a yellow/orange solid (4.91 g, 99.6 %). ^1H NMR (CDCl_3 , 400 MHz, 298 K): δ 8.85 (1 H, d, CH_{Ar} , $^3J_{\text{HH}} = 7.9$ Hz), δ 8.05 (1 H, d, CH_{Ar} , $^3J_{\text{HH}} = 8.3$ Hz), δ 7.85 (1 H, t, CH_{Ar} , $^3J_{\text{HH}} = 7.9$ Hz), δ 7.65 (1 H, t, CH_{Ar} , $^3J_{\text{HH}} = 8.3$ Hz), δ 7.55 (1 H, s, NCHN), δ 6.85 (2 H, s, CH_{Ar}), δ 3.80 (2 H, m, NCH₂), δ 3.10 (2 H, m, NCH₂), δ 2.55 (2 H, m, NCH₂CH₂), δ 2.40 (6 H, s, CH₃), δ 2.20 (3 H, s, CH₃), δ 1.85 (2 H, m, NCH₂CH₂). $^{13}\text{C}\{^1\text{H}\}$ NMR (CDCl_3 , 125 MHz, 298 K): δ 157.3 (NCHN), δ 142.9 (C_{Ar}), δ 139.8 (NC_{Ar}), δ 138.5 (NC_{Ar}), δ 135.5 (CH_{Ar}), δ 135.0 (CH_{Ar}), δ 131.3 (CH_{Ar}), δ 130.6 (CH_{Ar}), δ 125.0 (CH_{Ar}), δ 118.0 (C_{Ar}), δ 115.6 (C_{Ar}), δ 56.7 (NCH₂), δ 54.8 (NCH₂), δ 32.8 (CH₃), δ 24.4 (NCH₂CH₂), δ 23.9 (NCH₂CH₂), δ 20.0 (CH₃). MS(ES) m/z : [M^+] 338.1875 ($\text{C}_{20}\text{H}_{24}\text{N}_3\text{O}_2$ requires 338.1869).

Synthesis of 1-(2-nitrophenyl)-3-(2,4,6-trimethylphenyl)-3,4,5,6,7-tetrahydropyrimidin-1-ium tetrafluoroborate (7)

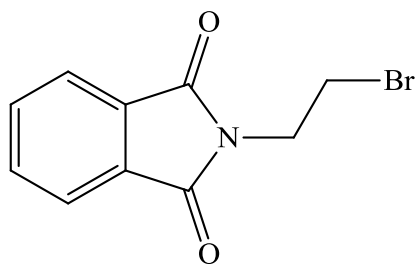


1-(2-nitrophenyl)-3-(2,4,6-trimethylphenyl)-3,4,5,6,7-tetrahydropyrimidin-1-ium bromide (1.00 g, 2.15 mmol, 1 eq) in acetone (20 ml), and a solution of sodium tetrafluoroborate (0.35 g, 3.23 mmol,

1.5 eq) in water (10 ml) were placed in a flask and stirred at room temperature for 1 hour. The organic solvent was then removed in *vacuo* producing the crude product as an oil. The oil was then dissolved in DCM and extracted from water. The DCM layer was then dried over magnesium sulphate and dried in *vacuo* yielding the crude product as a brown oil. This oil was then triturated in diethyl ether to give 1-(2-nitrophenyl)-3-(2,4,6-trimethylphenyl)-3,4,5,6,7-tetrahydropyrimidin-1-ium tetrafluoroborate as a light brown solid (0.63 g, 69.0 %). $^1\text{H NMR}$ (CDCl_3 , 400 MHz, 298 K): δ 8.40 (1 H, d, CH_{Ar} , $^3J_{\text{HH}} = 7.7$ Hz), δ 8.05 (1 H, d, CH_{Ar} , $^3J_{\text{HH}} = 8.0$ Hz), δ 7.85 (1 H, t, CH_{Ar} , $^3J_{\text{HH}} = 7.7$ Hz), δ 7.60 (1 H, t, CH_{Ar} , $^3J_{\text{HH}} = 8.0$ Hz), δ 7.40 (1 H, s, NCHN), δ 6.90 (2 H, s, CH_{Ar}), δ 4.70 (2 H, m, NCH₂), δ 3.80 (2 H, m, NCH₂), δ 2.45 (2 H, m, NCH₂CH₂), δ 2.40 (2 H, m, NCH₂CH₂), δ 2.35 (6 H, s, CH₂), δ 2.20 (3 H, s, CH₃). $^{13}\text{C}\{^1\text{H}\}$ NMR (CDCl_3 , 125 MHz, 298 K): δ 157.6 (NCHN), δ 143.0 (C_{Ar}), δ 139.3 (NC_{Ar}), δ 138.4 (NC_{Ar}), δ 135.6 (CH_{Ar}), δ 135.2 (CH_{Ar}), δ 130.6 (CH_{Ar}), δ 129.3 (CH_{Ar}), δ 125.0 (CH_{Ar}), δ 118.1 (C_{Ar}), δ 115.6 (C_{Ar}), δ 56.0 (NCH₂), δ 54.3 (NCH₂), δ 32.8 (CH₃), δ 24.2 (NCH₂CH₂), δ 23.9 (NCH₂CH₂), δ 19.9 (CH₃). MS(ES) m/z : [M^+] 338.1870 ($\text{C}_{20}\text{H}_{24}\text{N}_3\text{O}_2$ requires 338.1869).

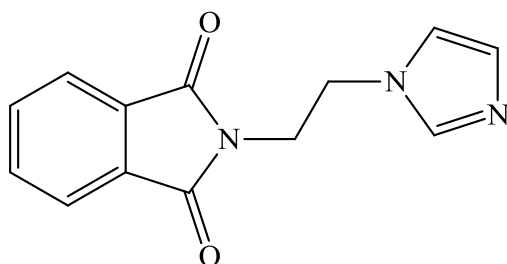
2.4.3: Experimental Data for the Initial Synthesis of Mixed Ring Size Bis-NHC Precursors

Synthesis of 2-(2-bromoethyl)-1*H*-isoindole-1,3-(2*H*)-dione (8)⁴⁵



Potassium phthalimide (1.48 g, 7.99 mmol, 1 eq) was placed in a flask containing 1,2-dibromoethane (1.38 ml, 15.97 mmol, 2 eq) in boiling acetone (25 ml) in four equal portions over a four hour period. The reaction mixture was then refluxed for 24 hours. The mixture was left to cool, the potassium bromide was removed by filtration and the acetone evaporated. The remaining residue was distilled under vacuum to give the crude product which was then recrystallised from ethanol yielding 2-(2-bromoethyl)-1*H*-isoindole-1,3-(2*H*)-dione as a white semicrystalline solid (3.09 g, 75.1 %). ¹H NMR (CDCl₃, 250 MHz, 298 K): δ 7.80 (2 H, m, CH_{Ar}), δ 7.65 (2 H, m, CH_{Ar}), δ 4.05 (2 H, t, NCH₂, ³J_{HH} = 6.7 Hz), δ 3.55 (2 H, t, CH₂Br, ³J_{HH} = 6.7 Hz).

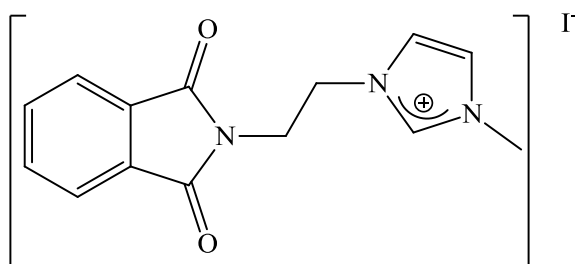
Synthesis of N-[2-(1*H*-imidazol-1-yl)ethyl]phthalimide (9)⁴⁶



Potassium bromide (0.23 g, 1.97 mmol, 1 eq) was added to melted imidazole (2.15 g, 31.50 mmol, 16 eq). To this mixture N-(2-bromoethyl)phthalimide (2.00 g, 7.88 mmol, 4 eq) was added in portions. The melted reaction mixture was stirred at 200 °C for 17 hours. The melted mixture was then refluxed in toluene (50 ml) for a further 24 hours. The reaction mixture was then left to cool to room temperature and the toluene was removed by evaporation to give the crude product. The crude product was then recrystallised from IPA to yield N-[2-(1*H*-imidazol-1-yl)ethyl]phthalimide as a white semicrystalline solid (1.47 g, 77.4 %). ¹H

NMR (DMSO, 400 MHz, 298 K): δ 7.85 (4 H, m, CH_{phthal}), δ 7.60 (1 H, s, NCHN), δ 7.15 (1 H, s, CH_{imid}), δ 6.85 (1 H, s, CH_{imid}), δ 4.30 (2 H, m, NCH₂), δ 3.95 (2 H, m, NCH₂). MS(ES) m/z : [M⁺ + H] 242.13 (C₁₃H₁₂N₃O₂ requires 242.16).

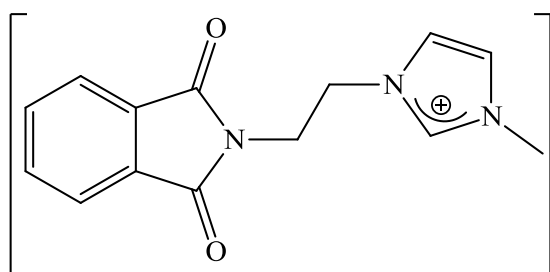
Synthesis of 1-[2-(1,3-dioxo-1,3-dihydro-2H-isoindole-2-yl)ethyl]-3-methyl-1H-imidazol-3-ium iodide (11)⁴⁷



N-[2-(1H-imidazol-1-yl)ethyl]phthalimide (0.90, 3.37 mmol, 1 eq) and methyl iodide (1.39 ml, 6 eq, excess) in THF (80 ml). The reaction mixture was heated to reflux for 2 hours.

The product precipitated out of THF, and was triturated in a further 3 x 30 ml of THF. The product was filtered and dried on a high vacuum line yielding 1-[2-(1,3-dioxo-1,3-dihydro-2H-isoindole-2-yl)ethyl]-3-methyl-1H-imidazol-3-ium iodide as an off white semicrystalline solid (0.87 g, 91.0 %). ¹H NMR (MeOD, 400 MHz, 298 K): δ 7.75 (4 H, m, CH_{phthal}), δ 7.70 (1 H, m, NCHN), δ 7.55 (1 H, m, CH_{imid}), δ 7.45 (1 H, m, CH_{imid}), δ 4.40 (2 H, m, NCH₂), δ 4.05 (2 H, m, NCH₂), δ 3.75 (3 H, s, CH₃). MS(ES) m/z : [M⁺] 256.11 (C₁₄H₁₄N₃O₂ requires 256.17), [M⁺ + H] 257.11 (C₁₄H₁₅N₃O₂ requires 257.17).

Synthesis of 1-[2-(1,3-dioxo-1,3-dihydro-2H-isoindole-2-yl)ethyl]-3-methyl-1H-imidazol-3-ium iodide (11)⁴⁷

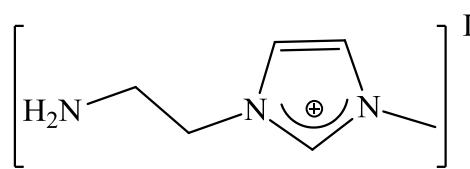


Potassium iodide (0.76 g, 4.57 mmol, 0.25 eq) was added to 1-methylimidazole (0.49 ml, 6.09 mmol, 0.33 eq). To this mixture N-(2-bromoethyl)phthalimide (4.64 g, 10.00

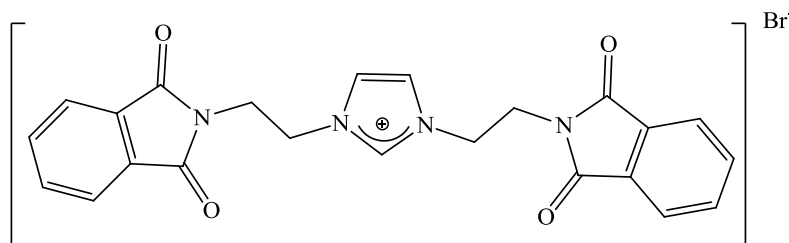
mmol, 1 eq) was added in portions and heated at 100 °C for 10 minutes at which point the solution solidified. Toluene was then added to the off white solid and refluxed for 1.5 hours. The mixture was left to cool to ambient temperatures, the crude product was

filtered and dried on a high vacuum line yielding 1-[2-(1,3-dioxo-1,3-dihydro-2*H*-isoindole-2-yl)ethyl]-3-methyl-1*H*-imidazol-3-ium iodide as a white powder (2.81 g, 60.1 %). ^1H NMR (CDCl_3 , 400 MHz, 298 K): δ 10.45 (1 H, s, NCHN), δ 7.75 (4 H, m, $\text{CH}_{\text{phthal}}$), δ 7.15 (2 H, m, CH_{imid}), δ 4.75 (2 H, t, NCH_2 , $^3J_{\text{HH}} = 5.4$ Hz), δ 4.20 (2 H, t, NCH_2 , $^3J_{\text{HH}} = 5.4$ Hz), δ 4.05 (3 H, s, CH_3). MS(ES) m/z : $[\text{M}^+]$ 256.11 ($\text{C}_{14}\text{H}_{14}\text{N}_3\text{O}_2$ requires 256.17), $[\text{M}^+ + \text{H}]$ 257.11 ($\text{C}_{14}\text{H}_{15}\text{N}_3\text{O}_2$ requires 257.17).

Synthesis of 1-(2-aminoethyl)-3-methyl-1*H*-imidazol-3-ium iodide (12)⁴⁷

 1-[2-(1,3-dioxo-1,3-dihydro-2*H*-isoindole-2-yl)ethyl]-3-methyl-1*H*-imidazol-3-ium iodide (2.79 g, 10.89 mmol, 1 eq) was dissolved in methoxyethanol (30 ml). To this solution hydrazine monohydrate (2.65 g, 54.49 mmol, 5 eq) was added and the reaction was heated to reflux for 3.5 hours. The reaction was then left to cool very slowly to ambient temperatures precipitating phthalhydrazide. The precipitate was then washed thoroughly with chloroform and filtered. The filtrate was then evaporated down to dryness yielding 1-(2-aminoethyl)-3-methyl-1*H*-imidazol-3-ium iodide as a yellow oil (3.39 g, 76.5 %). ^1H NMR (DMSO, 400 MHz, 298 K): δ 8.95 (1 H, s, NCHN), δ 7.55 (1 H, m, CH_{imid}), δ 7.50 (1 H, m, CH_{imid}), δ 3.95 (2 H, t, NCH_2 , $^3J_{\text{HH}} = 5.9$ Hz), δ 3.70 (3 H, s, CH_3), δ 2.75 (2 H, t, NH_2CH_2 , $^3J_{\text{HH}} = 5.9$ Hz). $^{13}\text{C}\{^1\text{H}\}$ NMR (DMSO, 125 MHz, 298 K): δ 135.5 (NCHN), δ 123.0 ($\text{CH}_{\text{phthal}}$), δ 122.5 ($\text{CH}_{\text{phthal}}$), δ 63.0 (NCH), δ 52.0 (NCH), δ 34.5 (CH_3).

Synthesis of 1,3-bis-[2-(1,3-dioxo-1,3-dihydro-2*H*-isoindol-2-yl)ethyl]-1*H*-imidazol-3-ium bromide (10)

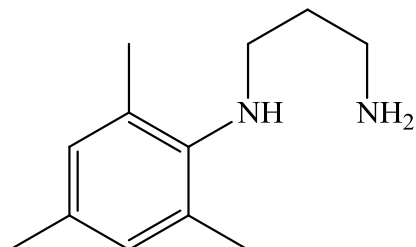


Potassium iodide (1.63 g, 9.79 mmol, 1 eq) was added to melted imidazole (1.00 g, 0.01 moles eq, 1.5 eq). N-(2-

bromoethyl)phthalimide (14.92 g, 0.06 moles, 6 eq) was then added in portions and stirred for 3 hours. Toluene was then added and the reaction was refluxed for 24 hours. After leaving to cool to ambient temperatures the toluene was removed by evaporation. The crude product was then recrystallised from IPA. The mixture of products was triturated in diethyl ether yielding 1,3-bis-[2-(1,3-dioxo-1,3-dihydro-2*H*-isoindol-2-yl)ethyl]-1*H*-imidazol-3-ium bromide as a white solid (3.29 g, 54.0 %). ^1H NMR (DMSO, 400 MHz, 298 K): δ 9.30 (1 H, s, NCHN), δ 7.85 (8 H, m, $\text{CH}_{\text{phthal}}$), δ 7.80 (2 H, m, CH_{imid}), δ 4.45 (4 H, m, NCH_2), δ 3.95 (4 H, m, NCH_2). $^{13}\text{C}\{^1\text{H}\}$ NMR (DMSO, 125 MHz, 298 K): δ 165.5 (CO), δ 156.5 (NCHN), δ 134.5 (CH_{imid}), δ 131.0 (C_{Ar}), δ 122.5 (CH), δ 122.0 (CH), δ 47.5 (NCH_2), δ 37.5 (NCH_2). MS(ES) m/z : [M^+] 415.14 ($\text{C}_{23}\text{H}_{19}\text{N}_4\text{O}_4$ requires 415.27), [$\text{M}^+ + \text{H}$] 416.15 ($\text{C}_{23}\text{H}_{20}\text{N}_4\text{O}_4$ requires 416.27), [$\text{M}^+ + 2\text{H}$] 417.15 ($\text{C}_{23}\text{H}_{21}\text{N}_4\text{O}_4$ requires 417.27).

2.4.4: Experimental Data for the Synthesis of Bis-NHC Precursors

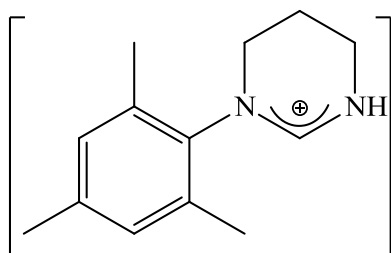
Synthesis of N-(2,4,6-trimethylphenyl)-1,3-propanediamine (15)²⁰



To a solution of 2,4,6-trimethylaniline (12.84 ml, 0.09 moles, 2 eq), in toluene (200 ml) was added 3-bromopropylamine hydrobromide (10.00 g, 0.05 moles, 1 eq) and the mixture was refluxed for 5 days.

The reaction mixture was then cooled to room temperature and poured into potassium hydroxide 2M and stirred until the organic layer became an homogenous brown oil. The aqueous layer was then separated and extracted into diethyl ether (3 x 50 ml). All the organic layers were then combined and reduced to dryness. The crude product was then extracted again using water and ethyl acetate. The aqueous layer was dried in *vacuo* yielding N-(2,4,6-trimethylphenyl)-1,3-propanediamine as a brown oil (3.74 g, 42.7 %). ¹H NMR (CDCl₃, 400 MHz, 298 K): δ 6.65 (2 H, s, CH_{Ar}), δ 5.75 (3 H, s, broad, NH + NH₂), δ 2.90 (2 H, t, NCH₂, ³J_{HH} = 7.2 Hz), δ 2.85 (2 H, t, NCH₂, ³J_{HH} = 6.6 Hz), δ 2.10 (9 H, s, CH₃), δ 1.80 (2 H, m, NCH₂CH₂). ¹³C{¹H} NMR (CDCl₃, 125 MHz, 298 K): δ 142.0 (C_{Ar}), δ 132.0 (C_{Ar}), δ 131.0 (C_{Ar}), δ 130.0 (CH_{Ar}), δ 46.5 (NCH₂), δ 38.0 (NCH₂), δ 29.5 (NCH₂CH₂), δ 21.0 (CH₃), δ 18.0 (CH₃). MS(ESI) *m/z*: [M⁺ + H] 193.1700 (C₁₂H₂₁N₂ requires 193.1705).

Synthesis of 1-(2,4,6-trimethylphenyl)-3,4,5,6-tetrahydropyrimidin-1-ium tetrafluoroborate (18)

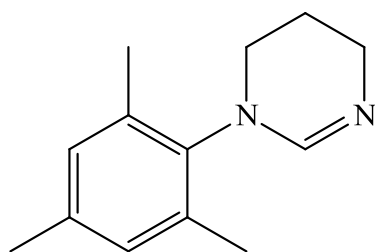


BF₄⁻ N-(2,4,6-trimethylphenyl)-1,3-propanediamine (3.60 g, 0.02 moles, 1 eq), triethylorthoformate (3.74 ml, 0.02 moles, 1.2 eq), and ammonium tetrafluoroborate were placed into a flask and refluxed for 5 days in acetonitrile (150 ml). The

reaction mixture was then left to cool slowly to room temperature, filtered, and reduced

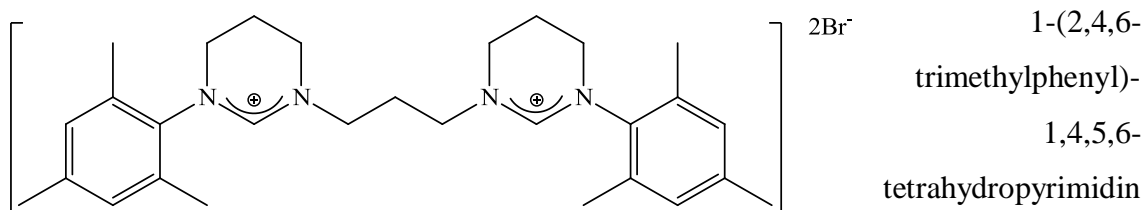
in *vacuo* yielding 1-(2,4,6-trimethylphenyl)-3,4,5,6-tetrahydropyrimidin-1-ium tetrafluoroborate (4.90 g, 90.2 %). ^1H NMR (CD_3CN , 125 MHz, 298 K): δ 7.85 (1 H, s, NCHN), δ 6.80 (2 H, s, CH_{Ar}), δ 3.35 (2 H, t, NCH_2 , $^3J_{\text{HH}} = 5.7$ Hz), δ 3.30 (2 H, t, NCH_2 , $^3J_{\text{HH}} = 5.8$ Hz), δ 2.30 (3 H, s, CH_3), δ 2.25 (6 H, s, CH_3), δ 1.85 (2 H, m, NCH_2CH_2). $^{13}\text{C}\{^1\text{H}\}$ NMR (CD_3CN , 125 MHz, 298 K): δ 154.0 (NCHN), δ 140.0 (C_{Ar}), δ 135.0 (C_{Ar}), δ 130.0 (C_{Ar}), δ 118.0 (CH_{Ar}), δ 47.0 (NCH_2), δ 38.0 (NCH_2), δ 20.0 (NCH_2CH_2), δ 18.0 (CH_3), δ 16.5 (CH_3). MS(ESI) m/z : [M^+] 203.1541 ($\text{C}_{13}\text{H}_{19}\text{N}_2$ requires 203.1548).

Synthesis of 1-(2,4,6-trimethylphenyl)-1,4,5,6-tetrahydropyrimidine (16)



1-(2,4,6-trimethylphenyl)-3,4,5,6-tetrahydropyrimidin-3-ium tetrafluoroborate (4.00 g, 0.01 moles, 1 eq) and potassium tertiarybutoxide (1.55 g, 0.01 moles, 1 eq) were placed in a flask containing THF (150 ml) and stirred at room temperature for 1 hour. After this time the solvent was removed in *vacuo*, the crude product redissolved in DCM and filtered through celite. The DCM was then evaporated yielding 1-(2,4,6-trimethylphenyl)-1,4,5,6-tetrahydropyrimidine (2.73 g, 97.9 %). ^1H NMR (CDCl_3 , 400 MHz, 298 K): δ 7.10 (1 H, s, NCHN), δ 6.80 (2 H, s, CH_{Ar}), δ 3.40 (2 H, m, NCH_2), δ 3.35 (2 H, t, NCH_2 , $^3J_{\text{HH}} = 5.8$ Hz), δ 2.20 (3 H, s, CH_3), δ 2.15 (6 H, s, CH_3), δ 2.05 (2 H, t, NCH_2CH_2 , $^3J_{\text{HH}} = 5.8$ Hz). MS(AP) m/z : [$\text{M}^+ + \text{H}^+$] 203.1548 ($\text{C}_{13}\text{H}_{19}\text{N}_2$ requires 203.1548).

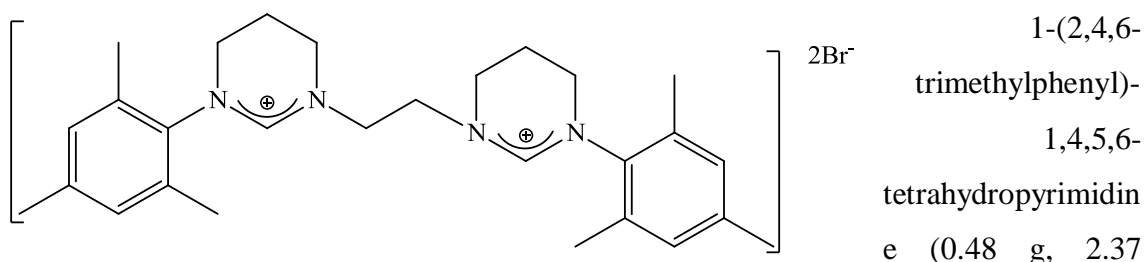
Synthesis of 1,1'-di-(2,4,6-trimethylphenyl)-3,3'-propylene-di-3,4,5,6-tetrahydropyrimidin-1-ium bisbromide (19)



(0.57 g, 2.82 mmol, 2.2 eq) was placed in a pressure tube and dissolved in THF (10 ml). To this 1,2-dibromopropane (0.13 ml, 1.28 mmol, 1 eq) was added and heated to

70 °C for 17 hours. The reaction mixture was then left to cool to room temperature, the supernatant was decanted and the crude product was triturated in diethyl ether (3 x 20 ml) then in THF (3 x 20 ml). The solvents were removed in *vacuo* yielding 1,1'-di-(2,4,6-trimethylphenyl)-3,3'-propylene-di-3,4,5,6-tetrahydropyrimidin-1-ium bisbromide (0.13 g, 17.0 %). ^1H NMR (CDCl_3 , 400 MHz, 298 K): δ 8.70 (2 H, s, NCHN), δ 6.85 (4 H, s, CH_{Ar}), δ 4.20 (4 H, m, NCH_2), δ 3.90 (4 H, m, NCH_2), δ 3.55 (4 H, t, NCH_2 , $^3J_{\text{HH}} = 5.6$ Hz), δ 2.40 (2 H, m, NCH_2CH_2), δ 2.25 (4 H, m, NCH_2CH_2), δ 2.20 (6 H, s, CH_3), δ 2.15 (12 H, s, CH_3). $^{13}\text{C}\{^1\text{H}\}$ NMR (CDCl_3 , 125 MHz, 298 K): δ 154.2 (NCHN), δ 141.0 (C_{Ar}), δ 136.0 (C_{Ar}), δ 134.0 (CH_{Ar}), δ 130.0 (C_{Ar}), δ 52.0 (NCH_2), δ 46.0 (NCH_2), δ 44.0 (NCH_2), δ 21.0 (CH_3), δ 19.0 (NCH_2CH_2) δ 18.0 (NCH_2CH_2), δ 17.0 (CH_3). MS(ES) m/z : [$\text{M}^+ + \text{Br}$] 525.2585 ($\text{C}_{29}\text{H}_{42}\text{N}_4\text{Br}$ requires 525.2593), [$\text{M}^+/2$] 223.1663 ($[\text{C}_{29}\text{N}_4\text{H}_{42}]/2$ requires 222.6748).

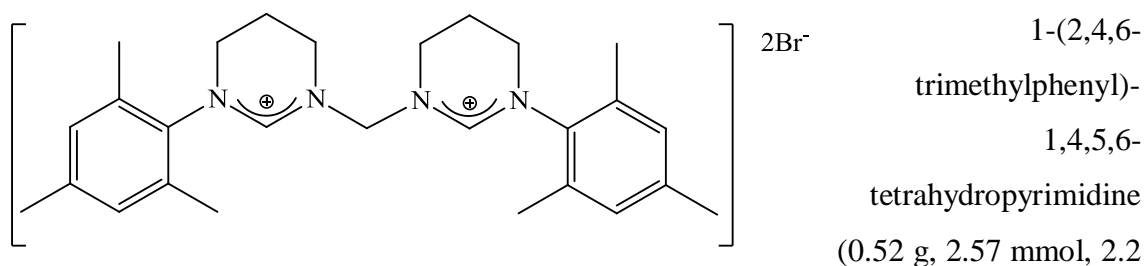
Synthesis of 1,1'-di-(2,4,6-trimethylphenyl)-3,3'-ethylene-di-3,4,5,6-tetrahydropyrimidin-1-ium bisbromide (17)



mmol, 2.2 eq) was placed in a pressure tube and dissolved in THF (10 ml). To this 1,2-dibromoethane (0.09 ml, 1.08 mmol, 1 eq) was added and heated to 70 °C for 4 hours. The reaction mixture was then left to cool to room temperature, the supernatant was decanted and the crude product was triturated in diethyl ether (3 x 20 ml) then in THF (3 x 20 ml). The solvents were removed in *vacuo* yielding 1,1'-di-(2,4,6-trimethylphenyl)-3,3'-ethylene-di-3,4,5,6-tetrahydropyrimidin-1-ium bisbromide (0.07 g, 10.2 %). ^1H NMR (CDCl_3 , 125 MHz, 298 K): δ 9.35 (2 H, s, NCHN), δ 6.85 (4 H, s, CH_{Ar}), δ 4.45 (4 H, s, NCH_2), δ 4.05 (4 H, t, NCH_2 , $^3J_{\text{HH}} = 5.0$ Hz), δ 3.50 (4 H, t, NCH_2 , $^3J_{\text{HH}} = 5.1$ Hz), δ 2.30 (4 H, m, NCH_2CH_2), δ 2.20 (12 H, s, CH_3), δ 2.10 (6 H, s, CH_3). $^{13}\text{C}\{^1\text{H}\}$ NMR (CDCl_3 , 125 MHz, 298 K): δ 155.3 (NCHN), δ 140.0 (C_{Ar}), δ 136.0 (C_{Ar}), δ 134.0 (C_{Ar}), δ 130.0 (CH_{Ar}), δ 52.0 (NCH_2), δ 46.0 (NCH_2), δ 45.0 (NCH_2), δ

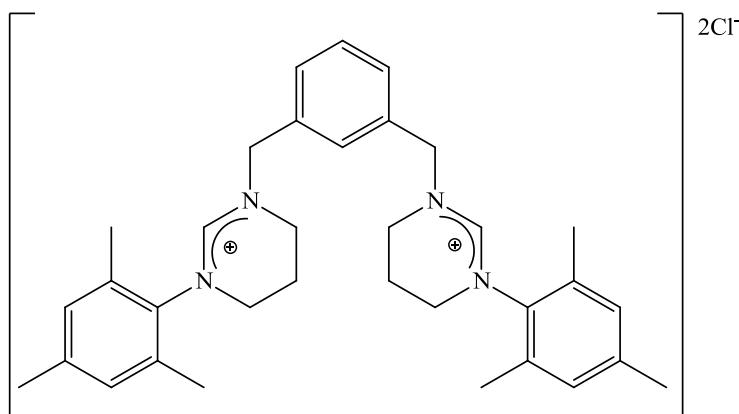
21.0 (CH₃), δ 19.0 (NCH₂CH₂), δ 18.0 (CH₃). MS(ES) *m/z*: [M⁺ + Br⁻] 511.2441 (C₂₈H₄₀N₄Br requires 511.2436), [M⁺/2] 216.1618 ([C₂₈H₄₆N₄]/2 requires 216.3262).

Synthesis of 1,1'-di-(2,4,6-trimethylphenyl)-3,3'-methylene-di-3,4,5,6-tetrahydropyrimidin-1-ium bisbromide (20)



eq) was placed in a pressure tube and dissolved in THF (10 ml). To this 1,2-dibromomethane (0.08 ml, 1.17 mmol, 1 eq) was added and heated to 70 °C for 4 hours. The reaction mixture was then left to cool to room temperature, the supernatant was decanted and the crude product was triturated in diethyl ether (3 x 20 ml) then in THF (3 x 20 ml). The solvents were removed in *vacuo* yielding 1,1'-di-(2,4,6-trimethylphenyl)-3,3'-methylene-di-3,4,5,6-tetrahydropyrimidin-1-ium bisbromide (0.12 g, 17.8 %). ¹H NMR (CDCl₃, 400 MHz, 298 K): δ 9.25 (2 H, s, NCHN), δ 6.85 (4 H, s, CH_{Ar}), δ 6.20 (2 H, s, NCH₂), δ 4.30 (4 H, m, NCH₂), δ 3.85 (4 H, m, NCH₂), δ 2.35 (4 H, m, NCH₂CH₂), δ 2.30 (12 H, s, CH₃), δ 2.25 (6 H, s, CH₃). ¹³C{¹H} NMR (CDCl₃, 125 MHz, 298 K): δ 155.5 (NCHN), δ 140.0 (C_{Ar}), δ 136.5 (C_{Ar}), δ 134.0 (CH_{Ar}), δ 130.0 (C_{Ar}), δ 71.0 (NCH₂), δ 47.0 (NCH₂), δ 43.0 (NCH₂), δ 21.0 (NCH₂CH₂), δ 19.0 (CH₃), δ 18.0 (CH₃). MS(ES) *m/z*: [M⁺ + Br⁻] 497.2285 (C₂₇H₃₈N₄Br requires 497.2280), [M⁺/2] 209.1535 ([C₂₇H₃₈N₄]/2 requires 208.6958).

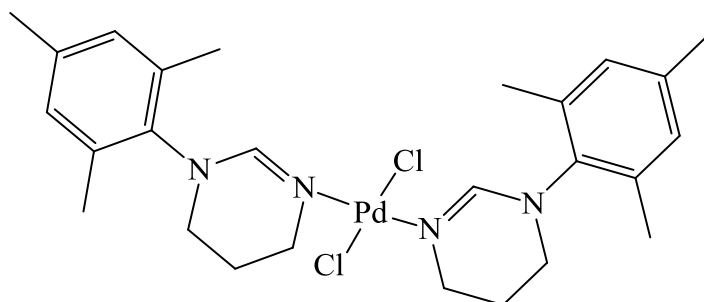
Synthesis of 1,1'-di-(2,4,6-trimethylphenyl)-3,3'-metaxylene-di-3,4,5,6-tetrahydropyrimidin-1-ium bischloride (21)



2Cl⁻ 1-(2,4,6-trimethylphenyl)-1,4,5,6-tetrahydropyrimidine (1.81 g, 8.96 mmol, 2 eq) was dissolved in DMF (20 ml) and *m*-xylene dichloride (0.78 g, 4.48 mmol, 1 eq) was added slowly. The reaction mixture was then

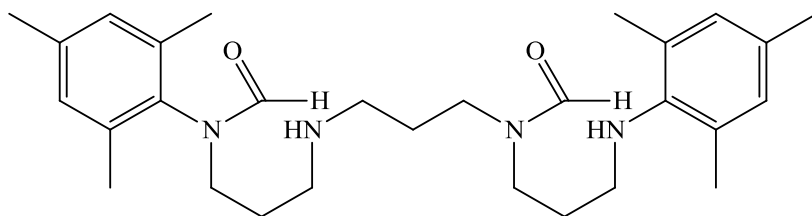
stirred at room temperature for 5 hours. The DMF was then removed by vacuum distillation. The crude product was first triturated in diethyl ether (3 x 20 ml) and then in THF (3 x 20 ml) yielding 1,1'-di-(2,4,6-trimethylphenyl)-3,3'-metaxylene-di-3,4,5,6-tetrahydropyrimidin-1-ium bischloride as a off white solid, (0.60 g, 23.1 %). ¹H NMR (CDCl₃, 125 MHz, 298 K): δ 9.45 (2 H, s, NCHN), δ 7.85 (1 H, s, CH_{Ar}), δ 7.25-7.40 (3 H, m, CH_{Ar}), δ 6.85 (4 H, s, CH_{Ar}), δ 5.20 (4 H, s, NCH₂), δ 3.55 (8 H, m, NCH₂), δ 2.25 (18 H, s, CH₃), δ 2.20 (4 H, m, NCH₂CH₂). ¹³C{¹H} NMR (CDCl₃, 125 MHz, 298 K): NCN not observed, δ 155.0 (NC_{Ar}), δ 139.5 (CH_{Ar}), δ 137.0 (CH_{Ar}), δ 134.5 (CH_{Ar}), δ 134.0 (C_{Ar}), δ 130.0 (CH_{Ar}), δ 129.5 (C_{Ar}), δ 129.0 (C_{Ar}), δ 58.5 (NCH₂), δ 46.5 (NCH₂), δ 43.5 (NCH₂), δ 21.5 (NCH₂CH₂), δ 19.5 (CH₃), δ 18.0 (CH₃). MS(ES) *m/z*: [M⁺ + Cl⁻] 543.3277 (C₃₄H₄₄N₄Cl requires 543.3255), [M⁺/2] 254.1774 ([C₂₇H₃₈N₄]/2 requires 254.3751).

2.4.5: Experimental Data for the Attempted Complexes of Bis-NHCs

Synthesis of bis-[1-(2,4,6-trimethylphenyl)-3,4,5,6-tetrahydropyrimidine] dichloropalladium (**25**)^{55,56}

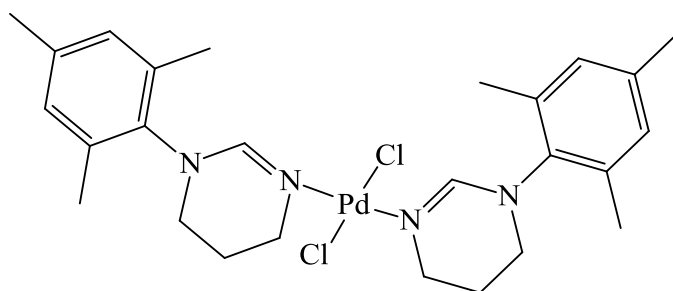
Compound **17** (0.07 g, 0.11 mmol, 1 eq) was placed in a flame dried Schlenk and dried under vacuum for 20 minutes. To this potassium tertiary

butoxide (0.03 g, 3.08 mmol, 2.4 eq) and toluene (15 ml) were added and stirred at room temperature for 20 minutes. The free carbene was then left to settle and filtered under nitrogen into a flame dried Schlenk containing Pd(1,5-COD)Cl₂ (0.03 g, 0.11 mmol, 1 eq) and stirred at room temperature under a nitrogen atmosphere for a further 17 hours. The resulting solution was then reduced to dryness on a high vacuum line, exposed to air and triturated in pentane (30 ml). The remaining solid was dried under vacuum yielding bis-[1-(2,4,6-trimethylphenyl)-3,4,5,6-tetrahydropyrimidine] dichloropalladium (0.03 g, 53.0 %). ¹H NMR (CDCl₃, 400 MHz, 298 K): δ 7.05 (2 H, s, NCHN), δ 6.80 (4 H, s, CH_{Ar}), δ 3.40 (4 H, t, NCH₂, ³J_{HH} = 5.3 Hz), δ 3.20 (4 H, t, NCH₂, ³J_{HH} = 5.8 Hz), δ 2.20 (6 H, s, CH₃), δ 2.10 (12 H, s, CH₃), δ 1.90 (4 H, m, NCH₂CH₂). ¹³C{¹H} NMR (CDCl₃, 125 MHz, 298 K): δ 153.5 (NCHN), δ 137.6 (C_{Ar}), δ 137.0 (C_{Ar}), δ 134.5 (C_{Ar}), δ 128.0 (CH_{Ar}), δ 45.0 (NCH₂), δ 44.0 (NCH₂), δ 21.0 (CH₃), δ 18.0 (CH₃), δ 15.0 (NCH₂CH₂). MS(ES) *m/z*: [M⁺ - Cl⁻ + MeCN] 587.19 (C₂₈H₃₉N₅PdCl requires 587.2), it was not possible to obtain HRMS for this complex.

Synthesis of 1,1'-di-(2,4,6-trimethylphenyl)-3,3'-aminopropyl-1,3'-formamide (24)

Compound **19** (0.03 g, 0.05 mmol, 1 eq) was placed in a round bottomed flask,

wrapped in tin foil, containing silver(I) oxide (0.01g, 0.05 mmol, 1 eq) and DCM (5 ml). The reaction mixture was stirred at room temperature for 2 days, filtered and reduced in *vacuo* yielding 1,1'-di-(2,4,6-trimethylphenyl)-3,3'-aminopropyl-1,3'-formamide (0.01 g, 48.0 %). ^1H NMR (CDCl_3 , 400 MHz, 298 K): δ 8.30 (1 H, s, NC(O)H), δ 7.90 (1 H, s, NC(O)H), δ 6.85 (4 H, s, CH_{Ar}), δ 3.50 (6 H, m, NCH_2), δ 2.55 (6 H, m, NCH_2), δ 2.20 (18 H, m, CH_3), δ 1.95 (2 H, m, NCH_2CH_2), δ 1.60 (4 H, m, NCH_2CH_2). MS(ES) m/z : [$\text{M}^+ + \text{H}$] 481.35 ($\text{C}_{29}\text{H}_{45}\text{N}_4\text{O}_2$ requires 481.33), it was not possible to obtain HRMS for this compound.

Synthesis of bis-[1-(2,4,6-trimethylphenyl)-3,4,5,6-tetrahydropyrimidine] dichloropalladium (25)^{55,56}

Compound **21** (0.50 g, 0.87 mmol, 1 eq), $\text{Pd}(\text{OAc})_2$ (0.19 g, 0.87 mmol, 1 eq) and DMSO (20 ml) were all placed in a round bottomed Schlenk under a nitrogen atmosphere and heated

to 60 °C for 5 hours. The reaction mixture was then left to cool slowly and the solvent was removed by vacuum distillation. The residue was then dissolved in chloroform, filtered through a pad of celite and reduced in *vacuo* yielding bis-[1-(2,4,6-trimethylphenyl)-3,4,5,6-tetrahydropyrimidine] dichloropalladium (0.03 g, 53.0 %). ^1H NMR (CDCl_3 , 400 MHz, 298 K): δ 7.05 (2 H, s, NCHN), δ 6.80 (4 H, s, CH_{Ar}), δ 3.40 (4 H, m, NCH_2), δ 3.20 (4 H, m, NCH_2), δ 2.20 (6 H, s, CH_3), δ 2.10 (12 H, s, CH_3), δ 1.90 (4 H, m, NCH_2CH_2).

2.5: References

- 1 Benhamou, L.; Chardon, E.; Lavigne, G.; Bellemin-Lapponnaz, S.; César, V. *Chem. Rev.* **2011**, 111, 4, 2705-2733.
- 2 Crudden, C. M.; Allen, D. P. *Coordination Chem. Revs.* **2004**, 248, 2247-2273.
- 3 Herrmann, W. A. *Angew. Chem. Int. Ed.* **2002**, 41, 8, 1290-1309.
- 4 Herrmann, W. A.; Köcher, C. *Angew. Chem. Int. Ed.* **1997**, 36, 20, 2162-2187.
- 5 Binobaid, A.; Iglesias, M.; Beetstra, D. J.; Kariuki, B.; Dervisi, A.; Fallis, I. A.; Cavell, K. J. *Dalton Trans.* **2009**, 35, 7099-7112.
- 6 Dunsford, J. J.; Cavell, K. J.; Kariuki, B. *J. Organomet. Chem.* **2011**, 696, 1, 188-194.
- 7 Kolychev, E. L.; Portnyagin, I. A.; Shuntikov, V. V.; Khrustalev, V. N.; Nechaev, M. S. *J. Organomet. Chem.* **2009**, 694, 15, 2454-2462.
- 8 Iglesias, M.; Beetstra, D. J.; Cavell, K. J.; Dervisi, A.; Fallis, I. A.; Kariuki, B.; Harrington, R. W.; Clegg, W.; Horton, P. N.; Coles, S. J.; Hursthouse, M. B. *Eur. J. Inorg. Chem.* **2010**, 11, 1604-1607.
- 9 Lu, W. Y.; Cavell, K. J.; Wixey, J. S.; Kariuki, B. *Organometallics* **2011**, 30, 21, 5649-5655.
- 10 Ahrens, S.; Zeller, A.; Taige, M.; Strassner, T. *Organometallics* **2006**, 25, 22, 5409-5415.
- 11 Viciano, M.; Poyatos, M.; Sanaú, M.; Peris, E.; Rossin, A.; Ujaque, G.; Lledós, A. *Organometallics* **2006**, 25, 5, 1120-1134.
- 12 Marshall, C.; Ward, M. F.; Harrison, W. T. A. *J. Organomet. Chem.* **2005**, 690, 17, 3970-3975.
- 13 Coberán, R.; Mas-Marzá, E.; Peris, E. *Eur. J. Inorg. Chem.* **2009**, 13, 1700-1716.
- 14 Vargas, V. C.; Rubio, R. J.; Hollis, T. K.; Salcido, M. E. *Org. Lett.* **2003**, 5, 25, 4847-4849.
- 15 Bessel, M.; Rominger, F.; Straub, B. F. *Synthesis* **2010**, 9, 1459-1466.
- 16 Marshall, C.; Ward, M. F.; Skakle, J. M. S. *Synthesis* **2006**, 6, 1040-1044.
- 17 Dyson, G.; Frison, J. -F.; Whitwood, A. C.; Douthwaite, R. E. *Dalton Trans.* **2009**, 7141-7151.

- 18 Alcade, E.; Ceder, R. M.; López, C.; Mesquida, N.; Muller, G.; Rodríguez, S. *Dalton Trans.* **2007**, 2696-2706.
- 19 Bessel, M.; Rominger, F.; Straub, B. F. *Synthesis* **2010**, 9, 1459-1466.
- 20 Paczal, A.; Bényei, A. C.; Kotschy, A. *J. Org. Chem.* **2006**, 71, 16, 5969-5979.
- 21 Kuhn, K. M.; Grubbs, R. H. *Org. Lett.* **2008**, 10, 10, 2075-2077.
- 22 Liu, J.; Chen, J.; Zhao, J.; Zhao, Y.; Li, L.; Zhang, H. *Synthesis* **2003**, 17, 2661-2666.
- 23 Cotton, F. A.; Lei, P.; Murillo, C. A.; Wang, L. -S. *Inorganica Chimica Acta* **2003**, 349, 165-172.
- 24 Boyd, P. D. W.; Edwards, A. J.; Gardiner, M. G.; Ho, C. C.; Lemée-Cailleau, M. -H.; McGuinness, D. S.; Riapanitra, A.; Steed, J. W.; Stringer, D. N.; Yates, B. F. *Angew. Chem. Int. Ed.* **2010**, 49, 36, 6315-6318.
- 25 Gardiner, M. G.; Herrmann, W. A.; Reisinger, C. -P.; Schwarz, J.; Spiegler, M. *J. Organomet. Chem.* **1999**, 572, 2, 239-247.
- 26 Nielsen, D. J.; Cavell, K. J.; Skelton, B. W.; White, A. H. *Organometallics* **2006**, 25, 20, 4850-4856.
- 27 Liu, B.; Liu, X.; Chen, C.; Chen, C.; Chen, W. *Organometallics* **2012**, 31, 1, 282-288.
- 28 Baker, M. V.; Brown, D. H.; Simpson, P. V.; Skelton, B. W.; White, A. H.; Williams, C. C. *J. Organomet. Chem.* **2006**, 691, 26, 5845-5855.
- 29 Özdemir, I.; Demir, S.; Gürbüz, N.; Çetinkaya, B.; Toupet, L.; Bruneau, C.; Dixneuf, P. H. *Eur. J. Inorg. Chem.* **2009**, 13, 1942-1949.
- 30 Azua, A.; Mata, J. A.; Peris, E.; Lamaty, F.; Martinez, J.; Colacino, E. *Organometallics* **2012**, 31, 10, 3911-3919.
- 31 Horn, S.; Gandolfi, C.; Albrecht, M. *Eur. J. Inorg. Chem.* **2011**, 18, 2863-2868.
- 32 Coberán, R.; Peris, E. *Organometallics* **2008**, 27, 8, 1954-1958.
- 33 Herrmann, W. A.; Elison, M.; Fischer, J.; Köcher, C.; Artus, G. R. *J. Angew. Chem. Int. Ed.* **1995**, 34, 21, 2371-2374.
- 34 Gaillard, S.; Slawin, A. M. Z.; Nolan, S. P. *Chem. Comm.* **2010**, 46, 2742-2744.
- 35 Díez-González, S.; Stevens, E. D.; Scott, N. M.; Petersen, J. L.; Nolan, S. P. *Chem. Eur. J.* **2007**, 14, 1, 158-168.
- 36 Silbestri, G. F.; Flores, J. C.; Jesús, E. *Organometallics* **2012**, 31, 8, 3355-3360.

- 37 Berthon-Gelloz, G.; Buisine, O.; Brière, J. -F.; Michaud, G.; Stérin, S.; Mignani, G.; Tinant, B.; Declercq, J. -P.; Chapon, D.; Markó, I. E. *J. Organomet. Chem.* **2005**, 690, 6156-6168.
- 38 Sprengers, J. W.; Mars, M. J.; Duin, M. A.; Cavell, K. J.; Elsevier, C. J. *J. Organomet. Chem.* **2003**, 679, 2, 149-152.
- 39 Mayr, M.; Wurst, K.; Ongania, K. -H.; Buchmeiser, M. R. *Chem. Eur. J.* **2004**, 10, 1256-1266.
- 40 Iglesias, M.; Beetstra, D. J.; Knight, J. C.; Ooi, L. -L.; Stasch, A.; Coles, S.; Male, L.; Hursthouse, M. B.; Cavell, K. J.; Dervisi, A.; Fallis, I. A. *Organometallics* **2008**, 27, 13, 3279-3289.
- 41 Dunsford, J. J.; Cavell, K. J. *Dalton Trans.* **2011**, 40, 9131-9135.
- 42 Binobaid, A.; Iglesias, M.; Beetstra, D.; Dervisi, A.; Fallis, I. A.; Cavell, K. J. *Eur. J. Inorg. Chem.* **2010**, 34, 5426-5431.
- 43 Alder, R. W.; Blake, M. E.; Bortolotti, C.; Bufali, S.; Butts, C. P.; Linehan, E.; Oliva, J. M.; Orpen, A. G.; Quayle, M. J. *Chem. Comm.* **1999**, 241-242.
- 44 Jazzar, R.; Liang, H.; Donnadiou, B.; Bertrand, G. *J. Organomet. Chem.* **2006**, 691, 14, 3201-3205.
- 45 Drake, N. L.; Garman, J. A. *J. Am. Chem. Soc.* **1949**, 71, 7, 2425-2427.
- 46 Popkov, S. V.; Skvortsova, M. N. *Russ. Chem. Bull. Int. Ed.* **2006**, 55, 10, 1848-1851.
- 47 Harjani, J. R.; Friščić, T.; MacGillivray, L. R.; Singer, R. D. *Dalton Trans.* **2008**, 4595-4601.
- 48 Herrmann, W. A.; Schneider, S. K.; Öfele, K.; Sakamoto, M.; Herdtweck, E. *J. Organomet. Chem.* **2004**, 689, 15, 2441-2449.
- 49 Herrmann, W. A.; Reisinger, C. -P.; Spigler, M. *J. Organomet. Chem.* **1998**, 557, 93-96.
- 50 Bonnette, F.; Kato, T.; Destarac, M.; Mignani, G.; Cossío, F. P.; Baceiredo, A. *Angew. Chem. Int. Ed.* **2007**, 46, 45, 8632-8635.
- 51 Hollóczki, O.; Terleczy, P.; Szieberth, D.; Mourgas, G.; Gudat, D.; Nyulászi, L. *J. Am. Chem. Soc.* **2011**, 133, 4, 780-789.
- 52 Abdellah, I.; Lepetit, C.; Canac, Y.; Duhayon, C.; Chauvin, R. *Chem. Eur. J.* **2010**, 16, 44, 13095-13108.

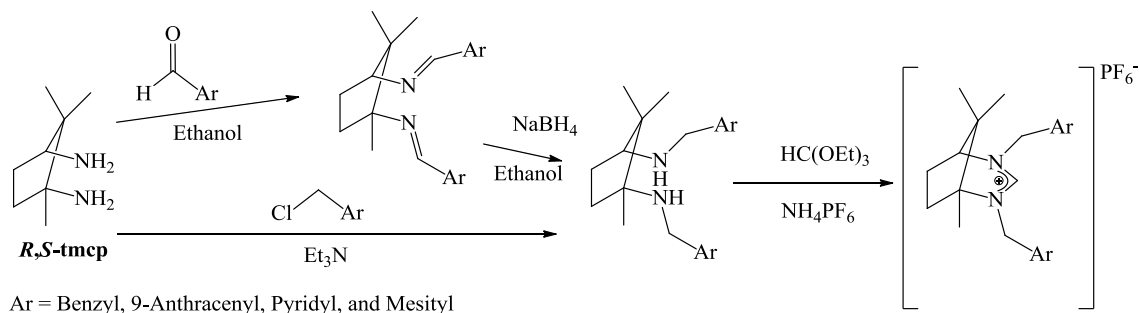
- 53 Zuo, W.; Braunstein, P. *Dalton Trans.* **2012**, 41, 636-643.
- 54 Denk, M. K.; Rodezno, J. M.; Gupta, S.; Lough, A. J. *J. Organomet. Chem.* **2001**, 617-618, 242-253.
- 55 Mao, P.; Yang, L.; Xiao, Y.; Yuan, J.; Liu, X.; Song, M. *J. Organomet. Chem.* **2012**, 705, 39-43.
- 56 Mao, P.; Liu, X.; Yang, L.; Yuan, J.; Song, M. *Acta Cryst.* **2011**, E67, m62.
- 57 Perrin, D. D.; Amarego, W. F. A. *Purification of Laboratory Chemicals*; Pergamon: Oxford, **1988**.
- 58 COLLECT; Nonius BV: Delft, The Netherlands, **1998**.
- 59 Otwinowski, Z.; Minor, W. *Methods Enzymol.* **1997**, 276, 307-326.
- 60 Altomare, A.; Cascarano, G.; Giacovazzo, C.; Guagliardi, A. *J. Appl. Crystallogr.* **1993**, 26, 343-350.
- 61 Sheldrick, G. M. *Acta Crystallogr. Sect. A* **2008**, A64, 112-122.
- 62 Blessing, R. H. *Acta Crystallogr. Sect. A* **1995**, 51, 33-38.

3. Synthesis of Novel Bicyclic N-Heterocyclic Carbenes and Their Coordination to Rhodium

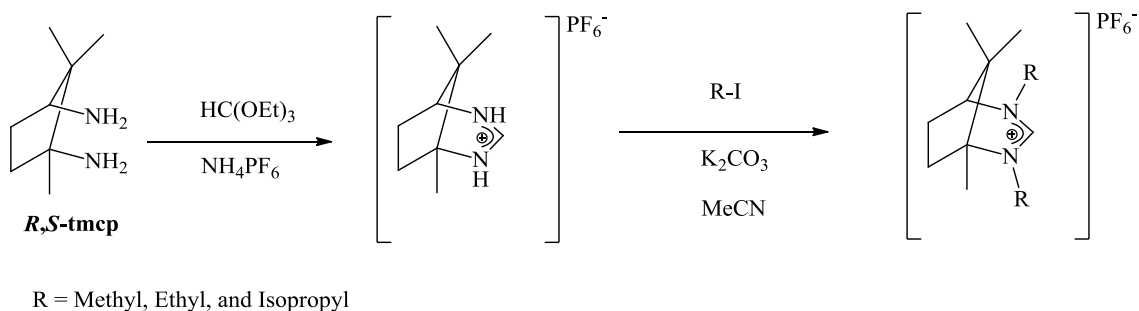
3.1: Introduction

There has been extensive research carried out into NHCs over recent years as shown in Chapter 1. However it has only been in more recent years that the interest has extended from 5-membered rings, their coordination to metals and catalytic reactions, to how expanded ring NHC architectures can be employed for coordination and catalysis.¹⁻³ It is not that well understood how the larger of the expanded rings, 7- and 8-membered, NHCs behave with only a few reports mostly from the Cavell⁴⁻⁶ and Stahl^{7,8} groups being reported. However, it is known that as the ring size increases there is an increase in basicity and therefore nucleophilicity along with a greater impact from steric demand, in turn causing larger NCN bond angles.^{4,5,9,10} The interest in the last few years has extended further to the behaviour of bicyclic NHCs, which contain at least one expanded ring, this is due to the prominent features of the bicyclic ring, where the ring is rigid, and therefore, unlike the expanded ring NHCs, will not twist in conformation to enable coordination. These ligand systems were first introduced by Wilhelm,¹¹ and Newman^{12,13} who reported the synthesis, coordination, and catalytic activity of a series of novel bicyclic N-heterocyclic carbenes.

There are two main synthetic routes to bicyclic NHC precursors, which are derived from camphoric acid via a Schmidt reaction with sodium azide yielding 1*R*-2*S*-diamino-1,2,2-trimethylcyclopentane (*R,S*-tmcp) as shown in Scheme 1 and 2.^{11,14-16} The first route involves the initial modification of the diamine through alkylation of the nitrogen proceeded by ring closure, as used by Wilhelm¹¹ and Newman,¹² shown in Scheme 1, whereas the second involves an initial ring closure and subsequent introduction of the exo N-substituents as shown in Scheme 2.



Scheme 1: First synthetic route to bicyclic NHC precursors.^{11,12}



Scheme 2: Second synthetic route to bicyclic NHC precursors.

There has been literature reported on a series of the bicyclic NHC precursors with successful coordinations to silver,¹² rhodium,^{12,13} iridium,^{12,13} nickel,¹² and copper¹⁷ with a few examples of these shown in Figure 1. Some applications of these complexes have also been noted.

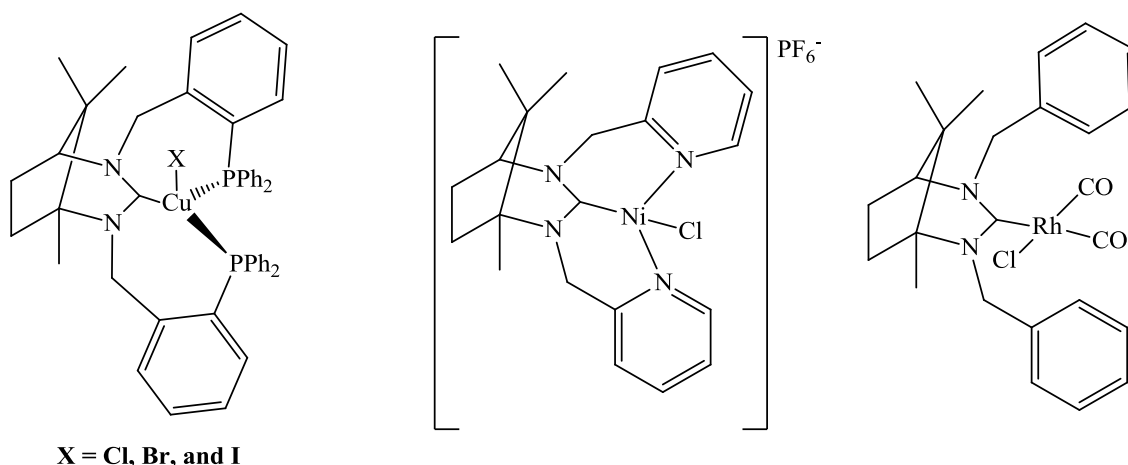


Figure 1: Three examples of bicyclic NHCs coordinated to metals.^{12,17}

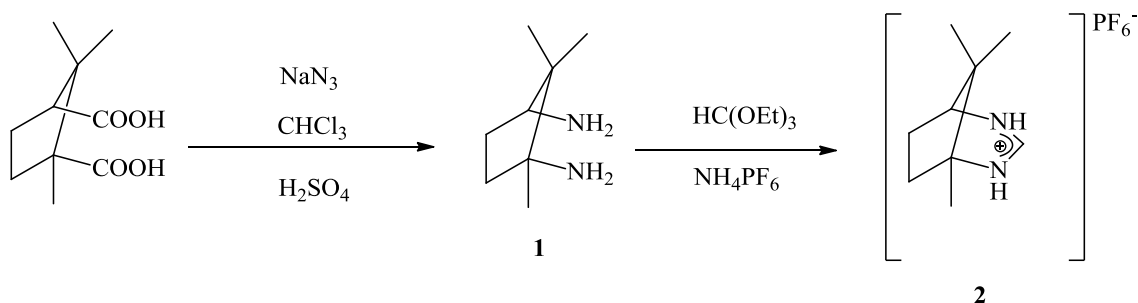
3.2: Results and Discussion

The few reports of bicyclic NHCs having the camphor-derived framework have benzylic type substituents and we were interested in exploring the related systems with simple alkyl groups in place of the benzylic functions. Therefore, the work in this chapter will concentrate on the synthesis of novel alkyl bicyclic ligands and their ability to coordinate. The metal which will be employed here will be rhodium, this is because complexation requires simple procedures, which are well explored in respect to coordination to NHCs.^{5,6,10,12,18,19} The complexes are usually stable to air and therefore simple to handle, and rhodium NHC compounds have been shown to possess excellent catalytic properties.^{13,19-22}

3.2.1: Synthesis and Characterisation of Alkylated Bicyclic NHC Ligands

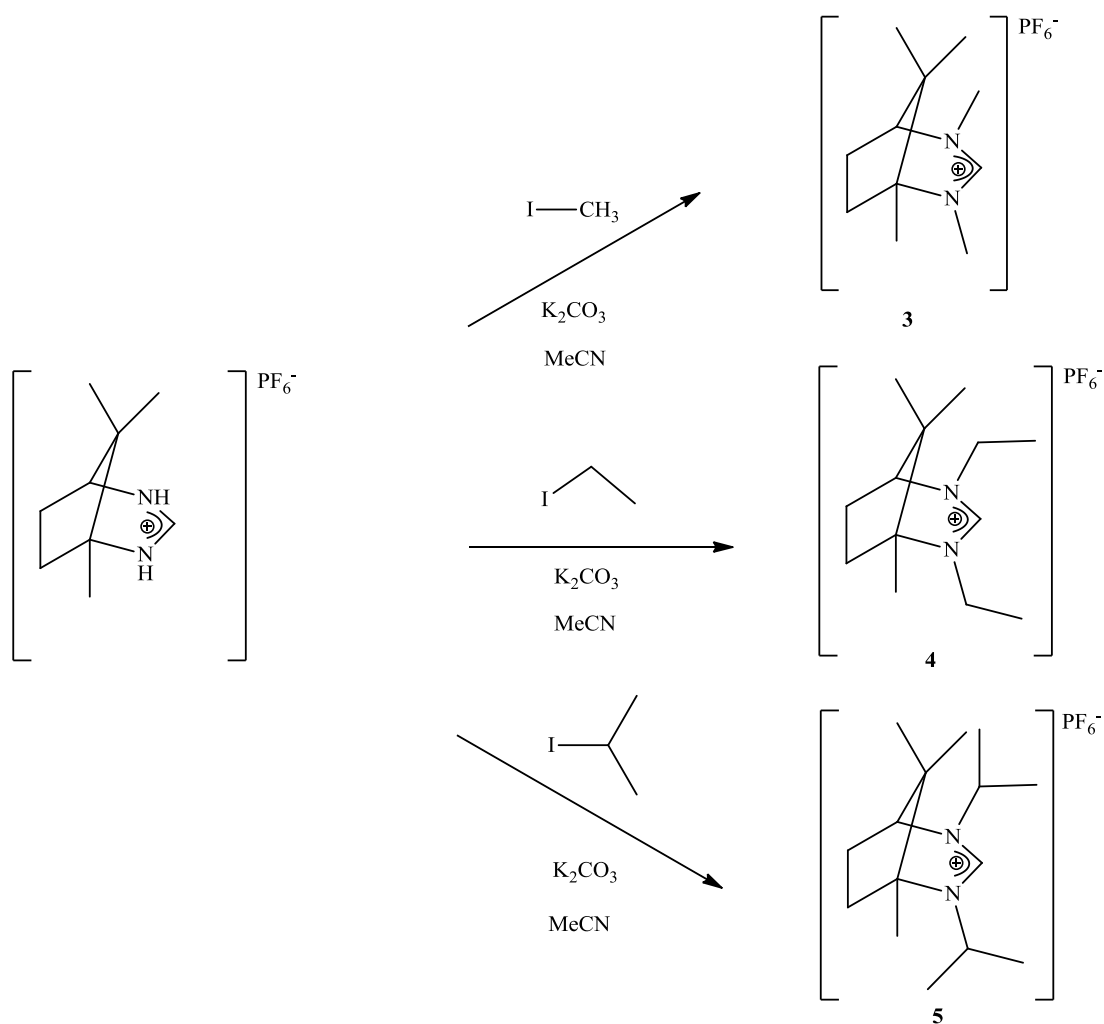
The route to the pro-ligands is shown in Scheme 3, and begins with a Schmidt reaction¹⁶ converting camphoric acid to the corresponding diamine (**1**). This is then followed by a

subsequent ring closure with triethyl orthoformate and ammonium hexafluorophosphate in equal amounts forming **2**.



Scheme 3: Synthesis of **2**.¹⁶

The ring closure was successful as shown by the appearance of the NCHN peak in both the carbon-13 NMR and proton NMR spectra at 151.4 ppm and 7.95 ppm respectively. Since the nitrogens in **2** are sufficiently reactive in the presence of a base, the alkyl derivatives were synthesised by deprotonation of the nitrogens, using potassium carbonate, and subsequent reaction with alkyl halides to form the alkyl derivatives, this was carried out in a similar way to that described by Dunsford²³ for the alkylation of the 6- and 7-membered expanded ring derivatives. The compounds synthesised are the methyl, ethyl, and isopropyl derivatives, **3-5**, as shown in Scheme 4.



Scheme 4: Synthesis of alkyl bicyclic NHC precursors, **3-5**.

Compounds **3-5** were fully characterised using ^1H NMR and $^{13}\text{C}\{^1\text{H}\}$ NMR spectroscopy, mass spectrometry, and single crystal X-ray crystallography. The $^{13}\text{C}\{^1\text{H}\}$ NMR spectra show that in all three cases the shift from the starting material is not large, with on average a shift of 1.27 ppm of the carbenic carbon, with **2** appearing at 151.4 ppm and **3**, **4**, and **5** appearing at 154.0 ppm, 153.0 ppm, and 151.0 ppm respectively. The differences in the proton NMR spectra between **3** and **5** for the NCHN peak and that of **2** is quite large, with the NCHN proton appearing at 7.95 ppm for **2** and 8.45 ppm for both **3** and **5** respectively. These shifts can be attributed to the presence of the alkyl moieties. The difference in shift for the NCHN peak between **2**

and **4** is not as large with the peak for **4** appearing at 7.70 ppm. However, other spectral data obtained clarifies the presence of the alkyl moieties. Crystals of **3**, **4**, and **5** were obtained from vapour diffusion of CDCl_3 and diethyl ether over a forty eight hour period. Figures 2, 3, and 4 show the ORTEP plots; Tables 1, 2, and 3 provide selected bond lengths and angles.

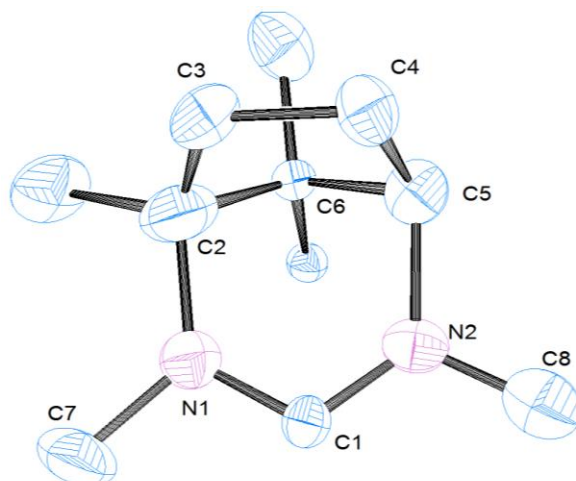


Figure 2: ORTEP ellipsoid plots at 50 % probability of the molecular structure of (5S)-1,2,4,8,8-pentamethyl-2,4-diazabicyclo[3.2.1]octan-2-ium, hexafluorophosphate(V) (**3**), the counterion is omitted for clarity.

Table 1: Selected bond lengths (Å) and angles (°) for (5*S*)-1,2,4,8,8-pentamethyl-2,4-diazabicyclo[3.2.1]octan-2-ium, hexafluorophosphate(V) (**3**).

Lengths (Å)		Angles (°)	
N(1)-C(1)	1.328(15)	N(1)-C(1)-N(2)	115.7(11)
N(2)-C(1)	1.338(15)	C(1)-N(1)-C(7)	108.7(11)
N(1)-C(2)	1.475(19)	C(1)-N(1)-C(2)	121.8(11)
N(1)-C(7)	1.481(18)	N(1)-C(2)-C(3)	124.6(16)
C(2)-C(3)	1.41(3)	C(2)-C(3)-C(4)	108.7(16)
C(3)-C(4)	1.54(2)	C(3)-C(4)-C(5)	104.2(13)
C(4)-C(5)	1.60(2)	C(4)-C(5)-N(2)	109.6(13)
C(5)-N(2)	1.553(18)	N(1)-C(2)-C(6)	101.6(12)
C(2)-C(6)	1.69(3)	C(2)-C(6)-C(5)	92.5(13)
C(6)-C(5)	1.64(2)	C(6)-C(5)-N(2)	99.8(11)
N(2)-C(8)	1.37(2)	C(5)-N(2)-C(8)	125.4(10)
		C(6)-C(5)-C(4)	103.3(13)
		C(6)-C(2)-C(3)	102.8(16)
		C(1)-N(2)-C(8)	118.1(10)
		C(7)-N(1)-C(2)	125.0(12)

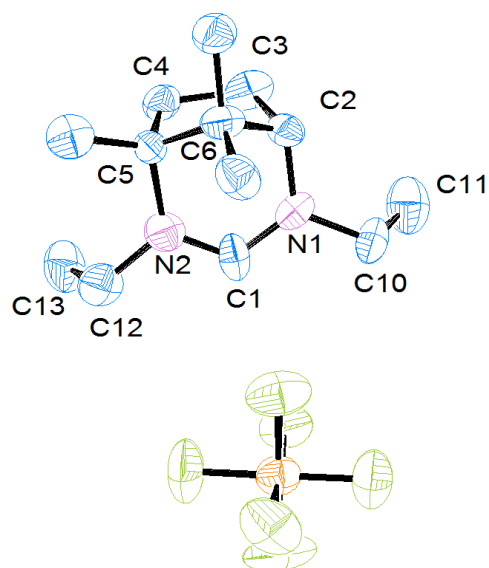


Figure 3: ORTEP ellipsoid plots at 50 % probability of the molecular structure of (1*R*,3*S*)-1,2,2-trimethylcyclopentane-1,3-diamine (5*S*)-2,4-diethyl-1,8,8-trimethyl-2,4-diazabicyclo[3.2.1]octan-2-ium, hexafluorophosphate(V) (**4**).

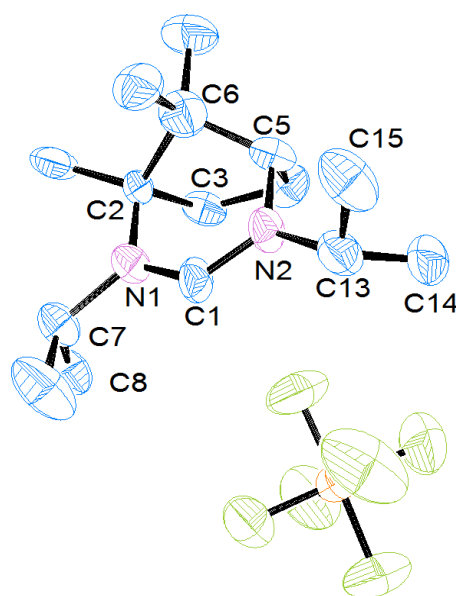


Figure 4: ORTEP ellipsoid plots at 50 % probability of the molecular structure of (5*S*)-2,4-diisopropyl-1,8,8-trimethyl-2,4-diazabicyclo[3.2.1]octan-2-ium, hexafluorophosphate(V) (**5**).

Table 2: Selected bond lengths (Å) and angles (°) for (1R,3S)-1,2,2-trimethylcyclopentane-1,3-diamine (5S)-2,4-diethyl-1,8,8-trimethyl-2,4-diazabicyclo[3.2.1]octan-2-ium, hexafluorophosphate(V) (**4**).

Lengths (Å)		Angles (°)	
N(1)-C(1)	1.328(13)	N(1)-C(1)-N(2)	120.4(11)
N(2)-C(1)	1.311(13)	C(1)-N(2)-C(12)	117.0(10)
N(2)-C(12)	1.474(14)	C(1)-N(2)-C(5)	121.4(10)
C(12)-C(13)	1.554(15)	C(1)-N(1)-C(10)	120.7(10)
N(2)-C(5)	1.533(13)	C(1)-N(1)-C(2)	120.3(9)
C(5)-C(4)	1.515(15)	N(1)-C(10)-C(11)	113.6(11)
C(4)-C(3)	1.571(17)	N(2)-C(12)-C(13)	111.9(10)
C(3)-C(2)	1.575(15)	N(2)-C(5)-C(4)	106.3(9)
C(2)-N(1)	1.460(12)	N(2)-C(5)-C(6)	105.1(9)
N(1)-C(10)	1.469(14)	C(5)-C(4)-C(3)	106.1(8)
C(10)-C(11)	1.493(17)	C(4)-C(3)-C(2)	103.1(9)
C(5)-C(6)	1.5649(15)	C(3)-C(2)-N(1)	106.9(8)
C(6)-C(2)	1.518(16)	N(1)-C(2)-C(6)	109.5(9)
		C(2)-C(6)-C(5)	99.4(9)

Table 3: Selected bond lengths (Å) and angles (°) for (5*S*)-2,4-diisopropyl-1,8,8-trimethyl-2,4-diazabicyclo[3.2.1]octan-2-ium, hexafluorophosphate(V) (**5**).

Lengths (Å)		Angles (°)	
N(1)-C(1)	1.303(12)	N(1)-C(1)-N(2)	124.6(9)
N(2)-C(1)	1.313(12)	C(1)-N(1)-C(7)	121.9(9)
N(1)-C(7)	1.481(12)	C(1)-N(1)-C(2)	118.2(8)
N(1)-C(2)	1.516(12)	N(1)-C(7)-C(8)	112.8(8)
C(7)-C(8)	1.507(12)	N(1)-C(7)-C(9)	112.7(8)
C(7)-C(9)	1.514(13)	N(1)-C(2)-C(3)	107.9(8)
C(2)-C(3)	1.549(13)	C(2)-C(3)-C(4)	105.8(7)
C(2)-C(6)	1.545(14)	C(3)-C(4)-C(5)	104.9(8)
C(6)-C(5)	1.532(15)	C(4)-C(5)-N(2)	109.9(8)
C(3)-C(4)	1.529(13)	C(5)-N(2)-C(1)	118.3(8)
C(4)-C(5)	1.541(12)	C(1)-N(2)-C(13)	119.8(9)
C(5)-N(2)	1.468(12)	N(2)-C(13)-C(14)	110.8(8)
N(2)-C(13)	1.469(12)	N(2)-C(13)-C(15)	110.3(9)
C(13)-C(14)	1.521(14)		
C(13)-C(15)	15.37(14)		

The crystal structure data, shown in Figures 2-4 and Tables 1-3, along with the distinctive peaks in the ^1H NMR and $^{13}\text{C}\{^1\text{H}\}$ NMR spectra and the mass spectra for **3**, **4**, and **5**, which show molecular ion peaks at 181.1708 amu, 209.2021 amu, and 237.2323 amu respectively, which have calculated values of 181.1705 amu, 209.2018 amu, and 237.2331 amu respectively, confirm the successful synthesis in high yields of 65-86 %. The NCN angles quoted for **3-5** are 115.7(11) °, 120.4(11) °, and 124.6(9) ° respectively. Between **3** and **5** there is an apparent increase, of the NCN angle, of 8.9 °, this can be attributed to the increase of steric demand from the different alkyl substituents, however due to the errors within the measurements these differences can

be considered negligible. The salt **3** has an NCN bond angle similar to that reported for 5-membered rings, whereas, **4** and **5** have angles similar to those reported for 6- and 7-membered rings as shown in Table 4. From the data shown in Table 4 it is apparent that as the steric demand increases so does the N-C_{NHC} bond length, this is apparent with **3** having similar lengths to that of the 5-Mes, with lengths of around 1.33 Å. This differs from that of **4**, **5**, and the expanded ring NHCs which have been reported where they exhibit lengths of around 1.31 Å. Within the error of the bond lengths this difference is negligible however the small observed changes can be attributed to influence of steric demand, this is also shown with the increase in C_{NHC}-N-C_R angles, where R = aryl and alkyl derivatives, with steric hindrance. In **3-5** the C_{NHC}-N-C_R angle increases in size from 118.1(10) ° to 120.7(10) °, this is a total increase of 2.6 °. This increase is not in accordance with the difference between the 5-membered and the 8-membered analogues reported, shown in Table 4, where the 5-membered has the largest C_{NHC}-N-C_R angle and the 8-membered has the smallest, which shows steric impact imparted by the N-substituents on the C_{NHC} centre, although within the error of the measurements this difference can be considered negligible. This is not as clearly shown in the bicyclic systems **3-5**, showing 118.1(10) °, 120.7(10) °, and 119.8(9) ° respectively, this is due to the extra steric hindrance from the methyl moiety in the backbone of the NHCs. However the diisopropyl derivative, **5**, has very similar steric bulk to that of the reported 6-*i*Pr.BF₄ and the 7-*i*Pr.HI salts shown in Table 4. This is not however the only aspects which influence these angles, ring size and flexibility are also considered to be contributing factors. The 7-membered NHCs appear to have a greater ability than the 6-membered NHCs to change the ring conformation to incorporate the N-substituents, the 8-membered NHCs do this to such a great extent that the backbone of the NHC is neatly folded over the central NHC carbon. Although the expanded ring NHCs have this capability, the bicyclic ring NHCs are very constrained due to their bicyclic nature, which will have an exacerbated influence on the angles mentioned above.

Table 4: Selected bond angles and lengths of **3-5** and their comparison to known literature.

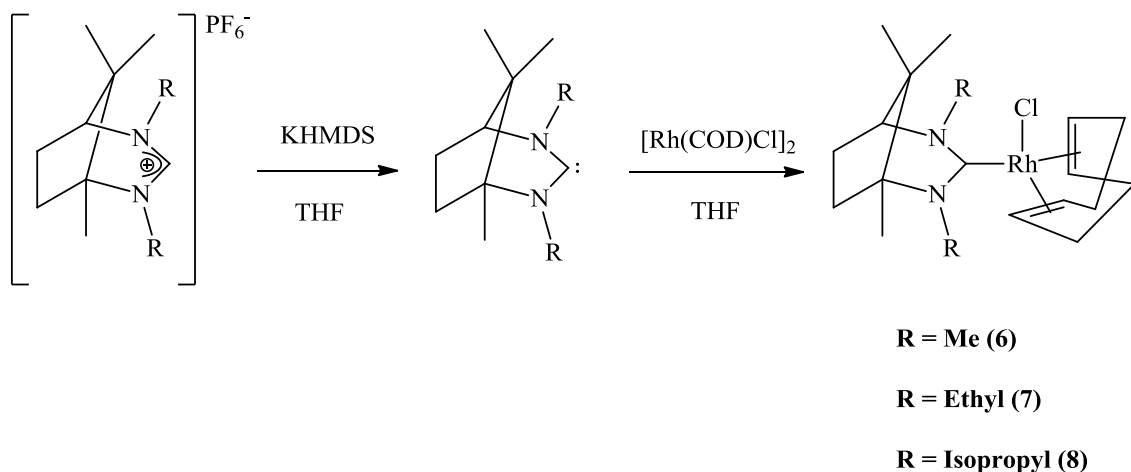
Compound	NCN Angle (°)	C _{NHC} -N-C _R (°)	N-C _{NHC} , N1-C1, N2, C1, distance (Å)
3	115.7(11)	118.1(10)	1.328(15), 1.338(15)
4	120.4(11)	120.7(10)	1.328(13), 1.311(13)
5	124.6(9)	119.8(9)	1.303(12), 1.313(12)
5-Mes ²⁴	113.1(4)	127.0(4)	1.327(5), 1.310(5)
6-iPr.BF₄ ²⁵	125.1(2)	119.6(2)	1.311(3), 1.310(2)
6-Mes.BF₄ ²⁶	124.72(15)	120.38(11)	1.3147(14), 1.3147(14)
7-iPr.HI ²³	130.2	118.5(13)	1.316(18), 1.310(17)
7-Cy.HPF₆ ²⁷	127.35(15)	118.11(13)	1.316(2), 1.318(2)
8-Mes ⁶	131.3(4)	115.8(3)	1.308(6), 1.490(4)

The steric bulk which is being exhibited by the bicyclic ligands, **3-5**, may have an effect on the coordination sphere when synthesising the metal complexes.

3.2.2: Coordination of Aliphatic Bicyclic NHC Precursors to Rhodium

Since the aryl bicyclic NHCs have been reported to coordinate to rhodium^{12,13} successfully in moderate yields, the same reactions were carried out with the novel alkyl bicyclic precursors, **3-5**. These reactions involved forming the free carbene from the NHC·HPF₆ salt, and 1.4 equivalents of KHMDS in THF. The free carbene was then

reacted with $[\text{Rh}(\text{COD})\text{Cl}]_2$ to form the corresponding rhodium complexes, **6-8**, as shown in Scheme 5.



Scheme 5: Synthesis of rhodium complexes **6-8**.

Compounds **6-8** were fully characterised using ^1H NMR and $^{13}\text{C}\{^1\text{H}\}$ NMR spectroscopy, mass spectrometry, and in the case of **6** through determination of its molecular structure by single crystal X-ray crystallography. From the proton NMR spectra of all three compounds it is clear to see that there are two isomers present in an approximately 2:1 ratio as shown in Figure 5, this is similar to that observed for the expanded ring NHCs reported by Iglesias.²⁸ Similar types of isomerisation are exhibited in the tridentate pyridyl analogues reported by Newman *et al.*¹² It is thought that this isomerisation is caused by the restricted rotation about the Rh-C_{NHC} bond; this causes two very different products, which in turn have different proton and carbon-13 NMR spectra. One of these products is isolated in the solid state as shown by the crystal structure in Figure 6. Here the C(6) carbon and its methyl groups lie *syn* to the *cis*-alkene of the COD. The second product, is where the C(6) carbon and its methyl groups lie *syn* to the *cis*-chloride.

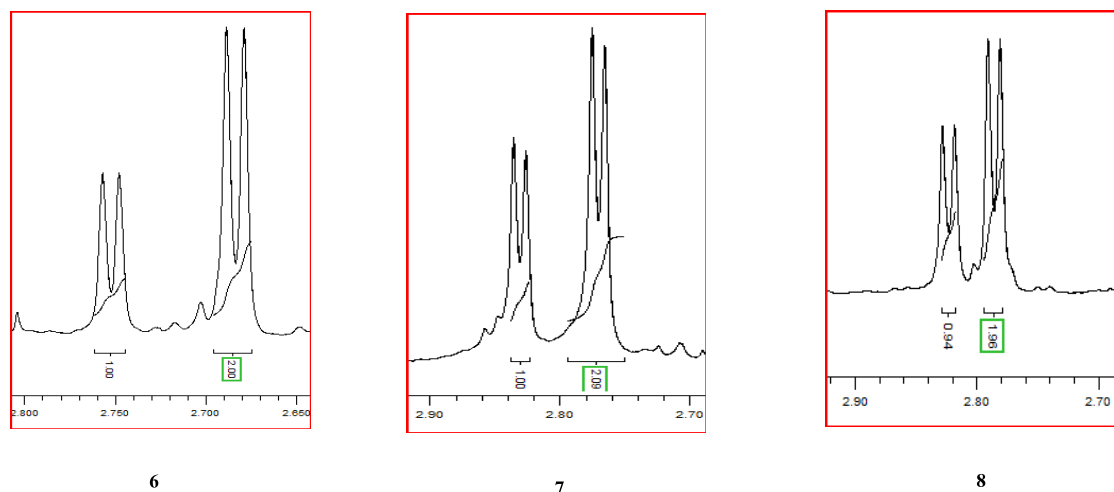


Figure 5: A section of the NMR spectra of **6-8** showing the 2:1 ratios of the NCH bridgehead proton.

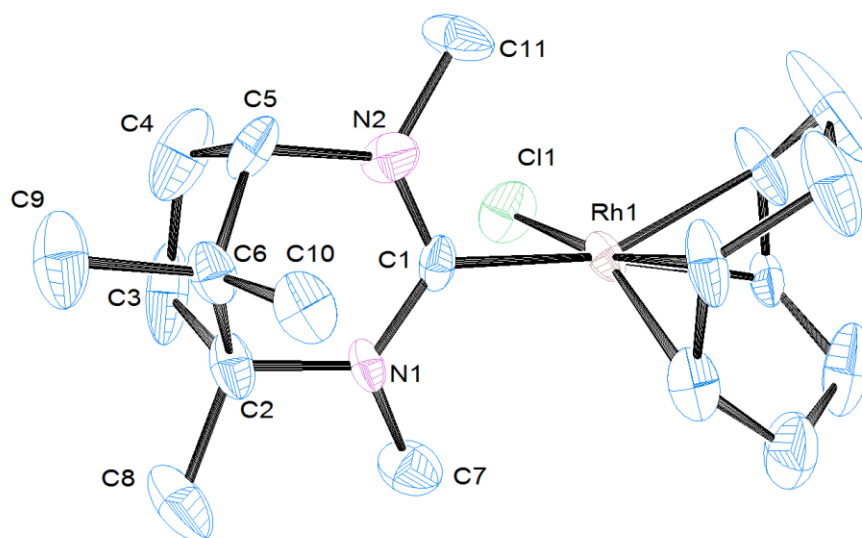


Figure 6: ORTEP ellipsoid plots at 50 % probability of the molecular structure of (5*S*)-2,4-dimethyl-1,8,8-trimethyl-2,4-diazabicyclo[3.2.1]octan-3-yl) rhodium (cyclooctadiene) chloride (**6**).

Table 5: Selected bond lengths (Å) and angles (°) for (5*S*)-2,4-dimethyl-1,8,8-trimethyl-2,4-diazabicyclo[3.2.1]octan-3-yl rhodium (cyclooctadiene) chloride (**6**).

Lengths (Å)		Angles (°)	
N(1)-C(1)	1.343(12)	N(1)-C(1)-N(2)	118.4(9)
N(2)-C(1)	1.323(12)	C(1)-N(1)-C(7)	118.9(8)
N(1)-C(7)	1.459(13)	C(1)-N(1)-C(2)	121.6(9)
N(1)-C(2)	1.490(11)	N(1)-C(2)-C(8)	111.3(11)
C(2)-C(3)	1.554(16)	N(1)-C(2)-C(3)	106.8(8)
C(2)-C(6)	1.550(15)	N(1)-C(2)-C(6)	107.8(8)
C(2)-C(8)	1.535(17)	C(2)-C(3)-C(4)	105.1(10)
C(3)-C(4)	1.565(19)	C(2)-C(6)-C(5)	98.4(8)
C(4)-C(5)	1.527(15)	C(3)-C(4)-C(5)	103.5(10)
C(5)-N(2)	1.482(14)	C(4)-C(5)-N(2)	108.1(9)
C(5)-C(6)	1.524(15)	C(4)-C(5)-C(6)	105.5(10)
N(2)-C(11)	1.462(13)	C(6)-C(5)-N(2)	108.2(8)
C(1)-Rh(1)	2.049(10)	C(5)-N(2)-C(1)	121.2(9)
Rh(1)-Cl(1)	2.366(3)	C(5)-N(2)-C(11)	115.5(9)
		C(2)-N(1)-C(7)	118.2(8)
		N(1)-C(1)-Rh(1)	124.0(8)
		N(2)-C(1)-Rh(1)	117.6(8)
		C(1)-Rh(1)-Cl(1)	86.6(3)

The crystal structure data found in Table 5 reveals that upon complexation, within the error of the measurements, the NCN bond angle does not change due to having values of 115.7(11) ° in the amidinium salt (**3**) and 118.4(9) ° in the rhodium complex (**6**).

The isomers are also observed in all three of the $^{13}\text{C}\{^1\text{H}\}$ NMR spectra where all of the peaks are duplicated in a 2:1 ratio, with the major isomer NCN-Rh peaks, for **6-8**,

appearing at 205.1 ppm, 203.6 ppm, 203.9 ppm respectively. All three compounds show doublets in the carbon-13 NMR spectra for the NCN-Rh peaks, since the carbon couples to the rhodium, the $^1J_{\text{Rh-C}}$ values, for the major isomers, were observed to be 46.5 Hz, 40.0 Hz, and 43.8 Hz for **6-8** respectively.

Table 6: Comparative data for **6-8** with literature values of 5-, 6-, 7-, and 8-membered analogues.^{5,6}

Compound	NCN angle (°)	NCN-Rh bond length (Å)	NCN-Rh peak in the $^{13}\text{C}\{^1\text{H}\}$ NMR spectrum (ppm)	$^1J_{\text{Rh-C}}$ (Hz)
6	118.4(9)	2.049(10)	205.1	46.5
7	-	-	203.6	40.0
8	-	-	203.9	43.8
Rh(5-Mes)(COD)Cl	107.29(12)	2.0513(14)	211.6	48.2
Rh(6-Mes)(COD)Cl	117.0(4)	2.078(4)	211.5	46.9
Rh(7-Mes)(COD)Cl	118.0(3)	2.085(3)	224.0	46.7
Rh(7-<i>o</i>-tolyl)(COD)Cl	117.2(3)	2.030(3)	222.8	45.0
Rh(8-<i>o</i>-tolyl)(COD)Cl	121.3(2)	2.061(3)	215.9	45.0

The carbon-13 NMR spectra of compounds **6-8** show that the NCN-Rh peak appears at 205.1 ppm, 203.6 ppm, and 203.9 ppm respectively, which are slightly upfield in comparison to the 5-, 6-, 7-, and 8-membered complexes as shown in Table 6. They are also significantly downfield in comparison to their amidinium salts, which appear at 154.0 ppm, 153.0 ppm, and 151.0 ppm for **3-5** respectively, which is a sign of

complexation. However the shift between amidinium salt and complex is not the most pertinent data obtainable from the carbon-13 NMR spectra as the shift observed between the free carbene and the complex is. This data was not obtained for **6-8** due to the *in situ* route to the complex.

The shift in the carbon-13 NMR data can also be an indication of how much σ -donating capability the NHC ligand has, this is due to the more downfield the carbon-13 NMR shift the more deshielded the NCN carbon will become, in turn producing a greater contribution of electron density towards the metal centre.^{29,30} Therefore with **6-8** having between 8 and 19 ppm shift upfield from their 5-, 6-, 7-, and 8-membered counterparts, Table 6, illustrates that these ligand systems have a slightly less de-shielded NCN carbon and therefore do not contribute as much electron density towards the metal centre as their 5-, 6-, 7- and 8-membered counterparts. The other noticeable difference between the carbon-13 NMR spectra of the salts **3-5** and the rhodium complexes **6-8** is that the NCHN peaks in the salts all appear as singlets, whereas in the complexes, due to coupling with the rhodium, the NCN-Rh peaks appear as doublets with couplings of 46.5 Hz, 40.0 Hz, and 43.8 Hz for **6-8** respectively. The $^1J_{\text{Rh-C}}$ values observed here are in accordance with the reported literature.^{5,6}

Due to the lack of crystallographic data for **7** and **8** it is not possible to say if the steric hindrance has an effect on the NCN angle. However, from data obtained for the NHC salts, Table 4, it is clear that as the steric bulk increases so does the NCN bond angle, therefore the likelihood is that this trend will continue for the metal complexes. From the literature it is also clear that as the ring size increases so does the NCN angle.⁵ It is also apparent that **6** is behaving more like a 6- or 7-membered NHC as the NCN bond angles after coordination are much closer to these values than those of the 5-membered or the 8-membered ring analogues. Although there appears to be large differences between the NCN angles of the different ring sizes, there does not appear to be a great change in the NCN-Rh bond lengths, this is also apparent with **6**, as there is only a 0.04 Å difference between **6** and the largest of the NCN-Rh bond lengths which is that of the Rh(7-Mes)(COD)Cl at 2.085(3) Å.

The mass spectrometry data is also in accordance with the production of **6**, **7**, and **8** due to observed peaks at 432.1882 amu, 460.2190 amu, and 488.2528 amu respectively,

which have calculated values of 432.1886 amu, 460.2199 amu, and 488.2512 amu respectively, which correspond in all three cases to $[M^+ - Cl^- + MeCN]$.

3.2.3: Catalysis

In recent years NHCs have been used as catalysts in many different types of reactions, including hydrosilylation,^{31,32} C-C coupling,²⁹ and transfer hydrogenation²¹ to name just a few. In this chapter the successful synthesis of a series of novel rhodium NHC complexes has been discussed, and it is these complexes which will be used as catalysts in the transfer hydrogenation of ketones. The reason for concentrating on transfer hydrogenations is due to the reported success of these transformations using a variety of NHCs, from 5-membered,³³⁻³⁵ to expanded rings,^{21,23} and to bicyclic NHCs.¹³

There are two proposed mechanisms for the transfer hydrogenation, which route the catalysis will take depends on the metal which is employed. For main group the mechanism is proposed to be a direct hydrogenation, through a concerted process, which forms a 6-membered cyclic transition state, Figure 7, made up of the hydrogen donor, 2-propanol; the hydrogen acceptor, the ketone substrate; and the metal.³⁶

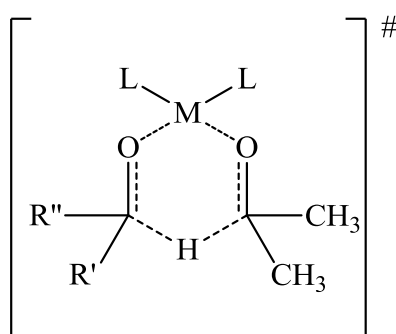
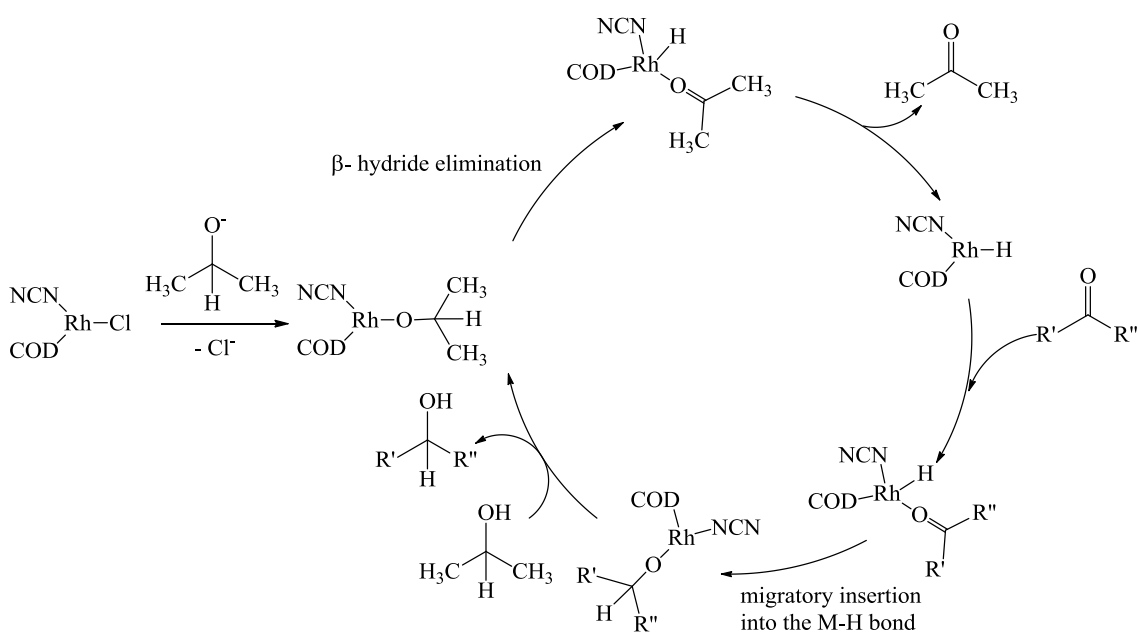


Figure 7: 6-Membered transition state for the direct transfer hydrogenation.

The second pathway is that of the hydride route, which is more common with transition metal complexes, this involves the production of a metal hydride species and is most probably the procedure which the catalysis reported in this chapter will follow. Within this mechanism there are two possible hydride species which could be formed, the mono hydride and the dihydride. It has been theorised using $[\text{Rh}(\text{diamine})(\text{COD})]$ as the catalytically active species that the reaction will predominantly proceed using a monohydride intermediate in a stepwise hydrogen transfer.³⁷



Scheme 6: Hypothesised mechanism for the transfer hydrogenation of ketones.

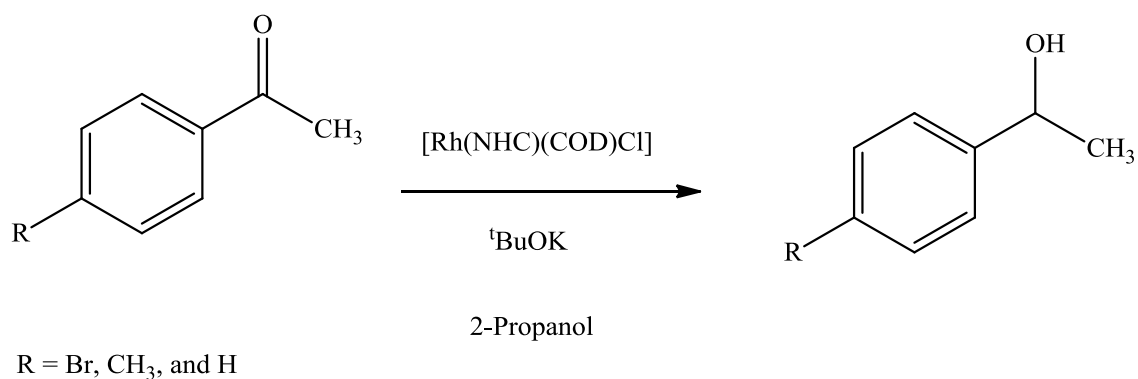
The proposed mechanism for the transfer hydrogenation, using a hydrogen donor such as 2-propanol, is shown in Scheme 6. This starts with the *in situ* generation of an alkoxide species, from the reaction with the $t\text{BuOK}$, which then coordinates to the rhodium complex. This is then followed by a β -hydride elimination to form the metal hydride species, which in turn eliminates acetone; it is this β -hydride elimination process which is the rate determining step. Once the rhodium hydride species has been formed it coordinates with the ketone substrate, which then undergoes a migratory

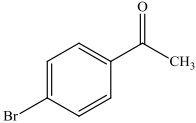
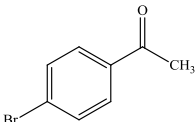
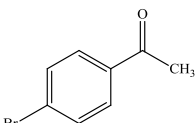
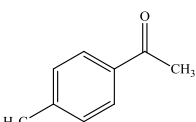
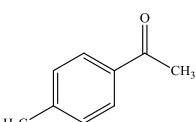
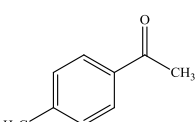
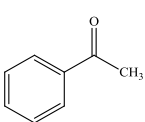
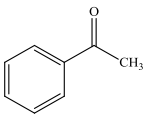
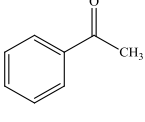
insertion into the rhodium hydride bond followed by an exchange of protons with the 2-propanol solvent releasing the reduction product from the cycle, in turn regenerating the rhodium alkoxide adduct ready for another rotation.

3.2.3.1: Catalytic Activity of Rhodium Bicyclic NHC Complexes

The catalytic procedure employed 0.1 mol % catalyst loading, 2-propanol and potassium tertiary butoxide at 80 °C for 23 hours. Three different substrates were used in this catalysis, 4-bromoacetophenone, 4-methylacetophenone, and acetophenone, these substrates have previously been employed for this type of catalysis when using the 6- and 7-membered rhodium and iridium complexes.^{20,21,23} The previously reported rhodium complexes, when using 4-bromoacetophenone as the substrate, show modest conversions of 63 % and 47 % when 1 mol % and 0.1 mol % catalysts loadings were employed respectively. The rhodium(I) complexes of the 5-, 6-, and 7-Mes saturated complexes show no activity in the transfer hydrogenation process,²¹ which has been attributed to the steric demand of the rhodium complex preventing substrate coordination prior to the reduction by the hydride.²¹

Table 7: Transfer hydrogenation of ketones using catalysts **6-8**.^a



Entry	Catalyst	Substrate	Time (hours)	Yield (%) ^b
1	6		23	23
2	7		23	14
3	8		23	14
4	6		23	37
5	7		23	12
6	8		23	36
7	6		23	22
8	7		23	11
9	8		23	17

^aReaction conditions: Substrate (1 mmol), catalyst (0.1 mol %), 2-propanol (5 ml), ^tBuOK (10 mol %), 80 °C for 23 hours. ^bPercentage yields measured through integrals by ¹H NMR.

As reported by Dunsford,²³ Iglesias,²¹ and Herrmann³⁸ the increase in the amount of catalyst from 0.1 mol % or 0.01 mol % to 1 mol % does not appear to have a large effect, with an increase of only 2 % when using [Ir(6-Neo)(COD)Cl], an increase of 16 % when employing [Rh(7-Cy)(COD)Cl], and an increase of about 10 % when using [Ir(5-Cy)(COD)Cl] as the catalyst. Due to these modest increases in percentage yield the amount of catalyst which has been employed in these catalytic processes is 0.1 mol %. The outcomes were similar to those reported by Dunsford²³ and Iglesias,²¹ with relatively low yields of a maximum of 37 %, which is a significant decrease from the bicyclic NHCs containing a secondary pyridyl donor reported by Newman,¹³ which have conversions of up to 60 % when employing rhodium as the metal, the results for catalysts **6-8** are also a significant decrease from the conversions which have been achieved by similar 5-membered catalysts^{34,38-40} where up to 100 % yields have been observed. A noteworthy point for these results is that on the whole, the less sterically hindered the catalyst the more effective the process, as shown with the methylated catalyst showing the largest percentage yield with all three substrates. However, the least catalytically active species was not the most hindered, it was the moderately hindered catalyst, which employed ethyl N-substituents, **7**, with the lowest yielding result being 11 %. Within the substrates the 4-methylacetophenone appears to have the largest conversions with 37 % and 36 % when employing catalyst **6** and **8** respectively. This can be attributed to the methyl substituent on the benzene ring of the substrate causing an activation of the ring, in turn increasing the yield of the product.^{21,38}

These results are not particularly surprising as it has been reported that the most effective transfer hydrogenation catalysts employ a hemilabile donor, which can facilitate the catalytic process. The other noteworthy feature is that the metal which has been employed in this catalysis is rhodium and it has been shown that iridium is a more successful catalyst than that of its rhodium analogues.^{21,41} The previously reported 5-membered³⁸ and expanded ring complexes of iridium,²¹ with the substrate as acetophenone, the expanded ring [Ir(COD)(7-MeOPh/Mes)Cl] showed to have 100 % conversion when using 1 mol %, yet when the catalyst loading was reduced to 0.1 mol % the conversion also decreased to 82 %, whereas the 5-membered catalyst [Ir(COD)(5-Cy)Cl] shows to have > 95 % yields when a catalyst loading of 1 mol % is employed, however when decreased to 0.01 mol % the conversion drops to about 85 %. This is an

increase of between 14 % and 37 % when iridium is employed as the metal instead of rhodium.

3.3: Conclusions

The overall aim of this section was to synthesise a range of novel bicyclic NHC precursors followed by coordination to rhodium metal.

A range of novel alkyl bicyclic NHCs were synthesised, **3-5**. The NCN angles shown in Tables 1-3, along with the NCHN peaks in the $^{13}\text{C}\{^1\text{H}\}$ NMR of **3-5** being 154.0 ppm, 153.0 ppm, and 151.0 ppm respectively, were all in accordance with the already published aryl bicyclic NHC precursors.

The novel ligands, **3-5**, were coordinated, to rhodium, via the free carbene, forming complexes **6-8**. The data obtained confirmed that a range of novel rhodium NHC complexes had been synthesised. The ^1H NMR and $^{13}\text{C}\{^1\text{H}\}$ NMR spectra of **6-8** show that there are two isomers present for each complex, one which is isolatable as a crystalline solid, as shown in Figure 6 for **6**, and one which is not isolatable as a crystalline solid. The isomer for **6** which was isolated through crystallisation, shows that the C(6) carbon and its methyl groups are *syn* to the *cis*-alkene, the second isomer is therefore where the C(6) carbon and its methyl groups are *syn* to the *cis*-chloride.

The transfer hydrogenation of ketones was carried out using 0.1 mol % of **6-8** as the catalysts. The outcomes were comparable to the reported data in which these reactions are relatively low yielding at this concentration of catalyst with a maximum yield of 37 %. It has also been found that with these complexes, the less sterically hindered the rhodium centre is then the more catalytically active the complexes are, with the methylated N-substituents (**17**) showing the most promising results.

3.4: Experimental

3.4.1: General Remarks

All air sensitive experiments were carried out using standard Schlenk techniques, under an atmosphere of argon or in a MBRAUN M72 glove box (N₂ atmosphere with > 0.1 ppm O₂ and H₂O) unless otherwise stated. Glassware was dried overnight in an oven at 120 °C and flame dried prior to use. Pentane of analytical grade was freshly collected from a MBRAUN sps 800 solvent purification system, THF was dried in a still over calcium hydride. All other solvents were used as purchased.

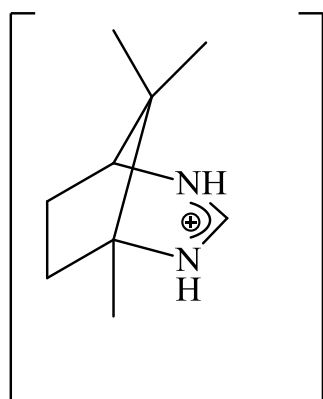
All NMR solvents used were purchased from Goss Scientific Ltd, and distilled from the appropriate drying agents under N₂ prior to use, following standard literature methods.⁴² All NMR spectra were obtained from a Bruker Avance AMX 250, 400, or 500 MHz and referenced to SiMe₄ and coupling constants *J* are expressed in Hertz as positive values regardless of their real individual signs. Mass spectrometry data was recorded, HRMS were obtained on a Waters Q-ToF micromass spectrometer and are reported as *m/z* (relative intensity) by the department of chemistry, Cardiff University.

All the X-ray Crystal structures were obtained on a Bruker Nonius Kappa CCD diffractometer using graphite mono-chromated Mo KR radiation ($\lambda(\text{Mo KR}) = 0.71073 \text{ \AA}$). An Oxford Cryosystems cooling apparatus was attached to the instrument, and all data were collected at 150 K. Data collection and cell refinement were carried out by Dr Benson Kariuki, using COLLECT⁴³ and HKL SCALEPACK.⁴⁴ Data reduction was applied using HKL DENZO and SCALEPACK.⁴⁴ The structures were solved using direct methods (Sir92)⁴⁵ and refined with SHELX-97.⁴⁶ Absorption corrections were performed using SORTAV.⁴⁷

Compound **1** was synthesised by known literature procedures¹⁶ and all other reagents were used as purchased.

3.4.2: Experimental Data for Aliphatic Bicyclic NHC Precursors

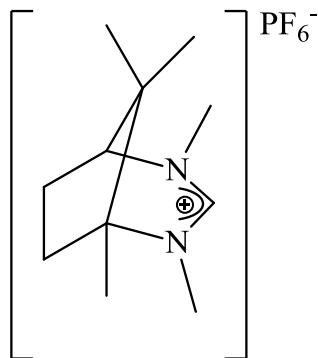
Synthesis of (5S)-1,8,8-trimethyl-2,4-diazabicyclo[3.2.1]octan-2-ium hexafluorophosphate(V) (2)



PF₆⁻ Ammonium hexafluorophosphate (17.34 g, 0.11 mol, 1 eq) was placed into a flask containing (1*R*,3*S*)-1,2,2-trimethylcyclopentane-1,3-diamine (15.00 g, 0.11 mol, 1 eq) and triethylorthoformate (17.77 ml, 0.11 mol, 1 eq). The reaction mixture was then heated to 120 °C for 3 hours. The reaction mixture was then left to cool to room temperature, and the solvents were removed *in vacuo*. The precipitate was then recrystallised from

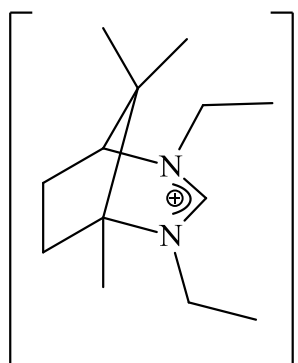
ethanol yielding (5*S*)-1,8,8-trimethyl-2,4-diazabicyclo[3.2.1]octan-2-ium hexafluorophosphate(V) as a white semicrystalline solid (17.70 g, 56.0 %). ¹H NMR (DMSO, 400 MHz, 298 K): δ 7.95 (1 H, s, NCHN), δ 3.35 (1 H, d, NCH, ³J_{HH} = 4.6 Hz), δ 2.20 (1 H, m, CH₂), δ 2.00 (3 H, m, CH₂), δ 1.15 (3 H, s, CH₃), δ 1.05 (3 H, s, CH₃), δ 0.90 (3 H, s, CH₃). ¹³C{¹H} NMR (DMSO, 100 MHz, 298 K): δ 151.4 (NCHN), δ 63.3 (NCH), δ 60.6 (NC), δ 42.2 (C), δ 38.3 (CH₂), δ 33.6 (CH₂), δ 20.3 (CH₃), δ 16.8 (CH₃), δ 16.0 (CH₃). MS (ES) *m/z*: [M⁺] 153.1396 (C₉H₁₇N₂ requires 153.1392).

Synthesis of (5S)-1,2,4,8,8-pentamethyl-2,4-diazabicyclo[3.2.1]octan-2-ium hexafluorophosphate(V) (3)



(5S)-1,8,8-trimethyl-2,4-diazabicyclo[3.2.1]octan-2-ium hexafluorophosphate(V) (0.50 g, 1.68 mmol, 1 eq) was placed in a pressure tube and potassium carbonate (0.56 g, 4.03 mmol, 2.4 eq), methyl iodide (0.52 ml, 8.39 moles, 5 eq), and acetonitrile (10 ml) were added. The pressure tube was then sealed and heated to 90 °C for 5 days. The pressure tube was then cooled slowly to room temperature the acetonitrile was removed on a rotary evaporator, the remaining solid was dissolved in DCM (50 ml), filtered to remove the base, and evaporated to dryness yielding (5S)-1,2,4,8,8-pentamethyl-2,4-diazabicyclo[3.2.1]octan-2-ium hexafluorophosphate(V) as a white semicrystalline solid (0.36 g, 65.8 %). ^1H NMR (CDCl_3 , 500 MHz, 298 K): δ 8.45 (1 H, s, NCHN), δ 3.25 (3 H, s, NCH₃), δ 3.15 (3 H, s, NCH₃), δ 3.00 (1 H, d, NCH, $^3J_{\text{HH}} = 5.0$ Hz), δ 2.50 (1 H, m, CH), δ 2.25 (1 H, m, CH), δ 2.05 (1 H, m, CH), δ 1.85 (1 H, m, CH), δ 1.25 (3 H, s, CH₃), δ 1.10 (3 H, s, CH₃), δ 1.05 (3 H, s, CH₃). $^{13}\text{C}\{^1\text{H}\}$ NMR (CDCl_3 , 125 MHz, 298 K): δ 154.0 (NCHN), δ 69.5 (NC), δ 69.0 (NCH), δ 41.0 (C), δ 40.5 (CH₃), δ 38.5 (CH₂), δ 37.0 (CH₃), δ 31.0 (CH₂), δ 22.0 (CH₃), δ 17.0 (CH₃), δ 14.0 (CH₃). MS (ES) m/z : [M^+] 181.1708 ($\text{C}_{11}\text{H}_{21}\text{N}_2$ requires 181.1705).

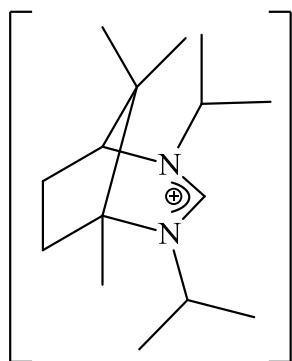
Synthesis of (5S)-2,4-diethyl-1,8,8-trimethyl-2,4-diazabicyclo[3.2.1]octan-2-ium hexafluorophosphate(V) (4)



PF_6^- (5S)-1,8,8-trimethyl-2,4-diazabicyclo[3.2.1]octan-2-ium hexafluorophosphate(V) (0.50 g, 1.68 mmol, 1 eq) was placed in a pressure tube and potassium carbonate (0.56 g, 4.03 mmol, 2.4 eq), 1-bromoethane (0.62 ml, 8.39 moles, 5 eq), and acetonitrile (10 ml) were added. The pressure tube was then sealed and heated to 90 °C for 2 days. The pressure tube was then cooled slowly to room temperature

the acetonitrile was removed on a rotary evaporator, the remaining solid was dissolved in DCM (50 ml), filtered to remove the base, and evaporated to dryness yielding (1S,2R)-2,4-diethyl-5,8,8-trimethyl-4-aza-2-azoniabicyclo[3.2.1]octan-2-ium hexafluorophosphate(V) as a white semicrystalline solid (0.50 g, 81.2 %). ^1H NMR (CDCl_3 , 400 MHz, 298 K): δ 7.70 (1 H, s, NCHN), δ 3.50 (2 H, m, NCH_2), δ 3.40 (2 H, m, NCH_2), δ 3.15 (1 H, d, NCH, $^3J_{\text{HH}} = 4.8$ Hz), δ 2.45 (1 H, m, CH), δ 2.15 (1 H, m, CH), δ 2.05 (1 H, m, CH), δ 1.95 (1 H, m, CH) δ 1.30 (3 H, s, CH_3), δ 1.25 (3 H, t, CH_3 , $^3J_{\text{HH}} = 5.6$ Hz), δ 1.10 (3 H, s, CH_3), δ 0.95 (3 H, s, CH_3). $^{13}\text{C}\{^1\text{H}\}$ NMR (CDCl_3 , 125 MHz, 298 K): δ 153.0 (NCHN), δ 70.0 (NC), δ 66.0 (NCH), δ 49.0 (NCH_2), δ 46.0 (NCH_2), δ 40.5 (CH_2), δ 40.0 (CH_2), δ 32.0 (C), δ 22.0 (CH_3), δ 17.0 (CH_3), δ 16.0 (CH_3), δ 14.0 (CH_3), δ 13.0 (CH_3). MS (ES) m/z : [M^+] 209.2021 ($\text{C}_{13}\text{H}_{25}\text{N}_2$ requires 209.2018).

Synthesis of (5S)-2,4-diisopropyl-1,8,8-trimethyl-2,4-diazabicyclo[3.2.1]octan-2-ium hexafluorophosphate(V) (5)

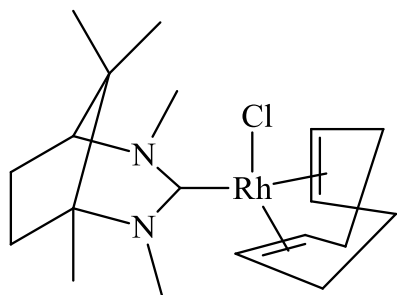


(5S)-1,8,8-trimethyl-2,4-diazabicyclo[3.2.1]octan-2-ium hexafluorophosphate(V) (1.50 g, 5.03 mmol, 1 eq) was placed in a pressure tube and potassium carbonate (1.66 g, 0.01 moles, 2.4 eq), isopropyl iodide (2.52 ml, 0.03 moles, 5 eq), and acetonitrile (10 ml) were added. The pressure tube was then sealed and heated to 90 °C for 18 hours. The pressure tube was then cooled slowly to room

temperature the acetonitrile was removed on a rotary evaporator, the remaining solid was dissolved in DCM (50 ml), filtered to remove the base, and evaporated to dryness. The solid was then redissolved in acetonitrile (10 ml) and isopropyl iodide (2.52 ml, 0.03 moles 5 eq), and potassium carbonate (1.66 g, 0.01 moles, 2.4 eq) were added and the pressure tube was sealed and heated to 90 °C for a further 48 hours. The pressure tube was then cooled slowly to room temperature and the acetonitrile was removed on a rotary evaporator, the remaining solid was dissolved in DCM (50 ml), filtered to remove the base, and evaporated to dryness yielding (5S)-2,4-diisopropyl-1,8,8-trimethyl-2,4-diazabicyclo[3.2.1]octan-2-ium hexafluorophosphate(V) as a white semicrystalline solid (1.66 g, 86.2 %). ^1H NMR (CDCl_3 , 400 MHz, 298 K): δ 8.45 (1 H, s, NCHN), δ 4.60 (1 H, m, NCH_{iso}), δ 3.85 (1 H, m, NCH), δ 3.25 (1 H, d, NCH, $^3J_{\text{HH}} = 5.6$ Hz), δ 2.40 (1 H, m, CH), δ 2.15 (1 H, m, CH), δ 2.10 (1 H, m, CH), δ 1.95 (1 H, m, CH), δ 1.50 (3 H, d, CH_3 , $^3J_{\text{HH}} = 6.8$ Hz), δ 1.40 (3 H, d, CH_3 , $^3J_{\text{HH}} = 6.8$ Hz), δ 1.30 (3 H, s, CH_3), δ 1.25 (3 H, d, CH_3 , $^3J_{\text{HH}} = 5.6$ Hz), δ 1.20 (3 H, d, CH_3 , $^3J_{\text{HH}} = 5.6$ Hz), δ 1.10 (3 H, s, CH_3), δ 0.90 (3 H, s, CH_3). $^{13}\text{C}\{^1\text{H}\}$ NMR (CDCl_3 , 125 MHz, 298 K): δ 151.0 (NCHN), δ 71.5 (C), δ 62.0 (NCH), δ 56.0 (NCH), δ 51.0 (NCH), δ 41.0 (CH_2), δ 40.5 (CH_2), δ 34.0 (C), δ 25.0 (CH_3), δ 23.0 (CH_3), δ 22.0 (CH_3), δ 21.5 (CH_3), δ 20.5 (CH_3), δ 17.5 (CH_3), δ 15.0 (CH_3). MS (ES) m/z : $[\text{M}^+]$ 237.2323 ($\text{C}_{15}\text{H}_{29}\text{N}_2$ requires 237.2331).

3.4.3: Experimental Data for Aliphatic Bicyclic NHC Rhodium Complexes

Synthesis of (5S)-2,4-dimethyl-1,8,8-trimethyl-2,4-diazabicyclo[3.2.1]octan-3-yl rhodium (cyclooctadiene) chloride (6)



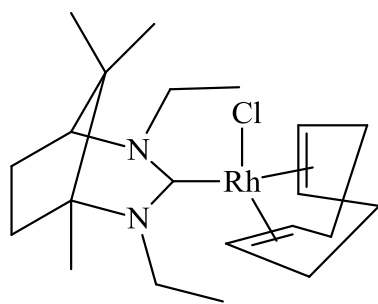
(5S)-1,2,4,8,8-pentamethyl-2,4-diazabicyclo[3.2.1]octan-2-ium

hexafluorophosphate(V) (0.07 g, 0.20 mmol, 1 eq) was placed in a flame dried Schlenk and dried for 20 minutes. To this Schenk KHMDS (0.06 g, 0.28 mmol, 1.4 eq) and THF (10 ml) were added and the mixture

was stirred for 20 minutes. After this time the free carbene produced was filtered under an inert atmosphere into a second flame dried Schlenk containing $[\text{Rh}(\text{COD})\text{Cl}]_2$ (0.05 g, 0.10 mmol, 0.5 eq) and the reaction was stirred at room temperature for 3 hours. The solvents were then removed under vacuum and the product extracted into pentane (10 ml) and reduced to dryness yielding (5S)-2,4-dimethyl-1,8,8-trimethyl-2,4-diazabicyclo[3.2.1]octan-3-yl rhodium (cyclooctadiene) chloride as a yellow solid (0.03 g, 30.1 %). ^1H NMR (CDCl_3 , 400 MHz, 298 K): (major : minor, 2 : 1): (major isomer) δ 4.75 (2 H, m, $\text{CH}_{(\text{COD})}$), δ 3.80 (3 H, s, CH_3), δ 3.75 (3 H, s, CH_3), δ 3.25 (2 H, m, $\text{CH}_{(\text{COD})}$), δ 2.70 (1 H, m, NCH), δ 2.25 (4 H, m, $\text{CH}_2_{(\text{COD})}$), δ 2.20 (1 H, m, CH_2), δ 2.00 (1 H, m, CH_2), δ 1.80 (1 H, m, CH_2), δ 1.75 (4 H, m, $\text{CH}_2_{(\text{COD})}$), δ 1.60 (1 H, m, CH_2), δ 1.10 (3 H, s, CH_3), δ 0.90 (3 H, s, CH_3), δ 0.75 (3 H, s, CH_3). (minor isomer) δ 4.75 (2 H, m, $\text{CH}_{(\text{COD})}$), δ 3.85 (3 H, s, CH_3), δ 3.80 (3 H, s, CH_3), δ 3.05 (2 H, m, $\text{CH}_{(\text{COD})}$), δ 2.75 (1 H, m, NCH), δ 2.25 (4 H, m, $\text{CH}_2_{(\text{COD})}$), δ 2.20 (1 H, m, CH_2), δ 2.00 (1 H, m, CH_2), δ 1.80 (1 H, m, CH_2), δ 1.75 (4 H, m, $\text{CH}_2_{(\text{COD})}$), δ 1.60 (1 H, m, CH_2), δ 1.15 (3 H, s, CH_3), δ 1.05 (3 H, s, CH_3), δ 0.85 (3 H, s, CH_3). $^{13}\text{C}\{^1\text{H}\}$ NMR (CDCl_3 , 125 MHz, 298 K): (major isomer) δ 205.1 (NCN, d, $^1J_{\text{Rh-C}} = 46.5$ Hz), δ 95.1 ($\text{CH}_{(\text{COD})}$), δ 94.8 ($\text{CH}_{(\text{COD})}$), δ 67.9 (NCH), δ 66.8 ($\text{CH}_{(\text{COD})}$), δ 66.5 ($\text{CH}_{(\text{COD})}$), δ 43.1 (CH_3), δ 40.1 (NC), δ 38.6 (CH_3), δ 36.0 (C), δ 31.8 ($\text{CH}_2_{(\text{COD})}$), δ 31.7 ($\text{CH}_2_{(\text{COD})}$), δ 30.2 (CH_2), δ 28.8 (CH_2), δ 28.6 ($\text{CH}_2_{(\text{COD})}$), δ 28.0 ($\text{CH}_2_{(\text{COD})}$), δ 21.4 (CH_3), δ 16.2 (CH_3), δ 14.6

(CH₃). (minor isomer) δ 204.8 (NCN), δ 95.4 (CH_(COD)), δ 95.2 (CH_(COD)), δ 68.1 (NCH), δ 66.6 (CH_(COD)), δ 66.2 (CH_(COD)), δ 44.1 (CH₃), δ 39.4 (NC), δ 38.1 (CH₃), δ 36.3 (C), δ 31.6 (CH_{2(COD)}), δ 31.4 (CH_{2(COD)}), δ 30.0 (CH₂), δ 28.5 (CH₂), δ 28.0 (CH_{2(COD)}), δ 27.7 (CH_{2(COD)}), δ 21.3 (CH₃), δ 16.5 (CH₃), δ 14.9 (CH₃). MS (ES) m/z : [M⁺ - Cl + MeCN] 432.1882 (C₂₁H₃₅N₃Rh requires 432.1886).

Synthesis of ((5S)-2,4-diethyl-1,8,8-trimethyl-2,4-diazabicyclo[3.2.1]octan-3-yl rhodium (cyclooctadiene) chloride (7)

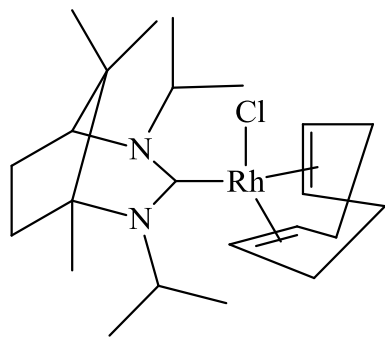


(1R,3S)-1,2,2-trimethylcyclopentane-1,3-diamine (5S)-2,4-diethyl-1,8,8-trimethyl-2,4-diazabicyclo[3.2.1]octan-2-ium hexafluorophosphate(V) (0.07 g, 0.20 mmol, 1 eq) was placed in a flame dried Schlenk and dried for 20 minutes. To this Schenk KHMDS (0.06 g, 0.28 mmol, 1.4 eq) and THF (10 ml)

were added and the mixture was stirred for 20 minutes. After this time the free carbene produced was filtered under an inert atmosphere into a second flame dried Schlenk containing [Rh(COD)Cl]₂ (0.05 g, 0.10 mmol, 0.5 eq) and the reaction was stirred at room temperature for 3 hours. The solvents were then removed under vacuum and the product extracted into pentane (10 ml) and reduced to dryness yielding ((5S)-2,4-diethyl-1,8,8-trimethyl-2,4-diazabicyclo[3.2.1]octan-3-yl rhodium (cyclooctadiene) chloride as a yellow solid (0.03 g, 33.2 %). ¹H NMR (CDCl₃, 500 MHz, 298 K): (major : minor, 2 : 1): (major isomer) δ 5.55 (1 H, m, NCH₂), δ 4.75 (2 H, m, CH_(COD)), δ 4.55 (1 H, m, NCH₂), δ 4.40 (1 H, m, NCH₂), δ 3.75 (1 H, m, NCH₂), δ 3.15 (2 H, m, CH_(COD)), δ 2.75 (1 H, d, NCH, ³J_{HH} = 7.5 Hz), δ 2.25 (4 H, m, CH_{2(COD)}), δ 2.20 (2 H, m, CH₂), δ 1.80 (4 H, m, CH_{2(COD)}), δ 1.70 (1 H, m, CH₂), δ 1.55 (1 H, m, CH₂), δ 1.35 (3 H, m, CH₃), δ 1.30 (3 H, m, CH₃), δ 1.20 (3 H, s, CH₃), δ 0.90 (3 H, s, CH₃), δ 0.65 (3 H, s, CH₃). (minor isomer), δ 4.75 (2 H, m, CH_(COD)), δ 4.70 (2 H, m, NCH₂), δ 4.50 (1 H, m, NCH₂), δ 4.20 (1 H, m, NCH₂), δ 3.30 (2 H, m, CH_(COD)), δ 2.80 (1 H, m, NCH), δ 2.25 (4 H, m, CH_{2(COD)}), δ 2.20 (2 H, m, CH₂), δ 1.90 (4 H, m, CH_{2(COD)}), δ

1.80 (2 H, m, CH₂), δ 1.25 (3 H, s, CH₃), δ 1.20 (3 H, m, CH₃), δ 1.20 (3 H, m, CH₃), δ 0.95 (3 H, s, CH₃), δ 0.85 (3 H, s, CH₃). ¹³C{¹H} NMR (CDCl₃, 125 MHz, 298 K): (major isomer) δ 203.6 (NCN, d, ¹J_{Rh-C} = 40.0 Hz), δ 94.5 (CH_(COD)), δ 94.4 (CH_(COD)), δ 69.2 (NCH), δ 67.2 (CH_(COD)), δ 67.1 (CH_(COD)), δ 64.0 (NC), δ 50.2 (NCH₂), δ 47.1 (NCH₂), δ 40.1 (CH_{2(COD)}), δ 38.8 (CH_{2(COD)}), δ 31.6 (C), δ 31.3 (CH_{2(COD)}), δ 30.3 (CH_{2(COD)}), δ 28.1 (CH₂), δ 27.4 (CH₂), δ 22.5 (CH₃), δ 16.5 (CH₃), δ 16.1 (CH₃), δ 14.0 (CH₃), δ 13.0 (CH₃). (minor isomer) δ 203.2 (NCN, d, ¹J_{Rh-C} = 40.0 Hz), δ 94.7 (CH_(COD)), δ 94.7 (CH_(COD)), δ 69.1 (NCH), δ 67.1 (CH_(COD)), δ 67.0 (CH_(COD)), δ 64.3 (NC), δ 50.7 (NCH₂), δ 47.4 (NCH₂), δ 40.3 (NCH₂), δ 39.7 CH_{2(COD)}), δ 32.0 (C), δ 31.2 (CH_{2(COD)}), δ 31.0 (CH_{2(COD)}), δ 28.5 (CH₂), δ 27.6 (CH₂), δ 22.8 (CH₃), δ 17.5 (CH₃), δ 17.0 (CH₃), δ 14.2 (CH₃), δ 13.2 (CH₃). MS (ES) *m/z*: [M⁺ - Cl + MeCN] 460.2190 (C₂₃H₃₉N₃Rh requires 460.2199).

Synthesis of ((5*S*)-2,4-diisopropyl-1,8,8-trimethyl-2,4-diazabicyclo[3.2.1]octan-3-yl rhodium (cyclooctadiene) chloride (8))



((5*S*)-2,4-diisopropyl-1,8,8-trimethyl-2,4-diazabicyclo[3.2.1]octan-2-ium

hexafluorophosphate(V) 0.07 g, 0.20 mmol, 1 eq) was placed in a flame dried Schlenk and dried for 20 minutes. To this Schenk KHMDS (0.06 g, 0.28 mmol, 1.4 eq) and THF (10 ml) were added and the mixture was stirred for 20 minutes. After this time the free carbene produced was filtered under an inert atmosphere into a second flame dried Schlenk containing [Rh(COD)Cl]₂ (0.05 g, 0.10 mmol, 0.5 eq) and the reaction was stirred at room temperature for 3 hours. The solvents were then removed under vacuum and the product extracted into pentane (10 ml) and reduced to dryness yielding ((5*S*)-2,4-diisopropyl-1,8,8-trimethyl-2,4-diazabicyclo[3.2.1]octan-3-yl rhodium (cyclooctadiene) chloride as a yellow solid (0.03 g, 28.6 %). ¹H NMR (CDCl₃, 500 MHz, 298 K): (major : minor, 2 : 1): (major isomer) δ 6.95 (1 H, m, NCH), δ 6.55 (1 H,

m, NCH), δ 4.70 (2 H, m, CH_(COD)), δ 3.45 (2 H, m, CH_(COD)), δ 2.75 (1 H, d, NCH, $^3J_{\text{HH}} = 5.8$ Hz), δ 2.45 (1 H, m, CH₂), δ 2.25 (4 H, m, CH_{2(COD)}), δ 2.10 (1 H, m, CH₂), δ 1.95 (1 H, m, CH₂), δ 1.80 (4 H, m, CH_{2(COD)}), δ 1.60 (1 H, m, CH₂), δ 1.50 (3 H, d, CH₃, $^3J_{\text{HH}} = 7.2$ Hz), δ 1.45 (3 H, d, CH₃, $^3J_{\text{HH}} = 7.2$ Hz), δ 1.26 (3 H, d, CH₃, $^3J_{\text{HH}} = 5.8$ Hz), δ 1.25 (3 H, s, CH₃), δ 1.20 (3 H, d, CH₃, $^3J_{\text{HH}} = 5.8$ Hz), δ 0.85 (3 H, s, CH₃), δ 0.70 (3 H, s, CH₃). (minor isomer) δ 7.05 (1 H, m, NCH), δ 6.55 (1 H, m, NCH), δ 4.70 (2 H, m, CH_(COD)), δ 3.45 (2 H, m, CH_(COD)), δ 2.80 (1 H, d, NCH, $^3J_{\text{HH}} = 5.5$ Hz), δ 2.45 (1 H, m, CH₂), δ 2.25 (4 H, m, CH_{2(COD)}), δ 2.10 (1 H, m, CH₂), δ 1.95 (1 H, m, CH₂), δ 1.80 (4 H, m, CH_{2(COD)}), δ 1.60 (1 H, m, CH₂), δ 1.55 (3 H, m, CH₃), δ 1.40 (3 H, d, CH₃, $^3J_{\text{HH}} = 7.2$ Hz), δ 1.35 (3 H, s, CH₃), δ 1.24 (3 H, d, CH₃, $^3J_{\text{HH}} = 5.5$ Hz), δ 1.19 (3 H, d, CH₃, $^3J_{\text{HH}} = 5.5$ Hz), δ 0.90 (3 H, s, CH₃), δ 0.80 (3 H, s, CH₃). $^{13}\text{C}\{^1\text{H}\}$ NMR (CDCl₃, 125 MHz, 298 K): (major isomer) δ 203.9 (NCN, d, $^1J_{\text{Rh-C}} = 43.8$ Hz), δ 93.4 (CH_(COD)), δ 93.1 (CH_(COD)), δ 69.6 (NC), δ 66.3 (CH_(COD)), δ 66.2 (CH_(COD)), δ 59.3 (NCH), δ 59.1 (NCH), δ 55.8 (NCH), δ 40.5 (CH₂), δ 39.2 (CH₂), δ 32.0 (C), δ 31.8 (CH_{2(COD)}), δ 31.5 (CH_{2(COD)}), δ 31.1 (CH_{2(COD)}), δ 30.5 (CH_{2(COD)}), δ 28.8 (CH₃), δ 27.6 (CH₃), δ 24.5 (CH₃), δ 22.5 (CH₃), δ 20.0 (CH₃), δ 17.5 (CH₃), δ 17.1 (CH₃). (minor isomer) δ 203.5 (NCN, d, $^1J_{\text{Rh-C}} = 45.0$ Hz), δ 93.5 (CH_(COD)), δ 93.4 (CH_(COD)), δ 68.9 (NC), δ 66.2 (CH_(COD)), δ 66.1 (CH_(COD)), δ 59.2 (NCH), δ 59.1 (NCH), δ 55.6 (NCH), δ 41.5 (CH₂), δ 40.0 (CH₂), δ 33.2 (C), δ 31.8 (CH_{2(COD)}), δ 31.2 (CH_{2(COD)}), δ 31.0 (CH_{2(COD)}), δ 30.1 (CH_{2(COD)}), δ 28.1 (CH₃), δ 27.0 (CH₃), δ 24.0 (CH₃), δ 22.8 (CH₃), δ 20.5 (CH₃), δ 18.0 (CH₃), δ 17.3 (CH₃). MS (ES) m/z : [M⁺ - Cl⁻ + MeCN] 488.2528 (C₂₅H₄₃N₃Rh requires 488.2512).

3.4.4: General Procedure for Transfer Hydrogenation

A flask was loaded with the desired substrate (1 mmol) and ^tBuOK (10 mol %), to this reagent grade 2-propanol (5 ml) was added followed by a stock solution of the catalyst in 2-propanol (0.1 mol %) and the solution heated to 80 °C for 23 hours. After this time the reaction mixture was left to cool slowly to room temperature, volatiles were evaporated and the final percentage conversions calculated by integrals from ¹H NMR.

3.5: References

- 1 Siemeling, U.; Färber, C.; Bruhn, C.; Fürmeier, S.; Schulz, T.; Kurlemann, M.; Tripp, S. *Eur. J. Inorg. Chem.* **2012**, 9, 1413-1422.
- 2 Bantu, B.; Wang, D.; Wurst, K.; Buchmeiser, M. R. *Tetrahedron* **2005**, 61, 12145-12152.
- 3 Davies, C. J. E.; Page, M. J.; Ellul, C. E.; Mahon, M. F.; Whittlesey, M. K. *Chem. Comm.* **2010**, 46, 5151-5153.
- 4 Iglesias, M.; Beetstra, D. J.; Knight, J. C.; Ooi, L.; Stasch, A.; Coles, S.; Male, L.; Hursthouse, M. B.; Cavell, K. J.; Dervisi, A.; Fallis, I. A.; *Organometallics* **2008**, 27, 13, 3279-3289.
- 5 Iglesias, M.; Beetstra, D. J.; Kariuki, B.; Cavell, K. J.; Dervisi, A.; Fallis, I. A. *Eur. J. Inorg. Chem.* **2009**, 1913-1919.
- 6 Lu, W. Y.; Cavell, K. J.; Wixey, J. S.; Kariuki, B. *Organometallics* **2011**, 30, 5649-5655.
- 7 Scarborough, C. C.; Guzei, L. A.; Stahl, S.S. *Dalton Trans.* **2009**, 2284-2286.
- 8 Scarborough, C. C.; Grady, M. J. W.; Guzei, L. A.; Ghandi, B. A.; Bunel, E. E.; Stahl, S. S. *Angew. Chem. Int. Ed.* **2005**, 44, 33, 5269-5272.
- 9 Siemeling, U.; Färber, C.; Leibold, M.; Bruhn, C.; Mücke, P.; Winter, R. F.; Sarkar, B.; Von Hopffgarten, M.; Frenking, G. *Eur. J. Inorg. Chem.* **2009**, 31, 4067-4612.
- 10 Mag, M. M.; Wurst, K.; Ongania, K. -H.; Buchmeiser, M. R. *Chem. Eur. J.* **2004**, 10, 5, 1256-1266.
- 11 Reddy, P. V. G.; Tabassum, S.; Blanrue, A.; Wilhelm, R. *Chem. Comm.* **2009**, 5910-5912.
- 12 Newman, P. D.; Cavell, K. J.; Kariuki, B. M. *Organometallics* **2010**, 29, 12, 2724-2734.
- 13 Newman, P. D.; Cavell, K. J.; Hallett, A. J.; Kariuki, B. M. *Dalton Trans.* **2011**, 40, 8807-8813.
- 14 Jaramillo, D.; Buck, D. P.; Collins, J. G.; Fenton, R. R.; Stootman, F. H.; Wheate, N. J.; Aldrich-Wright, J. R. *Eur. J. Inorg. Chem.* **2006**, 4, 839-849.

- 15 Palmere, R. M.; Conley, R. T. *J. Org. Chem.* **1970**, 35, 8, 2703-2707.
- 16 Schmidt, F. *Eur. J. Inorg. Chem* **1924**, 57, 4, 704-706.
- 17 Newman, P. D.; Cavell, K. J.; Kariuki, B. M. *Chem. Comm.* **2012**, 48, 6511-6513.
- 18 Voutchkova, A. M.; Appelhans, L. N.; Chianese, A. R.; Crabtree, R. H. *J. Am. Chem. Soc.* **2005**, 127, 50, 17624-17625.
- 19 Köcher, C.; Herrmann, W. A. *J. Organomet. Chem.* **1997**, 532, 261-265.
- 20 Binobaid, A.; Iglesias, M.; Beetstra, D. J.; Kariuki, B.; Dervisi, A.; Fallis, I. A.; Cavell, K. J. *Dalton Trans.* **2009**, 7099-7112.
- 21 Binobaid, A.; Iglesias, M.; Beetstra, D.; Dervisi, A.; Fallis, I.; Cavell, K. J. *Eur. J. Inorg. Chem.* **2010**, 34, 5426-5431.
- 22 Çetinkaya, B.; Özdemir, I.; Sixneuf, P. H. *J. Organomet. Chem.* **1997**, 534, 153-158.
- 23 Dunsford J. J. *PhD Thesis* **2012**
- 24 Arduengo, A. J.; Goerlich, J. R.; Marshall, W. J. *J. Am. Chem. Soc.* **1995**, 117, 44, 11027-11028.
- 25 Alder, R. W.; Blake, M. E.; Bortolotti, C.; Bufali, S.; Butts, C. P.; Lineham, E.; Oliva, J. M.; Orpen, A. G.; Quayle, M. J. *Chem. Comm.* **1999**, 241-242.
- 26 Herrmann, W. A.; Schneider, S. K.; Öfele, K.; Sakamoto, M.; Herdtweck, E. *J. Organomet. Chem.* **2004**, 689, 15, 2441-2449.
- 27 Iglesias, M.; Beetstra, D. J.; Stasch, A.; Horton, P. N.; Hursthouse, M. B.; Coles, S. J.; Cavell, K. J.; Dervisi, A.; Fallis, I. A. *Organometallics* **2007**, 26, 19, 4800-4809.
- 28 Iglesias, M. *PhD Thesis* **2008**
- 29 Dunsford, J. J.; Cavell, K. J. *Dalton Trans.* **2011**, 40, 9131-9135.
- 30 Dröge, T.; Glorius, F. *Angew. Chem. Int. Ed.* **2010**, 49, 6940-6952.
- 31 Berthon-Gelloz, G.; Buisine, O.; Brière, J. -F.; Michaud, G.; Stéin, S.; Mignani, G.; Tinant, B.; Declercq, J. -P.; Chapon, D.; Markó, I. E. *J. Organomet. Chem.* **2005**, 690, 6156-6168.
- 32 Dunsford, J. J.; Cavell, K. J.; Kariuki, B. *J. Organomet. Chem.* **2011**, 696, 1, 188-194.
- 33 Albrecht, M.; Crabtree, R. H.; Mata, J.; Peris, E. *Chem. Comm.* **2002**, 32-33.
- 34 Hillier, A. C.; Lee, H. M.; Stevens, E. D.; Nolan, S. P. *Organometallics* **2001**, 20, 20, 4246-4252.

- 35 Page, M. J.; Wagler, J.; Messerlem, B. A. *Dalton Trans.* **2009**, 7029-7038.
- 36 Palmer, M. J.; Wills, M. *Tetrahedron: Asymmetry* **1999**, 10, 11, 2045-2061.
- 37 Bernard, M.; Guiral, V.; Delbecq, F.; Fache, F.; Sautet, P.; Lemaire, M. *J. Am. Chem. Soc.* **1998**, 120, 7, 1441-1446.
- 38 Zinner, S. C.; Rentzsch, C. F.; Herdtweck, E.; Herrmann, W. A.; Kühn, F. *Dalton Trans* **2009**, 7055-7062.
- 39 Mas-Marzá, E.; Poyatos, M.; Sanaú, M.; Peris, E. *Organometallics* **2004**, 23, 3, 323-325.
- 40 Hahn, F. E.; Holtgrewe, C.; Pape, T.; Martin, M.; Sola, E.; Oro, L. A. *Organometallics* **2005**, 24, 9, 2203-2209.
- 41 Dyson, G.; Frison, J. -C.; Whitwood, A. C.; Douthwaite, R. E. *Dalton Trans.* **2009**, 7141-7151.
- 42 Perrin, D. D.; Amarego, W. F. A. *Purification of Laboratory Chemicals*; Pergamon: Oxford, **1988**.
- 43 COLLECT; Nonius BV: Delft, The Netherlands, **1998**.
- 44 Otwinowski, Z.; Minor, W. *Methods Enzymol.* **1997**, 276, 307-326.
- 45 Altomare, A.; Cascarano, G.; Giacovazzo, C.; Guagliardi, A. *J. Appl. Crystallogr.* **1993**, 26, 343-350.
- 46 Sheldrick, G. M. *Acta Crystallogr. Sect. A* **2008**, A64, 112-122.
- 47 Blessing, R. H. *Acta Crystallogr. Sect. A* **1995**, 51, 33-38.

4: Coordination of Expanded Ring N-Heterocyclic Carbenes to Copper(I)

4.1: Introduction

There has been a substantial amount of work on the coordination of NHCs to late transition metals such as palladium, platinum, rhodium, and iridium over recent years,¹⁻⁴ which has led to an extensive insight into how these complexes act as catalysts. The outcomes have been excellent with the catalysts proving to be very efficient across a large range of catalytic processes.⁵⁻⁸ However, the metals above are not very abundant, they are expensive and generally have a large impact on the environment, therefore it is of interest to replace these with cheaper, more abundant, and more benign metals. This has led to the complexation of group XI metals (Cu, Ag, and Au), since they are generally cheaper, even gold is more cost effective than platinum or palladium, and their natural abundance is significantly greater than that of platinum for example. There has already been some quite extensive work carried out on silver(I) complexes,⁹⁻¹¹ and Nolan *et al.*¹²⁻¹⁵ and Buchmeiser *et al.*¹⁶ have shown that copper(I) NHC complexes can be very useful in a range of catalytic processes. Therefore due to these successes and the already reported literature on silver, this chapter will concentrate on the synthesis of copper(I) complexes.

4.2: Results and Discussion

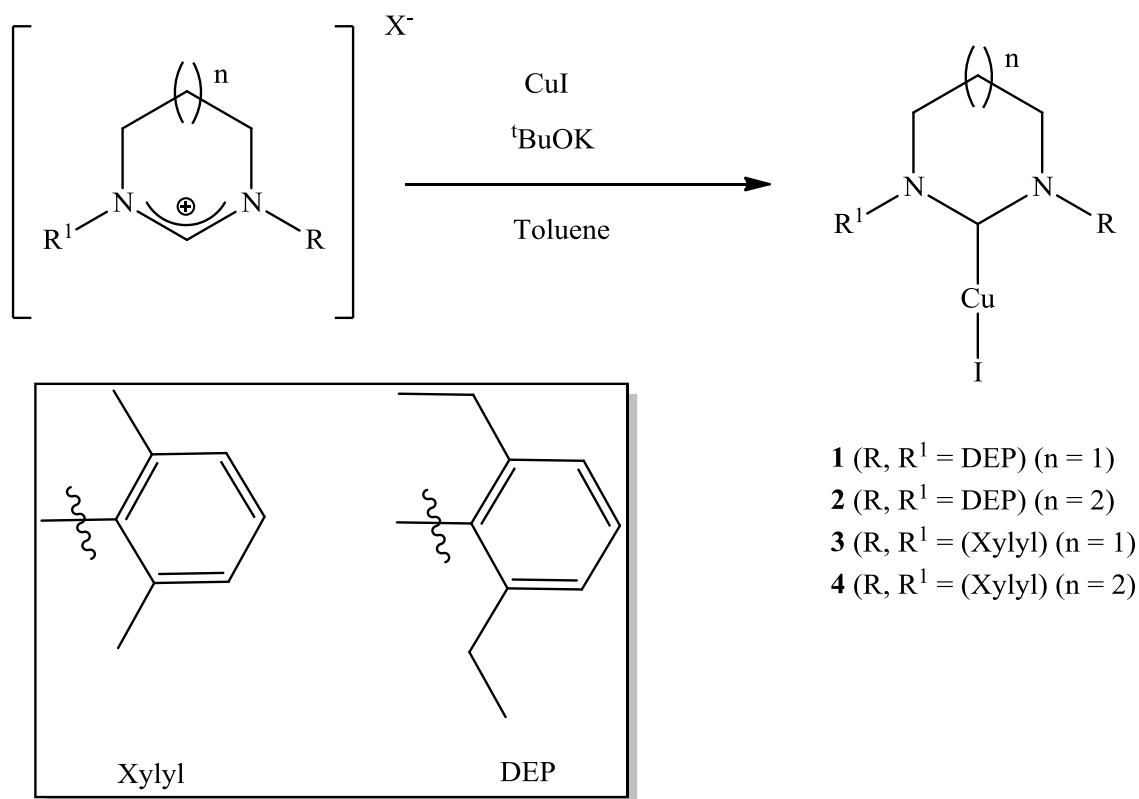
There has been a number of reports of expanded ring N-heterocyclic carbenes coordinated to transition metals.¹⁷⁻²² However it has only been in recent years that coordination of coinage metals such as gold(I) and copper(I) has been carried out. Nolan has had success with the applications of 5-membered copper(I) NHCs of general formula [Cu(NHC)X] (where X = Cl, Br, and I) in catalytic processes such as

hydrosilylation.^{12,13} Buchmeiser *et al.* have published that the 6-membered derivatives of these types of systems can be successful in C=O cyanosilylation.¹⁶ More recently the Cavell group have shown that expanded ring copper(I) complexes 6-NHC and 7-NHC of general formula [Cu(NHC)X] (where X = Cl, Br, and I) and [Cu(NHC)OH] also show good catalytic properties in hydrosilylation, carboxylation, and C-H activation.²³ The [Cu(NHC)X] complexes can very easily be converted to the copper(I) hydroxide complexes of the general formula [Cu(NHC)OH] as Nolan and the Cavell group have shown.^{14,23} These complexes have been used for two different types of catalysis, C-H activation and carboxylation.^{15,23}

Due to these exciting developments with expanded NHCs and coinage metals the research described in this chapter will focus on the coordination to copper(I) of expanded ring NHCs and bicyclic NHCs.

4.2.1: Synthetic Route to Copper(I) Complexes

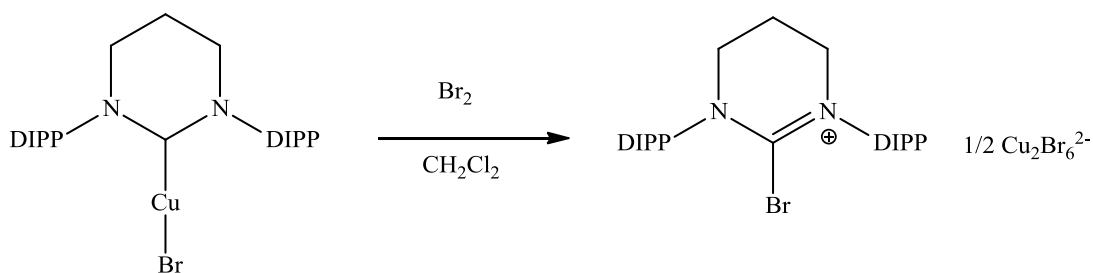
The synthetic route employed in this work for the coordination of the expanded ring NHCs to copper(I) (**1-4**) is similar to that reported by Buchmeiser and co-workers,¹⁶ which is an *in situ* deprotonation of the appropriate NHC·HX (where X = Br, or I) salt with ^tBuOK (1.4 eq) in the presence of copper(I) iodide as shown in Scheme 1. This route appears to be much simpler and cheaper than the transmetallation from silver reported by Nechaev.⁹



Scheme 1: Synthesis of copper(I) complexes with general formula [Cu(NHC)X].

Compounds **1-4** were shown to be relatively stable in air in the solid state, however decomposition was observed over a period of one week as the white solid slowly turned green. This observation of a colour change and apparent decomposition has been observed by Nechaev.²⁴ This group reacted Br₂ with the [Cu(NHC)X] complex in CD₂Cl₂ to show that the haloamidinium salt is a result of the decomposition of [Cu(NHC)X], as shown in Scheme 2. This elimination has also been observed by Stack *et al.* where they used a specific oxidant to aid elimination to the haloamidinium.²⁵

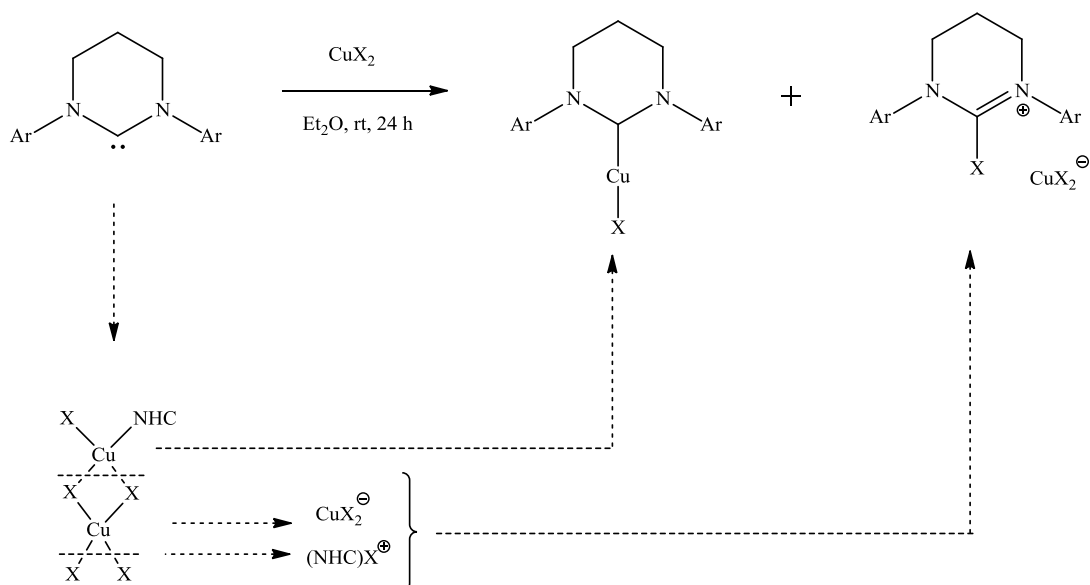
When dissolved in chlorinated solvents these compounds are susceptible to oxidation and production of the haloamidinium is much faster (1-2 hours). This decomposition can be slowed by passing the chlorinated solvent through a small column of basic alumina to remove any HCl present in the solvent.



Scheme 2: Proof of decomposition to the haloamidinium.²⁴

This process was also evident when Nechaev attempted to synthesise the copper(II) halide salts by reacting the free carbene with CuX_2 , where $X = \text{Cl}$ or Br . The reaction did not produce the $[\text{Cu}(\text{NHC})\text{X}_2]$ as predicted, instead it produced $[\text{Cu}(\text{NHC})\text{X}]$ and $[(\text{NHC})\text{X}]$ as shown in Scheme 3.

Nachaev tried using $[\text{Ag}(\text{NHC})\text{Br}]$ to make CuX_2 , where $X = \text{Cl}$ or Br , through transmetallation, however $[\text{Cu}(\text{NHC})\text{X}_2]$ was not isolated as predicted, instead the haloamidinium was the only isolated product with $\text{Cu}_2\text{Br}_6^{2-}$ and CuBr_2^- anions. The final route that Nachaev attempted with the copper(II) salts was that of the free carbene with $\text{Cu}(\text{OAc})_2$, this was successful in the formation of $[\text{Cu}(\text{NHC})(\text{OAc})_2]$.



Scheme 3: Reaction of free carbene with copper(II) salts.²⁴

A series of expanded ring copper(II) complexes were attempted here, however the reactions were not successful in producing the copper(II) NHC species, instead they yielded compounds that gave incomprehensible ^1H NMR spectra. Due to this, the following discussion will concentrate on the synthesis of copper(I) complexes and their applications.

4.2.2: Copper(I) Complexes with Monocyclic Expanded Ring NHC Ligands

4.2.2.1: Synthesis and Characterisation of Compounds with the General Formula $[\text{Cu}(\text{NHC})\text{X}]$, Where $\text{X} = \text{I}$ or Br

Compounds **1-4** were fully characterised using ^1H NMR and $^{13}\text{C}\{^1\text{H}\}$ NMR spectroscopy, mass spectrometry, and in the case of $[\text{Cu}(\text{7-xylyl})\text{I}]$, **4**, X-ray crystal structure data. The ^1H NMR spectra show that there is, in all four cases, a

disappearance of the NCHN peak, and a shift upfield, of on average 0.84 ppm, of the NCH₂ peak. In the case of compound **1** this is from 4.20 ppm to 3.35 ppm. The other important spectroscopic indicator is the NCN peak in the ¹³C{¹H} NMR spectra. For **1** it appears at 202.5 ppm, which is a significant shift downfield from the NHC·HX salt (153.34 ppm). The ¹³C{¹H} NMR data for **1** is in accordance with that reported by Nechaev *et al.*⁹ for copper(I) complexes, and also that shown by Dunsford with the NCN peak for [Cu(6-Mes)Cl] and [Cu(7-Mes)Cl] appearing at 202.41 ppm and 209.18 ppm respectively.²³ For **2**, **3**, and **4** the NCN peak in the ¹³C{¹H} NMR spectra was not observed but the mass spectra for **3** and **4** shows [M⁺ - I⁻ + MeCN] at 396.1490 amu and 410.1643 amu respectively, which have calculated values of 396.1501 amu and 410.1643 amu respectively, which is clarification that these compounds were synthesised. The peaks in the mass spectra which Dunsford observed were also the acetonitrile adducts, with the [Cu(6-Mes)Cl] molecular ion appearing at 424.1834 amu, and the [Cu(7-Mes)I] appearing at 438.1967 amu.²³ Attempts were made to obtain micro analytical data, however due to the slight decomposition over time a pure sample was not obtainable. The crystal structure of **4** was obtained from vapour diffusion of THF and *n*-pentane over a period of 72 hours and is shown in Figure 1 and Table 1.

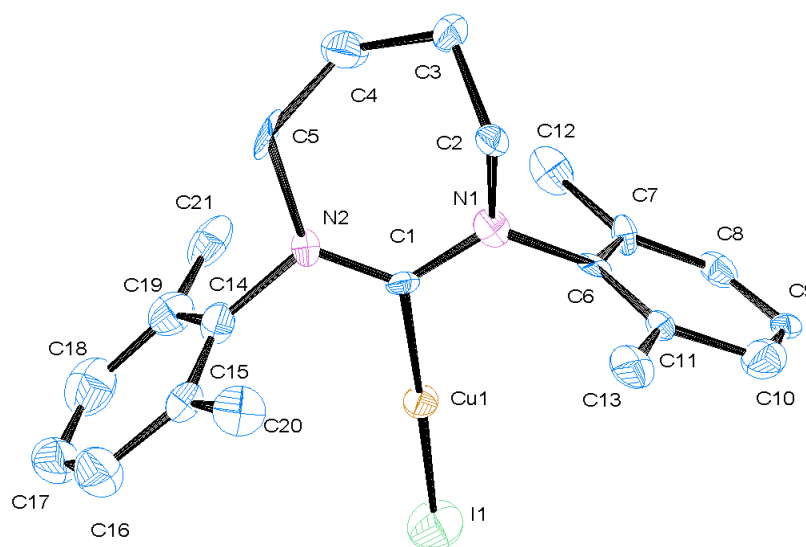


Figure 1: ORTEP ellipsoid plots at 50 % probability of the molecular structure of [Cu(7-xylyl)I] (**4**).

Table 1: Selected bond lengths (Å) and angles (°) for [Cu(7-xylyl)I] (**4**).

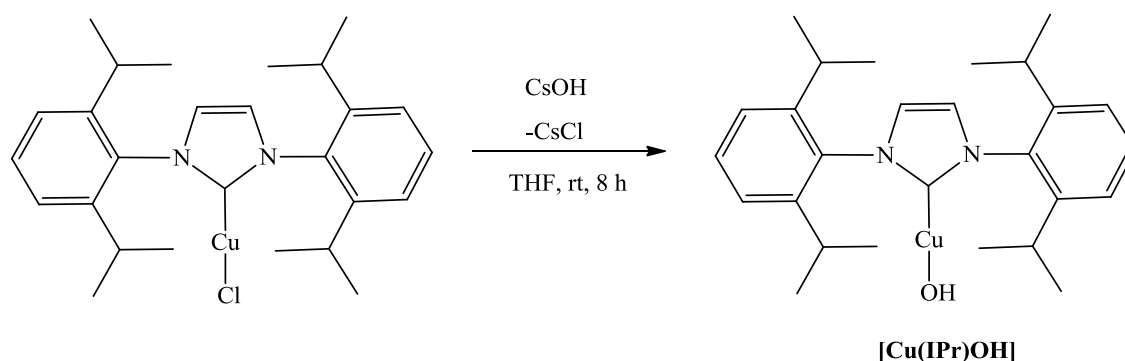
Lengths (Å)		Angles (°)	
C(1)-N(1)	1.36(2)	N(1)-C(1)-N(2)	119.9(18)
C(1)-N(2)	1.31(3)	C(1)-N(1)-C(2)	124.2(17)
N(2)-C(5)	1.51(3)	C(1)-N(1)-C(6)	117.7(15)
C(5)-C(4)	1.50(3)	N(1)-C(2)-C(3)	113.4(18)
C(4)-C(3)	1.52(3)	C(2)-C(3)-C(4)	11.4(17)
C(3)-C(2)	1.48(3)	C(3)-C(4)-C(5)	114.3(19)
C(2)-N(1)	1.47(2)	C(4)-C(5)-N(2)	111.0(19)
N(2)-C(14)	1.48(3)	C(5)-N(2)-C(1)	129.7(17)
C(14)-C(19)	1.41(3)	C(1)-N(2)-C(14)	115.8(17)
C(14)-C(15)	1.39(3)	C(5)-N(2)-C(14)	114.3(16)
N(1)-C(6)	1.43(2)	N(2)-C(14)-C(19)	119.0(2)
C(6)-C(7)	1.42(3)	N(2)-C(14)-C(15)	118.0(2)
C(6)-C(11)	1.35(3)	C(2)-N(1)-C(6)	117.2(15)
C(1)-Cu(1)	1.93(2)	N(1)-C(6)-C(7)	119.5(19)
Cu(1)-I(1)	2.312(3)	N(1)-C(6)-C(11)	119.0(2)
		C(7)-C(6)-C(11)	121.0(19)
		C(19)-C(14)-C(15)	122.0(2)
		N(1)-C(1)-Cu(1)	119.5(14)
		N(2)-C(1)-Cu(1)	120.4(15)
		C(1)-Cu(1)-I(1)	175.6(6)

As shown in Table 1 the N(1)-C(1)-N(2) angle is 119.9(18) °, which is in accordance with the data reported by Nechaev showing the [Cu(7-DIPP)Br] NCN angle to be

119.4(4) °. Also a noteworthy angle in this structure is that of C(1)-Cu(1)-I(1) (175.6(6) °), which is virtually linear. It has been reported by Nechaev⁹ that the silver and copper complexes form almost linear metal halide bonds of 177.59(5) ° and 173.5(2) ° respectively, therefore the results obtained here are consistent with this data.

4.2.2.2: Synthesis and Characterisation of Compounds with the General Formula [Cu(NHC)OH]

Nolan *et al.* have established the preparation of 5-membered copper(I) hydroxide complexes from [Cu(5-NHC)Cl] by reaction with caesium hydroxide (two equivalents) as shown in Scheme 4.¹⁴

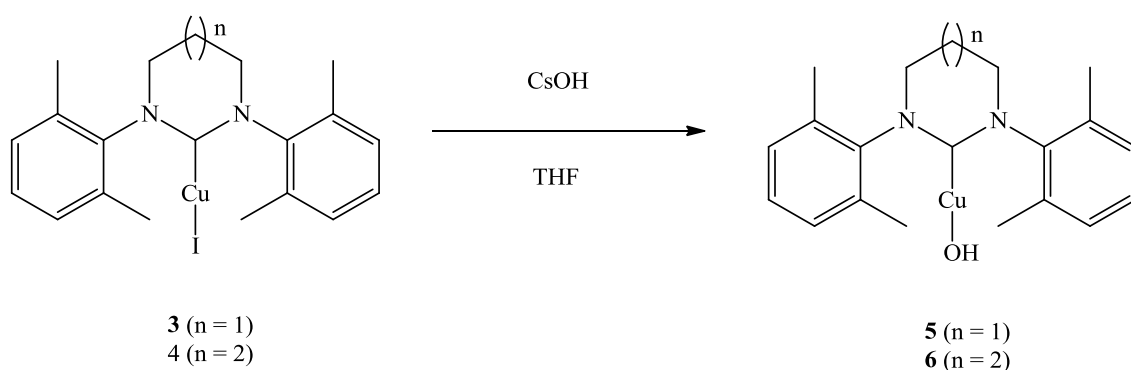


Scheme 4: Synthetic route to [Cu(IPr)OH].¹⁴

These hydroxide complexes have been shown to be a versatile reagent for creating a library of different copper(I) species,¹⁴ this is due to the copper hydroxide being more reactive than that of the parent iodide complex. This increase in reactivity can be attributed to the increase in basicity of the hydroxide co-ligand in comparison to the iodide co-ligand in the parent complex. Nolan *et al.* have shown that the [Cu(NHC)OH] could react with several different species to form new copper(I)

with converting the [Cu(6-Mes)I] and [Cu(7-Mes)I] to their hydroxide derivatives. Compounds **5** and **6** were synthesised analogously to that of Nolan *et al.*¹⁴

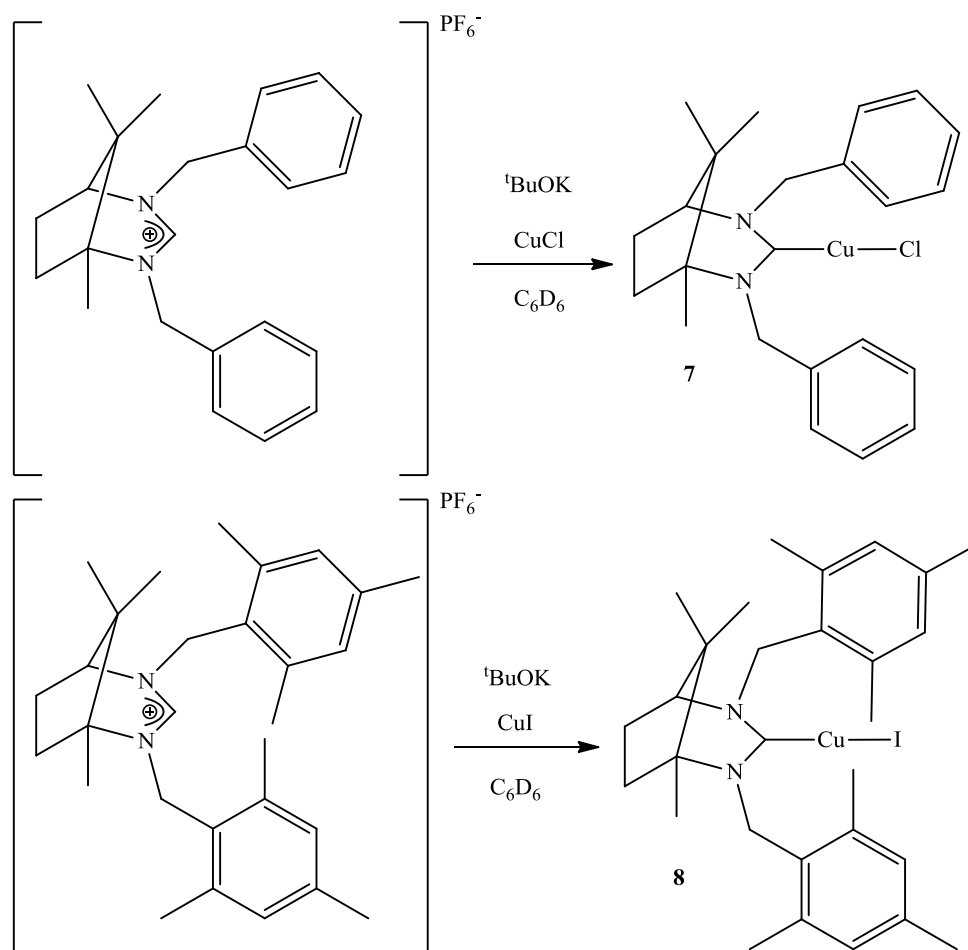
The spectroscopic data for **5** and **6** were very similar to that of **3** and **4**, with the NCH₂ protons in **5** not shifting at all from that of **3** and the NCH₂CH₂ protons only shifting downfield by 0.05 ppm from that of **3** in the ¹H NMR spectrum. It is a similar case for **6**, however the NCH₂ protons shift upfield from 3.85 ppm in **4** to 3.60 ppm in **6**. The NCH₂CH₂ protons in **6** have also shifted upfield by 0.3 ppm from that of **4**. The mass spectra of **5** and **6** show [M⁺ - OH + MeCN] at 396.1467 amu and 410.1679 amu respectively, which have calculated values of 396.1501 amu and 410.1657 amu, which is the same adduct as for **3** and **4**. As there are only small differences in ppm between the [Cu(NHC)I] complexes and the [Cu(NHC)OH] complexes and the mass spectra showing the same acetonitrile adducts, the only diagnostic data for formation of the hydroxo species is provided by the infra red spectra. The infra red spectra showed a broad peak for the OH in both **5** and **6** at 3380.0 cm⁻¹ and 3402.3 cm⁻¹ respectively, indicating that **5** and **6** were synthesised. It was attempted to obtain elemental analysis of **5** and **6**, however due to the slight decomposition of the compounds over time, these were unsuccessful.



Scheme 5: Synthesis of [Cu(NHC)OH], **5** and **6**.

4.2.3: Synthesis and Characterisation of Copper(I) Complexes with Bicyclic Expanded Ring NHC Ligands

There have been reports by Newman *et al.* of novel, relatively unexplored, bicyclic N-heterocyclic carbene ligands and their complexes and although the silver(I) dibenzyl derivative was prepared no copper(I) complexes were reported,^{26,27} therefore the coordination of these bicyclic systems to copper(I) has been investigated (Scheme 6, **7-9**). The route was the same as for the monocyclic derivatives,²³ however these systems appear to be more sensitive than those of the monocyclic rings, since they appear to decompose (turn green) over about a thirty minute period on exposure to air, which is much quicker than the expanded ring analogues. Therefore, the reactions were carried out under an inert atmosphere and using dry deuterated benzene as the solvent instead of toluene. Two alkyl derivatives with aryl substituents were synthesised, the benzyl bicyclic **7** and the mesityl bicyclic **8**, as shown in Scheme 6.



Scheme 6: Synthesis of bicyclic copper(I) complexes **7** and **8**.

Another alkyl derivative (iso-propyl) was also synthesised, **9**, as shown in Figure 3. The characterisation of these three compounds was undertaken with NMR spectroscopy. The ^1H NMR spectra of **7** and **8** show a large downfield shift of the benzylic hydrogens (NCH_2), which is due to the change from a cationic species to a coordinated species, which is an indication that complexation has occurred. The $^{13}\text{C}\{^1\text{H}\}$ NMR spectrum also provides evidence that **7** was synthesised as there is a peak at 197.88 ppm which corresponds to the NCN. As with the expanded ring copper(I) complexes mentioned in Chapter 4.2.2.1 the shift in ppm between the parent salt and the copper(I) complex for the NCN peak is shifted downfield. The parent salt for **7** appears at 153.7 ppm.²⁶ The $^{13}\text{C}\{^1\text{H}\}$ NMR spectrum of **9** shows a peak at 193.9 ppm, which again is downfield

from the parent salt where it appears at 151.0 ppm, these two values are in accordance with literature values for the copper(I) complexes.^{9,27}

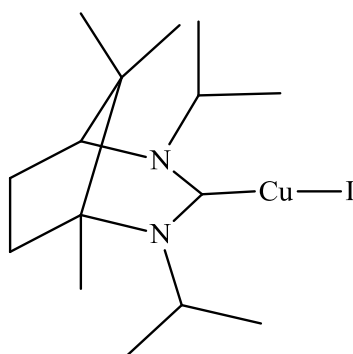


Figure 3: Structure of **9**.

For the characterisation of **8** an X-ray crystal structure was obtained. Crystals were grown by vapour diffusion of C₆D₆ and hexane in a glove box. The structure is shown in Figure 4 and selected bond lengths and angles in Table 2. The structure showed an unexpected feature as the C(11)-Cu(1)-(I) angle was significantly shifted from linearity at 158.4(6) ° (Table 2). This change in linearity is due to an apparent non covalent interaction between the mesityl ring and the copper. There is no covalent bond present, as there is no observed perturbation to the aromatic ring system.

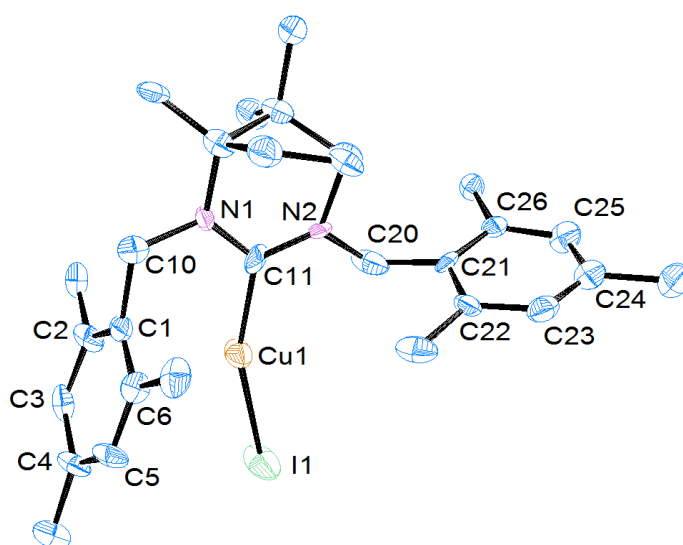


Figure 4: ORTEP ellipsoid plots at 50 % probability of the molecular structure of **8**.

Table 2: Selected bond lengths (Å) and angles (°) for **8**.

Lengths (Å)		Angles (°)	
N(1)-C(11)	1.34(2)	N(1)-C(11)-N(2)	117.7(17)
N(2)-C(11)	1.33(2)	C(11)-N(1)-C(10)	120.0(15)
C(11)-Cu(1)	1.943(18)	C(11)-N(2)-C(20)	120.9(15)
Cu(1)-I(1)	2.426(3)	N(1)-C(11)-Cu(1)	122.3(15)
N(2)-C(20)	1.50(2)	N(2)-C(11)-Cu(1)	120.0(13)
C(20)-C(21)	1.55(3)	C(11)-Cu(1)-I(1)	158.4(6)
C(21)-C(22)	1.40(3)	N(1)-C(10)-C(1)	117.9(15)
C(21)-C(26)	1.43(2)	C(10)-C(1)-C(2)	117.4(18)
N(1)-C(10)	1.47(2)	C(10)-C(1)-C(6)	120.9(18)
C(10)-C(1)	1.54(2)	C(6)-C(1)-C(2)	121.3(17)
C(1)-C(2)	1.41(3)	N(2)-C(20)-C(21)	112.4(15)
C(1)-C(6)	1.38(3)	C(20)-C(21)-C(22)	119.3(17)
C(2)-C(3)	1.40(2)	C(20)-C(21)-C(26)	116.7(16)
C(3)-C(4)	1.45(3)	C(26)-C(21)-C(22)	123.3(17)
C(4)-C(5)	1.37(2)	C(1)-C(2)-C(3)	119.7(18)
C(5)-C(6)	1.39(2)	C(2)-C(3)-C(4)	118.7(18)
		C(3)-C(4)-C(5)	118.3(17)
		C(4)-C(5)-C(6)	123.3(18)
		C(5)-C(6)-C(1)	118.3(18)

To probe this apparent interaction, density functional theory (DFT) calculations and further computational calculations and other computational methods were carried out. The optimised structure retains the interaction between the copper and the mesityl ring

system, as shown in Figure 5, and is similar to that provided by the crystal structure data, as the C(11)-Cu(1)-I(1) calculated bond angle is 162.8 °.

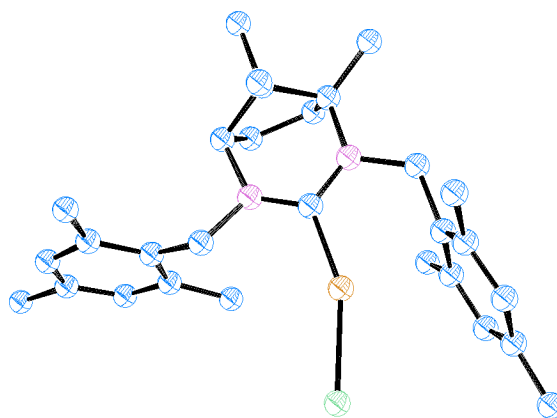


Figure 5: B97-D optimised structure of **8**.

In light of the optimised structure, Figure 5, quantum theory atoms in molecules (QTAIM) analysis of the wavefunction was carried out to further probe these interactions, using the AIM 2000 package.²⁸ The Cu... π interaction value comes out as 0.0233 indicating that this is indeed non covalent, as shown in Figure 6. A covalent interaction would be an order of magnitude larger than this, for example for the C-C bonds in the mesityl ring the value is 0.3049. The values are indicative of electron density between two atoms, these are arbitrary values and are not comparable to any other systems. The interactions observed in Figure 6 between the iodine atom and the mesityl rings are incorrect and can be disregarded, this is due to iodine having an effective core potential (ECP), which is where the core electrons are considered as a potential and only the outer electrons are involved in the calculation, this is a known shortcoming of QTAIM.

It was thought that the iodine may have an influence on the C(11)-Cu(1)-I(1) angle due to steric bulk. However the optimisation of the corresponding chlorine and bromine

complexes were carried out using the same methodology as before. It was found that the bond angle of the chlorine derivative was 165.9° and the bromine adduct was 164.37° . These angles are also lower than that found in the literature,⁹ having moved the angle away from linearity. From these calculations and the corresponding crystal data it is clear that an interaction does occur and it is this interaction which is causing the C(11)-Cu(1)-I(1) bond angles to decrease and move away from linearity and not steric bulk due to the halide moiety. This interaction does not appear to occur in **7** as shown by the optimised structure (Figure 7). This is due to the CH₂ adjacent to the aromatic ring having more rotational freedom, allowing the aromatic ring to flip out of the plain of the molecule.

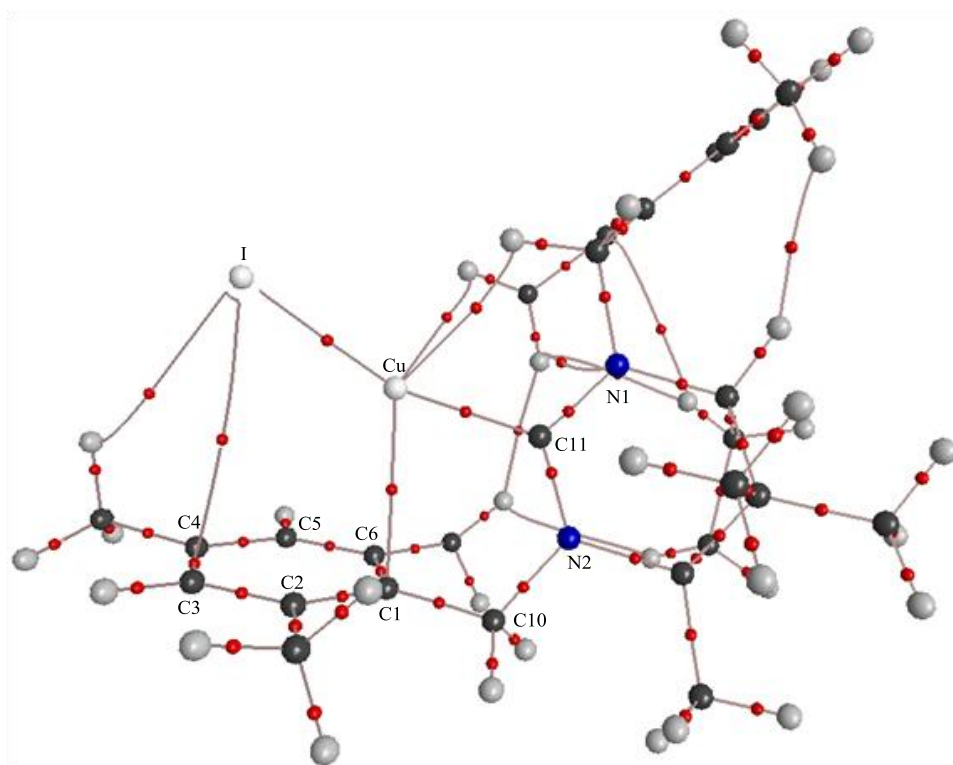


Figure 6: QTAIM analysis of **8** (blue atoms are nitrogens, black atoms are carbons, white atoms are hydrogens except where specified with the Cu and I atoms. Red dots show favourable interactions).

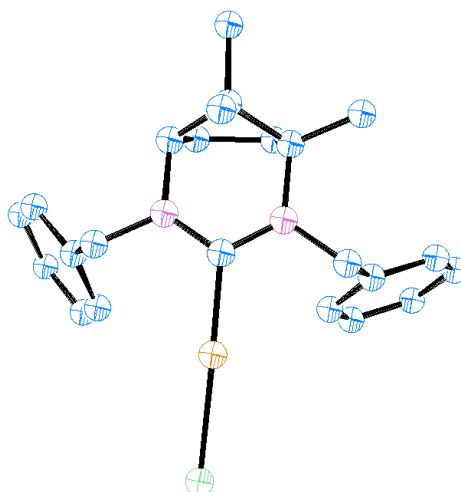


Figure 7: B97-D optimised structure of **7**.

This interaction does not occur in the expanded ring complexes, due to the bicyclic benzyl moiety having an added flexibility. The flexibility arises because of the presence of the benzylic type CH_2 group adjacent to the nitrogens. Therefore, the interaction is much less likely to occur in the expanded ring NHC complexes, due to the limited rotation of the aromatic moiety.

4.2.4: Attempted Formation of Other Copper(I) Complexes

4.2.4.1: The Attempted Synthesis and Characterisation of Expanded Ring Copper(I) Complexes

Although several copper(I) complexes have been successfully synthesised, **1-8**, there have been many that have not had the expected outcome. Other examples of expanded ring copper(I) complexes were attempted using the same methodology applied for **1-8**.

However these reactions appeared to be unsuccessful in the formation of copper complexes. Attempts to make $[\text{Cu}(6\text{-}o\text{-tolyl)I}]$ and $[\text{Cu}(7\text{-DEP)I}]$, resulted only in **10** and **11** being isolated, as shown in Figure 8.

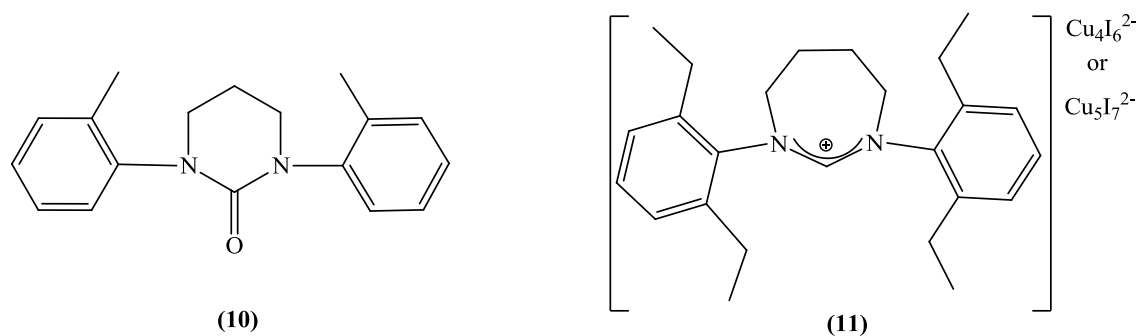


Figure 8: Compounds **10** and **11**.

These compounds were fully characterised using ^1H NMR and $^{13}\text{C}\{^1\text{H}\}$ NMR spectroscopy, mass spectrometry, and X-ray crystallography. The ^1H NMR spectra for these two compounds were obtained. In complex **11**, which has previously been made, **2**, the NCH_2 proton was shifted upfield to 3.60 ppm, which is 0.25 ppm different from that of **2**. This change in shift leads to the conclusion that this compound was not equivalent to that of **2**. A similar shift upfield is apparent in **10**. The $^{13}\text{C}\{^1\text{H}\}$ NMR spectra also shows the absence of the NCN peak at about 200 ppm, however peaks at 158.7 ppm for **11** and 152.6 ppm for **10** were observed and could not be assigned. It was unclear what the structure of these compounds was until the crystal structure data was obtained, as shown in Figure 9 and Table 3 for **10** and Figure 10 and Table 4 for **11**.

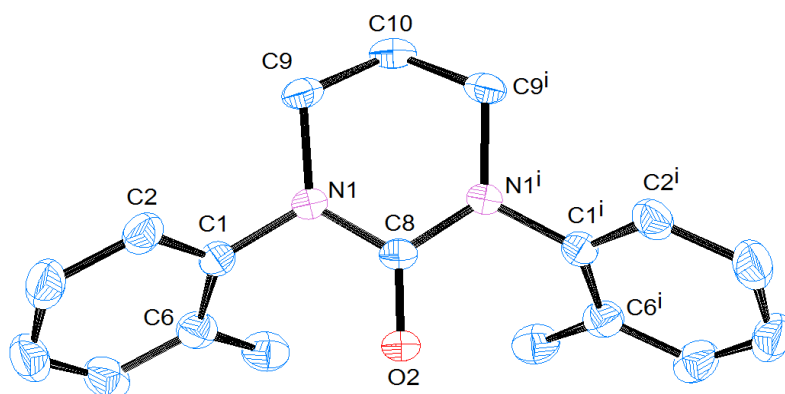


Figure 9: ORTEP ellipsoid plots at 50 % probability of the molecular structure of **10**.

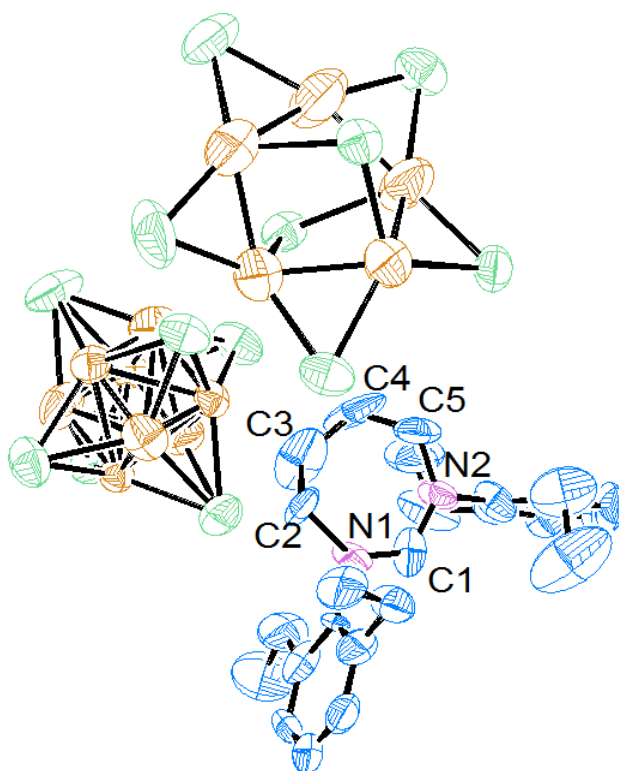


Figure 10: ORTEP ellipsoid plots at 50 % probability of the molecular structure of [7-DEP]⁺ [X]⁻, where X = [Cu₅I₇]²⁻ or [Cu₄I₆]²⁻, **11**.

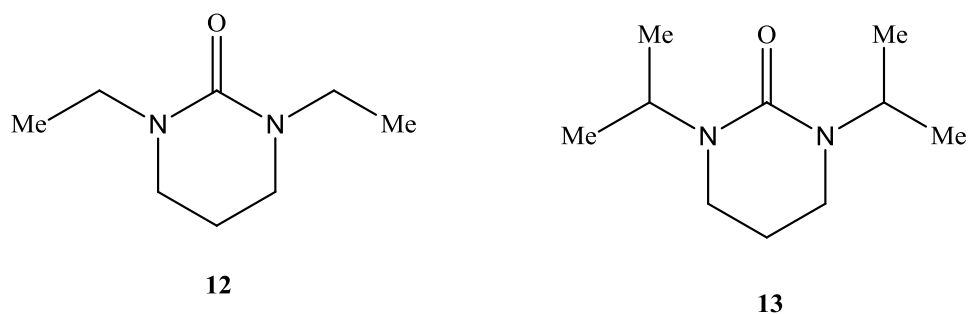
Table 3: Selected bond lengths (Å) and angles (°) for **10**.

Lengths (Å)		Angles (°)	
N(1)-C(8)	1.3771(14)	N(1)-C(8)-N(1 ⁱ)	116.74(15)
C(8)-O(2)	1.226(2)	N(1)-C(8)-O(2)	121.62(8)
N(1)-C(9)	1.4715(18)	N(1 ⁱ)-C(8)-O(2)	121.62(8)
C(9)-C(10)	1.5038(18)	C(8)-N(1)-C(9)	122.6(11)
C(10)-C(9 ⁱ)	1.5038(18)	C(8)-N(1 ⁱ)-C(9 ⁱ)	122.6(11)
C(9 ⁱ)-N(1 ⁱ)	1.4715(18)	N(1)-C(9)-C(10)	110.09(13)
N(1)-C(1)	1.4367(17)	C(9)-C(10)-C(9 ⁱ)	108.75(16)
C(1)-C(6)	1.399(2)	C(10)-C(9 ⁱ)-N(1 ⁱ)	110.09(13)
C(1)-C(2)	1.3885(18)	C(9)-N(1)-C(1)	117.17(11)
N(1 ⁱ)-C(1 ⁱ)	1.4367(17)	C(9 ⁱ)-N(1 ⁱ)-C(1 ⁱ)	117.17(11)
C(1 ⁱ)-C(2 ⁱ)	1.3885(18)	N(1)-C(1)-C(2)	118.92(12)
C(1 ⁱ)-C(6 ⁱ)	1.399(2)	N(1)-C(1)-C(6)	120.63(12)
C(8)-N(1 ⁱ)	1.3771(14)	N(1 ⁱ)-C(1 ⁱ)-C(6 ⁱ)	120.63(12)
		C(6)-C(1)-C(2)	120.37(12)
		C(6 ⁱ)-C(1 ⁱ)-C(2 ⁱ)	120.37(12)
		C(8)-N(1)-C(1)	
		C(8 ⁱ)-N(1 ⁱ)-C(1 ⁱ)	

Table 4: Selected bond lengths (Å) and angles (°) for [7-DEP]⁺ [X]⁻, where X = [Cu₅I₇]²⁻ or [Cu₄I₆]²⁻, **11**.

Lengths (Å)		Angles (°)	
N(1)-C(1)	1.30(3)	N(1)-C(1)-N(2)	126.0(2)
N(2)-C(1)	1.38(3)	C(1)-N(1)-C(2)	130.0(2)
N(1)-C(2)	1.48(3)	N(1)-C(2)-C(3)	111.0(2)
C(2)-C(3)	1.510(18)	C(2)-C(3)-C(4)	117.0(3)
C(3)-C(4)	1.53(4)	C(3)-C(4)-C(5)	115.5(18)
C(4)-C(5)	1.521(19)	C(4)-C(5)-N(2)	109.6(15)
C(5)-N(2)	1.492(19)	C(5)-N(2)-C(1)	120.9(16)

The structure obtained for **10** shows it to be the urea derivative of the N-heterocyclic carbene, where oxygen has bonded to the carbene, in turn eliminating the copper halide, this is probably due to the reaction of the free carbene with oxygen, as Alici *et al.* have reported similar reactions.²⁹ The mass spectrum of **10** is in accordance with the crystal data as there is a peak at 281.18 amu, which has a calculated value of 281.00 amu, which corresponds to [M⁺ - Cu - I + O + H⁺]. The ¹³C{¹H} NMR spectroscopic data has previously been reported for similar 5-membered and 6-membered NHCs containing a urea moiety and Widenhoefer states that the NC(O)N peak in the ¹³C{¹H} NMR appears at 155.6 ppm for **12** and 155.2 ppm for **13** as shown in Figure 11.³⁰

**Figure 11:** Compounds **12** and **13**.³⁰

The X-ray crystal structure data of **11** shows a different compound to that of **10**. This shows that the NHC salt is still present; however instead of having a halide as the counterion, there are now two copper anions, $[\text{Cu}_4\text{I}_6]^{2-}$ and $[\text{Cu}_5\text{I}_7]^{2-}$ present. This is probably due to the way in which these compounds were synthesised, with an *in situ* route. This could cause an anion exchange process instead of the expected deprotonation of the salt, followed by coordination to the metal. The shift in ppm in the proton NMR spectrum of the NCH_2 is still an anomaly as the counterion exchange would not be expected to alter the ^1H NMR spectrum significantly. The only reasoning is that the large shift in ppm of the NCH_2 protons are due to a strong ion pair interaction between the NCHN salt and the copper anion, whereas the halide counterion has a weaker ion pair interaction, hence causing the shift.

The compound shown in Figure 10 is also found in the mass spectrum, which shows a peak at 363.28 amu, which has a calculated value of 363.56 amu, corresponding to $[\text{NCN} + \text{H}^+]$ as the counterion is not observed, showing that the predicted coordination of the copper has not proceeded as expected.

4.2.4.2: The Attempted Synthesis and Characterisation of Bicyclic Copper(I) Complexes

Although the synthesis of compounds **7-9** had been successful, problems occurred upon attempting to synthesise different variations of these copper complexes. The route taken to the bicyclic complexes was the same as for **7-9**, however THF was used as the solvent for **14** and toluene was used as the solvent for **15** and **16** instead of deuterated benzene. The complexes sought were the diethyl (**14**), diisopropyl (**15**), and the copper iodide analogue of the benzyl (**16**) as shown in Figure 12.

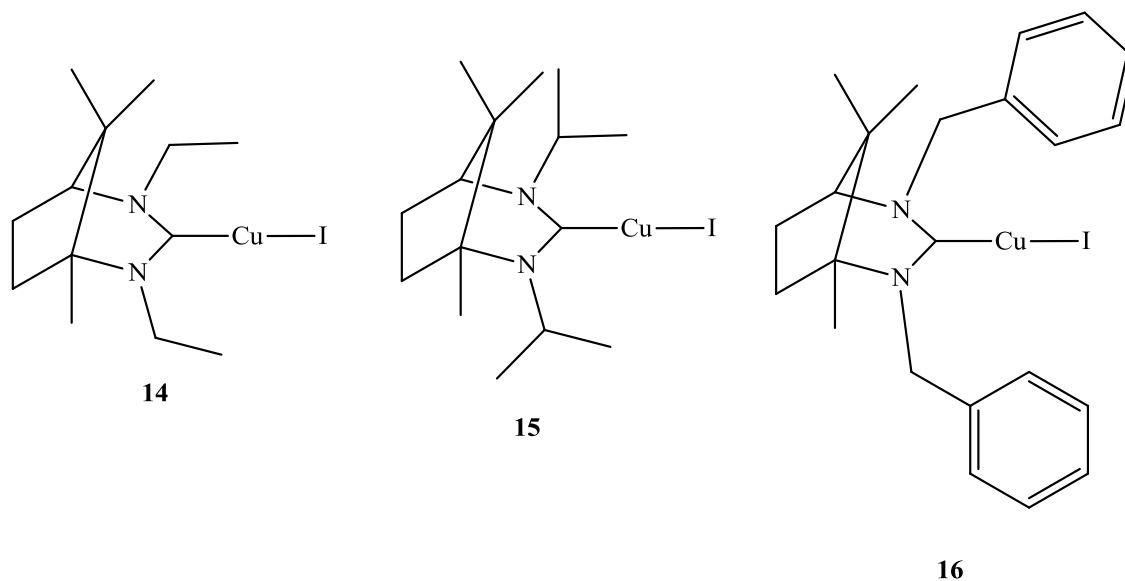


Figure 12: Expected structures compounds **14-16**.

They all showed very similar $^{13}\text{C}\{^1\text{H}\}$ NMR spectroscopic results where the NCN peak could not be observed but there was a very strong peak at 154.1 ppm, 154.9 ppm, and 155.8 ppm for the diisopropyl, diethyl, and benzyl derivatives respectively. These peaks suggest one of three things: the first would be the same as **10**, where a urea derivative is formed;³⁰ the second being where the NCN bridges between two copper(I) centres;³¹⁻³⁴ and the third being where a haloamidinium species is formed as shown by Nechaev *et al.*²⁴ Compounds **17-19**, **20-22**, and **23-25**, Figure 13, show the possible outcomes of these reactions. The mass spectra of **14**, **15**, and **16** show peaks at 225.19 amu, 253.2280 amu, and 349.2275 amu respectively, which correspond to $[\text{NCN} + \text{O}]$, which have calculated values of 225.00 amu, 253.2280 amu, and 349.2285 amu respectively. There are also absences for the bridging NCN peaks in all three, and it is therefore assumed that the unexpected compounds which have been formed are the urea type compounds **17-19**.

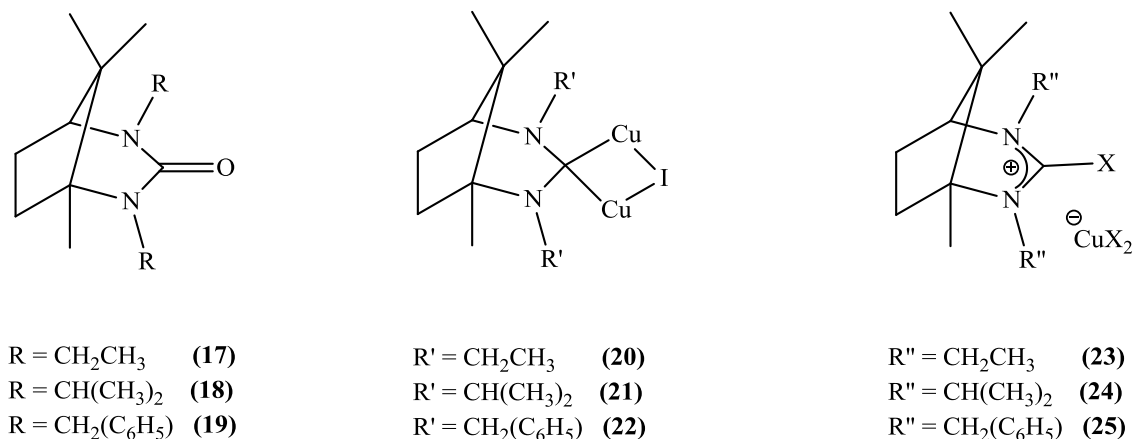


Figure 13: Predicted structures, 17-25.

It cannot be completely discerned which of these structures is correct as the hydrogen NMR spectra obtained along with the $^{13}\text{C}\{^1\text{H}\}$ NMR spectra were not conclusive due to the similarity in peaks around 150 ppm in the $^{13}\text{C}\{^1\text{H}\}$ NMR spectra. The mass spectrometry on its own is not conclusive enough to predict the structure between the three possibilities shown in Figure 13. The only way to attain these structures is to obtain the X-ray crystallography data, which has been attempted but was unsuccessful.

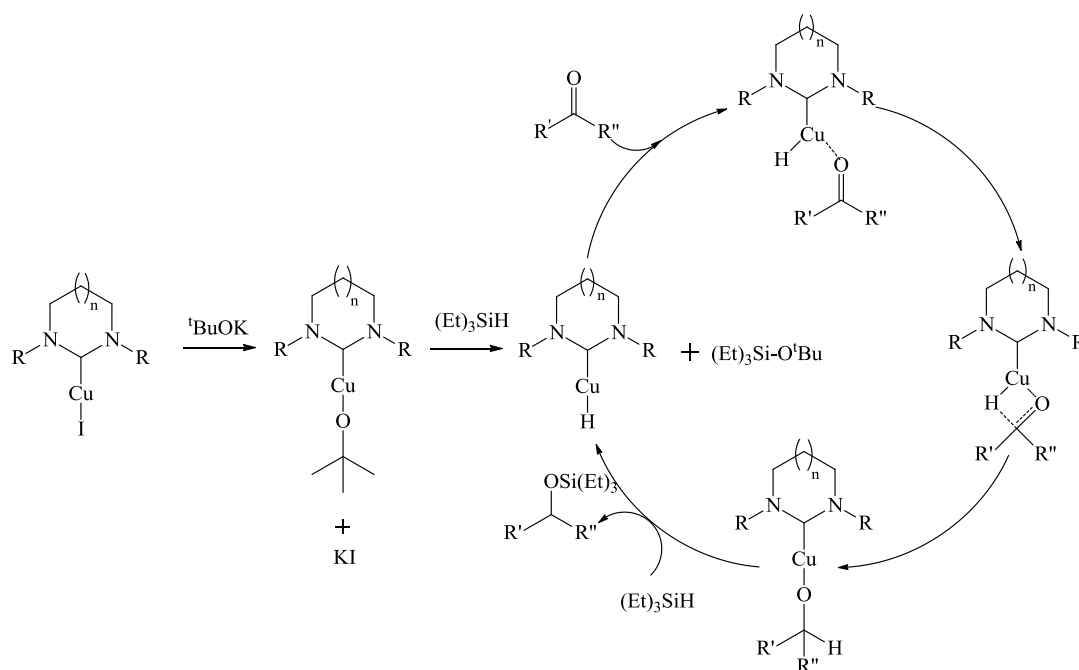
4.2.5: Catalysis

Nolan and co-workers have extensively researched the 5-membered copper(I) complexes as catalysts for hydrosilylation and have shown that at a catalyst loading of 3 mol % and 80 °C impressive yields of above 90 % are achieved.^{32,35-37} The best conversions were observed with isopropyl N-substituents and this is attributed to the steric bulk at the copper(I) centre.^{35,36} Due to these highly active catalyst being reported by Nolan and the success which the Cavell group have had with the expanded ring NHCs it was of interest to explore whether an active catalytic species could be

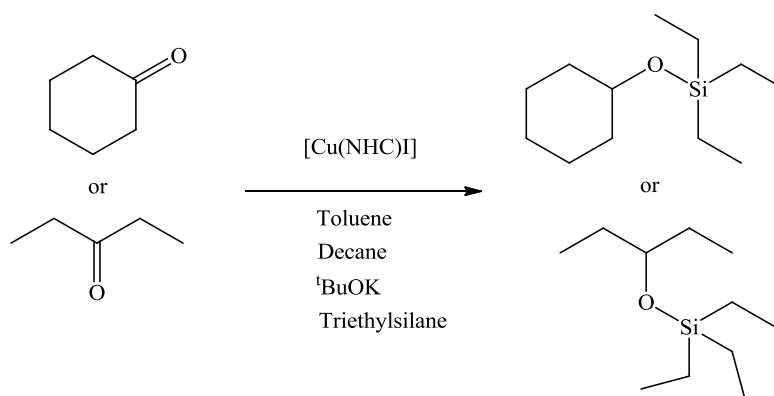
generated here. Therefore the catalysts employed here combine the two properties of an expanded ring NHC and highly sterically encumbered N-substituents.

4.2.5.1: Catalytic Activity of Expanded Ring Copper(I) Complexes

Nolan and co-workers have proposed a mechanism for the hydrosilylation of ketones using copper(I) complexes of the general formula $[\text{Cu}(\text{NHC})\text{X}]$ where $\text{X} = \text{Cl}, \text{Br}, \text{or I}$, Scheme 7.³⁷ This mechanism starts with the activation of the copper(I) complex by abstracting the halide and forming the $[\text{Cu}(\text{NHC})(^t\text{BuO})]$ complex, this is then reacted with triethylsilane forming the copper(I) hydride species which in turn reacts with the ketone substrate through a four membered transition state. This four membered transition state then produces the alkoxide adduct, which after insertion of the silane substrate eliminates the target product and regenerates the copper(I) hydride species. The complexes **1-4** and $[\text{Cu}(7\text{-DIPP})\text{I}]$, as synthesised by Nachaev,⁹ are expected to operate through the cycle shown in Scheme 7.



Scheme 7: Hypothesised mechanism for the hydrosilylation of ketones using $[\text{Cu}(\text{NHC})\text{I}]$ as the catalyst.

Table 5: Hydrosilylation of ketones using **1-4** and [Cu(7-DIPP)I] as catalysts.^a

Entry	Catalyst	Substrate	Time (hours)	Yield (%) ^b
1	1		18	0
2	1		18	0
3	2		18	0
4	2		18	0
5	3		18	0
6	3		18	0
7	4		18	0
8	4		18	0
9	[Cu(7-DIPP)I]		18	0
10	[Cu(7-DIPP)I]		18	0

^aReaction conditions: Substrate (1 mmol), catalyst (1 mol %), toluene (2 ml), ^tBuOK (12 mol %), decane (internal standard, 1 mmol), triethylsilane (3 eq), room temperature 18 hours. ^bPercentage yields based upon consumption of substrate by GCMS.

The results of the hydrosilylation reactions are summarised in Table 5. Unfortunately there was no conversion with any substrate with any catalyst. This was contrary to that observed by Dunsford,²³ where conversions of up to 100 % occurred with [Cu(6-Mes)Cl] as the catalyst, at a loading of 3 mol %. The lack of conversion observed with **1-4** and [Cu(7-DIPP)I] could be due to the low amount of catalyst loading. The other reason for no catalytic activity could be due to decomposition of the complex over time. Due to time constraints no further catalytic testing was carried out.

4.3: Conclusions

In conclusion a series of expanded ring copper(I) complexes were synthesised, **1-4**, in a similar way to that of the Cavell group for the [Cu(6-Mes)Cl] and [Cu(7-Mes)Cl].²³ This methodology has proved to be cheaper and simpler than that of Nechaev *et al.*⁹ A few of these complexes of the general formula [Cu(NHC)X], where X = I, have then been converted to the copper(I) hydroxide derivatives using the methodology of Nolan *et al.*¹⁴ producing **5** and **6**.

A series of bicyclic N-heterocyclic carbenes were also coordinated to copper(I) through a similar route to that of the expanded ring carbenes, except the solvent was switched from toluene to deuterated benzene and the entire reaction was carried out in a glove box under an inert atmosphere, in turn producing **7-9**. There were no unexpected results with **7** and **9**; however **8** showed an interaction between the mesityl ring and the copper in the crystal structure. This was confirmed using DFT calculations and QTAIM analysis, which was in accordance with that of the crystal structure data, showing a non covalent interaction between the mesityl ring and the copper.

A number of other compounds were also synthesised, however the results of these were not as expected, with **10** and **11** being formed instead of their [Cu(NHC)X] analogues. This unexpected synthesis was shown using ¹³C{¹H} NMR spectroscopy, where there was a peak at 152.6 ppm and 158.7 ppm for **10** and **11** respectively, which are more in accordance with the urea type moiety for **10**³⁰ and the NCHN salt for **11** than that of the

copper N-heterocyclic carbene which was expected. The crystal structures of **10** and **11** were conclusive in showing that the expected complexes had not been formed and the urea type compound, and the exchange of the copper counterion for **11** had been synthesised. The bicyclic compounds, which did not produce the expected complexes **14-16**, were not conclusive in confirming what was produced as X-ray crystal structure data was not obtainable.

Hydrosilylation of cyclohexanone and 3-pentanone was carried out using catalysts **1-4**, however the outcome was not as expected with no conversion for any of the catalytic processes. This could be explained by the decrease in catalyst loading from 3 mol %, which had been previously employed by Nolan^{32,35-37} and Dunsford,²³ to 1 mol %. Due to the lack of activity it was not possible to observe whether the steric hindrance from the N-substituents along with the expanded ring NHC increased the activity of the catalyst.

The overall synthesis of the copper(I) complexes with general formula [Cu(NHC)X], where X =Cl and I, and [Cu(NHC)OH] (**1-9**) were successful.

4.4: Experimental

4.4.1: General Remarks

All air sensitive experiments were carried out using standard Schlenk techniques, under an atmosphere of argon or in a MBRAUN M72 glove box (N₂ atmosphere with > 0.1 ppm O₂ and H₂O) unless otherwise stated. Glassware was dried overnight in an oven at 120 °C and flame dried prior to use. Toluene, pentane, hexane, and DCM of analytical grade were freshly collected from a MBRAUN sps 800 solvent purification system. All other solvents were used as purchased.

All NMR solvents used were purchased from Goss Scientific Ltd, and distilled from the appropriate drying agents under N₂ prior to use, following standard literature methods.³⁸ All NMR spectra were obtained from a Bruker Avance AMX 400 or 500 MHz and referenced to SiMe₄ and coupling constants *J* are expressed in Hertz as positive values regardless of their real individual signs. Mass spectrometry data was recorded, HRMS were obtained on a Waters Q-ToF micromass spectrometer and are reported as *m/z* (relative intensity) by the department of chemistry, Cardiff University.

All computational calculations were carried out by the Platts group on the Merlin cluster at Cardiff University. DFT optimisation of compound **8** was carried out using the crystal structure coordinates as a starting point. This was done using the B97 functional with an empirical dispersion correction of the type D2,³⁹ using the def2-TZVP basis set,⁴⁰ with resolution of identity (ri), within turbomole version 5.10.⁴¹ Resolution of identity uses auxiliary fitting basis sets to speed up the calculation of some two electron integrals. QTAIM analysis was carried out using the AIM 2000 package to find (3,-1) bond critical points.²⁸

All the X-ray Crystal structures were obtained on a Bruker Nonius Kappa CCD diffractometer using graphite mono-chromated Mo KR radiation ($\lambda(\text{Mo KR}) = 0.71073 \text{ \AA}$). An Oxford Cryosystems cooling apparatus was attached to the instrument, and all data were collected at 150 K. Data collection and cell refinement were carried out by

Dr Benson Kariuki, using COLLECT⁴² and HKL SCALEPACK.⁴³ Data reduction was applied using HKL DENZO and SCALEPACK.⁴³ The structures were solved using direct methods (Sir92)⁴⁴ and refined with SHELX-97.⁴⁵ Absorption corrections were performed using SORTAV.⁴⁶

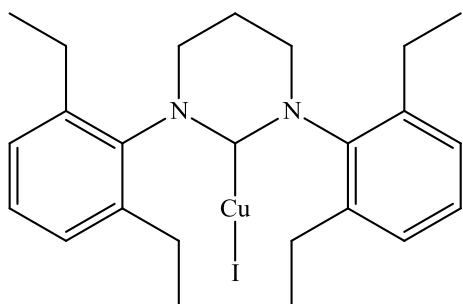
GC-MS data was obtained on an Agilent Technologies 6890N GC system with an Agilent Technologies 5973 iner MS detector with MSD.

Elemental analysis was obtained from the service provided by MEDAC Ltd.

N-heterocyclic carbene precursors to compounds **1**, **2**, **3**, **4**, **7**, **10**, and **11** were synthesised by known literature procedures.^{26,47-49} The NHC salts for compounds **8**, **9**, **17**, **18**, and **19** were synthesised by methodologies reported in Chapter 3 of this thesis. All other reagents were used as purchased unless otherwise stated.

4.4.2: Experimental Data for Copper(I) Complexes

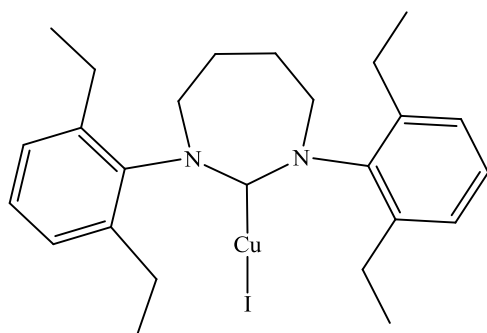
Synthesis of [Cu(6-DEP)I] (1)



[6-(DEPH)Br] (0.50 g, 1.17 mmol, 1 eq) was placed in a flame dried Schlenk and dried for 20 minutes. To this Schlenk CuI (0.27 g, 1.40 mmol, 1.2 eq), potassium tertiary butoxide (0.18 g, 1.63 mmol, 1.4 eq) and toluene (15 ml) were all added in a glove box and the reaction mixture was then

stirred outside of the glove box for 18 hours. The toluene was then removed in *vacuo*, DCM (20 ml) was added and then filtered through a pad of celite. The DCM was then removed yielding [Cu(6-(DEP)I] as a white solid (0.08 g, 13.1 %). ^1H NMR (CDCl_3 , 400 MHz, 298 K): δ 7.25 (2 H, m, CH_{Ar}), δ 7.10 (4 H, d, CH_{Ar} , $^3J_{\text{HH}} = 7.6$ Hz), δ 3.35 (4 H, t, NCH_2 , $^3J_{\text{HH}} = 5.8$ Hz), δ 2.15 (8 H, m, CH_2), δ 2.30 (2 H, m, NCH_2CH_2), δ 1.25 (12 H, t, CH_3 , $^3J_{\text{HH}} = 7.6$ Hz). $^{13}\text{C}\{^1\text{H}\}$ NMR (CDCl_3 , 125 MHz, 298 K): δ 202.5 (NCN), δ 143.0 (NC_{Ar}), δ 140.0 (C_{Ar}), δ 129.0 (CH_{Ar}), δ 127.5 (CH_{Ar}), δ 45.5 (NCH_2), δ 24.0 (CH_2), δ 20.5 (NCH_2CH_2), δ 15.5 (CH_3). MS(ES) m/z : [$\text{M}^+ - \text{I} + \text{MeCN}$] 452.2132 ($\text{C}_{26}\text{H}_{35}\text{N}_3\text{Cu}$ requires 452.2127).

Synthesis of [Cu(7-DEP)I] (2)

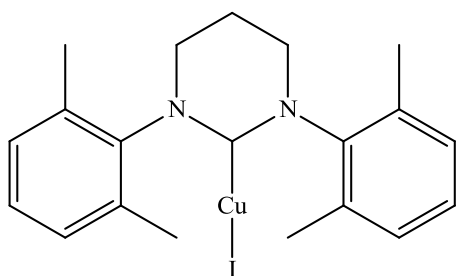


[(7-DEPH)I] (0.50 g, 1.53 mmol, 1 eq) was placed in a flame dried Schlenk and dried for 20 minutes. To this Schlenk CuI (0.35 g, 1.84 mmol, 1.2 eq), potassium tertiary butoxide (0.24 g, 2.15 mmol, 1.4 eq) and THF (15 ml) were all added in a glove box and the reaction mixture was then stirred outside of the glove box for 36

hours. The THF was then removed in *vacuo*, DCM (20 ml) was added and then filtered

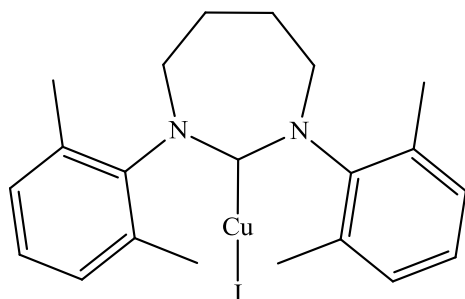
through a pad of celite. The DCM was then removed yielding [Cu(7-DEP)I] as an off white solid (0.29 g, 33.7 %). ^1H NMR (CDCl_3 , 400 MHz, 298 K): δ 7.20 (2 H, t, CH_{Ar} , $^3J_{\text{HH}} = 7.6$ Hz), δ 7.10 (4 H, d, CH_{Ar} , $^3J_{\text{HH}} = 7.6$ Hz), δ 3.85 (4 H, m, NCH_2), δ 2.75 (4 H, q, CH_2 , $^3J_{\text{HH}} = 7.5$ Hz), δ 2.65 (4 H, q, CH_2 , $^3J_{\text{HH}} = 7.5$ Hz), δ 2.25 (4 H, m, NCH_2CH_2), δ 1.30 (12 H, t, CH_3 , $^3J_{\text{HH}} = 7.5$ Hz). $^{13}\text{C}\{^1\text{H}\}$ NMR (CDCl_3 , 125 MHz, 298 K): NCN not observed, δ 144.3 (NC_{Ar}), δ 139.0 (C_{Ar}), δ 127.6 (CH_{Ar}), δ 126.0 (CH_{Ar}), δ 52.5 (NCH_2), δ 24.6 (NCH_2CH_2), δ 23.4 (CH_2), δ 23.2 (CH_2), δ 13.6 (CH_3). MS(ES) m/z : [$\text{M}^+ - \text{I} + \text{MeCN}$] 466.2284 ($\text{C}_{27}\text{H}_{37}\text{N}_3\text{Cu}$ requires 466.2283).

Synthesis of [Cu(6-xylyl)I] (3)



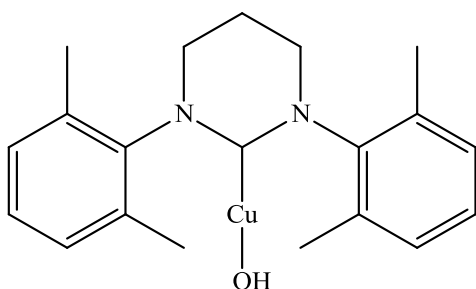
[(6-xylyl)H]Br] (0.50 g, 1.34 mmol, 1 eq) was placed in a flame dried Schlenk and dried for 20 minutes. To this Schlenk CuI (0.31 g, 1.61 mmol, 1.2 eq), potassium tertiary butoxide (0.21 g, 1.88 mmol, 1.4 eq) and toluene (15 ml) were all added in a glove box and the reaction mixture was then

stirred outside of the glove box for 18 hours. The toluene was then removed in *vacuo*, DCM (20 ml) was added and then filtered through a pad of celite. The DCM was then removed yielding [Cu(6-xylyl)I] as a white solid (0.28 g, 43.3 %). ^1H NMR (CDCl_3 , 500 MHz, 298 K): δ 7.15 (2 H, m, CH_{Ar}), δ 7.05 (4 H, m, CH_{Ar}), δ 3.30 (4 H, m, NCH_2), δ 2.30 (2 H, m, NCH_2CH_2), δ 2.25 (12 H, s, CH_3). $^{13}\text{C}\{^1\text{H}\}$ NMR (CDCl_3 , 125 MHz, 298 K): NCN not observed, δ 143.0 (NC_{Ar}), δ 134.0 (C_{Ar}), δ 128.0 (CH_{Ar}), δ 127.5 (CH_{Ar}), δ 43.5 (NCH_2), δ 20.0 (NCH_2CH_2), δ 17.0 (CH_3). MS(ES) m/z : [$\text{M}^+ - \text{I} + \text{MeCN}$] 396.1490 ($\text{C}_{22}\text{H}_{27}\text{N}_3\text{Cu}$ requires 396.1501). IR (Nujol Mull, cm^{-1}): 2924 (C-C), 2853 (C-H).

Synthesis of [Cu(7-xylyl)I] (4)

[(7-xylyl)H]Br] (0.50 g, 1.29 mmol, 1 eq) was placed in a flame dried Schlenk and dried for 20 minutes. To this Schlenk CuI (0.30 g, 1.55 mmol, 1.2 eq), potassium tertiary butoxide (0.20 g, 1.81 mmol, 1.4 eq) and toluene (15 ml) were all added in a glove box and the reaction mixture

was then stirred outside of the glove box for 18 hours. The toluene was then removed *in vacuo*, DCM (20 ml) was added and then filtered through a pad of celite. The DCM was then removed yielding [Cu(7-xylyl)I] as an off white solid (0.33 g, 51.9 %). ^1H NMR (CDCl_3 , 400 MHz, 298 K): δ 7.05 (6 H, m, CH_{Ar}), δ 3.85 (4 H, m, NCH_2), δ 2.40 (12 H, s, CH_3), δ 2.25 (4 H, m, NCH_2CH_2). $^{13}\text{C}\{^1\text{H}\}$ NMR (CDCl_3 , 125 MHz, 298 K): NCN not observed, δ 145.0 (NC_{Ar}), δ 134.0 (C_{Ar}), δ 128.0 (CH_{Ar}), δ 127.0 (CH_{Ar}), δ 52.0 (NCH_2), δ 25.0 (NCH_2CH_2), δ 18.0 (CH_3). MS(ES) m/z : [$\text{M}^+ - \text{I} + \text{MeCN}$] 410.1643 ($\text{C}_{23}\text{H}_{29}\text{N}_3\text{Cu}$ requires 410.1643). IR (Nujol Mull, cm^{-1}): 2923 (C-C), 2853 (C-H).

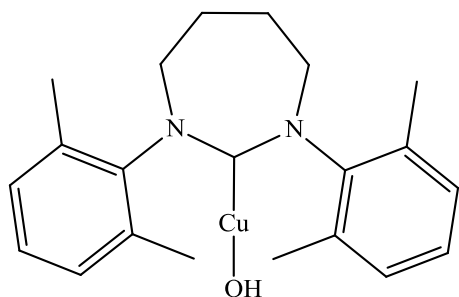
Synthesis of [Cu(6-xylyl)OH] (5)

[6-(xylyl)CuI] (0.10 g, 0.21 mmol, 1 eq) was placed in a flame dried Schlenk and dried for 20 minutes. CsOH.H₂O (0.07 g, 0.41 mmol, 2 eq) and THF (15 ml) were then added and stirred at room temperature for 18 hours. The resulting solution was then filtered through a pad of celite

and reduced to dryness yielding [Cu(6-xylyl)OH] as a off white solid (0.03 g, 38.9 %). ^1H NMR (CDCl_3 , 500 MHz, 298 K): δ 7.10 (2 H, m, CH_{Ar}), δ 7.05 (4 H, m, CH_{Ar}), δ 3.55 (2 H, t, NCH_2 , $^3J_{\text{HH}} = 5.0$ Hz), δ 3.30 (2 H, t, NCH_2 , $^3J_{\text{HH}} = 5.0$ Hz), δ 2.35 (2 H,

m, NCH_2CH_2), δ 2.30 (6 H, s, CH_3), δ 2.25 (6 H, s, CH_3). $^{13}\text{C}\{^1\text{H}\}$ NMR (CDCl_3 , 125 MHz, 298 K): NCN not observed, δ 135.0 (NC_{Ar}), δ 134.0 (C_{Ar}), δ 128.0 (CH_{Ar}), δ 127.0 (CH_{Ar}), δ 47.5 (NCH_2), δ 43.5 (NCH_2), δ 18.0 (NCH_2CH_2), δ 17.5 (CH_3), δ 17.5 (CH_3). MS(ES) m/z : [$\text{M}^+ - \text{I} + \text{MeCN}$] 396.1467 ($\text{C}_{22}\text{H}_{27}\text{N}_3\text{Cu}$ requires 396.1501). IR (Nujol Mull, cm^{-1}): 3380 (O-H).

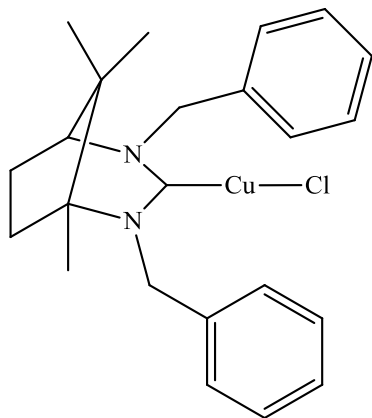
Synthesis of $[\text{Cu}(7\text{-xylyl})\text{OH}]$ (6)



$[\text{7-(xylyl)CuI}]$ (0.10 g, 0.20 mmol, 1 eq) was placed in a flame dried Schlenk and dried for 20 minutes. $\text{CsOH}\cdot\text{H}_2\text{O}$ (0.07 g, 0.40 mmol, 2 eq) and THF (15 ml) were then added and stirred at room temperature for 18 hours. The resulting solution was then filtered through a pad of celite

and reduced to dryness yielding $[\text{Cu}(7\text{-xylyl})\text{OH}]$ as a pale yellow solid (0.02 g, 25.7 %). ^1H NMR (CDCl_3 , 400 MHz, 298 K): δ 7.05 (2 H, m, CH_{Ar}), δ 6.95 (4 H, m, CH_{Ar}), δ 3.60 (4 H, m, NCH_2), δ 2.25 (12 H, s, CH_3), δ 1.95 (4 H, m, NCH_2CH_2). $^{13}\text{C}\{^1\text{H}\}$ NMR (CDCl_3 , 125 MHz, 298 K): NCN not observed, δ 143.0 (NC_{Ar}), δ 135.0 (C_{Ar}), δ 127.0 (CH_{Ar}), δ 126.0 (CH_{Ar}), δ 50.5 (NCH_2), δ 26.5 (NCH_2CH_2), δ 18.0 (CH_3). MS(ES) m/z : [$\text{M}^+ - \text{I} + \text{MeCN}$] 410.1679 ($\text{C}_{23}\text{H}_{29}\text{N}_3\text{Cu}$ requires 410.1657). IR (Nujol Mull, cm^{-1}): 3402 (O-H).

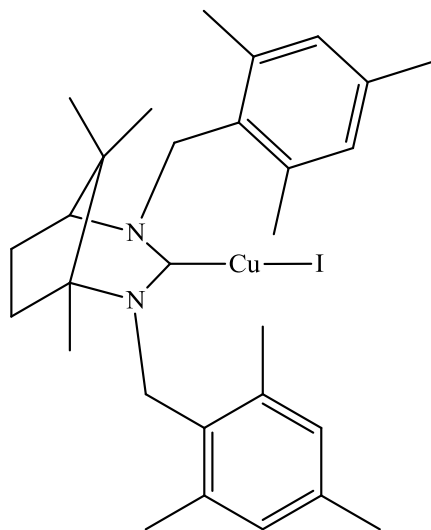
Synthesis of ((5S)-2,4-dibenzyl-1,8,8-trimethyl-2,4-diazabicyclo[3.2.1]octan-3-yl)copper(I) chloride (7)



(1R, 5S)-2,4-dibenzyl-1,8,8-trimethyl-4-aza-2-azoniabicyclo-[3.2.1]oct-2-ene hexafluorophosphate (0.05 g, 0.11 mmol, 1 eq) was placed in a flame dried Schlenk and dried for 20 minutes. To this Schlenk CuCl (0.01 g, 0.13 mmol, 1.2 eq), potassium tertiary butoxide (0.02 g, 0.15 mmol, 1.4 eq) and toluene (10 ml) were all added in a glove box and the reaction mixture was then stirred outside of the glove box for 18 hours. The

toluene was then removed in *vacuo* and the crude product was taken back into the glove box, benzene (5 ml) was added and then filtered through cotton wool. This solution was then reduced in *vacuo* yielding ((5S)-2,4-dibenzyl-1,8,8-trimethyl-2,4-diazabicyclo[3.2.1]octan-3-yl)copper(I) chloride as a white solid (0.02 g, 39.9 %). ^1H NMR (C_6D_6 , 400 MHz, 298 K): δ 7.40 - 6.90 (10 H, m, CH_{Ar}), δ 4.75 - 4.35 (4 H, m, NCH_2), δ 2.45 (1 H, d, NCH , $^3J_{\text{HH}} = 4.6$ Hz), δ 2.15 (1 H, m, CH), δ 2.00 (3 H, s, CH_3), δ 1.90 (1 H, m, CH), δ 1.15 (1 H, m, CH), δ 0.75 (1 H, m, CH), δ 0.60 (3 H, s, CH_3), δ 0.55 (3 H, s, CH_3). $^{13}\text{C}\{^1\text{H}\}$ NMR (C_6D_6 , 125 MHz, 298 K): δ 197.8 (NCN), δ 138.0 (C_{Ar}), δ 136.5 (C_{Ar}), δ 128.0 (CH_{Ar}), δ 128.0 (CH_{Ar}), δ 125.5 (CH_{Ar}), δ 125.5 (CH_{Ar}), δ 124.0 (CH_{Ar}), δ 124.0 (CH_{Ar}), δ 68.0 (NCH), δ 65.0 (NC), δ 60.0 (NCH_2), δ 56.5 (NCH_2), δ 49.0 (CH), δ 48.0 (C), δ 30.0 (CH), δ 20.0 (CH_3), δ 17.5 (CH_3), δ 14.0 (CH_3). MS (ES) m/z : [$\text{M}^+ + \text{MeCN}$] 436.1817 ($\text{C}_{25}\text{H}_{31}\text{N}_3\text{Cu}$) requires 436.1814).

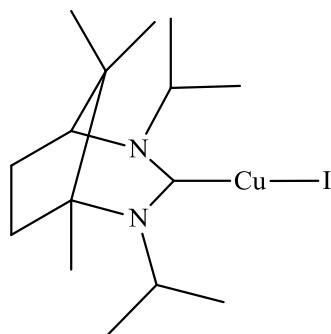
Synthesis of ((5S)-1,8,8-trimethyl-2,4-bis(2,4,6-trimethylbenzyl)-2,4-diazabicyclo[3.2.1]octan-3-yl)copper(I) iodide (8)



(1S)-5,8,8-trimethyl-2,4-bis(2,4,6-trimethylbenzyl)-4-aza-2-azoniabicyclo[3.2.1]octane hexafluorophosphate(V) (0.10 g, 0.17 mmol, 1 eq) was placed in a flame dried Schlenk and dried for 20 minutes. To this Schlenk CuI (0.04 g, 0.25 mmol, 1.2 eq), potassium tertiary butoxide (0.04 g, 0.21 mmol, 1.4 eq) and toluene (10 ml) were all added in a glove box and the reaction mixture was then stirred outside of the glove box for 18 hours. The toluene was then removed in *vacuo* and the crude

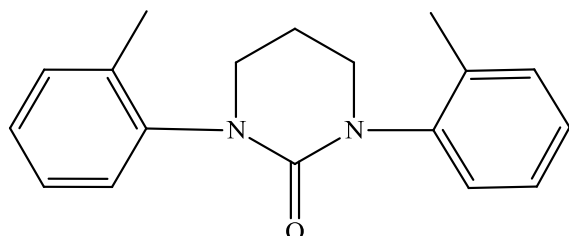
product was taken back into the glove box, benzene (5 ml) was added and then filtered through cotton wool. This solution was then reduced in *vacuo* yielding ((5S)-1,8,8-trimethyl-2,4-bis(2,4,6-trimethylbenzyl)-2,4-diazabicyclo[3.2.1]octan-3-yl)copper(I) iodide as a white solid (0.05 g, 46.0 %). ^1H NMR (C_6D_6 , 400 MHz, 298 K): δ 7.10 (1 H, s, CH_{Ar}), δ 6.90 (1 H, s, CH_{Ar}), δ 6.85 (1 H, s, CH_{Ar}), δ 6.75 (1 H, s, CH_{Ar}), δ 5.50 – 4.00 (4 H, m, 2 x NCH_2), δ 2.75 (1 H, d, NCH , $^3J_{\text{HH}} = 5.0$ Hz), δ 2.55 (6 H, s, CH_3), δ 2.50 (3 H, s, CH_3), δ 2.35 (6 H, s, CH_3), δ 2.25 (3 H, s, CH_3), δ 1.85 (1 H, m, CH), δ 1.55 (1 H, m, CH), δ 1.35 (2 H, m, CH_2), δ 1.05 (3 H, s, CH_3), δ 0.80 (3 H, s, CH_3), δ 0.75 (3 H, s, CH_3). $^{13}\text{C}\{^1\text{H}\}$ NMR (C_6D_6 , 125 MHz, 298 K): NCN not observed, δ 135.9 (CH), δ 135.4 (CH), δ 132.0 (C_{Ar}), δ 130.2 (C_{Ar}), δ 129.8 (C_{Ar}), δ 129.5 (C_{Ar}), δ 129.3 (C_{Ar}), δ 125.6 (C_{Ar}), δ 68.7 (NC), δ 62.9 (NCH), δ 56.9 (NCH_2), δ 43.2 (NCH_2), δ 36.2 (C), δ 30.5 (CH_2), δ 29.4 (CH_2), δ 22.8 (CH_3), δ 21.4 (CH_3), δ 21.0 (CH_3), δ 20.9 (CH_3), δ 20.6 (CH_3), δ 20.3 (CH_3), δ 17.8 (CH_3). MS(ES) m/z : [$2 \text{M}^+ - 2\text{I} + \text{CN}$] 986.5022 ($\text{C}_{59}\text{H}_{80}\text{N}_5\text{Cu}_2$ requires 986.5012). Analysis calculated for $\text{C}_{29}\text{N}_2\text{H}_{40}\text{CuI}$: C, 57.37; H, 6.64; N, 4.61. Found C, 58.56; H, 7.52; N, 4.62, which was inclusive of 1/3 hexane.

Synthesis of ((5S)-2,4-diisopropyl-1,8,8-trimethyl-2,4-diazabicyclo[3.2.1]octan-3-yl)copper(I) iodide (9)



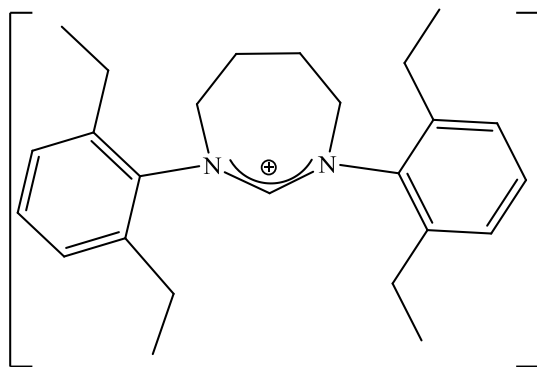
(5S)-2,4-diisopropyl-1,8,8-trimethyl-2,4-diazabicyclo[3.2.1]octan-2-ium hexafluorophosphate(V) (0.30 g, 0.85 mmol, 1 eq) was placed in a flame dried Schlenk and dried for 20 minutes. To this Schlenk CuI (0.19 g, 1.02 mmol, 1.2 eq), potassium tertiary butoxide (0.13 g, 1.19 mmol, 1.4 eq) and THF (10 ml) were all added in a glove box and the reaction mixture was then stirred outside of the glove box for 18 hours. The THF was then removed in *vacuo*, deuterated benzene (3 ml) was added and then filtered through a pad of cotton wool all inside the glove box. Recrystallisation from C₆D₆ and hexane yielded ((5S)-2,4-diisopropyl-1,8,8-trimethyl-2,4-diazabicyclo[3.2.1]octan-3-yl)copper(I) iodide as a yellow solid (0.13 g, 35.6 %). ¹H NMR (C₆D₆, 400 MHz, 298 K): δ 4.75 (1 H, m, NCH), δ 3.40 (1 H, m, NCH), δ 2.50 (1 H, d, NCH, ³J_{HH} = 5.1 Hz), δ 1.70 (1 H, m, CH₂), δ 1.55 (1 H, m, CH₂), δ 1.50 (3 H, m, CH₃), δ 1.30 (2 H, m, CH₂), δ 1.25 (3 H, m, CH₃), δ 1.20 (3 H, m, CH₃), δ 0.80 (3 H, d, CH₃, ³J_{HH} = 6.7 Hz), δ 0.75 (3 H, s, CH₃), δ 0.60 (3 H, s, CH₃), δ 0.45 (3 H, s, CH₃). ¹³C{¹H} NMR (C₆D₆, 125 MHz, 298 K): δ 193.9 (NCN), δ 66.5 (NC), δ 66.0 (NCH), δ 59.6 (NCH), δ 59.1 (NCH), δ 39.0 (CH₂), δ 38.7 (C), δ 31.9 (CH₂), δ 31.6 (CH₃), δ 24.4 (CH₃), δ 23.5 (CH₃), δ 21.9 (CH₃), δ 20.5 (CH₃), δ 20.2 (CH₃), δ 17.5 (CH₃). MS(ES) *m/z*: [M⁺ - I + MeCN] 340.20 (C₁₇H₃₁N₃Cu requires 340.99), it was not possible to obtain HRMS data for this complex.

4.4.3: Experimental Data for the Attempted Synthesis of Copper(I) Complexes

Synthesis of [(6-*o*-tolyl)O] (10)

[(6-*o*-tolylH)Br] (0.50 g, 1.45 mmol, 1 eq) was placed in a flame dried Schlenk and dried for 20 minutes. To this Schlenk CuI (0.33 g, 1.74 mmol, 1.2 eq), potassium tertiary butoxide (0.23 g, 2.03

mmol, 1.4 eq) and THF (15 ml) were all added in a glove box and the reaction mixture was then stirred outside of the glove box for 18 hours. The THF was then removed in *vacuo*, DCM (20 ml) was added and then filtered through a pad of celite. The DCM was then removed yielding [(6-*o*-tolyl)O] as an off white solid (0.22 g, 53.7 %). ^1H NMR (CDCl_3 , 400 MHz, 298 K): δ 7.20 (2 H, m, CH_{Ar}), δ 7.15 (2 H, m, CH_{Ar}), δ 7.10 (2 H, m, CH_{Ar}), δ 7.05 (2 H, m, CH_{Ar}), δ 3.70 (2 H, m, NCH_2), δ 3.55 (2 H, m, NCH_2), δ 2.25 (6 H, s, CH_3), δ 2.20 (2 H, m, NCH_2CH_2). $^{13}\text{C}\{^1\text{H}\}$ NMR (CDCl_3 , 125 MHz, 298 K): δ 152.6 (NC(O)N), δ 141.6 (NC_{Ar}), δ 135.0 (C_{Ar}), δ 135.0 (C_{Ar}), δ 130.6 (CH_{Ar}), δ 127.6 (CH_{Ar}), δ 125.9 (CH_{Ar}), δ 125.7 (CH_{Ar}), δ 48.4 (NCH_2), δ 22.4 (NCH_2CH_2), δ 16.8 (CH_3). MS(ES) m/z : [$\text{M}^+ - \text{Cu} - \text{I} + \text{O} + \text{H}^+$] 281.18 ($\text{C}_{18}\text{H}_{21}\text{N}_2\text{O}$ requires 281.00), it was not possible to obtain HRMS data for this complex.

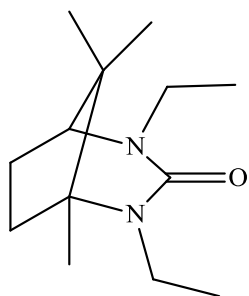
Synthesis of [(7-DEPH)]⁺ [X], where X = [Cu₄I₆]²⁻ or [Cu₅I₇]²⁻ (11)

$\text{Cu}_4\text{I}_6^{2-}$ [(7-DEPH)I] (0.50 g, 1.02 mmol, 1 eq) or $\text{Cu}_5\text{I}_7^{2-}$ was placed in a flame dried Schlenk and dried for 20 minutes. To this Schlenk CuI (0.23 g, 1.22 mmol, 1.2 eq), potassium tertiary butoxide (0.16 g, 1.43 mmol, 1.4 eq) and toluene (15 ml) were all added in

a glove box and the reaction mixture was then stirred outside of the glove box for 54

hours. The toluene was then removed in *vacuo*, DCM (20 ml) was added and then filtered through a pad of celite. The DCM was then removed yielding [7-DEPH]⁺ [X], where X = [Cu₄I₆]²⁻ or [Cu₅I₇]²⁻ as an off white solid (0.16 g, 18.6 %). ¹H NMR (CDCl₃, 400 MHz, 298 K): δ 7.10 (4 H, t, CH_{Ar}, ³J_{HH} = 6.5 Hz), δ 7.05 (1 H, s, NCHN), δ 7.00 (4 H, d, CH_{Ar}, ³J_{HH} = 6.5 Hz), δ 3.60 (4 H, m, NCH₂), δ 2.70 (4 H, m, CH₂), δ 2.60 (4 H, m, CH₂), δ 1.95 (4 H, m, NCH₂CH₂), δ 1.20 (12 H, t, CH₃, ³J_{HH} = 4.6 Hz). ¹³C{¹H} NMR (CDCl₃, 125 MHz, 298 K): δ 158.7 (NCHN), δ 141.9 (NC_{Ar}), δ 140.6 (C_{Ar}), δ 126.6 (CH_{Ar}), δ 125.5 (CH_{Ar}), δ 52.5 (NCH₂), δ 25.8 (NCH₂CH₂), δ 23.7 (CH₂), δ 23.5 (CH₂), δ 13.9 (CH₃). MS(ES) *m/z*: [M⁺ + H⁺] 363.28 (C₂₅H₃₅N₂ requires 363.56), it was not possible to obtain HRMS data for this complex.

Synthesis of (5S)-2,4-diethyl-1,8,8-trimethyl-2,4-diazabicyclo[3.2.1]octan-3-one (17)

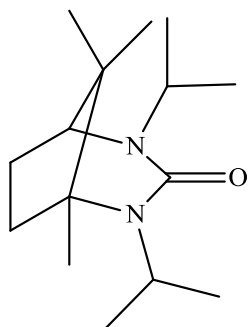


(1R,3S)-1,2,2-trimethylcyclopentane-1,3-diamine (5S)-2,4-diethyl-1,8,8-trimethyl-2,4-diazabicyclo[3.2.1]octan-2-ium hexafluorophosphate(V) (0.30 g, 0.85 mmol, 1 eq) was placed in a flame dried Schlenk and dried for 20 minutes. To this Schlenk CuI (0.19 g, 1.02 mmol, 1.2 eq), potassium tertiary butoxide (0.13 g, 1.19 mmol, 1.4 eq) and THF (10 ml) were all added in a glove box

and the reaction mixture was then stirred outside of the glove box for 54 hours. The toluene was then removed in *vacuo*, DCM (20 ml) was added and then filtered through a pad of celite. The DCM was then removed yielding (5S)-2,4-diethyl-1,8,8-trimethyl-2,4-diazabicyclo[3.2.1]octan-3-one as a yellow solid (0.11 g, 58.2 %). ¹H NMR (CDCl₃, 400 MHz, 298 K): δ 3.55 (1 H, m, NCH₂), δ 3.30 (2 H, q, NCH₂, ³J_{HH} = 7.0 Hz), δ 3.00 (1 H, m, NCH₂), δ 2.85 (1 H, d, NCH, ³J_{HH} = 4.6 Hz), δ 2.05 (1 H, m, CH₂), δ 1.90 (1 H, m, CH₂), δ 1.75 (2 H, m, CH₂), δ 1.15 (3 H, s, CH₃), δ 1.05 (6 H, m, CH₃), δ 0.95 (3 H, s, CH₃), δ 0.90 (3 H, s, CH₃). ¹³C{¹H} NMR (CDCl₃, 125 MHz, 298 K): δ 154.9 (NC(O)N), δ 66.2 (NC), δ 64.6 (NCH), δ 41.5 (C), δ 40.5 (NCH₂), δ 37.7 (CH₂), δ 36.3 (NCH₂), δ 29.9 (CH₂), δ 21.9 (CH₃), δ 16.7 (CH₃), δ 16.0 (CH₂), δ 15.6 (CH₃), δ

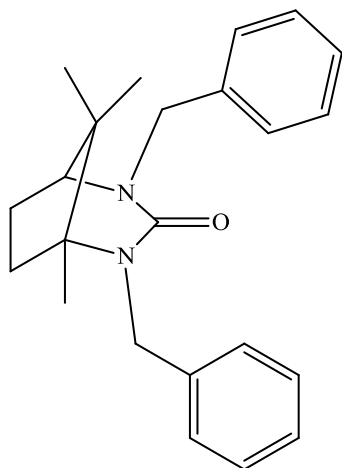
13.0 (CH₃). MS(ES) *m/z*: [M⁺ - I - Cu + O] 225.19 (C₁₃H₂₅N₂O requires 225.00), it was not possible to obtain HRMS data for this complex.

Synthesis of (5*S*)-2,4-diisopropyl-1,8,8-trimethyl-2,4-diazabicyclo[3.2.1]octan-3-one (18)



(5*S*)-2,4-diisopropyl-1,8,8-trimethyl-2,4-diazabicyclo[3.2.1]octan-2-ium hexafluorophosphate(V) (0.30 g, 0.79 mmol, 1 eq) was placed in a flame dried Schlenk and dried for 20 minutes. To this Schlenk CuI (0.18 g, 0.94 mmol, 1.2 eq), potassium tertiary butoxide (0.12 g, 1.10 mmol, 1.4 eq) and toluene (10 ml) were all added in a glove box and the reaction mixture was then stirred outside of the glove box for 18 hours. The toluene was then removed in *vacuo*, DCM (20 ml) was added and then filtered through a pad of celite. The DCM was then removed yielding (5*S*)-2,4-diisopropyl-1,8,8-trimethyl-2,4-diazabicyclo[3.2.1]octan-3-one as an off white solid (0.08 g, 36.2 %). ¹H NMR (CDCl₃, 400 MHz, 298 K): δ 4.65 (1 H, m, NCH), δ 3.50 (1 H, m, NCH), δ 2.90 (1 H, d, NCH, ³J_{HH} = 5.7 Hz), δ 2.00 (2 H, m, CH₂), δ 1.65 (2 H, m, CH₂), δ 1.35 (3 H, d, CH₃, ³J_{HH} = 6.7 Hz), δ 1.30 (3 H, d, CH₃, ³J_{HH} = 6.7 Hz), δ 1.15 (3 H, s, CH₃), δ 1.05 (3 H, d, CH₃, ³J_{HH} = 5.7 Hz), δ 0.95 (3 H, d, CH₃, ³J_{HH} = 5.7 Hz), δ 0.90 (3 H, s, CH₃), δ 0.85 (3 H, s, CH₃). ¹³C{¹H} NMR (CDCl₃, 125 MHz, 298 K): δ 154.1 (NC(O)N), δ 67.6 (NC), δ 57.6 (NCH), δ 45.5 (NCH), δ 42.3 (NCH), δ 41.8 (CH₂), δ 36.8 (C), δ 32.3 (CH₂), δ 23.8 (CH₃), δ 22.6 (CH₃), δ 21.6 (CH₃), δ 20.6 (CH₃), δ 20.1 (CH₃), δ 17.5 (CH₃), δ 16.5 (CH₃). MS(ES) *m/z*: [M⁺ - I - Cu + O] 253.2280 (C₁₅H₂₉N₂O requires 253.2280).

Synthesis of (5S)-2,4-dibenzyl-1,8,8-trimethyl-2,4-diazabicyclo[3.2.1]octan-3-one (19)



(1R, 5S)-2,4-dibenzyl-1,8,8-trimethyl-4-aza-2-azoniabicyclo-[3.2.1]oct-2-ene hexafluorophosphate (0.10 g, 0.21 mmol, 1 eq) was placed in a flame dried Schlenk and dried for 20 minutes. To this Schlenk CuI (0.05 g, 0.25 mmol, 1.2 eq), potassium tertiary butoxide (0.03 g, 0.29 mmol, 1.4 eq) and toluene (10 ml) were all added in a glove box and the reaction mixture was then stirred outside of the glove box for 18 hours. The toluene was then removed in *vacuo* and DCM (20 ml) was added. The precipitate was

filtered through a canular, and the filtrate was reduced to dryness yielding (5S)-2,4-dibenzyl-1,8,8-trimethyl-2,4-diazabicyclo[3.2.1]octan-3-one as a white solid (0.02 g, 29.7 %). ^1H NMR (C_7D_8 , 400 MHz, 298 K): δ 7.25 (2 H, d, CH_{Ar} , $^3J_{\text{HH}} = 7.2$ Hz), δ 7.15 (2 H, d, CH_{Ar} , $^3J_{\text{HH}} = 7.2$ Hz), δ 7.00 (2 H, m, CH_{Ar}), δ 6.95 (2 H, m, CH_{Ar}), δ 6.90 (1 H, m, CH_{Ar}), δ 6.85 (1 H, m, CH_{Ar}), δ 4.25 (1 H, m, NCH_2), δ 4.70 (1 H, m, NCH_2), δ 4.15 (1 H, m, NCH_2), δ 3.95 (1 H, m, NCH_2), δ 2.50 (1 H, d, NCH , $^3J_{\text{HH}} = 4.7$ Hz), δ 1.70 (1 H, m, CH_2), δ 1.45 (1 H, m, CH_2), δ 1.30 (1 H, m, CH_2), δ 1.10 (1 H, m, CH_2), δ 0.70 (3 H, s, CH_3), δ 0.60 (3 H, s, CH_3), δ 0.25 (3 H, s, CH_3). $^{13}\text{C}\{^1\text{H}\}$ NMR (C_7D_8 , 125 MHz, 298 K): δ 155 (NC(O)N), δ 142.0 (C_{Ar}), δ 139.0 (C_{Ar}), δ 127.0 (CH_{Ar}), δ 127.0 (CH_{Ar}), δ 126.5 (CH_{Ar}), δ 126.5 (CH_{Ar}), δ 126.0 (CH_{Ar}), δ 125.0 (CH_{Ar}), δ 67.0 (NC), δ 64.0 (NCH), δ 50.0 (NCH_2), δ 46.0 (NCH_2), δ 42.0 (C), δ 36.0 (CH_2), δ 28.5 (CH_2), δ 21.0 (CH_3), δ 16.5 (CH_3), δ 16.0 (CH_3). MS(ES) m/z : [$\text{M}^+ - \text{I} - \text{Cu} + \text{O}$] 349.2275 ($\text{C}_{23}\text{H}_{29}\text{N}_2\text{O}$ requires 349.2285).

4.4.4: General Procedure for Hydrosilylation of Ketones

A flask containing [Cu(NHC)I] (1 mol %) and ^tBuOK (12 mol %) had toluene (2 ml) added and the solution was stirred at room temperature for 5 minutes. To this mixture triethylsilane (3 eq) and decane (internal standard, 1 mmol) were added and stirred for a further 5 minutes at room temperature. The substrate (1 mmol) was then added and reaction mixture was stirred for a further 18 hours at ambient temperatures. Samples were prepared for GCMS analysis by the dilution of 0.2 ml of reaction mixture in HPLC DCM (2 ml) and eluted through a small column of Celite and activated charcoal. Program analysis: initial temperature at 40 °C, held for 2.5 minutes, ramp 5 °C/minute next 150 °C, ramp 10 °C/minute next 220 °C held for 10 minutes. The temperature of the injector and detector were maintained at 240 °C.

4.5: References

- 1 Herrmann, W. A. *Angew. Chem. Int. Ed.* **2002**, 41, 8, 1290-1309.
- 2 Crudden, M. C.; Allen, D. P. *Coord. Chem. Revs.* **2004**, 248, 2247-2273.
- 3 Doyle, M. J.; Lappert, M. F.; McLaughlin, G. M.; McMeeking, J. *J. Chem. Soc. Dalton Trans.* **1974**, 1494-1501.
- 4 Viciu, M. S.; Germaneau, R. F.; Navarro-Fernandez, O.; Stevens, E. D.; Nolan, S. P. *Organometallics* **2002**, 21, 25, 5470-5472.
- 5 Díez-González, S.; Marion, N.; Nolan, S. P. *Chem. Revs.* **2009**, 109, 8, 3612-3676.
- 6 Wang, F.; Liu, L. -J.; Wang, W.; Li, S.; Shi, M. *Coord. Chem. Revs.* **2012**, 256, 804-853.
- 7 Schwarz, J.; Böhm, V. P. W.; Gardiner, M. G.; Grosche, M.; Herrmann, W. A.; Hieringer, W.; Raudaschl-Sieber, G. *Chem. Eur. J.* **2000**, 6, 10, 1773-1780.
- 8 Berthon-Gelloz, G.; Buisine, O.; Brière, J. -F.; Michaud, G.; Stérin, S.; Mignani, G.; Tinant, B.; Declercq, J. -P.; Chapon, D.; Markó, I. E. *J. Organomet. Chem.* **2005**, 690, 6156-6168.
- 9 Kolychev, E. L.; Portnyagin, I. A.; Shuntikov, V. V.; Khrustalev, V. N.; Nechaev, M. S. *J. Organomet. Chem.* **2009**, 694, 15, 2454-2462.
- 10 Herrmann, W. A.; Schneider, S. K.; Öfele, K.; Sakamoto, M.; Herdtweck, E. *J. Organomet. Chem.* **2004**, 689, 15, 2441-2449.
- 11 Kascatan-Nebioglu, A.; Panzner, M. J.; Tessier, C. A.; Cannon, C. L.; Youngs, W. *J. Coord. Chem. Revs.* **2007**, 251, 884-895.
- 12 Díez-González, S.; Kaur, H.; Zinn, F. K.; Stevens, E. D.; Nolan, S. P. *J. Org. Chem.* **2005**, 70, 12, 4784-4796.
- 13 Díez-González, S.; Correa, A.; Cavallo, L.; Nolan, S. P. *Chem. Eur. J.* **2006**, 12, 29, 7558-7564.
- 14 Fortman, G. C.; Slawin, A. M. Z.; Nolan, S. P. *Organometallics* **2010**, 29, 17, 3966-3972.
- 15 Boogaerts, I. I. F.; Fortman, G. C.; Furst, M. R. L.; Cazin, C. S. J.; Nolan, S. P. *Angew. Chem. Int. Ed.* **2010**, 49, 46, 8674-8677.
- 16 Bantu, B.; Wang, D.; Wurst, K.; Buchmeiser, M. R. *Tetrahedron* **2005**, 61, 51, 12145-12152.
- 17 Dunsford, J. J.; Cavell, K. J.; Kariuki, B. M. *Organometallics* **2012**, 31, 11, 4118-4121.

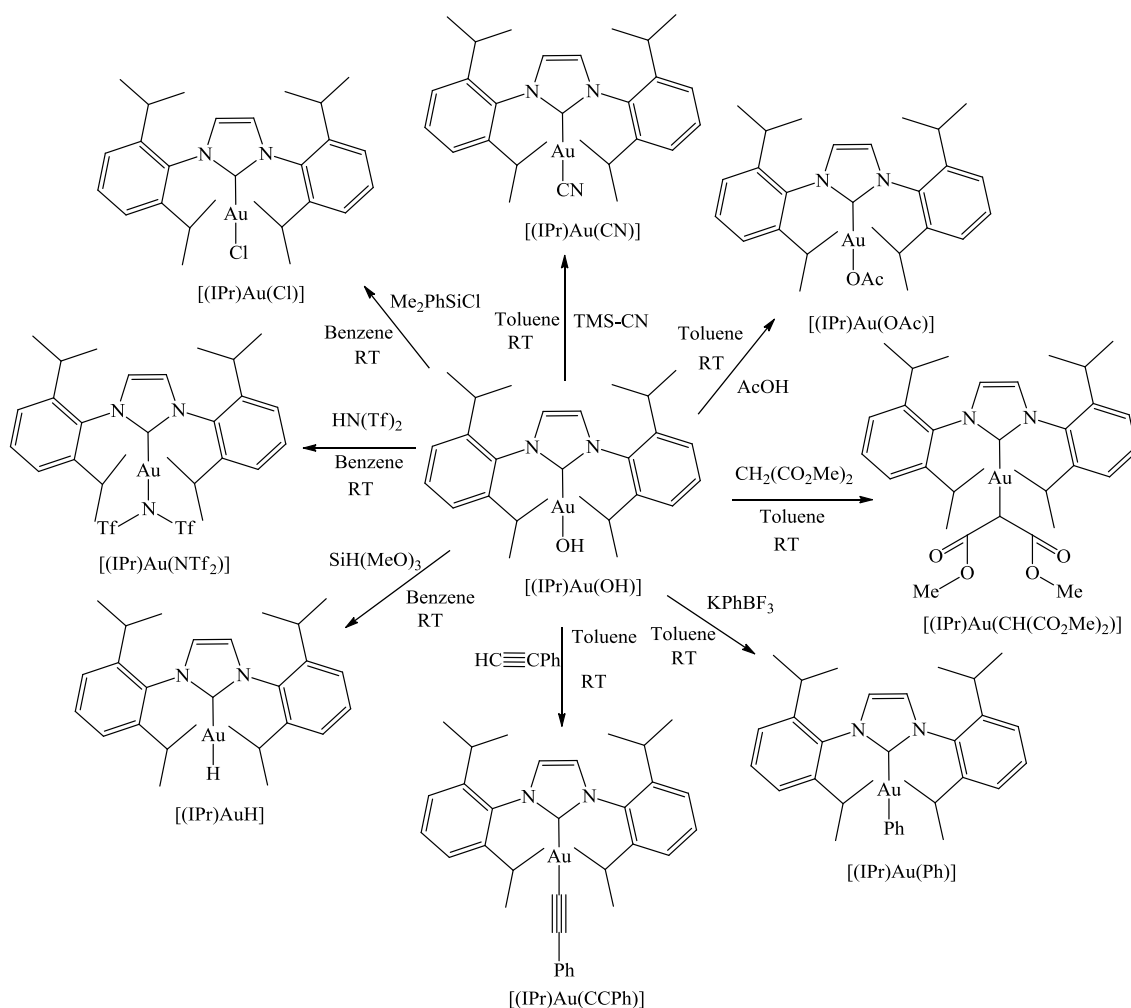
- 18 Lu, W. Y.; Cavell, K. J.; Wixey, J. S.; Kariuki, B. *Organoemetallics* **2011**, 30, 21, 5649-5655.
- 19 Binobaid, A.; Cavell, K. J.; Nechaev, M. S.; Kariuki, B. M. *Australian J. Chem.* **2011**, 64, 8, 1141-1147.
- 20 Binobaid, A.; Iglesias, M.; Beetstra, D.; Dervisi, A.; Fallis, I.; Cavell, K. J. *Eur. J. Inorg. Chem.* **2010**, 34, 5426-5431.
- 21 Dunsford, J. J.; Cavell, K. J. *Dalton Trans.* **2011**, 40, 9131-9135.
- 22 Mag, M. M.; Wurst, K.; Omgania, K. -H.; Buchmeiser, M. R. *Chem. Eur. J.* **2004**, 10, 5, 1256-1266.
- 23 Dunsford, J. J. *PhD Thesis* **2012**.
- 24 Kolychev, E. L.; Shuntikov, V. V.; Khrustalev, V. N.; Bush, A. A.; Nechaev, M. S. *Dalton Trans.* **2011**, 40, 3074-3076.
- 25 Lin, B. -L.; Kang, P.; Stack, D. P. *Organometallics* **2010**, 29, 17, 3683-3685.
- 26 Newman, P. D.; Cavell, K. J.; Kariuki, B. M. *Organometallics* **2010**, 29, 12, 2724-2734.
- 27 Newman, P. D.; Cavell, K. J.; Kariuki, B. M. *Chem. Comm.* **2012**, 48, 6511-6513.
- 28 Bader, R. F. W. *Pure Appl. Chem.* **1988**, 60, 145-155.
- 29 Alici, B.; Hökelek, T.; Çetinkaya, E.; Çetinkaya, B. *Heteroatom Chem.* **2003**, 14, 1, 82-87.
- 30 Zhang, Z.; Lee, S. D.; Widenhoefer, R. A. *J. Am. Chem. Soc.* **2009**, 131, 15, 5372-5373.
- 31 Catalano, V. J.; Munro, L. B.; Stasser, C. E.; Samin, A. F. *Inorg. Chem.* **2011**, 50, 17, 8465-8476.
- 32 Díez-González, S.; Escudero-Adán, E. C.; Benet-Buchholz, J.; Stevens, E. D.; Slawin, A. M. Z. Nolan, S. P. *Dalton Trans.* **2010**, 39, 7595-7606.
- 33 Catalano, V. J.; Malwitz, M. A. *Inorg. Chem.* **2003**, 42, 18, 5483-5485.
- 34 Gischig, S.; Togni, A. *Organometallics* **2005**, 24, 2, 203-205.
- 35 Díez-González, S.; Scott, N. M.; Nolan, S. P. *Organometallics* **2006**, 25, 9, 2355-2358.
- 36 Kaur, H.; Zinn, F. K.; Stevens, E. D.; Nolan, S. P. *Organometallics* **2004**, 23, 5, 1157-1160.
- 37 Díez-González, S.; Stevens, E. D.; Scott, N. M.; Petersen, J. L.; Nolan, S. P. *Chem. Eur. J.* **2007**, 14, 1, 158-168.

- 38 Perrin, D. D.; Amarego, W. F. A. *Purification of Laboratory Chemicals*; Pergamon: Oxford, **1988**.
- 39 Grimme, S. *J Comput Chem* **2006**, *27*, 1787-1799.
- 40 Weigend, F.; Ahlrichs, R. *Phys.Chem.Chem.Phys.* **2005**, *7*, 3297.
- 41 Ahlrichs, R.; Bar, M.; Haser, M.; Horn, H.; Kolmel, C. *Chem Phys Lett* **1989**, *162*, 165-169.
- 42 COLLECT; Nonius BV: Delft, The Netherlands, **1998**.
- 43 Otwinowski, Z.; Minor, W. *Methods Enzymol.* **1997**, *276*, 307-326.
- 44 Altomare, A.; Cascarano, G.; Giacovazzo, C.; Guagliardi, A. *J. Appl. Crystallogr.* **1993**, *26*, 343-350.
- 45 Sheldrick, G. M. *Acta Crystallogra. Sect. A* **2008**, *A64*, 112-122.
- 46 Blessing, R. H. *Acta Crystallogra. Sect. A* **1995**, *51*, 33-38.
- 47 Dunsford, J. J.; Cavell, K. J.; Kariuki, B. *J. Organomet. Chem.* **2011**, *696*, 1, 188-194.
- 48 Iglesias, M.; Beetstra, D. J.; Knight, J. C.; Ooi, L. -L.; Stasch, A.; Coles, S.; Male, L.; Hursthouse, M. B.; Cavell, K. J.; Dervisi, A.; Fallis, I. A. *Organometallics* **2008**, *27*, 13, 3279-3289.
- 49 Iglesias, M.; Beetstra, D. J.; Kariuki, B.; Cavell, K. J.; Dervisi, A.; Fallis, I. A. *Eur. J. Inorg. Chem.* **2009**, *13*, 1913-1919.

5: Synthesis and Coordination of Expanded Ring N-Heterocyclic Carbenes to Gold(I)

5.1: Introduction

Over the recent years there has been important research concentrating on the synthesis, coordination and application of expanded ring NHCs (any NHC with a ring size greater than 5).¹⁻⁸ Along with the expanded ring NHCs there has also been reports of the synthesis of novel bicyclic NHCs, their coordination and application,⁹⁻¹² however these are relatively unexplored in comparison to the expanded ring NHCs and especially the 5-membered analogues. As mentioned in Chapter 4, metals such as rhodium, iridium, platinum and palladium are expensive and non abundant, therefore the interest in recent years has moved away from these metals in a hope to find a cheaper more abundant alternative, this has led to the research into the reactivity and application of metals such as silver, copper, and gold. In recent years this has been mainly with silver(I) and copper(I), however more recently the interest has moved towards gold(I) mediated transformations,^{13,14} especially those containing sterically demanding NHC ancillary ligands.¹⁵⁻¹⁷ Nolan and co workers have also found that it is not just the halide analogues of the gold(I) complexes with general formula $[\text{Au}(\text{NHC})\text{X}]$, where X = Cl, Br, or I, that are versatile in catalysis. The hydroxide adducts, with general formula $[\text{Au}(\text{NHC})\text{OH}]$, have successful applications, especially in the stoichiometric C-H activation of a range of aromatic substrates.¹⁸ The key factor in this application is that the aromatic substrates should bear moderately acidic protons, therefore have a maximum pK_a of 30. It has also been shown that a large library of gold(I) complexes can be synthesised from the $[\text{Au}(\text{NHC})\text{OH}]$ adducts with relative ease, Scheme 1, this could lead to an extensive range of catalytic possibilities.



Scheme 1: Transformations of $[\text{Au}(\text{NHC})\text{OH}]$.¹⁸

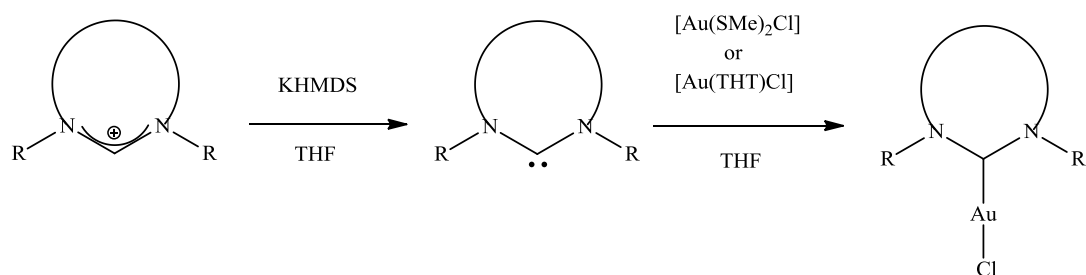
5.2: Results and Discussion

As mentioned in Chapter 4 there has been extensive work carried out on metals such as palladium, platinum, rhodium, and iridium over the years.¹⁹⁻²² Chapter 4 exhibits how coinage metals, such as copper, can be used in place of these expensive, non abundant metals in synthesising novel complexes, which can then be used for catalysis. Therefore, due to the copper(I) complexes being successful along with the fact that gold has a proven catalytic heritage for novel transformations and is cheaper than iridium, rhodium, platinum, and palladium, gold complexes were prepared. Due to there already being several silver metal complexes reported^{1,6,23} and the success that Nolan¹⁸ and

Dunsford²⁴ have had with their coordination of 5-membered and expanded ring NHCs respectively to gold and their subsequent catalysis this chapter concentrates solely on the coordination of a series of expanded ring NHCs to gold and their subsequent catalytic properties.

5.2.1: General Synthesis of Gold(I) Complexes

The route that was employed, for the coordination of the NHC precursors to gold(I) to give complexes with general formula $[\text{Au}(\text{NHC})\text{Cl}]$, is analogous to that of Dunsford *et al.*²⁴ as shown in Scheme 2. The NHC precursor is deprotonated using KHMDS in THF forming the free carbene in solution, which is then added dropwise to a stirring solution of either $[\text{Au}(\text{SMe}_2)\text{Cl}]$ or $[\text{Au}(\text{THT})\text{Cl}]$, THT = Tetrahydrothiophene, in THF at ambient temperature. After purification the reaction yields the target compounds as air stable semi crystalline solids.



Scheme 2: General procedure for the synthesis of gold(I) complexes with the general formula $[\text{Au}(\text{NHC})\text{Cl}]$.

5.2.2: The Synthesis of Expanded Ring NHC Gold(I) Complexes

A series of gold(I) complexes were synthesised with a range of expanded ring NHC precursors. Due to the success in synthesis and catalytic activity that Dunsford *et al.*²⁴

had with the mesityl and diisopropyl derivatives and the steric impact from the N-substituents, which was found using percentage buried volumes, a series of expanded ring aromatic gold(I) complexes were synthesised, Figure 1, to attempt to relate steric demand to catalytic activity. As well as the library of aromatic expanded ring complexes, Figure 1, a range of alkylated expanded ring precursors were also coordinated to gold forming a range of gold(I) complexes of the general formula $[\text{Au}(\text{NHC})\text{Cl}]$, Figure 2.

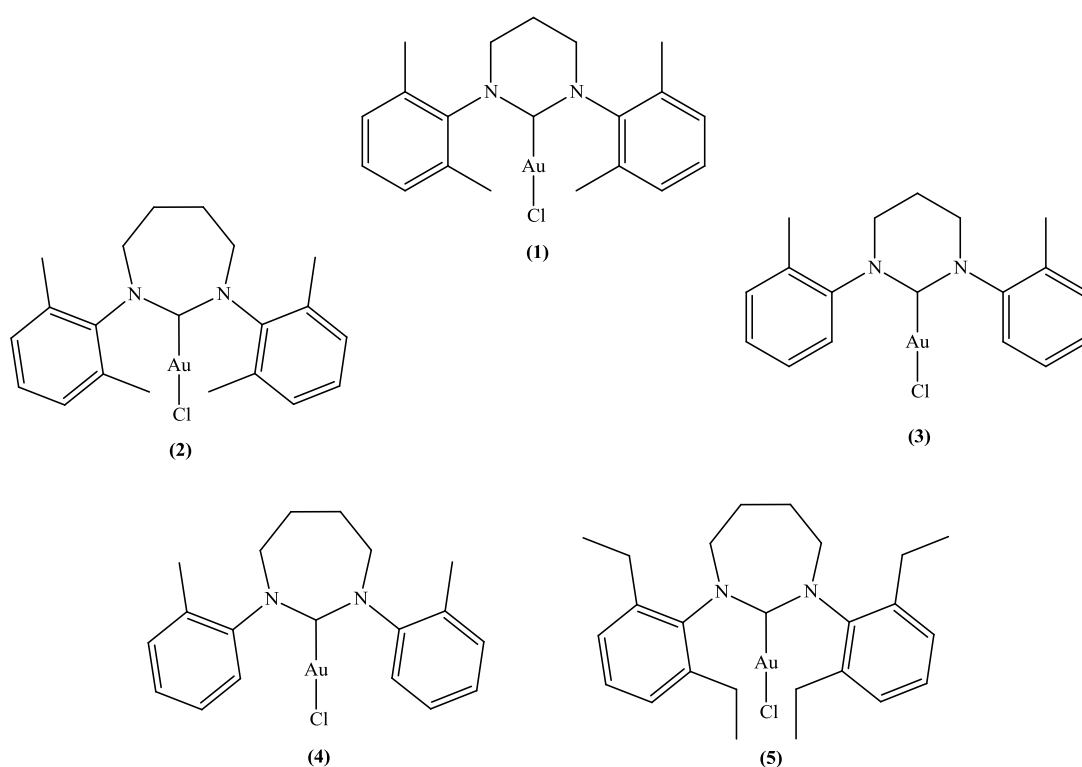


Figure 1: Aromatic expanded ring gold(I) complexes of general formula $[\text{Au}(\text{NHC})\text{Cl}]$ (1-5).

Table 1: A comparison between the NHC·HX, where X = Br or I, salts and the gold(I) complexes of general formula [Au(NHC)Cl].

Derivative	NCN-H peak in the amidinium salt (ppm)	NCN-Au peak (ppm)	Total shift during complexation (ppm)
7-Xylyl	157.6	201.1	43.49
6-<i>o</i>-tolyl	153.7	191.1	37.40
7-DEP	157.8	201.7	43.87
6-Mes	153.5	192.6	39.05
7-Mes	157.8	193.1	35.26
6-DIPP	152.8	200.9	48.05
7-DIPP	157.0	200.5	43.47

As can be seen from the data in Table 1, the average shift downfield in the $^{13}\text{C}\{^1\text{H}\}$ NMR spectra for compounds **2**, **3**, and **5** is 41.59 ppm, this is a substantial shift and is also shown in the mesityl and diisopropylphenyl derivatives (Table 1), and is therefore conclusive in demonstrating that **2**, **3** and **5** have been successfully synthesised.

The other noticeable shift is that of the NCH_2 protons in the backbone of the NHC in the ^1H NMR spectrum where a shift from on average 4.28 ppm in the amidinium salts of general formula $\text{NHC}\cdot\text{HX}$, where X = Br, I and BF_4^- , to 3.40 ppm, 3.85 ppm, 3.50 ppm, 3.65-4.10 ppm, and 3.85 ppm for complexes **1-5** respectively, Table 2, is observed. This upfield shift (average 0.58 ppm) is as expected when going from a cationic species to a coordinated species. This shift can therefore be attributed to the successful coordination to gold producing **1-5**.

Table 2: Comparison of NCH₂ peaks in the ¹H NMR spectra between the amidinium salts of general formula NHC·HX, where X = Br, I, or BF₄, and **1-5**.

Derivative	NCH ₂ peak in amidinium salt (ppm)	NCH ₂ peak in gold(I) complexes (ppm)	Total shift in NCH ₂ peaks during complexation (ppm)
6-Xylyl	4.21	3.40	0.81
7-Xylyl	4.61	3.85	0.76
6-<i>o</i>-tolyl	3.71	3.50	0.21
7-<i>o</i>-tolyl	4.34	3.65 - 4.10	0.47
7-DEP	4.52	3.85	0.67

High resolution mass spectrometry data for **1-5** was collected and for all five complexes the results were very similar, with **1-4** showing [M⁺ - Cl + MeCN], with the molecular ion peaks at 529.43 amu, 544.2005 amu, 502.1567 amu, and 516.1732 amu respectively, and **5** showing [M⁺ + MeCN] with a molecular ion peak at 635.1718 amu, which have calculated values of 529.97 amu, 544.2027 amu, 502.1558 amu, 516.1714 amu, and 635.1823 amu for **1-5** respectively.

Crystals were obtained from vapour diffusion of *n*-pentane into a concentrated solution of **1-5** in CDCl₃ over a 24 hour period and X-ray crystal data was obtained. The structures obtained for **1-5** are shown in Figure 3, and selected bond lengths and angles are exhibited in Table 3.

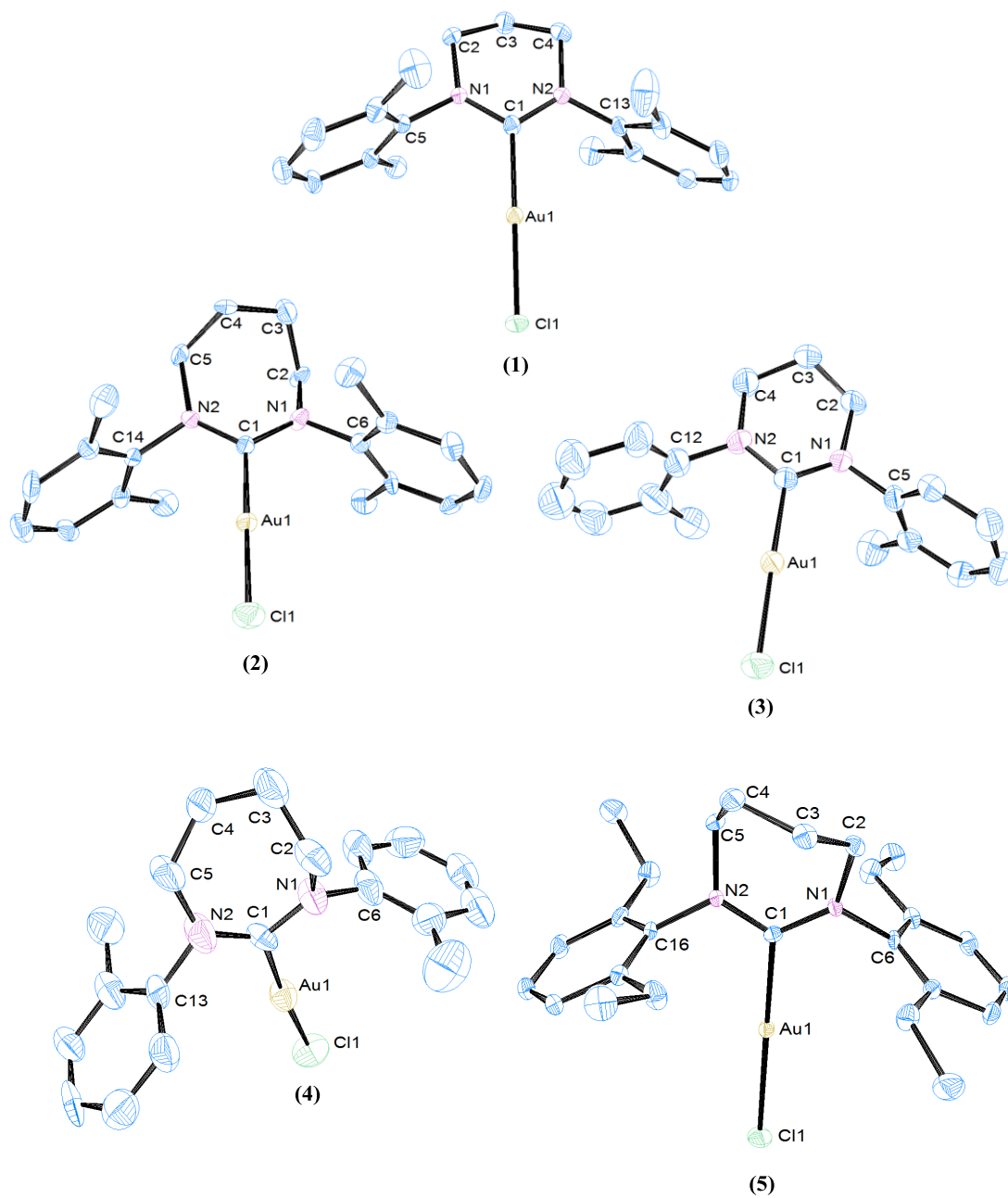


Figure 3: ORTEP ellipsoid plots at 50 % probability of the molecular structure of (1-5), hydrogens have been omitted for clarity.

Table 3: Selected bond lengths (Å) and angles (°) for **(1-5)**.

	(1)	(2)	(3)	(4)	(5)
N(1)-C(1)	1.343(5)	1.344(10)	1.315(12)	1.354(13)	1.349(4)
N(2)-C(1)	1.331(5)	1.344(9)	1.343(11)	1.342(14)	1.332(4)
C(1)-Au(1)	2.001(4)	2.001(7)	1.984(9)	1.993(11)	2.006(3)
Au(1)-Cl(1)	2.2933(10)	2.290(2)	2.285(2)	2.286(3)	2.2915(8)
N(1)-C(1)-N(2)	117.9(3)	119.9(7)	117.8(8)	117.8(10)	120.3(3)
N(2)-C(1)-Au(1)	121.1(3)	119.4(5)	121.9(7)	124.2(8)	119.9(2)
N(1)-C(1)-Au(1)	120.8(3)	120.4(5)	120.3(6)	118.0(8)	119.7(2)
C(1)-Au(1)-Cl(1)	176.32(11)	175.8(2)	179.1(3)	175.8(3)	173.99(8)

As can be observed in the crystal structures of **1-5**, Figure 3, the conformations of the NHCs vary. The 6-membered NHCs are in the plane with the NCN bond, however when it comes to the 7-membered NHCs, there is bending in the NHC backbone causing part of the NHC structure not to be in the same plane as the NCN bond. As the NHC ring increases in size it behaves more like an acyclic NHC, this is due to the greater flexibility of the bigger expanded rings. This flexibility leads to larger NCN bond angles and pushes the N-substituents closer to the metal centre on coordination.

The crystal structure data shows that compounds **1-5** follow the same trend as their copper(I) and silver(I) counterparts, with a decrease in the N(1)-C(1)-N(2) angle on coordination from around 124 ° in the amidinium salts to on average 118.7 ° in **1-5**. Also similarly to that of the copper(I) complexes, mentioned in Chapter 4, the C(1)-Au(1)-Cl(1) angle in **1-5** is virtually linear at on average 176.2 °. The C(1)-Au(1) bond appears to be comparable to that of the 6-Mes, 6-DIPP, and 7-DIPP analogues as reported by Dunsford with all the lengths appearing between 1.984(9) Å and 2.012(6) Å.²⁴

It is apparent that as the N-substituents are modified there is an increase in steric bulk, however this steric bulk is not as large as that evident in the [Au(6-Mes)Cl], [Au(7-Mes)Cl], [Au(6-DIPP)Cl], and the [Au(7-DIPP)Cl] as reported by Dunsford *et al.*²⁴ The percentage buried volumes were obtained for complexes **1-5** using their crystal structure data and found to exhibit large steric demand, however the percentage buried volumes were in general not as large as those reported by Dunsford for the [Au(6-DIPP)Cl] and the [Au(7-DIPP)Cl] as shown in Table 4. It is shown from all the data collected that **1-5** have successfully been synthesised as white semicrystalline solids in yields of 24 - 42 %.

Table 4: Percentage buried volume (% V_{bur}) values of gold(I) complexes.

Compound	Buried Volume (% V_{bur})
[Au(6-Xylyl)Cl] (1)	41.5
[Au(7-Xylyl)Cl] (2)	42.9
[Au(6- <i>o</i> -tolyl)Cl] (3)	41.1
[Au(7- <i>o</i> -tolyl)Cl] (4)	40.8
[Au(7-DEP)Cl] (5)	43.3
[Au(6-Mes)Cl] ²⁴	42.2
[Au(6-DIPP)Cl] ²⁴	50.8
[Au(7-DIPP)Cl] ²⁴	52.6

5.2.2.2: The Characterisation of Alkylated Expanded Ring NHC Gold(I)

Complexes

Compounds **6-8**, Figure 2, were fully characterised using ^1H NMR and $^{13}\text{C}\{^1\text{H}\}$ NMR spectroscopy, mass spectrometry, single crystal X-ray crystallography, elemental analysis, and percentage buried volumes. The proton NMR spectra for **6-8** were obtained and all showed a shift upfield of the NCH_2 ring protons from their amidinium salt precursors, with the NHC salts appearing at on average 3.60 ppm shifting to 3.05 ppm, 3.25 ppm, and 3.45 ppm for **6-8** respectively, Table 5. This is a considerable shift upfield and can therefore be used to show that **6-8** have been formed. The carbon-13 NMR spectra for **6-8** also indicate that these complexes were successfully synthesised with the large shift downfield of the NCN peak. In the amidinium salt precursors the NCN peak appears on average at 155.3 ppm with **6-8** appearing at 187.0 ppm, 199.0 ppm, and 204.5 ppm respectively. As shown in Table 5 this is a shift of on average 41.5 ppm. These shifts are comparable to the shifts mentioned previously in this chapter with **1-5** and are also in accordance with the shifts discussed in Chapter 4 for the copper(I) complexes.

Table 5: ^1H NMR and $^{13}\text{C}\{^1\text{H}\}$ NMR spectra data comparing the amidinium precursors and complexes **6-8**.

	^1H NMR Spectra Data			$^{13}\text{C}\{^1\text{H}\}$ NMR Spectra Data		
	NCHN Peak (ppm)	NCN-Au Peak (ppm)	Total Shift (ppm)	NCH_2 Peak in the Salt (ppm)	NCH_2 Peak in the Complex (ppm)	Total Shift (ppm)
6	150.0	187.0	37.0	3.34	3.05	0.29
7	155.6	199.0	43.4	3.65	3.25	0.40
8	160.4	204.5	44.1	3.80	3.45	0.35

X-ray crystallographic data has also been obtained for complexes **6-8**. Crystals of complexes **6-8** were grown from vapour diffusion of *n*-pentane into a concentrated solution of the corresponding complex in CDCl₃ over a period of 24 hours. The structures obtained are shown in Figure 4 and selected bond angles and lengths are shown in Table 6. In comparison to that of the salt precursors the N(1)-C(1)-N(2) angle in all three complexes **6-8** has decreased in size on complexation as observed for the copper(I) complexes in Chapter 4 and complexes **1-5** in this chapter. The change is quite dramatic in some cases with the 7-Neo (Neo = neopentyl) amidinium salt having a N(1)-C(1)-N(2) angle of 127.4(5) ° and in **8** it has decreased to 117.3(3) °, that is a total decrease in bond angle of over 10 °. A similar pattern occurs between 7-*i*Pr and **7**, with the NHC precursor having an angle of 130.2 ° and complex **7** having an angle of 120.7(4) °, Table 6. The C(1)-Au(1) bond lengths for **6-8** are slightly longer than those of **1-5**, however they are still in the same region, the slight increase could be due to sterics as the isopropyl and neopentyl moieties are very bulky. The other bond angle to note is that of C(1)-Au(1)-Cl(1) for **1-5** as mentioned in this chapter in 5.2.2.1 they are virtually linear with angles of on average 176.2 °, which is comparable to that of the copper(I) complexes mentioned in Chapter 4. This bond angle for **6-8** is an average 173.6 °, this is slightly further away from linearity than those of **1-5** and this can be rationalised as due to steric hindrance from the bulky N-substituents. The other noteworthy bond angles for complexes **6-8** is that of the C_{carbene}-N-C_{Alkyl} angles, which are dependent on the size of the NCN bond angle. As the NCN bond angle increases the C_{carbene}-N-C_{Alkyl} angle decreases, pushing the N-substituents towards the metal centre.

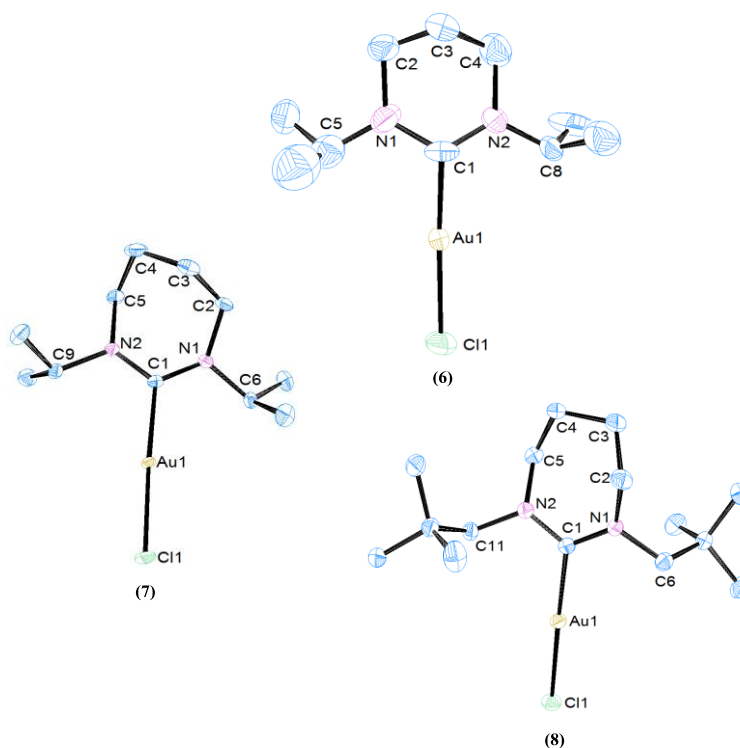


Figure 4: ORTEP ellipsoid plots at 50 % probability of the molecular structure of **6-8**, hydrogens have been omitted for clarity.

Table 6: Selected bond lengths (Å) and angles (°) for **6-8**.

	(6)	(7)	(8)
N(1)-C(1)	1.442(19)	1.346(6)	1.341(4)
N(2)-C(1)	1.337(17)	1.330(6)	1.353(4)
C(1)-Au(1)	2.072(11)	2.026(4)	2.016(3)
Au(1)-Cl(1)	2.363(2)	2.2946(10)	2.3056(8)
N(1)-C(1)-N(2)	116.8(13)	120.7(4)	117.3(3)
N(2)-C(1)-Au(1)	117.4(10)	121.4(3)	121.8(2)
N(1)-C(1)-Au(1)	110.8(10)	117.8(3)	120.9(2)
C(1)-Au(1)-Cl(1)	166.8(5)	176.31(12)	177.81(9)
C(5/6)-N(1)-C(1)	119.3(12)	118.2(4)	120.0(3)
C(8/9/11)-N(2)-C(1)	123.3(9)	120.8(4)	118.4(3)

Since X-ray crystal structures were obtained for **6-8** it was therefore possible to calculate the percentage buried volumes to see how sterically hindered these complexes are, Table 7. The percentage buried volumes of **6-8** are surprisingly small, they are considerably less than those of **1-5** and the recently reported, sterically imposing, [Au(6-DIPP)Cl] and [Au(7-DIPP)Cl],²⁴ they are also slightly less sterically hindered than that of the reported [Au(IMes)Cl] and the [Au(SIMes)Cl] with these having values of 36.5 % and 36.9 % respectively.²⁶ This decrease in percentage buried volume in comparison to the reported 5- and 6-membered analogues shows that when the N-substituent is an aromatic moiety then the steric hindrance is increased quite considerably in comparison to when the N-substituents are alkyl moieties. This appears to be the case even when the alkyl moieties are large bulky groups like isopropyl and neopentyl.

Table 7: Percentage buried volume (% V_{bur}) values of **6-8**.

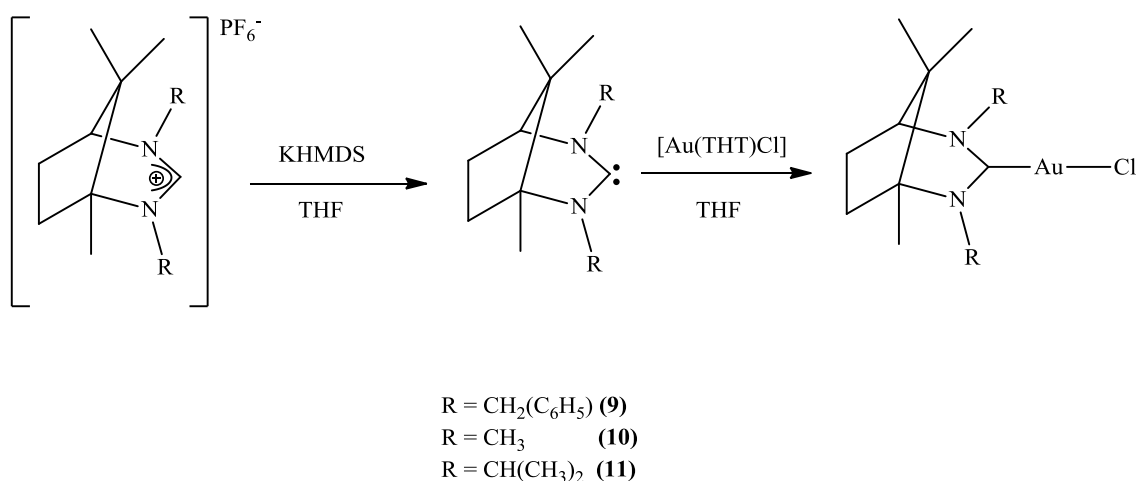
Compound	Buried Volume (% V_{bur})
[Au(6-iPr)Cl] (6)	32.2
[Au(7-iPr)Cl] (7)	33.5
[Au(7-Neo)Cl] (8)	33.6
[Au(IMes)Cl] ²⁶	36.5
[Au(SIMes)Cl] ²⁶	36.9
[Au(6-Mes)Cl] ²⁴	42.2
[Au(6-DIPP)Cl] ²⁴	50.8
[Au(7-DIPP)Cl] ²⁴	52.6

The mass spectrometry data was obtained for **6-8**, however the molecular ion adducts were dissimilar. This was shown with molecular ion peaks at 446.1926 amu exhibiting $[M^+ - Cl + 2MeCN]$, 453.0777 amu showing $[M^+ + K^+]$, and 517.37 amu giving $[M^+ - Cl + 2MeCN + H^+]$, for **6-8** respectively, which have calculated values of 466.1855 amu, 453.0774 amu, and 517.97 amu for **6-8** respectively.

Elemental analytical data for **6-8** was obtained, confirming that these complexes were successfully synthesised and isolated in their pure form, which is in accordance with the other data obtained, 1H NMR and $^{13}C\{^1H\}$ NMR spectra, mass spectra, and X-ray crystallographic data.

5.2.3: The Synthesis and Characterisation of Bicyclic NHC Gold(I) Complexes

Analogously to that of the saturated expanded ring gold(I) complexes a range of fused ring bicyclic NHC gold(I) complexes of general formula $[Au(NHC)Cl]$ were synthesised as shown in Scheme 3.



Scheme 3: Synthesis of **9-11**.

Complexes **9-11** were fully characterised using elemental analysis, mass spectrometry and NMR techniques, however the single crystal X-ray crystallographic data and percentage buried volumes were only obtainable for **10** and **11**. Using these techniques it was demonstrated that these three complexes had been successfully synthesised. In the proton NMR spectra, disappearance of the NCHN proton for the amidinium salts was apparent, the other noticeable shift in the proton NMR spectra is that of the NCH bridge head proton as shown in Table 8. For complexes **9** and **10** these protons on coordination shift slightly upfield and for **11** it appears to shift very slightly downfield. The carbon-13 NMR spectra were also collected for **9-11** and as with the proton NMR they are conclusive in showing that these complexes have been successfully formed, this is due to the large shift of the NCN peak, of on average, 46.2 ppm downfield from the amidinium precursors, however the NCN peak was not observed for **10**.

These shifts in the proton NMR spectra and the carbon-13 NMR spectra are consistent with those of the copper(I) complexes synthesised in Chapter 4 and that obtained for complexes **1-8** mentioned earlier in this chapter. These similar shifts in carbon-13 NMR spectra have also been reported by Dunsford *et al.* for the mesityl and DIPP expanded ring gold(I) analogues.²⁴ The shift observed in carbon-13 NMR spectra is however slightly larger than that of the 5-membered analogues reported by Nolan²⁶ with the NCN peak for the [Au(IMes)Cl], and the [Au(IPr)Cl] shifting from 134.8 ppm, and 132.2 ppm, in the amidinium salts, to 173.4 ppm and 175.1 ppm in the complexes. This shift in ppm in the carbon-13 NMR spectra, during complexation, can be attributed to the size of the N-heterocyclic carbene ring with 5-membered analogues having the smallest shift, with an increase as you move from the 6-membered to the 7-membered and this increase is predicted to extend to the 8-membered NHCs. The bicyclic NHCs appear to have shifts in the $^{13}\text{C}\{^1\text{H}\}$ NMR spectra more like that of the 6-membered expanded ring analogues, rather than that of the 5-membered analogues.

Table 8: ^1H NMR and $^{13}\text{C}\{^1\text{H}\}$ NMR spectra data comparing the amidinium precursors and **9-11**.

	$^{13}\text{C}\{^1\text{H}\}$ NMR Spectra Data			^1H NMR Spectra Data		
	NCHN Peak (ppm)	NCN-Au Peak (ppm)	Total Shift (ppm)	NCH (Bridge Head) Peak in Salt (ppm)	NCH (Bridge Head) Peak in Complex (ppm)	Total Shift (ppm)
9	153.7	190.0	36.3	3.20	3.00	0.20
10	-	-	-	3.25	2.95	0.30
11	151.0	207.1	56.1	3.00	3.05	0.05

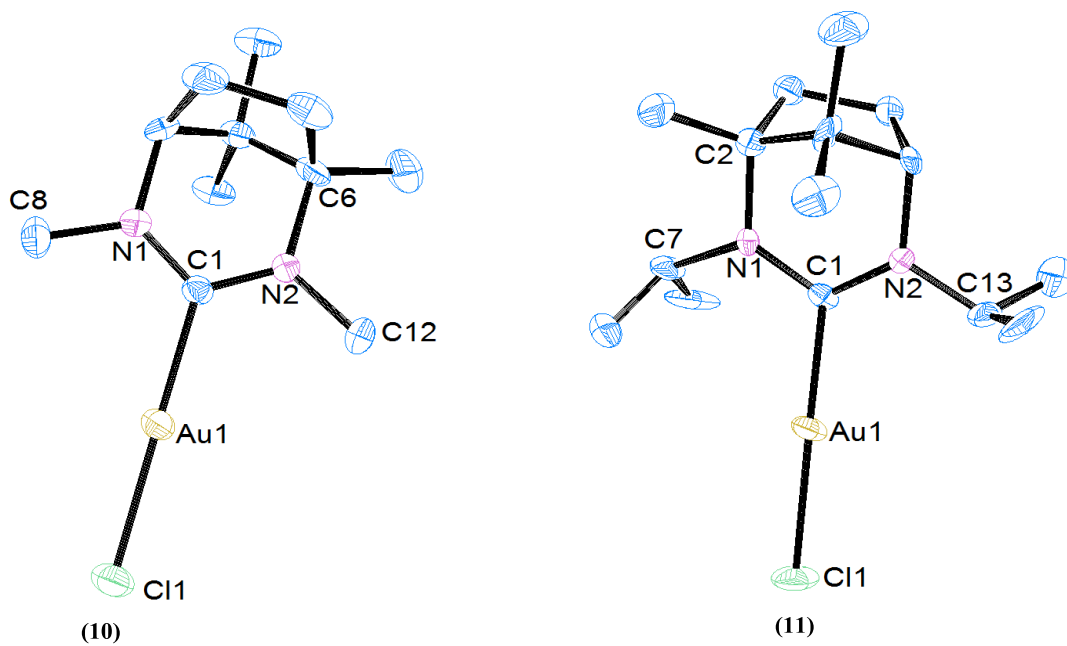
**Figure 5:** ORTEP ellipsoid plots at 50 % probability of the molecular structure of **10** and **11**, hydrogens have been omitted for clarity.

Table 9: Selected bond lengths (Å) and angles (°) for **10** and **11**.

	10	11
N(1)-C(1)	1.331(7)	1.383(16)
N(2)-C(1)	1.337(7)	1.323(15)
C(1)-Au(1)	2.024(5)	2.008(9)
Au(1)-Cl(1)	2.2937(15)	2.310(2)
N(1)-C(1)-N(2)	117.7(5)	117.1(9)
N(1)-C(1)-Au(1)	120.8(4)	119.9(9)
N(2)-C(1)-Au(1)	121.3(4)	121.5(8)
C(1)-Au(1)-Cl(1)	177.36(18)	178.2(6)

As observed for complexes **1-8** complexation causes the N(1)-C(1)-N(2) bond angle to decrease in size in **11** from 124.6(9) ° to 117.1(9) °, this however does not occur for the methyl analogue (**10**). In complex **10**, within the error of the measurements, the N(1)-C(1)-N(2) bond angles are the same between the amidinium salt and **10**. The C(1)-Au(1) bond lengths, are 2.024(5) Å and 2.008(9) Å for **10** and **11** respectively. These values are in accordance with those observed with **1-8**, and those reported by Dunsford.²⁴ They are slightly larger, as expected, than those of the 5-membered analogues reported by Nolan.²⁶

Since crystallographic data were obtained for **10** and **11** it is therefore possible to calculate the percentage buried volume of these gold(I) complexes, Table 10. From Table 10 it is clear that **10** and **11** have percentage buried volumes more in accordance with those of the 5-membered gold(I) analogues, [Au(IMes)Cl] and [Au(SIMes)Cl] rather than those of the 6-membered or 7-membered analogues. The results are also very similar to those of alkylated expanded ring gold(I) complexes shown in Table 7. This indicates that steric hindrance and hence the percentage buried volume is largest for aromatic moieties with large groups present as the N-substituents.

Other data obtained was mass spectrometry data. This was also helpful in showing that **9-11** were successfully synthesised. The molecular ion peaks for **9-11** were 587.2426

amu, 418.20 amu, and 474.2161 amu respectively, which have calculated values of 587.2429 amu, 418.97 amu, and 474.2184 amu for **9-11** respectively. These show two different adducts in the mass spectra, this first is that of **9** which gives a $[M^+ + Na]$ peak and the second is for **10** and **11** which show the peak to be $[M^+ - Cl + MeCN]$. The elemental analysis of **9-11** confirmed their purity.

Table 10: Percentage buried volume (% V_{bur}) values of **10** and **11**.

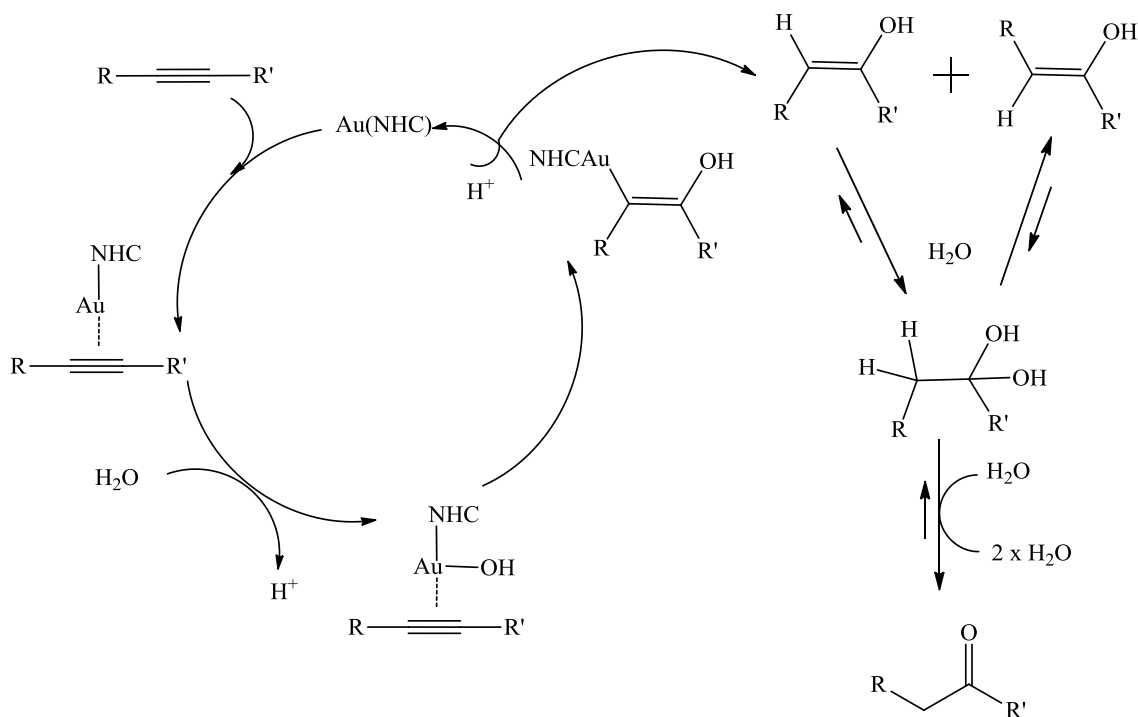
Complex	Percentage Buried Volume (% V_{bur})
10	29.5
11	36.9
$[Au(IMes)Cl]^{26}$	36.5
$[Au(SIMes)Cl]^{26}$	36.9
$[Au(6-Mes)Cl]^{24}$	42.2
$[Au(6-DIPP)Cl]^{24}$	50.8

5.2.4: Catalysis

In recent years there has been an increase in interest in gold transformations,¹³ especially with those using gold(I) complexes of general formula $[Au(NHC)X]$, where $X = Cl, Br, I, \text{ or } OH$.^{15,18,24} These have shown that gold(I) complexes can be used for a range of catalytic processes including, the hydration of alkynes,^{24,27,28} activation of alkenes,²⁹ and catalysed intermolecular bis-cyclopropanation of enynes with alkenes.³⁰ These catalytic processes have shown that even when an impressively low loading of catalyst is employed (as low as 0.001 mol %) it is still possible to achieve high yields of 84 %.²⁷ Nolan and co workers have employed low levels of catalyst to achieve

excellent results, in the hydration of alkynes. Dunsford *et al.* have shown the same outcome with slightly higher catalyst amounts (0.1 mol %) with conversions up to 100 % for the expanded ring NHCs. The following catalysis work will concentrate on the hydration of internal and terminal alkynes.

The exact mechanism for the hydration of alkynes is not known however, a postulated route is shown in Scheme 4 and starts with the coordination of the alkyne to the catalyst, this is then followed by the addition of water to the alkyne in a tri-coordinated transition state. An addition of the alcohol across the triple bond then occurs subsequently followed by a protodeauration to regenerate the catalyst and forming an enolic species. This enolic species then further reacts with water forming a bis-alcohol compound which then undergoes elimination of two waters forming the desired ketone species.³¹ Selectivity, for this transformation, is observed when an internal alkyne is employed as the substrate and this regioselectivity is predicted by Markovnikov's rule.

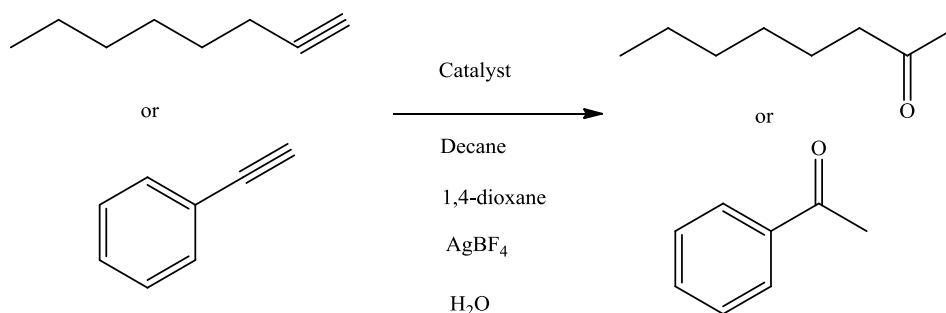


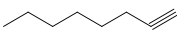
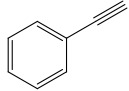
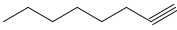
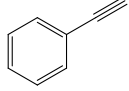
Scheme 4: Postulated route taken by gold(I) catalysts in the hydration of alkynes.³¹

5.2.4.1: Catalytic Activity of Expanded Ring Gold(I) Complexes

Dunsford and co workers have showed that sterically encumbered gold(I) complexes do not show any conversion of terminal alkynes unlike the 5-membered analogues which show excellent conversion. As the slightly less sterically hindered gold(I) complexes **1** and **2** lie between the complexes of Dunsford and the 5-membered NHCs it was of interest to see how they behaved catalytically, as shown in Table 11.

Table 11: Hydration of terminal alkynes using **1** and **2**.^a

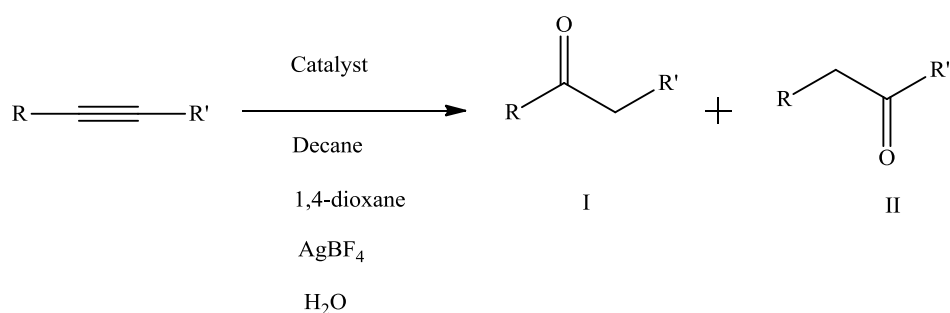


Entry	Catalyst	Substrate	Time (hours)	Yield (%)
1	1		17	43
2	1		17	44
3	2		17	69
4	2		17	31

^aReaction conditions: Substrate (1 mmol), catalyst (0.1 mol %), 1,4-dioxane (660 μ l), AgBF₄ (5 mg), decane (internal standard, 1 mmol), water (330 μ l), 80 °C for 17 hours. ^bPercentage yields based upon consumption of substrate by GCMS.

As shown in Table 11 the hydration of terminal alkynes to their corresponding ketones, entries **1-4**, was successful. 1-Octyne was converted with yields of 43 % and 69 %, and phenylacetylene formed acetophenone in yields of 44 % and 31 % for catalysts **1** and **2** respectively. These outcomes contrast with those of Dunsford *et al.* who observed no catalytic activity with expanded ring catalysts.²⁴ The results for internal alkynes are shown in Table 12.

Table 12: Hydration of internal alkynes using **1** and **2**.^a



Entry	Catalyst	Substrate	Time(hours)	Yield (%) ^b	Selectivity I:II ^c
1	1	2-Hexyne	17	100	36:64
2	2	2-Hexyne	17	100	30:70
3	1	Diphenylacetylene	17	32	-
4	2	Diphenylacetylene	17	4	-
5	1	4-Octyne	17	48	-
6	2	4-Octyne	17	99	-

^aReaction conditions: Substrate (1 mmol), catalyst (0.1 mol %), 1,4-dioxane (660 μ l), AgBF₄ (5 mg), decane (internal standard, 1 mmol), water (330 μ l), 80 °C for 17 hours. ^bPercentage yields based upon consumption of substrate by GCMS. ^cSelectivity determined by integration of GCMS peaks.

The hydration of internal alkynes were slightly more successful than that of the terminal alkynes, with 2-hexyne being completely converted to 2-hexanone and 3-hexanone with both catalyst **1** and **2**; this is in accordance with the data reported by Dunsford, where complete conversion for 2-hexyne is observed when the catalyst is [Au(6-Mes)Cl] and [Au(7-Mes)Cl].²⁴ However, the conversions of 4-octyne did not follow quite the same pattern as reported by Dunsford, with catalyst **2** exhibiting a near complete conversion of 99 % and catalyst **1** yielding a significantly lower 48 %. This can likely be explained by the size of the NHC, with catalyst **2** having a larger 7-membered ring causing the increase in the activity. Although the conversion of 4-octyne was not as high yielding as that reported by Dunsford it was still an enormous improvement in activity in comparison to the 5-membered counterparts, which are found to be inactive in this transformation.²⁷ As for catalysis when the substrate is diphenylacetylene, the outcome was better than that reported by Dunsford, as in this work conversions were up to 32 %. Although catalyst **1** yields 32 % for the conversion of diphenylacetylene catalyst **2** merely yields 4 % for the same conversion. The reason for this can be due to the steric demand imparted by both the NHC and the substrate.

5.3: Conclusions

The aim of this section was to synthesise a library of novel NHC gold(I) complexes of the general formula [Au(NHC)X], where X = Cl, Br, or I. This aim has successfully been achieved with a large range of novel [Au(NHC)X] complexes being made with NHCs, varying from expanded ring N-heterocyclic carbenes (**1-8**) to bicyclic N-heterocyclic carbenes (**9-11**).

The complexes were characterised by the disappearance of the carbene peak in the proton NMR spectra and a shift of the NCN peak in the carbon-13 NMR spectra. It has been found that this shift is greater in the expanded ring NHC gold(I) complexes than it is in the 5-membered analogues.

Molecular structures of complexes **1-8**, **10**, and **11** were obtained, and unlike the bicyclic benzyl copper(I) complex, compound **8** in Chapter 4, there is limited deviations of the C(1)-Au(1)-Cl(1) bond angle away from linearity. The angle does appear to differ slightly depending on the steric bulk situated on the N-substituents, with smaller N-substituents causing a greater deviation from the expected linearity. The other bond angle of interest was that of N(1)-C(1)-N(2), which, just like the copper(I) analogues and the reported data, shows a decrease in angle between the amidinium salt and the complex. In one case, **8**, this decrease in angle was above 10 °.

Percentage buried volume calculations showed the NHCs to be moderately bulky with little difference between the 6- and 7-membered alkylated expanded ring complexes and bicyclic rings with values of around 30 %, however the aryl substituted expanded ring complexes have larger buried volume values of around 40 %. The percentage buried volumes appear to show greatest effect when the N-substituents are altered over the make up of the NHC itself. This is apparent for the gold(I) complexes with large N-alkyl substituents, **6-8**, having percentage buried volumes more comparable to that of the [Au(IMes)Cl] than that of the [Au(6-Mes)Cl].

Hydration of terminal alkynes was carried out employing **1** and **2** as the catalyst; this was partially successful with conversions of 1-octyne to its ketone in yields of 43 % and 69 %, which had not been previously observed for expanded ring NHC gold complexes. The interest then moved from terminal alkynes to internal alkynes employing the same catalysts, this showed variable results with 2-hexyne yielding 100 % product in reasonable selectivity of around 30:70. 4-Octyne was converted to its corresponding ketone in 99 % yield when catalyst **2** is employed. However, diphenylacetylene gave limited conversion of 32 % and 4 % when employing **1** and **2** respectively. This is attributed to the steric hindrance of both the substrate and catalyst. This activity shown by the catalysts for the hydration of diphenylacetylene is a big improvement on that reported by Dunsford where only a trace of ketone product was observed.²⁴

5.4: Experimental

5.4.1: General Remarks

All air sensitive experiments were carried out using standard Schlenk techniques, under an atmosphere of argon or in a MBRAUN M72 glove box (N₂ atmosphere with > 0.1 ppm O₂ and H₂O) unless otherwise stated. Glassware was dried overnight in an oven at 120 °C and flame dried prior to use. Pentane of analytical grade was freshly collected from a MBRAUN sps 800 solvent purification system, THF was dried in a still over calcium hydride. All other solvents were used as purchased.

All NMR solvents used were purchased from Goss Scientific Ltd, and distilled from the appropriate drying agents under N₂ prior to use, following standard literature methods.³² All NMR spectra were obtained from a Bruker Avance AMX 250, 400, or 500 MHz and referenced to SiMe₄ and coupling constants *J* are expressed in Hertz as positive values regardless of their real individual signs. Mass spectrometry data was recorded, HRMS were obtained on a Waters Q-ToF micromass spectrometer and are reported as *m/z* (relative intensity) by the department of chemistry, Cardiff University.

All the X-ray Crystal structures were obtained on a Bruker Nonius Kappa CCD diffractometer using graphite mono-chromated Mo KR radiation ($\lambda(\text{Mo KR}) = 0.71073 \text{ \AA}$). An Oxford Cryosystems cooling apparatus was attached to the instrument, and all data were collected at 150 K. Data collection and cell refinement were carried out by Dr Benson Kariuki, using COLLECT³³ and HKL SCALEPACK.³⁴ Data reduction was applied using HKL DENZO and SCALEPACK.³⁴ The structures were solved using direct methods (Sir92)³⁵ and refined with SHELX-97.³⁶ Absorption corrections were performed using SORTAV.³⁷

Percentage buried volumes were calculated using SambVca.³⁸ Parameters applied for SambVca calculations: 3.50 Å was selected as the value for the sphere radius, 2.00 Å was used as distances for the metal–ligand bond, hydrogen atoms were omitted, and Bondi radii scaled by 1.17 were used. The above parameters applied are identical to

those of all literature examples discussed, allowing a direct comparison of calculated values.

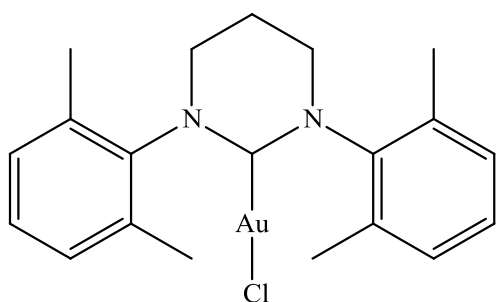
GC-MS data was obtained on an Agilent Technologies 6890N GC system with an Agilent Technologies 5973 inert MS detector with MSD.

Elemental analysis was obtained from the service provided by London Metropolitan University.

[Au(THT)Cl] and the amidinium salt precursors for **1-9** were synthesised by known literature procedures,^{8,10,39-42} amidinium salt precursors for **10** and **11** were synthesised as shown in Chapter 3 and all other reagents were used as purchased.

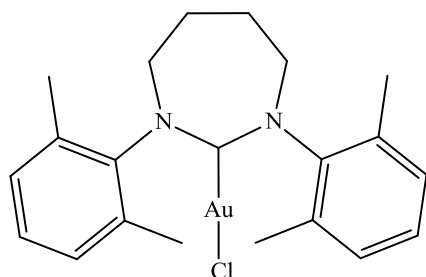
5.4.2: Experimental Data for Expanded Ring Gold(I) Complexes

Synthesis of [Au(6-xylyl)Cl] (1)



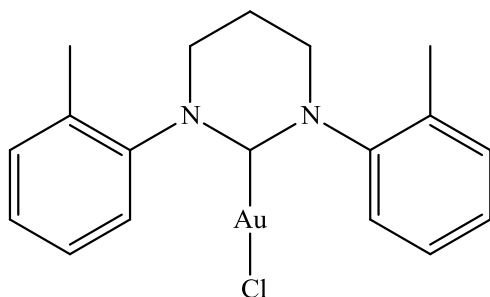
[6-xylylH]Br] (0.06 g, 0.17 mmol, 1 eq) was placed in a flame dried Schlenk and dried for 20 minutes. To this KHMDS (0.05 g, 0.24 mmol, 1.4 eq) and THF (5 ml) were added and stirred at room temperature for 20 minutes.

The free carbene solution was then filtered, under an atmosphere of nitrogen, on to a solution of [Au(SMe₂)Cl] (0.05 g, 0.17 mmol, 1 eq) in THF (5 ml) and stirred for a further hour. The reaction mixture was then exposed to air and activated charcoal was added and stirred for 30 minutes. The resulting solution was then filtered through a pad of oven dried celite and the filtrate was then reduced to dryness yielding [Au(6-xylyl)Cl] as a white solid (0.032 g, 35.9 %). ¹H NMR (CDCl₃, 400 MHz, 298 K): δ 7.15 (2 H, m, CH_{Ar}), δ 7.05 (4 H, d, CH_{Ar}, ³J_{HH} = 7.5 Hz), δ 3.40 (4 H, t, NCH₂, ³J_{HH} = 5.9 Hz), δ 2.30 (2 H, m, NCH₂CH₂), δ 2.25 (12 H, s, CH₃). ¹³C{¹H} NMR (CDCl₃, 125 MHz, 298 K): NCN not observed, δ 144.3 (C_{Ar}), δ 134.8 (C_{Ar}), δ 129.2 (CH_{Ar}), δ 128.7 (CH_{Ar}), δ 45.3 (NCH₂), δ 20.7 (NCH₂CH₂), δ 18.0 (CH₃). MS(ES) *m/z*: [M⁺ - Cl⁻ + MeCN] 529.43 (C₂₂H₂₇N₃Au requires 529.97), it was not possible to obtain HRMS data for this complex. Analysis calculated for C₂₀H₂₄N₂AuCl: C, 45.77; H, 4.61; N, 5.34. Found: C, 45.86; H, 4.59; N, 5.46.

Synthesis of [Au(7-xylyl)Cl] (2)

[(7-xylylH)Br] (0.07 g, 0.17 mmol, 1 eq) was placed in a flame dried Schlenk and dried for 20 minutes. To this KHMDS (0.05 g, 0.24 mmol, 1.4 eq) and THF (5 ml) were added and stirred at room temperature for 20 minutes. The free carbene solution was then filtered, under an atmosphere of

nitrogen, on to a solution of [Au(SMe₂)Cl] (0.05 g, 0.17 mmol, 1 eq) in THF (5 ml) and stirred for a further hour. The reaction mixture was then exposed to air and activated charcoal was added and stirred for 30 minutes. The resulting solution was then filtered through a pad of oven dried celite and the filtrate was then reduced to dryness yielding [Au(7-xylyl)Cl] as a white solid (0.038 g, 41.6 %). ¹H NMR (CDCl₃, 400 MHz, 298 K): δ 7.15 (2 H, m, CH_{Ar}), δ 7.05 (4 H, d, CH_{Ar}, ³J_{HH} = 7.3 Hz), δ 3.85 (4 H, m, NCH₂), δ 2.30 (12 H, s, CH₃), δ 2.25 (4 H, m, NCH₂CH₂). ¹³C{¹H} NMR (CDCl₃, 125 MHz, 298 K): δ 201.1 (NCN), δ 146.6 (C_{Ar}), δ 134.5 (C_{Ar}), δ 129.3 (CH_{Ar}), δ 128.4 (CH_{Ar}), δ 53.1 (NCH₂), δ 25.1 (NCH₂CH₂), δ 18.6 (CH₃). MS (ES) *m/z*: [M⁺ - Cl⁻ + MeCN] 544.2005 (C₂₃H₂₉N₃Au requires 544.2027). Analysis calculated for C₂₁H₂₆N₂AuCl: C, 46.81; H, 4.86; N, 5.20. Found: C, 46.78; H, 4.76; N, 5.17.

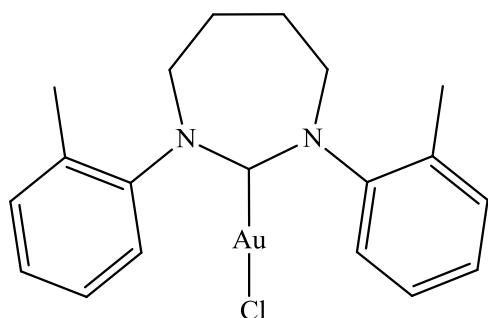
Synthesis of [Au(6-*o*-tolyl)Cl] (3)

[(6-*o*-tolylH)Br] (0.06 g, 0.17 mmol, 1 eq) was placed in a flame dried Schlenk and dried for 20 minutes. To this KHMDS (0.05 g, 0.24 mmol, 1.4 eq) and THF (5 ml) were added and stirred at room temperature for 20 minutes. The free carbene solution was then filtered, under an

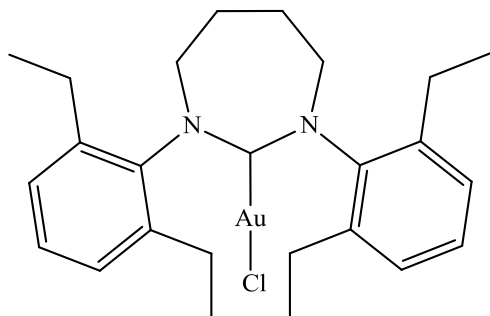
atmosphere of nitrogen, on to a solution of [Au(SMe₂)Cl] (0.05 g, 0.17 mmol, 1 eq) in THF (5 ml) and stirred for a further hour. The reaction mixture was then exposed to air

and activated charcoal was added and stirred for 30 minutes. The resulting solution was then filtered through a pad of oven dried celite and the filtrate was then reduced to dryness yielding [Au(6-*o*-tolyl)Cl] as a white solid (0.028 g, 33.2 %). ^1H NMR (CDCl_3 , 400 MHz, 298 K): δ 7.10 – 7.20 (8 H, m, CH_{Ar}), δ 3.50 (4 H, m, NCH_2), δ 2.30 (2 H, m, NCH_2CH_2), δ 2.25 (6 H, m, CH_3). $^{13}\text{C}\{^1\text{H}\}$ NMR (CDCl_3 , 125 MHz, 298 K): δ 191.1 (NCN), δ 145.9 (C_{Ar}), δ 134.6 (C_{Ar}), δ 131.5 (CH_{Ar}), δ 128.8 (CH_{Ar}), δ 128.1 (CH_{Ar}), δ 127.3 (CH_{Ar}), δ 47.0 (NCH_2), δ 21.0 (NCH_2CH_2), δ 17.8 (CH_3). MS(ES) m/z : [$\text{M}^+ - \text{Cl}^- + \text{MeCN}$] 502.1567 ($\text{C}_{20}\text{H}_{23}\text{N}_3\text{Au}$ requires 502.1558). Analysis calculated for $\text{C}_{18}\text{H}_{20}\text{N}_2\text{AuCl}$: C, 43.52; H, 4.06; N, 5.64. Found: C, 43.43; H, 3.98; N, 5.69.

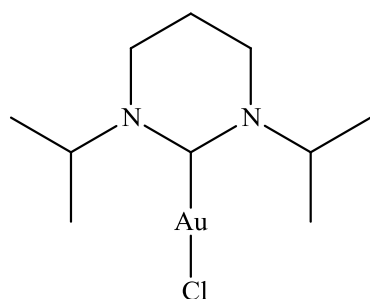
Synthesis of [Au(7-*o*-tolyl)Cl] (4)



[(7-*o*-tolyl)H]Br (0.06 g, 0.16 mmol, 1 eq) was placed in a flame dried Schlenk and dried for 20 minutes. To this KHMDS (0.04 g, 0.22 mmol, 1.4 eq) and THF (5 ml) were added and stirred at room temperature for 20 minutes. The free carbene solution was then filtered, under an atmosphere of nitrogen, on to a solution of [Au(THT)Cl] (0.05 g, 0.16 mmol, 1 eq) in THF (5 ml) and stirred for a further hour. The reaction mixture was then exposed to air and activated charcoal was added and stirred for 30 minutes. The resulting solution was then filtered through a pad of oven dried celite and the filtrate was then reduced to dryness yielding [Au(7-*o*-tolyl)Cl] as a white solid (0.019 g, 23.9 %). ^1H NMR (CDCl_3 , 400 MHz, 298 K): δ 7.10 – 7.20 (8 H, m, CH_{Ar}), δ 3.65 – 4.10 (4 H, m, NCH_2), δ 2.25 (4 H, m, CH_3), δ 2.15 (4 H, m, NCH_2CH_2). $^{13}\text{C}\{^1\text{H}\}$ NMR (CDCl_3 , 125 MHz, 298 K): NCN not observed, δ 134.6 (C_{Ar}), δ 131.8 (C_{Ar}), δ 128.6 (CH_{Ar}), δ 128.2 (CH_{Ar}), δ 127.6 (CH_{Ar}), δ 127.3 (CH_{Ar}), δ 54.3 (NCH_2), δ 24.6 (NCH_2CH_2), δ 18.1 (CH_3). MS(ES) m/z : [$\text{M}^+ - \text{Cl}^- + \text{MeCN}$] 516.1732 ($\text{C}_{21}\text{H}_{25}\text{N}_3\text{Au}$ requires 516.1714). Elemental analysis could not be obtained for unknown reasons.

Synthesis of [Au(7-DEP)Cl] (5)

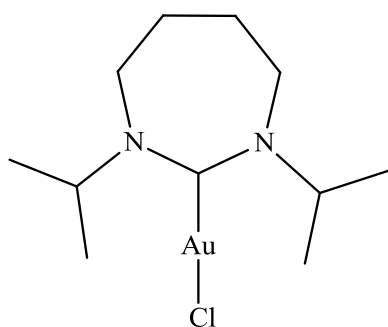
[(7-DEPH)Br] (0.08 g, 0.16 mmol, 1 eq) was placed in a flame dried Schlenk and dried for 20 minutes. To this KHMDS (0.04 g, 0.22 mmol, 1.4 eq) and THF (5 ml) were added and stirred at room temperature for 20 minutes. The free carbene solution was then filtered, under an atmosphere of nitrogen, on to a solution of [Au(THT)Cl] (0.05 g, 0.16 mmol, 1 eq) in THF (5 ml) and stirred for a further hour. The reaction mixture was then exposed to air and activated charcoal was added and stirred for 30 minutes. The resulting solution was then filtered through a pad of oven dried celite and the filtrate was then reduced to dryness yielding [Au(7-DEP)Cl] as a white solid (0.034 g, 37.6 %). ^1H NMR (CDCl_3 , 250 MHz, 298 K): δ 7.20 (2 H, t, CH_{Ar} , $^3J_{\text{HH}} = 7.9$ Hz), δ 7.10 (4 H, d, CH_{Ar} , $^3J_{\text{HH}} = 7.9$ Hz), δ 3.85 (4 H, m, NCH_2), δ 2.85 (4 H, m, NCH_2), δ 2.60 (4 H, m, CH_2), δ 2.20 (4 H, m, NCH_2CH_2), δ 1.30 (12 H, t, CH_3 , $^3J_{\text{HH}} = 7.5$ Hz). $^{13}\text{C}\{^1\text{H}\}$ NMR (CDCl_3 , 125 MHz, 298 K): δ 201.7 (NCN), δ 145.7 (C_{Ar}), δ 139.9 (C_{Ar}), δ 128.6 (CH_{Ar}), δ 126.7 (CH_{Ar}), δ 54.3 (NCH_2), δ 24.9 (NCH_2CH_2), δ 24.0 (CH_2), δ 14.4 (CH_3). MS(ES) m/z : [$\text{M}^+ + \text{MeCN}$] 635.1718 ($\text{C}_{27}\text{H}_{37}\text{N}_3\text{AuCl}$ requires 635.1823). Analysis calculated for $\text{C}_{25}\text{H}_{34}\text{N}_2\text{AuCl}$: C, 50.47; H, 5.76; N, 4.71. Found: C, 50.53; H, 5.79; N, 4.88.

Synthesis of [Au(6-iPr)Cl] (6)

[(6-iPrH)I] (0.05 g, 0.16 mmol, 1 eq) was placed in a flame dried Schlenk and dried for 20 minutes. To this KHMDS (0.04 g, 0.22 mmol, 1.4 eq) and THF (5 ml) were added and stirred at room temperature for 20 minutes. The free carbene solution was then filtered, under an atmosphere of nitrogen, on to a solution of [Au(THT)Cl] (0.05 g, 0.16 mmol, 1 eq) in THF (5 ml) and stirred for a further hour. The reaction mixture was then exposed to air and activated charcoal was added and

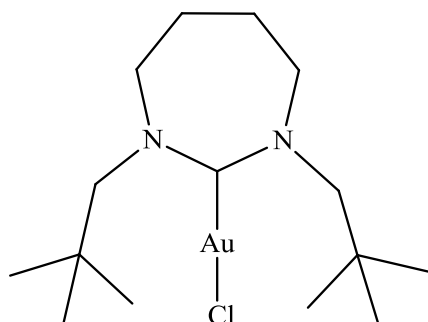
stirred for 30 minutes. The resulting solution was then filtered through a pad of oven dried celite and the filtrate was then reduced to dryness yielding $[\text{Au}(6\text{-iPr})\text{Cl}]$ as a white solid (0.026 g, 42.2 %). ^1H NMR (CDCl_3 , 400 MHz, 298 K): δ 5.25 (2 H, m, NCH), δ 3.05 (4 H, m, NCH_2), δ 1.85 (2 H, m, NCH_2CH_2), δ 1.10 (12 H, d, CH_3 , $^3J_{\text{HH}} = 6.8$ Hz). $^{13}\text{C}\{^1\text{H}\}$ NMR (CDCl_3 , 125 MHz, 298 K): δ 187.0 (NCN), δ 60.1 (NCH), δ 38.3 (NCH_2), δ 20.5 (NCH_2CH_2), δ 20.0 (CH_3). MS(ES) m/z : $[\text{M}^+ - \text{Cl} + 2 \text{MeCN}]$ 446.1926 ($\text{C}_{14}\text{H}_{26}\text{N}_4\text{Au}$ requires 446.1855). Analysis calculated for $\text{C}_{10}\text{H}_{20}\text{N}_2\text{AuCl}$: C, 29.98; H, 5.03; N, 6.99. Found: C, 29.89; H, 4.97; N, 6.98.

Synthesis of $[\text{Au}(7\text{-iPr})\text{Cl}]$ (7)



$[(7\text{-iPrH})\text{I}]$ (0.05 g, 0.16 mmol, 1 eq) was placed in a flame dried Schlenk and dried for 20 minutes. To this KHMDS (0.04 g, 0.22 mmol, 1.4 eq) and THF (5 ml) were added and stirred at room temperature for 20 minutes. The free carbene solution was then filtered, under an atmosphere of nitrogen, on to a solution of $[\text{Au}(\text{THT})\text{Cl}]$ (0.05 g, 0.16 mmol, 1 eq) in THF (5 ml) and stirred for a further hour. The reaction mixture was then exposed to air and activated charcoal was added and stirred for 30 minutes. The resulting solution was then filtered through a pad of oven dried celite and the filtrate was then reduced to dryness yielding $[\text{Au}(7\text{-iPr})\text{Cl}]$ as a white solid (0.027 g, 41.9 %). ^1H NMR (CDCl_3 , 400 MHz, 298 K): δ 5.10 (2 H, m, NCH), δ 3.25 (4 H, t, NCH_2 , $^3J_{\text{HH}} = 5.6$ Hz), δ 1.75 (4 H, m, NCH_2CH_2), δ 1.20 (12 H, d, CH_3 , $^3J_{\text{HH}} = 6.8$ Hz). $^{13}\text{C}\{^1\text{H}\}$ NMR (CDCl_3 , 125 MHz, 298 K): δ 199.0 (NCN), δ 60.2 (NCH), δ 44.1 (NCH_2), δ 25.0 (NCH_2CH_2), δ 20.2 (CH_3). MS(ES) m/z : $[\text{M}^+ + \text{K}^+]$ 453.0777 ($\text{C}_{11}\text{H}_{22}\text{N}_2\text{AuClK}$ requires 453.0774). Analysis calculated for $\text{C}_{11}\text{H}_{22}\text{N}_2\text{AuCl}$: C, 31.86; H, 5.35; N, 6.75. Found: C, 31.97; H, 5.46; N, 6.72.

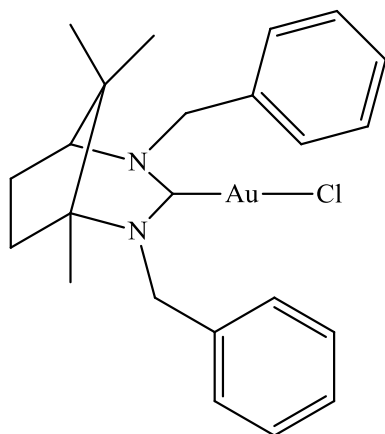
Synthesis [Au(7-Neo)Cl] (8)



[(7-NeoH)I] (0.06 g, 0.16 mmol, 1 eq) was placed in a flame dried Schlenk and dried for 20 minutes. To this KHMDS (0.04 g, 0.22 mmol, 1.4 eq) and THF (5 ml) were added and stirred at room temperature for 20 minutes. The free carbene solution was then filtered, under an atmosphere of nitrogen, on to a solution of [Au(THT)Cl] (0.05 g, 0.16 mmol, 1 eq) in THF (5 ml) and stirred for a further hour. The reaction mixture was then exposed to air and activated charcoal was added and stirred for 30 minutes. The resulting solution was then filtered through a pad of oven dried celite and the filtrate was then reduced to dryness yielding [Au(7-Neo)Cl] as a white solid (0.024 g, 32.6 %). ^1H NMR (CDCl_3 , 400 MHz, 298 K): δ 3.90 (4 H, s, NCH_2), δ 3.45 (4 H, t, NCH_2 , $^3J_{\text{HH}} = 5.0$ Hz), δ 1.75 (4 H, m, NCH_2CH_2), δ 0.85 (18 H, s, CH_3). $^{13}\text{C}\{^1\text{H}\}$ NMR (CDCl_3 , 125 MHz, 298 K): δ 204.5 (NCN), δ 74.7 (NCH_2), δ 56.0 (NCH_2), δ 33.3 (C), δ 28.8 (CH_3), δ 24.7 (NCH_2CH_2). MS(ES) m/z : [$\text{M}^+ - \text{Cl} + 2 \text{MeCN} + \text{H}$] 517.37 ($\text{C}_{19}\text{H}_{37}\text{N}_4\text{Au}$ requires 517.97), it was not possible to obtain HRMS data for this complex. Analysis calculated for $\text{C}_{15}\text{H}_{30}\text{N}_2\text{AuCl}$: C, 38.27; H, 6.42; N, 5.95. Found: C, 38.41; H, 6.42; N, 6.05.

5.4.3: Experimental Data for Bicyclic Gold(I) Complexes

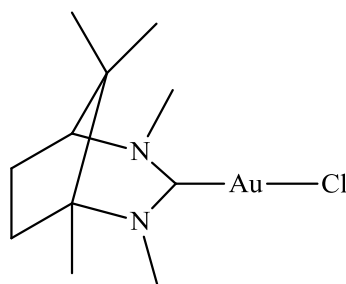
Synthesis of ((5S)-2,4-dibenzyl-1,8,8-trimethyl-2,4-diazabicyclo[3.2.1]octan-3-yl)gold(I) chloride (9)



(1R, 5S)-2,4-dibenzyl-1,8,8-trimethyl-4-aza-2-azoniabicyclo-[3.2.1]oct-2-ene hexafluorophosphate (0.07 g, 0.16 mmol, 1 eq) was placed in a flame dried Schlenk and dried for 20 minutes. To this KHMDS (0.04 g, 0.22 mmol, 1.4 eq) and THF (5 ml) were added and stirred at room temperature for 20 minutes. The free carbene solution was then filtered, under an atmosphere of nitrogen, on to a solution of

[Au(THT)Cl] (0.05 g, 0.16 mmol, 1 eq) in THF (5 ml) and stirred for a further hour. The reaction mixture was then exposed to air and activated charcoal was added and stirred for 30 minutes. The resulting solution was then filtered through a pad of oven dried celite and the filtrate was then reduced to dryness yielding ((5S)-2,4-dibenzyl-1,8,8-trimethyl-2,4-diazabicyclo[3.2.1]octan-3-yl)gold(I) chloride as a white solid (0.046 g, 52.8 %). ^1H NMR (CDCl_3 , 400 MHz, 298 K): δ 7.45 (1 H, d, CH_{Ar} , $^3J_{\text{HH}} = 6.2$ Hz), δ 7.40 (1 H, d, CH_{Ar} , $^3J_{\text{HH}} = 7.2$ Hz), δ 7.25 (4 H, m, CH_{Ar}), δ 7.20 (1 H, m, CH_{Ar}), δ 7.15 (1 H, d, CH_{Ar} , $^3J_{\text{HH}} = 6.8$ Hz), δ 5.40 (2 H, m, NCH_2), δ 5.05 (1 H, m, NCH_2), δ 4.75 (1 H, m, NCH_2), δ 3.00 (1 H, m, NCH), δ 2.05 (1 H, m, CH_2), δ 1.60 (1 H, m, CH_2), δ 1.25 (2 H, m, CH_2), δ 1.10 (3 H, s, CH_3), δ 0.80 (3 H, s, CH_3), δ 0.70 (3 H, s, CH_3). $^{13}\text{C}\{^1\text{H}\}$ NMR (CDCl_3 , 125 MHz, 298 K): δ 190.0 (NCN), δ 138.3 (C_{Ar}), δ 135.4 (C_{Ar}), δ 129.5 (CH_{Ar}), δ 129.0 (CH_{Ar}), δ 128.7 (CH_{Ar}), δ 128.1 (CH_{Ar}), δ 127.7 (CH_{Ar}), δ 126.0 (CH_{Ar}), δ 70.9 (NC), δ 66.3 (NCH), δ 62.3 (NCH_2), δ 58.5 (NCH_2), δ 40.4 (CH_2), δ 39.1 (CH_2), δ 31.4 (C), δ 21.8 (CH_3), δ 18.0 (CH_3), δ 16.9 (CH_3). MS(ES) m/z : [$\text{M}^+ + \text{Na}$] 587.2426 ($\text{C}_{23}\text{H}_{28}\text{N}_2\text{AuClNa}$ requires 587.2429). Analysis calculated for $\text{C}_{23}\text{H}_{28}\text{N}_2\text{AuCl}$: C, 48.90; H, 5.00; N, 4.96. Found: C, 49.61; H, 5.24; N, 4.86, which was inclusive of 1/6 pentane.

Synthesis of ((5S)-2,4-dimethyl-1,8,8-trimethyl-2,4-diazabicyclo[3.2.1]octan-3-yl)gold(I) chloride (10)



((5S)-2,4-dimethyl-1,8,8-trimethyl-2,4-

diazabicyclo[3.2.1]octan-2-ium hexafluorophosphate(V)

(0.05 g, 0.16 mmol, 1 eq) was placed in a flame dried

Schlenk and dried for 20 minutes. To this KHMDS (0.04

g, 0.22 mmol, 1.4 eq) and THF (5 ml) were added and

stirred at room temperature for 20 minutes. The free

carbene solution was then filtered, under an atmosphere of nitrogen, on to a solution of

[Au(THT)Cl] (0.05 g, 0.16 mmol, 1 eq) in THF (5 ml) and stirred for a further hour.

The reaction mixture was then exposed to air and activated charcoal was added and

stirred for 30 minutes. The resulting solution was then filtered through a pad of oven

dried celite and the filtrate was then reduced to dryness yielding ((5S)-2,4-dimethyl-

1,8,8-trimethyl-2,4-diazabicyclo[3.2.1]octan-3-yl)gold(I) chloride as a white solid

(0.024 g, 37.5 %). ^1H NMR (CDCl_3 , 400 MHz, 298 K): δ 3.40 (3 H, s, CH_3), δ 3.35 (3

H, s, CH_3), δ 2.95 (1 H, d, NCH, $^3J_{\text{HH}} = 4.0$ Hz), δ 2.20 (1 H, m, CH_2), δ 1.95 (2 H, m,

CH_2), δ 1.75 (1 H, m, CH_2), δ 1.15 (3 H, s, CH_3), δ 0.95 (3 H, s, CH_3), δ 0.90 (3 H, s,

CH_3). $^{13}\text{C}\{^1\text{H}\}$ NMR (CDCl_3 , 125 MHz, 298 K): NCN not observed, δ 69.1 (NCH), δ

68.6 (NC), δ 46.2 (CH_3), δ 41.6 (CH_3), δ 37.9 (C), δ 34.1 (CH_2), δ 30.3 (CH_2), δ 22.1

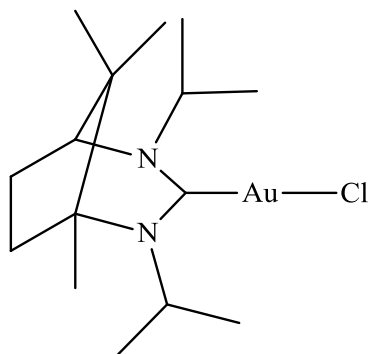
(CH_3), δ 17.6 (CH_3), δ 16.2 (CH_3). MS(ES) m/z : [$\text{M}^+ - \text{Cl} + \text{MeCN} + \text{H}$] 418.20

($\text{C}_{13}\text{H}_{24}\text{N}_3\text{Au}$ requires 418.97), it was not possible to obtain HRMS data for this

complex. Analysis calculated for $\text{C}_{11}\text{H}_{20}\text{N}_2\text{AuCl}$: C, 32.01; H, 4.88; N, 6.79. Found: C,

31.88; H, 4.73; N, 6.83.

Synthesis of ((5S)-2,4-diisopropyl-1,8,8-trimethyl-2,4-diazabicyclo[3.2.1]octan-3-yl)gold(I) chloride (11)



(5S)-2,4-diisopropyl-1,8,8-trimethyl-2,4-

diazabicyclo[3.2.1]octan-2-ium hexafluorophosphate(V)

(0.06 g, 0.16 mmol, 1 eq) was placed in a flame dried

Schlenk and dried for 20 minutes. To this KHMDS (0.04

g, 0.22 mmol, 1.4 eq) and THF (5 ml) were added and

stirred at room temperature for 20 minutes. The free

carbene solution was then filtered, under an atmosphere of nitrogen, on to a solution of

[Au(THT)Cl] (0.05 g, 0.16 mmol, 1 eq) in THF (5 ml) and stirred for a further hour.

The reaction mixture was then exposed to air and activated charcoal was added and

stirred for 30 minutes. The resulting solution was then filtered through a pad of oven

dried celite and the filtrate was then reduced to dryness yielding ((5S)-2,4-diisopropyl-

1,8,8-trimethyl-2,4-diazabicyclo[3.2.1]octan-3-yl)gold(I) chloride as a white solid

(0.043 g, 58.2 %). ^1H NMR (CDCl_3 , 400 MHz, 298 K): δ 5.80 (1 H, m, NCH), δ 3.75

(1 H, m, NCH), δ 3.05 (1 H, d, NCH, $^3J_{\text{HH}} = 5.2$ Hz), δ 2.20 (1 H, m, CH_2), δ 2.05 (1 H,

m, CH_2), δ 1.85 (2 H, m, CH_2), δ 1.75 (3 H, m, CH_3), δ 1.70 (3 H, m, CH_3), δ 1.20 (3 H,

s, CH_3), δ 1.20 (3 H, d, CH_3 , $^3J_{\text{HH}} = 6.8$ Hz), δ 1.10 (3 H, d, CH_3 , $^3J_{\text{HH}} = 6.7$ Hz), δ 0.95

(3 H, s, CH_3), δ 0.80 (3 H, s, CH_3). $^{13}\text{C}\{^1\text{H}\}$ NMR (CDCl_3 , 125 MHz, 298 K): δ 207.1

(NCN), δ 72.0 (NCH), δ 60.5 (NC), δ 59.3 (NCH), δ 48.6 (NCH), δ 39.5 (C), δ 38.1

(CH_2), δ 31.6 (CH_2), δ 28.7 (CH_3), δ 26.2 (CH_3), δ 23.5 (CH_3), δ 21.8 (CH_3), δ 20.3

(CH_3), δ 19.7 (CH_3), δ 17.5 (CH_3). MS(ES) m/z : [$\text{M}^+ - \text{Cl}^- + \text{MeCN}$] 474.2161

($\text{C}_{17}\text{H}_{31}\text{N}_3\text{Au}$ requires 474.2184). Analysis calculated for $\text{C}_{15}\text{H}_{28}\text{N}_2\text{AuCl}$: C, 38.43; H,

6.02; N, 5.98. Found: C, 38.66; H, 6.16; N, 5.82.

5.4.4: General Procedure for the Hydration of Alkynes

A vial equipped with a magnetic stirrer bar was loaded with the appropriate catalyst (0.1 mol %, THF stock solution), decane (1 mmol, internal standard), and 1,4-dioxane (660 μ l). AgBF_4 (5 mg) was added to the reaction mixture and stirred for 5 minutes at room temperature. The alkyne substrate (1 mmol) was added followed by deionised water (330 μ l) and the reaction mixture was then heated to 80 $^\circ\text{C}$ for 17 hours. After this time the reaction mixture was left to cool slowly to room temperature before being extracted into HPLC DCM (2 ml). 0.2 ml was then taken and eluted through a small silica column for GCMS analysis. Program analysis: initial temperature at 40 $^\circ\text{C}$, held for 2.5 minutes, ramp 5 $^\circ\text{C}/\text{minute}$ next 150 $^\circ\text{C}$, ramp 10 $^\circ\text{C}/\text{minute}$ next 220 $^\circ\text{C}$ held for 10 minutes. The temperature of the injector and detector were maintained at 240 $^\circ\text{C}$.

5.5: References

- 1 Herrmann, W. A.; Schneider, S. K.; Öfele, K.; Sakamoto, M.; Herdtweck, E. J. *Organomet. Chem.* **2004**, 689, 2441-2449.
- 2 Scarborough, C. C.; Popp, B. V.; Guzei, I. A.; Stahl, S. S. *J. Organomet. Chem.* **2005**, 690, 6143-6155.
- 3 Yasar, S.; Özdemir, I.; Cetinkaya, B.; Renaud, J. -L.; Bruneau, C. *Eur. J. Org. Chem.* **2008**, 2142-2149.
- 4 Mayr, M.; Wurst, K.; Ongania, K. -H.; Buchmeiser, M. R. *Chem. Eur. J.* **2004**, 10, 1256-1266.
- 5 Binobaid, A.; Iglesias, M.; Beetstra, D. J.; Kariuki, B.; Dervisi, A.; Fallis, I. A.; Cavell, K. J. *Dalton Trans.* **2009**, 7099-7112.
- 6 Kolychev, E. L.; Portnyagin, I. A.; Shuntikov, V. V.; Khrustlaev, V. N.; Nechaev, M. S. *J. Organomet. Chem.* **2009**, 694, 2454-2462.
- 7 Lu, W. Y.; Cavell, K. J.; Wixey, J. S.; Kariuki, B. *Organometallics* **2011**, 30, 5649-5655.
- 8 Iglesias, M.; Beetstra, D. J.; Knight, J. C.; Ooi, L. -L.; Stasch, A.; Coles, S.; Male, L.; Hursthouse, M. B.; Cavell, K. J.; Dervisi, A.; Fallis, I. A. *Organometallics* **2008**, 27, 13, 3279-3289.
- 9 Reddy, P. V. G.; Tabassum, S.; Blanrue, A.; Wilhelm, R. *Chem. Comm.* **2009**, 5910-5912.
- 10 Newman, P. D.; Cavell, K. J.; Kariuki, B. M. *Organometallics* **2010**, 29, 12, 2724-2734.
- 11 Newman, P. D.; Cavell, K. J.; Hallett, A. J.; Kariuki, B. M. *Dalton Trans.* **2011**, 40, 8807-8813.
- 12 Newman, P. D.; Cavell, K. J.; Kariuki, B. M. *Chem. Comm.* **2012**, 48, 6511-6513.
- 13 Stephen, A.; Hashmi, K.; Hutchings, G. J. *Angew. Chem. Int. Ed.* **2006**, 45, 47, 7896-7936.
- 14 Boorman, T. C.; Larrosa, I. *Chem. Soc. Rev.* **2011**, 40, 1910-1925.
- 15 Marion, N.; Nolan, S. P. *Chem. Soc. Rev.* **2008**, 37, 1776-1782.
- 16 Nolan, S. P. *Acc. Chem. Res.* **2011**, 44, 2, 91-100.

- 17 Czégéni, C. E.; Papp, G.; Kathó, Á.; Joó, F. *J. Mol. Cat. A: Chem.* **2011**, 340, 1-8.
- 18 Gaillard, S.; Slawin, A. M. Z.; Nolan, S. P. *Chem. Comm.* **2010**, 46, 2742-2744.
- 19 Herrmann, W. A. *Angew. Chem. Int. Ed.* **2002**, 41, 8, 1290-1309.
- 20 Crudden, C. M.; Allen, D. P. *Coord. Chem. Revs.* **2004**, 248, 2247-2273.
- 21 Doyle, M. J.; Lappert, M. F.; McLaughlin, G. M.; McMeeking, J. *J. Chem. Soc. Dalton Trans.* **1974**, 1494-1501.
- 22 Viciu, M. S.; Germaneau, R. F.; Navarro-Fernandez, O.; Stevens, E. D.; Nolan, S. P. *Organometallics* **2002**, 21, 25, 5470-5472.
- 23 Kascatan-Nebioglu, A.; Panzner, M. J.; Tessier, C. A.; Cannon, C. I.; Youngs, W. J. *Coord. Chem. Revs.* **2007**, 251, 884-895.
- 24 Dunsford, J. J.; Cavell, K. J.; Kariuki, B. M. *Organometallics* **2012**, 31, 4118-4121.
- 25 Dunsford, J. J.; Cavell, K. J. *Dalton Trans.* **2011**, 40, 9131-9135.
- 26 De Frémont, P.; Scott, N. M.; Stevens, E. D.; Nolan, S. P. *Organometallics* **2005**, 24, 10, 2411-2418.
- 27 Marion, N.; Ramón, R. S.; Nolan, S. P. *J. Am. Chem. Soc.* **2009**, 131, 2, 448-449.
- 28 Hudnall, T. W.; Tennyson, A. G.; Bielawski, C. W. *Organometallics* **2010**, 29, 20, 4569-4578.
- 29 Coberán, R.; Ramírez, J.; Poyatos, M.; Peris, E.; Fernández, E. *Tetrahedron: Asymm.* **2006**, 17, 12, 1759-1762.
- 30 López, S.; Gerrero-Gómez, E.; Pérez-Galán, P.; Nieto-Oberhuber, C.; Echavarren, A. M. *Angew. Chem. Int. Ed.* **2006**, 45, 36, 6029-6032.
- 31 Leyva, A.; Corma, A. *J. Org. Chem.* **2009**, 74, 5, 2067-2074.
- 32 Perrin, D. D.; Amarego, W. F. A. *Purification of Laboratory Chemicals*; Pergamon: Oxford, **1988**.
- 33 COLLECT; Nonius BV: Delft, The Netherlands, **1998**.
- 34 Otwinowski, Z.; Minor, W. *Methods Enzymol.* **1997**, 276, 307-326.
- 35 Altomare, A.; Cascarano, G.; Giacovazzo, C.; Guagliardi, A. *J. Appl. Crystallogr.* **1993**, 26, 343-350.
- 36 Sheldrick, G. M. *Acta Crystallogr. Sect. A* **2008**, A64, 112-122.
- 37 Blessing, R. H. *Acta Crystallogr. Sect. A* **1995**, 51, 33-38.
- 38 Poater, A.; Cosenza, B.; Correa, A.; Giudice, S.; Ragone, F.; Scarano, V.; Cavallo, L. *Eur. J. Inorg. Chem.* **2009** 1759-1766.

- 39 Hasmi, A. S. K.; Braun, I.; Rudolph, M.; Rominger, F. *Organoemtallics* **2012**, 31, 2, 644-661.
- 40 Dunsford, J. J.; Cavell, K. J.; Kariuki, B. *J. Organomet. Chem.* **2011**, 696, 1, 188-194.
- 41 Iglesias, M.; Beetstra, D. J.; Kariuki, B.; Cavell, K. J.; Dervisi, A.; Fallis, I. A. *Eur. J. Inorg. Chem.* **2009**, 13, 1913-1919.
- 42 Dunsford, J. J. *PhD Thesis* **2012**.

6. Coordination of Expanded Ring N-Heterocyclic Carbenes to Nickel(I)

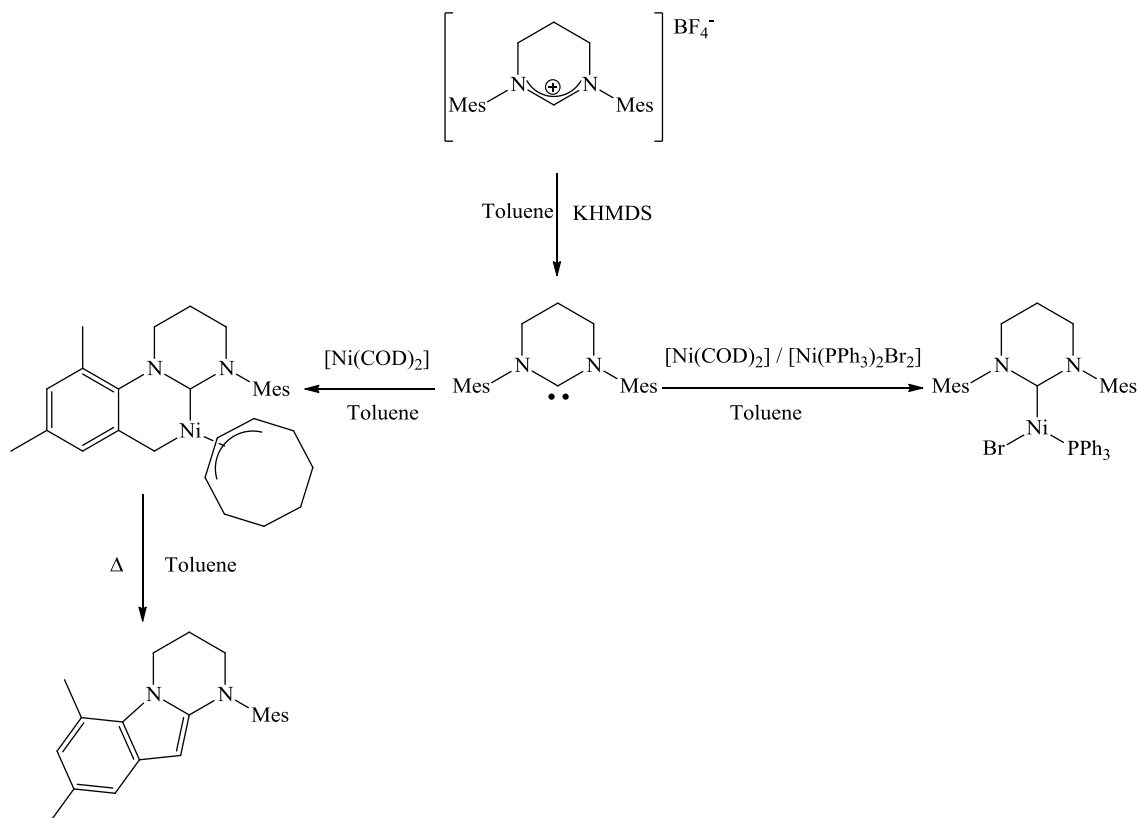
6.1: Introduction

In recent years the interest in paramagnetic metal complexes of NHCs and their characterisation using electron paramagnetic resonance (EPR) have been appearing, with the main reports coming from the Cavell group¹ and the Whittlesey group^{2,3}. These complexes, although relatively unexplored, have been shown to be useful in catalytic processes, such as cross coupling reactions^{2,4-6} and alkene oligomerisation¹ due to their abilities to undergo one and two electron processes. The two electron process has been exhibited by Vicic and co-workers where they employ nickel(I) complexes and it is hypothesised that the catalytic process is not a transmetallation affording the Ni(II) complex but a Ni(I)-Ni(III) redox pathway.⁷ It was not until 2010 that Whittlesey and co-workers reported an expanded ring NHC coordinated to nickel(I), yielding a three coordinate nickel(I) complex, and have shown that it could be employed in cross coupling catalytic reactions with conversions of greater than 99 %.² Due to this discovery by Whittlesey, this chapter will concentrate on the coordination of a series of expanded ring NHCs to nickel(I).

6.2: Results and Discussion

It has been found by Whittlesey and co-workers that certain expanded ring NHC nickel complexes are susceptible to carbene C-H activations.² This was apparent when first attempting to synthesise the nickel(I) complex [Ni(6-Mes)(COD)Cl]. A nickel(II) C-H activation complex was synthesised by reacting one equivalent of 6-Mes NHC precursor with a solution of [Ni(COD)₂] in toluene, yielding, after just one hour, a deep red nickel(II) species, Scheme 1. This nickel(II) species then undergoes an indole

elimination upon heating. It was found that using half an equivalent each of $[\text{Ni}(\text{COD})_2]$ and $[\text{Ni}(\text{PPh}_3)_2\text{Br}_2]$ gave a three coordinate, nickel(I) complex in a yield of 43 % as shown in Scheme 1.



Scheme 1: Synthesis of the expanded ring NHCs nickel complexes by Whittlesey and co-workers.²

6.2.1: Synthesis of Nickel(I) Complexes

The synthetic route to expanded ring NHC nickel(I) complexes, which was employed to synthesise a series of complexes, was analogous to that of Whittlesey and co-workers shown in Scheme 1. The NHC precursors, which were used to synthesise these

complexes were the 6-DEPH·Br, 7-DEPH·I (DEPH = diethylphenyl amidinium salt), 6-*o*-tolyIH·Br, and the 7-*o*-tolyIH·Br amidinium salts. After producing the free carbene via an *in situ* reaction with KHMDS they were reacted with half an equivalent of both nickel(0) and nickel(II) adduct and after continuous stirring for eighteen hours formed the nickel(I) complexes, **1-4**, in yields of up to 35 %, Figure 1, these were then purified by recrystallisation from toluene and hexane.

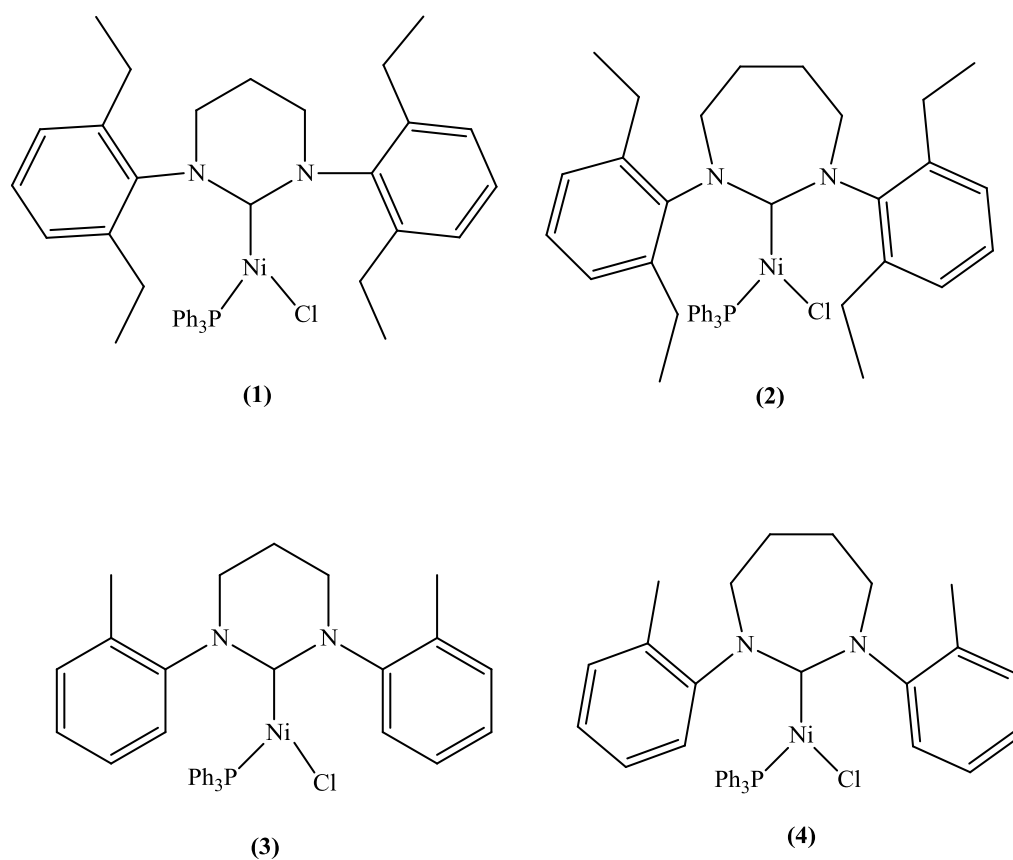


Figure 1: Nickel(I) complexes of expanded ring NHCs, **1-4**.

Although compounds **1-4** were successfully isolated, on exposure to air and moisture the yellow precipitate darkened indicating facile decomposition. Therefore the compounds were synthesised and stored inside a glove box.

6.2.2: Characterisation of Nickel(I) Complexes

Complexes **1-4** were characterised by single crystal X-ray crystallography (Figures 2-5), mass spectrometry, and EPR studies. Crystals suitable for single crystal X-ray crystallography were obtained from vapour diffusion of hexane into a concentrated solution of **1-4** in THF in the freezer inside the glove box over a period of four days. Crystallographic data for **1-4** is shown in Tables 1-4 respectively.

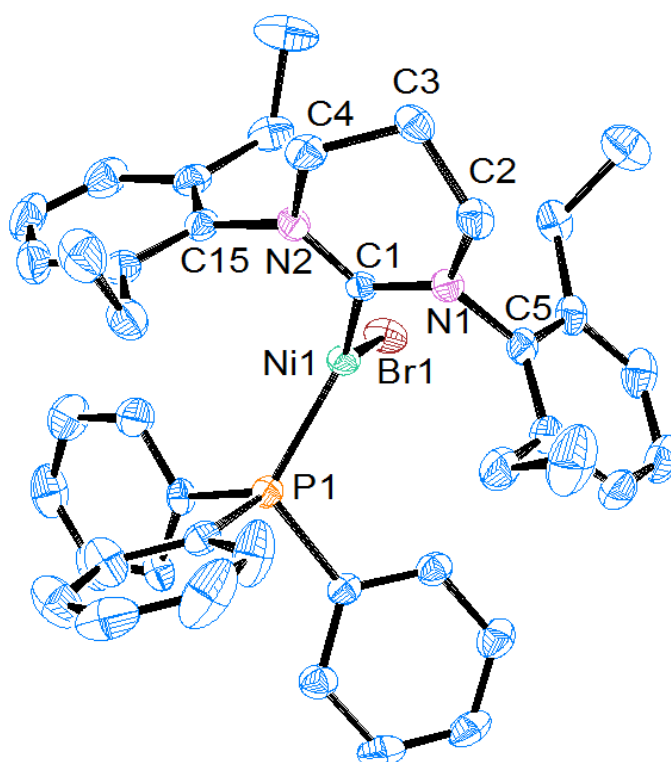


Figure 2: ORTEP ellipsoid plots at 50 % probability of the molecular structure of $[\text{Ni}(\text{6-DEP})(\text{PPh}_3)\text{Cl}/\text{Br}]$ (**1**).

Table 1: Selected bond lengths (Å) and angles (°) for [Ni(6-DEP)(PPh₃)Cl/Br] (**1**).

Lengths (Å)		Angles (°)	
N(1)-C(1)	1.348(3)	N(1)-C(1)-N(2)	116.5(2)
N(2)-C(1)	1.352(3)	C(1)-N(2)-C(15)	119.6(2)
N(2)-C(15)	1.439(3)	C(1)-N(2)-C(4)	124.1(2)
N(2)-C(4)	1.475(3)	C(15)-N(2)-C(4)	116.3(2)
C(4)-C(3)	1.508(4)	N(2)-C(4)-C(3)	109.5(2)
C(3)-C(2)	1.509(4)	C(4)-C(3)-C(2)	108.1(2)
C(2)-N(1)	1.479(3)	C(3)-C(2)-N(1)	108.8(2)
N(1)-C(5)	1.442(3)	C(2)-N(1)-C(5)	116.4(2)
C(1)-Ni(1)	1.946(2)	C(2)-N(1)-C(1)	125.0(2)
Ni(1)-Br(1)	2.3226(3)	C(5)-N(1)-C(1)	118.4(2)
Ni(1)-P(1)	2.2100(7)	N(1)-C(1)-Ni(1)	121.30(18)
		N(2)-C(1)-Ni(1)	121.88(17)
		C(1)-Ni(1)-Br(1)	132.48(7)
		C(1)-Ni(1)-P(1)	116.74(7)
		Br(1)-Ni(1)-P(1)	110.78(2)

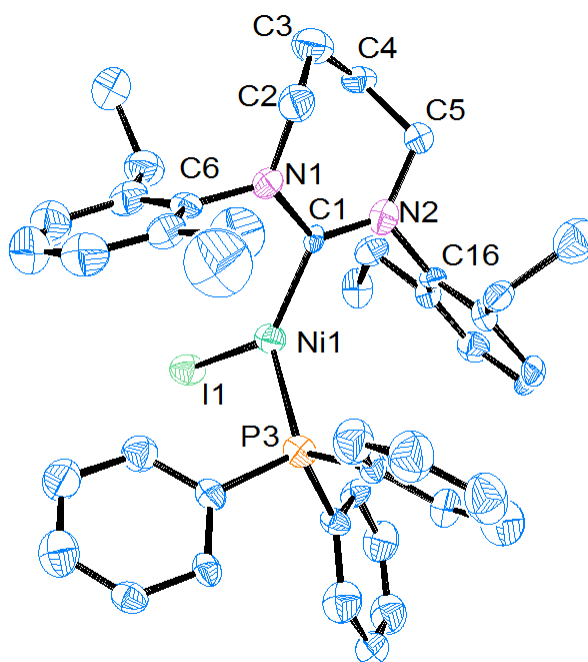


Figure 3: ORTEP ellipsoid plots at 50 % probability of the molecular structure of $[\text{Ni}(7\text{-DEP})(\text{PPh}_3)\text{Cl}/\text{I}]$ (**2**).

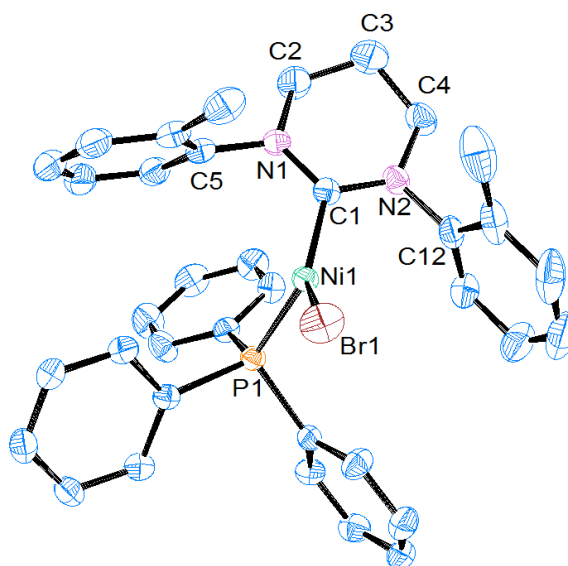


Figure 4: ORTEP ellipsoid plots at 50 % probability of the molecular structure of $[\text{Ni}(6\text{-}o\text{-tolyl})(\text{PPh}_3)\text{Br}/\text{Cl}]$ (**3**).

Table 2: Selected bond lengths (Å) and angles (°) for [Ni(7-DEP)(PPh₃)Cl/I] (**2**).

Lengths (Å)		Angles (°)	
N(1)-C(1)	1.36(2)	N(1)-C(1)-N(2)	118.8(16)
N(2)-C(1)	1.35(2)	C(1)-N(1)-C(6)	118.2(15)
N(1)-C(6)	1.46(2)	C(1)-N(1)-C(2)	124.9(15)
N(1)-C(2)	1.50(2)	C(6)-N(1)-C(2)	115.9(14)
C(2)-C(3)	1.51(2)	N(1)-C(2)-C(3)	112.7(15)
C(3)-C(4)	1.50(2)	C(2)-C(3)-C(4)	115.3(15)
C(4)-C(5)	1.52(2)	C(3)-C(4)-C(5)	110.9(15)
C(5)-N(2)	1.50(2)	C(4)-C(5)-N(2)	112.1(14)
N(2)-C(16)	1.45(2)	C(5)-N(2)-C(1)	130.5(15)
C(1)-Ni(1)	1.939(17)	C(5)-N(2)-C(16)	112.4(14)
Ni(1)-I(1)	2.520(3)	C(1)-N(2)-C(16)	117.1(15)
Ni(1)-P(3)	2.243(5)	N(1)-C(1)-Ni(1)	119.5(13)
		N(2)-C(1)-Ni(1)	120.5(13)
		C(1)-Ni(1)-I(1)	130.2(5)
		C(1)-Ni(1)-P(3)	121.0(5)
		I(1)-Ni(1)-P(3)	108.66(13)

Table 3: Selected bond lengths (Å) and angles (°) for [Ni(6-*o*-tolyl)(PPh₃)Br/Cl] (**3**).

Lengths (Å)		Angles (°)	
N(1)-C(1)	1.350(4)	N(1)-C(1)-N(2)	116.9(3)
N(1)-C(5)	1.432(5)	C(1)-N(1)-C(5)	119.5(3)
C(1)-N(2)	1.343(4)	C(1)-N(1)-C(2)	123.6(3)
N(2)-C(12)	1.439(5)	N(1)-C(2)-C(3)	109.8(3)
N(1)-C(2)	1.478(5)	C(2)-C(3)-C(4)	110.7(4)
C(2)-C(3)	1.495(7)	C(3)-C(4)-N(2)	109.4(3)
C(3)-C(4)	1.507(6)	C(1)-N(2)-C(4)	126.1(3)
C(4)-N(2)	1.480(5)	C(1)-N(2)-C(12)	117.4(3)
C(1)-Ni(1)	1.925(3)	N(1)-C(1)-Ni(1)	125.0(3)
Ni(1)-Br(1)	2.2966(6)	N(2)-C(1)-Ni(1)	118.1(2)
Ni(1)-P(1)	2.1901(10)	C(1)-Ni(1)-Br(1)	137.03(10)
		C(1)-Ni(1)-P(1)	108.54(10)
		P(1)-Ni(1)-Br(1)	114.43(3)
		C(5)-N(1)-C(2)	116.8(3)
		C(4)-N(2)-C(12)	116.4(3)

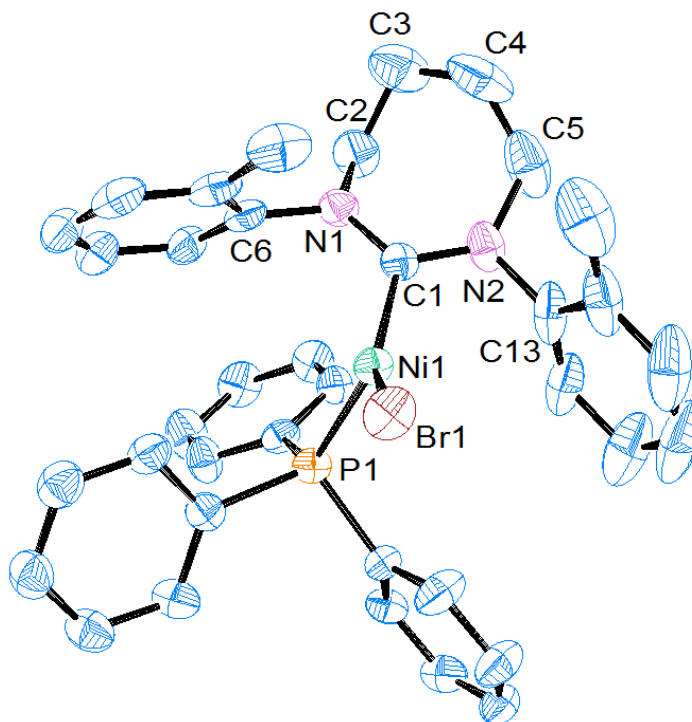


Figure 5: ORTEP ellipsoid plots at 50 % probability of the molecular structure of $[\text{Ni}(7\text{-}o\text{-tolyl})(\text{PPh}_3)\text{Br/Cl}]$ (**4**).

The geometries of nickel(I) complexes are varied with reports of three coordinate systems which are trigonal planar⁸⁻¹⁰ or T-shaped^{4,6,11} and four coordinate systems which are either tetrahedral^{12,13} or square planar.^{14,15} The more bulky the ligand architecture the more likely they are to be three coordinate.

Table 4: Selected bond lengths (Å) and angles (°) for [Ni(7-*o*-tolyl)(PPh₃)Br/Cl] (**4**).

Lengths (Å)		Angles (°)	
C(1)-N(1)	1.346(6)	N(1)-C(1)-N(2)	117.3(4)
C(1)-N(2)	1.347(6)	C(1)-N(1)-C(6)	118.1(4)
N(1)-C(2)	1.493(6)	C(1)-N(1)-C(2)	124.3(4)
N(1)-C(6)	1.449(6)	C(6)-N(1)-C(2)	116.6(4)
C(2)-C(3)	1.496(9)	N(1)-C(2)-C(3)	112.0(5)
C(3)-C(4)	1.500(10)	C(2)-C(3)-C(4)	111.9(6)
C(4)-C(5)	1.513(10)	C(3)-C(4)-C(5)	111.8(6)
C(5)-N(2)	1.525(8)	C(4)-C(5)-N(2)	113.3(5)
N(2)-C(13)	1.444(7)	C(5)-N(2)-C(1)	129.0(5)
C(1)-Ni(1)	1.918(5)	C(5)-N(2)-C(13)	114.7(5)
Ni(1)-Br(1)	2.3169(8)	C(1)-N(2)-C(13)	115.5(4)
Ni(1)-P(1)	2.1901(14)	N(1)-C(1)-Ni(1)	125.5(4)
		N(2)-C(1)-Ni(1)	117.1(4)
		C(1)-Ni(1)-Br(1)	136.87(14)
		C(1)-Ni(1)-P(1)	108.26(14)
		P(1)-Ni(1)-Br(1)	114.86(4)

The geometry of the bis-5-membered NHC nickel(I) complex, [Ni(IPr)₂Cl], synthesised by Matsubara and co workers is T-shaped,⁴ which is the same as the [Ni(IMes)₂I] synthesised by Zhang,⁶ whereas the three coordinate [Ni(6-Mes)(PPh₃)Br] synthesised by Whittlesey and the range of Ni(I) expanded ring NHC complexes synthesised by Cavell have a trigonal planar geometry.^{2,3} The structures of **1-4** are the same as those of Whittlesey's and Cavell's and approximate to trigonal planar. This difference can in part be attributed to the size and bulk of the nickel co-ligands, as in the expanded ring

nickel(I) complexes this is a triphenylphosphine moiety and in the bis-5-membered NHCs this is a chlorine. Therefore, the steric demand of the bulkier co-ligands on the nickel in the expanded ring complexes favours the formation of the trigonal planar geometries over the T-shaped conformation of the bis-5-membered NHC complexes. The other notable feature of the expanded ring Ni(I) NHC complexes is that of the $C_{\text{carbene}}\text{-Ni-X}$, where X = halide, exceeds the ideal 120° , which is expected for the perfect trigonal planar complex. The values obtained for **1-4** are $132.48(7)^\circ$, $130.2(5)^\circ$, $137.03(10)^\circ$, and $136.87(14)^\circ$ respectively, which is a considerable increase from 120° . These are also in the same region as those reported by Whittlesey and Cavell, which have an average value of 135° .^{2,3}

The crystallographic data in Tables 1-4 shows that on coordination, in the same way as the rhodium, copper, and gold complexes shown in previous chapters of this thesis, the NCN bond angle is decreased from its amidinium salt precursors. The NCN bond angle of the four complexes **1-4** differs by a total of 2.3° , with the 7-DEP and 7-*o*-tolyl derivatives having the largest angles of $118.8(16)^\circ$ and $117.3(4)^\circ$ respectively, which is due to the larger ring size. These angles are in accordance with that of $[\text{Ni}(6\text{-Mes})(\text{PPh}_3)\text{Br}]$, which has an NCN bond angle of $116.5(2)^\circ$.² The other notable angles in the crystal structure data are those of the C-N-C_{Ar} link, which have values of between $115.5(4)^\circ$ and $119.6(2)^\circ$, which is a total increase of 3.9° . In this case the largest angles are related to the smaller ring sizes. Hindrance coming from the N-substituents and the back bone of the NHC result in larger NCN bond angles, therefore, the larger the NCN bond angle the smaller the C-N-C_{Ar} angle has to be. There is also a correlation between steric hindrance from the N-substituents, with the larger substituents **1** and **2** resulting in larger C-N-C_{Ar} angles of $119.6(2)^\circ$ and $118.2(15)^\circ$ for 6-DEP and 7-DEP derivatives respectively. These observations are also in accordance with the literature data on the 6-Mes derivative, where the angle is on average 118.4° .² It has been reported by Whittlesey that the bond lengths between the nitrogen and the carbene carbon atom for the 6-Mes derivative are on average 1.35 \AA^2 and compounds **1-4** fall between values of $1.343(4) \text{ \AA}$ and $1.36(2) \text{ \AA}$. There is a relatively small difference between the value for the 6-Mes derivative and the 7-DEP derivative with a difference of 0.012 \AA and this is due to the size of the NCN ring with the greater value being for the larger ring, although this difference is within the error of the measurements. The

final bond length, which is of importance for these four compounds is that of the C-Ni bond, which for the 6-Mes derivative is 1.942(2) Å and for **1-4** is 1.946(2) Å, 1.939(17) Å, 1.925(3) Å, and 1.918(5) Å respectively. The values obtained for the Ni-C bond distances for complexes **1-4** are in accordance with the recent report by Whittlesey and Cavell where the length of the Ni-C bond for the 6-anisidine, 6-anisidine/Mes, 7-*o*-tolyl, 8-Mes, and 8-*o*-tolyl are 1.9346(19) Å, 1.942(2) Å, 1.925(3) Å, 1.979(5) Å, and 1.949(4) Å respectively.^{2,3} The lengths reported for the 8-membered derivatives are larger than the other expanded ring derivatives and can be attributed to large steric bulk around the metal centre in part due to the extensive size of the ring. The smallest C-Ni bond length is assigned to the smallest ring size with the smallest amount of steric bulk, which is the 6-*o*-tolyl derivative.

Table 5: Percentage buried volume (%V_{bur}) values for compounds **1-4** and [Ni(6-Mes)(PPh₃)Br].

Compound	Buried Volume (%V _{bur})
[Ni(6-DEP)(PPh ₃)Cl] (1)	41.5
[Ni(7-DEP)(PPh ₃)Cl] (2)	43.0
[Ni(6- <i>o</i> -tolyl)(PPh ₃)Cl] (3)	41.5
[Ni(7- <i>o</i> -tolyl)(PPh ₃)Cl] (4)	42.5
[Ni(6-Mes)(PPh ₃)Br] ²	42.4

Since the single crystal X-ray crystallographic data was obtained it was therefore possible to obtain the percentage buried volumes for these four compounds, Table 5. The calculated percentage buried volumes range from 41.5 % to 43.0 %, with **2** having the largest value, which is as expected as it has the most sterically encumbered NHC. These percentage buried volume values are in accordance with that obtained for the 6-

Mes derivative² and also the gold complexes in Chapter 5 of this thesis. However, due to the nature of the N-substituents these values are not quite as large as those reported by Dunsford for the sterically encumbered [Au(6-DIPP)Cl] and [Au(7-DIPP)Cl] complexes.¹⁶

It was also found from the crystallographic data that the halide was not 100 % chlorine, the actual values are shown in Table 6. These values are due to the *in situ* route which was taken to prepare the complexes. This meant that there were small amounts of the halide counterion still in solution and therefore reacted to produce the unwanted ratio of Br:Cl or I:Cl in the products. This problem can be resolved by replacing the halide in the pro-ligand with the BF₄⁻ or using the same halide in both precursors. This has been shown by Whittlesey and Cavell.³ The crystal structure parameters are based on a weighted average between the halides and as such the exact values may differ from those of the pure single halide species.

Table 6: Ratios of halides in compounds **1-4**.

Compound	Ratio of halides
	Br/I : Cl
[Ni(6-DEP)(PPh ₃)Cl/Br] (1)	81 : 19
[Ni(7-DEP)(PPh ₃)Cl/I] (2)	98 : 2
[Ni(6- <i>o</i> -tolyl)(PPh ₃)Cl/Br] (3)	77 : 23
[Ni(7- <i>o</i> -tolyl)(PPh ₃)Cl/Br] (4)	89 : 11

This mixture of halides in the products (**1-4**) could be the reason why it was not possible to obtain the elemental analysis even after pure products in the form of crystals were attained. The mass spectrometry data was obtained for all four complexes, **1-4**. **1** and **2** showed the absence of a halide and either a proton addition (**1**, [M⁺ - Cl + H⁺]) or two

amounts of acetonitrile added (**2**, $[M^+ - Cl + 2MeCN + H^+]$) with peaks at 669.34 amu and 765.34 amu respectively, which have calculated values of 669.50 amu and 765.63 amu respectively. However, **3** and **4** showed molecular ion peaks, $[M^+]$, with values of 619.1597 amu and 633.1752 amu respectively, which have calculated values of 619.1580 amu and 633.1736 amu respectively. Although the outcomes were slightly different, these results along with the crystal data are conclusive in showing that **1-4** were successfully synthesised.

6.2.3: EPR Studies

6.2.3.1: Background to EPR

Electron paramagnetic resonance (EPR) is a magnetic resonance technique which studies unpaired electrons, therefore making it possible to detect species such as radicals and paramagnetic compounds. EPR informs you about the electronic and structural aspects of a system¹⁷ and therefore is extremely useful not only in chemistry but across a vast range of disciplines including areas of medicine, physics, and industrial uses to name just a few.

Most compounds are characterised using NMR spectroscopic methods, however when a paramagnetic metal is analysed in this way, including the nickel(I) complexes discussed in this chapter, the spectra becomes broadened and therefore less useful. EPR, just like NMR, is capable of studying different systems under a variety of conditions, these include solid state, solutions, variable temperature and variable pressure. The other added benefit of EPR over NMR is its sensitivity. EPR techniques require as little as 10^{-7} molar quantities and NMR has a detection limit of around 10^{-1} molar quantities. This makes this technique the most direct and sensitive method for doing such analysis.

Electrons in the same orbital abide by the Pauli exclusion principle and are therefore paired and of opposite spins, this in turn causing the compounds to be EPR silent.¹⁸ For

a compound to be EPR active at least one unpaired electron is required, transition metals containing this are suitable for being analysed by this technique.

6.2.3.2: Basic Principles of EPR

The basic principles of EPR are very similar to those of NMR with differences to allow for the larger magnetic moment, which is associated with the electron in comparison to a proton. Every electron has a magnetic moment (μ_s) because they are negatively charged particles spinning on their own axis, and this magnetic moment is related to its spin (spin angular momentum, S), since they are co-linear and antiparallel to each other. The relationship between the two is exhibited in Equation 1, where g_e = the free electron g value = 2.0023 and μ_B = Bohr magneton ($9.274 \times 10^{-24} \text{ J T}^{-1}$).

$$\mu_S = - g_e \mu_B S \quad \text{(Equation 1)}$$

The interaction between the magnetic moment and an external applied magnetic field is given as Equation 2, where B = the applied magnetic field (or magnetic flux given in units of Tesla (T) or Gauss (G)).

$$E = - \mu_S B \quad \text{(Equation 2)}$$

Therefore the overall equation for the interaction between the magnetic moment and the external magnetic field is given by Equation 3.

$$E = g_e \mu_B S B \quad \text{(Equation 3)}$$

An electron can exist in two spin states, $+\frac{1}{2}$ and $-\frac{1}{2}$, in the absence of an external magnetic field these two spin states are degenerate, however when a magnetic field is applied the spin states split in energy.¹⁹ The higher of these two levels are where the electrons spin is antiparallel to that of the magnetic field and the lower more stable energy is where the two spins are parallel to each other. These two levels are known as the Zeeman levels and the difference is known as the Zeeman splitting, as shown in Figure 6 and Equation 4, where h = Planck's constant and ν = the frequency of electromagnetic radiation. The transition between the two Zeeman levels can be induced by absorption of a photon of the exact frequency, hence $\Delta E = h\nu$ as shown in Equation 4.

$$\Delta E = h\nu = g_e \mu_B B \quad \text{(Equation 4)}$$

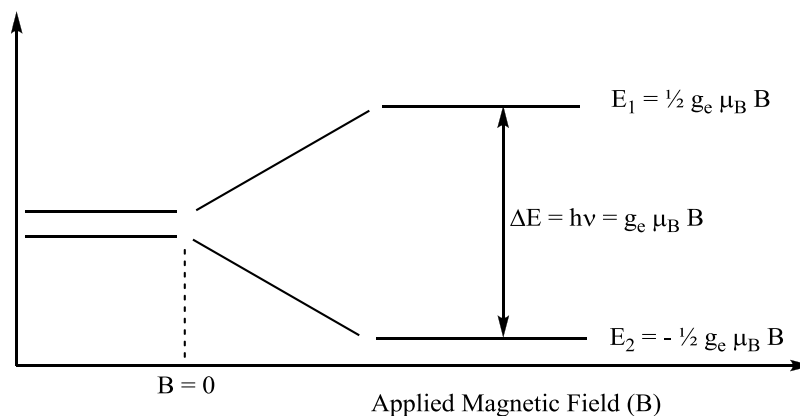


Figure 6: The Electronic Zeeman Effect (this is for a system containing one unpaired electron and no nuclei interactions).

The transition between the two Zeeman levels is the basis of EPR spectroscopy. The g value, which is obtained, is the position of transition and is analogous to the chemical

shift in NMR spectroscopy and is therefore dependant on the species. The g value can be calculated by a rearrangement of the Zeeman splitting equation to give Equation 5.

$$g = h \nu / \mu_B B \quad \text{(Equation 5)}$$

6.2.3.3: Multi-Electron Systems

So far it has been discussed how free electrons are characterised by EPR techniques, however molecules and complexes have additional interactions, which in turn cause the Zeeman levels to split, Figure 7. In a system larger than a free electron, the electrons have interactions with the spin-active nuclei, where the spin $\geq \frac{1}{2}$ of the complexes. The origin of these interactions comes from the interaction of both the electron and nuclear magnetic moments with the external magnetic field, giving rise to electron and nuclear Zeeman splitting, respectively and the interaction of the electron and nuclear magnetic moments with each other, giving rise to the hyperfine interaction (A).

For any allowed transition between two energy levels the process must obey selection rules and these are $\Delta M_I = 0$ when $\Delta M_S = \pm 1$. These selection rules lead to two possible transitions as shown in Equations 6, 7, and Figure 7, where E_A and E_B = the allowed transitions and A_o = hyperfine coupling interaction.

$$\Delta E_A = EPR\ 1 = g \mu_B B + \frac{1}{2} h A_o \quad \text{(Equation 6)}$$

$$\Delta E_B = EPR\ 2 = g \mu_B B - \frac{1}{2} h A_o \quad \text{(Equation 7)}$$

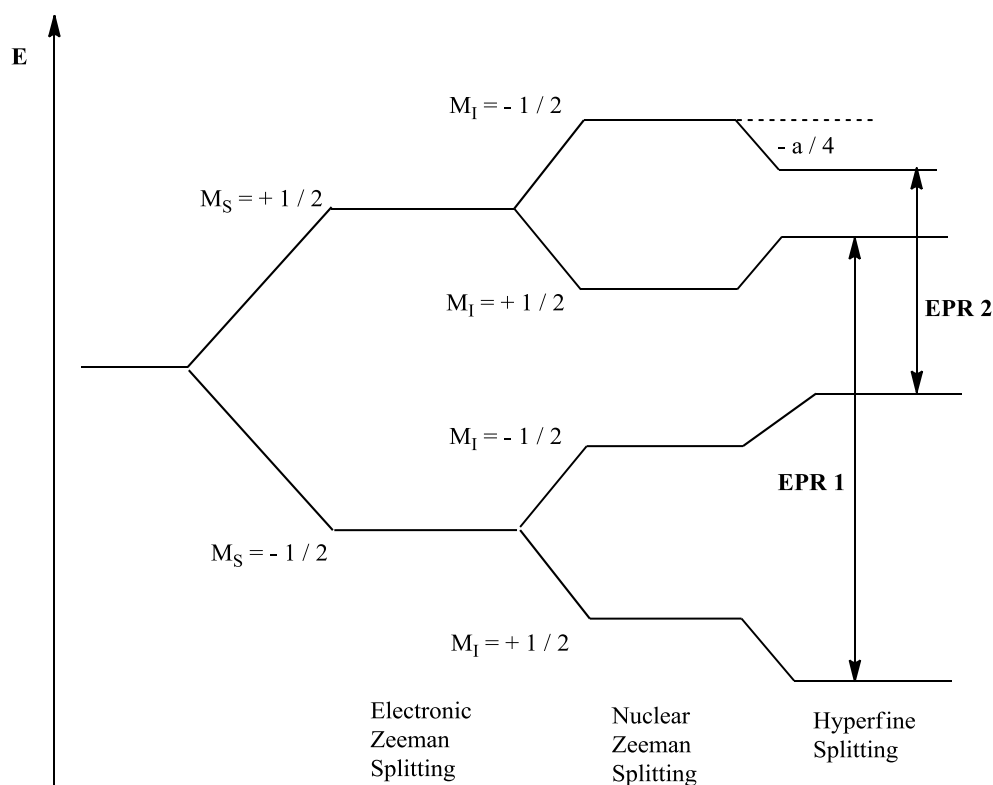


Figure 7: Energy level diagram showing the interaction between an unpaired electron ($S = 1/2$) and a spin active ($I = 1/2$) nucleus in an applied field.

There are three types of EPR spectral outcomes, which can be obtained and these are dependent on the symmetry of the system. When the system is of perfect cubic symmetry, therefore tetrahedral or octahedral, the spectrum observed will be of an isotropic profile. Isotropic profile is where the spectra are symmetrical and therefore all the g factors are equal, hence $g_{xx} = g_{yy} = g_{zz}$. When only two of the g values are equal, $g_{xx} = g_{yy} \neq g_{zz}$, then the spectrum observed is known to have axial symmetry and has two peaks. The g_{zz} term is also known as the g parallel due to its position being parallel to the direction of the magnetic field and the $g_{xx} = g_{yy}$ terms are referred to as the g perpendicular factor as they lie perpendicular to the direction of the magnetic field. When none of the g factors are equal, $g_{xx} \neq g_{yy} \neq g_{zz}$, then the spectra observed is said to have orthorhombic symmetry and three peaks will be observed.

The samples analysed in this thesis are all of frozen samples and therefore any orientations of the molecule with respect to the magnetic field will be observed in the spectra obtained.

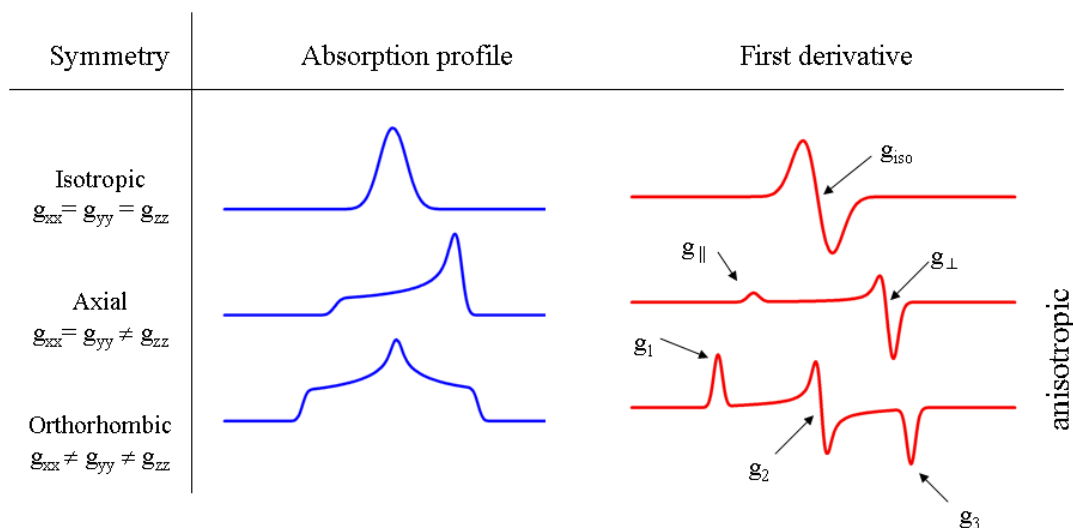


Figure 8: A diagram showing the three types of spectra observed in EPR, Isotropic, Axial, and Orthorhombic, where g_{iso} = the isotropic g value, g_{\parallel} = g parallel and g_{\perp} = g perpendicular.

6.2.3.4: EPR Studies of Nickel(I) Complexes

In recent years there have been only a few studies of nickel(I) NHC complexes reported.²⁻⁴ These complexes are shown to be three coordinate 15-electron d^9 nickel(I) complexes and along with complexes **1-4**, due to their paramagnetic nature, are deemed incompatible with NMR techniques and have therefore been analysed using EPR techniques. Compounds **1-4** were analysed using X-band continuous wave (CW) EPR techniques at 140 K and 10 K and the spectra obtained are shown in Figure 9.

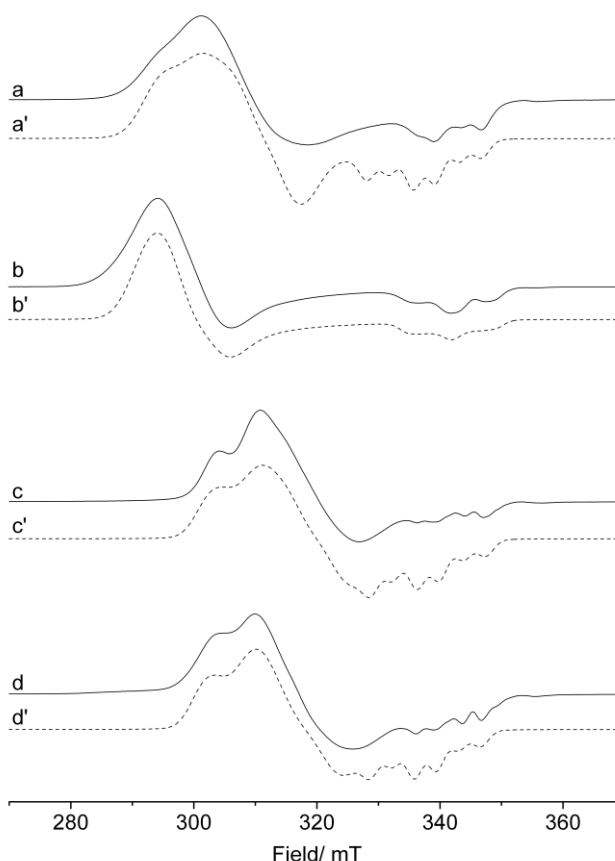


Figure 9: CW (10 K) EPR spectra of (a) [Ni(6-DEP)(PPh₃)Cl/Br] (**1**), (b) [Ni(7-DEP)(PPh₃)Cl/Br] (**2**), (c) [Ni(6-*o*-tolyl)(PPh₃)Cl/Br] (**3**), and (d) [Ni(7-*o*-tolyl)(PPh₃)Cl/Br] (**4**). The corresponding simulations are shown in a' - d'.

The four complexes, **1-4**, display orthorhombic symmetry, which is in accordance with the reported EPR data of the series of expanded ring nickel(I) NHC complexes synthesised by Whittlesey and Cavell.³ The line widths as reported by Whittlesey and Cavell are also broadened on the spectra obtained for **1-4**, which is due to the larger superhyperfine couplings of the ³¹P and ^{79,81}Br nuclei. As mentioned in section 6.2.3.3, the rhombic systems are apparent when none of the *g* values are equivalent therefore $g_{xx} \neq g_{yy} \neq g_{zz}$, and these systems are known as anisotropic. It has also been reported for three coordinate nickel(I) complexes that a trend in *g* tensors is observed of $g_3 - g_2 > g_2 - g_1$,²⁰⁻²³ however for the [Ni(N[^]N)^{Me}(CO)]²¹ and the more recent NHC nickel(I)

complexes³ the opposite trend was observed with $g_3 - g_2 < g_2 - g_1$. The outcome of **1-4** was the same as that reported by Stephen and Whittlesey where the trends show that $g_3 - g_2 < g_2 - g_1$. This is a result of the NCN and the N-substituents having a larger effect on the g tensor than that of the vibronic interactions.

Table 7: Spin Hamiltonian parameters for [Ni(NHC)(PPh₃)X] complexes (recorded in THF) in comparison to other reported Ni(I) species.

Complex	^a $g_{3(z)}$	g_2	g_1	^P A_3 / MHz	^P A_2 / MHz	^P A_1 / MHz	Ref
[Ni(6-Mes)(PPh ₃)X]	2.365	2.270	2.073	186	206	208	3
(X = Br)				^b 22	20	90	
[Ni(7- <i>o</i> -tolyl)(PPh ₃)X]	2.275	2.200	2.072	206	169	228	3
(X = Br)				^b 22	20	100	
[Ni(8-Mes)(PPh ₃)X]	2.405	2.322	2.034	146	146	188	3
(X = Br/Cl)							
[Ni(8- <i>o</i> -tolyl)(PPh ₃)X]	2.312	2.216	2.066	186	206	208	3
(X = Br)				^b 22	20	90	
[Ni(8- <i>o</i> -tolyl)(PPh ₃)X]	2.307	2.216	2.037	186	106	208	3
(X = Cl)							
[Ni(O-8- <i>o</i> -tolyl)(PPh ₃)X]	2.322	2.216	2.072	186	206	228	3
(X = Br/Cl)				^b 22	20	100	
(1) X = Br/Cl	2.352	2.246	2.0760	206	169	228	t.w.
				22	20	100	

(2) X = I/Cl	2.382	2.326	2.0460	<i>116</i>	<i>169</i>	<i>208</i>	t.w.
				<i>22</i>	<i>20</i>	<i>66</i>	
(3) X = Br/Cl	2.282	2.186	2.0725	<i>216</i>	<i>159</i>	<i>229</i>	t.w.
				<i>42</i>	<i>20</i>	<i>100</i>	
(4) X = Br/Cl	2.286	2.196	2.0725	<i>216</i>	<i>159</i>	<i>209</i>	t.w.
				<i>42</i>	<i>20</i>	<i>100</i>	
[Ni(PPh ₃) ₃][BF ₄]	2.38	2.12	2.07	^c 171	179	226	23,24
				^c 168	171	179	
[Ni(PPh ₃) ₂ Br]	2.435	2.209	2.112	159	159	216	22
				102	105	105	
				^d 42	93	21	
[Ni(PPh ₃) ₂ Cl]	2.446	2.167	2.111	^c 165	165	201	22
				^c 105	117	123	
[Ni(N [^] N) ^{Me} (dppm)]	2.43	2.16	2.03				20
[Ni(N [^] N) ^{Me} (CO)]	2.19	2.17	2.01				21
[Ni(CO)(H ₂ O) ₂] ⁺	2.357	2.249	2.017				25

^a *g* values ± 0.005 ; ^b Br couplings; ^c the two or three P nuclei are inequivalent in these literature complexes, hence the two ^PA values; ^d resolved Br coupling in [Ni(PPh₃)₂Br]; ^{t.w.} = This work. Note; *The italicised values of A₃/A₂ for the NHC complexes represent an estimated upper limit, as these couplings were not resolved in the broad experimental spectra.*

As shown in Table 7, the spin Hamiltonian parameters are affected not only by ring size but by the N-substituent and the halide as well, this is apparent because d⁹ metal centres are extremely sensitive to coordination environment. This sensitivity is shown by the effects on the *g*₃ and *g*₂ tensors with values of 2.382 and 2.326 for **2** and 2.282 and 2.186 for **3**. This however does not affect the *g*₁ value as much with values of 2.0460 and 2.0725 for **2** and **3** respectively. This observation is a result of the *g*₃ and *g*₂ tensors being in an in-plane d_σ-orbital whereas the *g*₁ tensor is in an out of plane d_σ-orbital.

Large $^{\text{P}}\text{A}$ values for nickel(I) complexes containing a phosphorus moiety have been reported^{3,22-24} and this is also apparent in complexes **1-4** with values of up to 229 MHz. These bigger $^{\text{P}}\text{A}$ values are due to the greater extent of covalency found in the Ni-P bond. Additional superhyperfine coupling originating from the Br counter-ion can also be resolved in spectra a, c, and d.

EPR spectroscopy has been used to provide a detailed characterisation of these complexes, relating their ground state SOMOs to ligand structure and choice of halide ion. This information may prove useful in the investigation of these complexes for catalysis, in reactions such as cross couplings, in particular probing mechanistic pathways and changes in metal environment during the catalytic cycle.

6.3: Conclusions

The aim of this chapter was to synthesise a series of expanded ring nickel(I) complexes and analyse them using EPR techniques. These aims were achieved with complexes **1-4** being successfully synthesised, although a mix of halide products were obtained, in yields of up to 35 %.

This was exhibited by the single crystal X-ray crystallographic data which was obtained for all four complexes. This showed that all four complexes were trigonal planar, which is the same as was reported by Whittlesey for a series of expanded ring nickel(I) complexes.^{2,3} Although the complexes were observed as trigonal planar the $\text{C}_{\text{carbene}}\text{-Ni-X}$, where X =halide, angles exceeded the ideal 120 °, with **1-4** having corresponding angles of up to 137.03(10) °.

A correlation between the size of the NCN angle and the size of the $\text{C}_{\text{carbene}}\text{-N-C}_{\text{Ar}}$ angle was observed with the larger the NCN angle the smaller the $\text{C}_{\text{carbene}}\text{-N-C}_{\text{Ar}}$ angle and is in part due to the steric hindrance from the N-substituents. The C-Ni bond lengths and the NCN bond angles are all in accordance with the literature values, however the 8-membered derivatives exhibit a much larger C-Ni bond length due to the huge steric demand surrounding the metal centre.

The percentage buried volumes of **1-4** were calculated from their crystal structure data and the results showed that they were sterically hindered but not quite as much as the [Au(6-DIPP)Cl] and [Au(7-DIPP)Cl] complexes reported by Dunsford.¹⁶

The EPR spectroscopic analysis shows that in a similar way to the reported literature³ **1-4** exhibit orthorhombic g profiles. The g values for **1-4** were obtained and showed a sensitivity to coordination through the g_2 and g_3 values, which are considerably effected by the size of the NHC, the N-substituents, and the halide which is present. The other noticeable feature of **1-4** was that of the trend in g tensor which exhibited that $g_3 - g_2 < g_2 - g_1$, which is the same as reported by Whittlesey³ and Stephen²¹ but the opposite to the early reports on nickel(I) complexes.²⁰⁻²³

6.4: Experimental

6.4.1: General Remarks

All air sensitive experiments were carried out using standard Schlenk techniques, under an atmosphere of argon or in a MBRAUN M72 glove box (N₂ atmosphere with > 0.1 ppm O₂ and H₂O) unless otherwise stated. Glassware was dried overnight in an oven at 120 °C and flame dried prior to use. Hexane and toluene of analytical grade was freshly collected from a MBRAUN sps 800 solvent purification system, THF was dried in a still over calcium hydride. All other solvents were used as purchased.

Mass spectrometry data was recorded, HRMS were obtained on a Waters Q-ToF micromass spectrometer and are reported as *m/z* (relative intensity) by the department of chemistry, Cardiff University.

All the X-ray Crystal structures were obtained on a Bruker Nonius Kappa CCD diffractometer using graphite mono-chromated Mo KR radiation ($\lambda(\text{Mo KR}) = 0.71073 \text{ \AA}$). An Oxford Cryosystems cooling apparatus was attached to the instrument, and all data were collected at 150 K. Data collection and cell refinement were carried out by Dr Benson Kariuki, using COLLECT²⁶ and HKL SCALEPACK.²⁷ Data reduction was applied using HKL DENZO and SCALEPACK.²⁷ The structures were solved using direct methods (Sir92)²⁸ and refined with SHELX-97.²⁹ Absorption corrections were performed using SORTAV.³⁰

Percentage buried volume was calculated using SambVca.³¹ Parameters applied for SambVca calculations: 3.50 Å was selected as the value for the sphere radius, 2.00 Å was used as distances for the metal–ligand bond, hydrogen atoms were omitted, and Bondi radii scaled by 1.17 were used. The above parameters applied are identical to those of all literature examples discussed, allowing a direct comparison of calculated values.

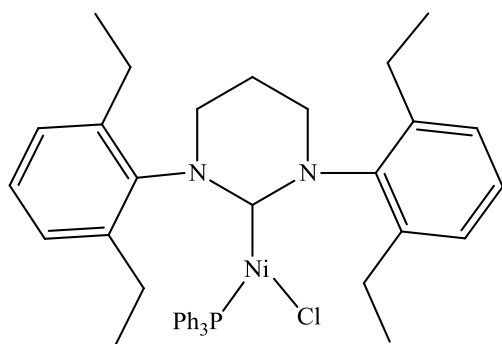
Samples for EPR measurements were prepared under an inert N₂ atmosphere in a glove box. A solution of each complex was prepared by dissolving 5 mg of

[Ni(NHC)(PPh₃)X] in 150 μ L dry THF to give pale yellow solutions. The solutions were transferred to an EPR tube and sealed in the glove box. The samples were cooled to 77 K before rapid transfer to the pre-cooled EPR cavity; all measurements were performed at 10 K or 140 K. All X-band CW measurements were performed on a Bruker EMX spectrometer with an ER4119HS resonator. EPR simulations were performed using the Easyspin toolbox.³²

The amidinium salt precursors for **1-4** were synthesised by known literature procedures^{33,34} and all other reagents were used as purchased.

6.4.2: Experimental Data for Nickel(I) Complexes

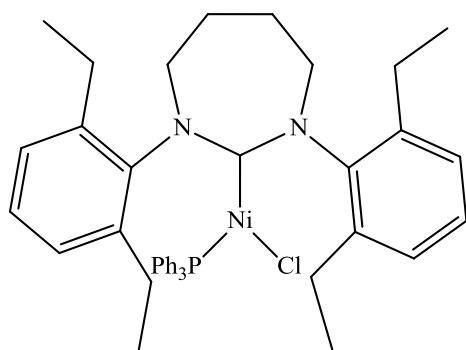
Synthesis of [Ni(6-DEP)(PPh₃)Cl/Br] (1)



The free carbene of 6-DEP was prepared using the pyrimidinium salt (6-DEPH)Br (0.20 g, 0.47 mmol, 1 eq) with KHMDS (0.13 g, 0.63 mmol, 1.4 eq) in toluene (10 ml) for 20 minutes. This solution was then added to a solution of [Ni(COD)₂] (0.06 g, 0.23 mmol, 0.5 eq) and [Ni(PPh₃)₂Cl₂] (0.15 g, 0.23 mmol,

0.5 eq) in toluene (5 ml) and stirred for a further 17 hours. The resulting solution was then filtered, under an atmosphere of nitrogen, into an empty Schlenk. The residue was washed with THF (10 ml) and then filtered again into the same Schlenk as before. The filtrate was then reduced under vacuum to 2 ml and hexane (10 ml) was added to precipitate [Ni(6-DEP)(PPh₃)Cl] as a bright yellow solid, yield (0.11 g, 32.0 %). MS(ES) *m/z*: [M⁺ - Cl + H⁺] 669.34 (C₄₂H₄₈N₂PNi) requires 669.50), it was not possible to obtain HRMS data for this complex.

Synthesis of [Ni(7-DEP)(PPh₃)Cl/I] (2)

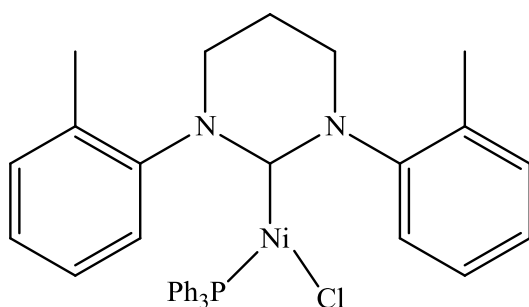


The free carbene of 7-DEP was prepared using the pyrimidinium salt (7-DEPH)I (0.20 g, 0.41 mmol, 1 eq) with KHMDS (0.11 g, 0.57 mmol, 1.4 eq) in toluene (10 ml) for 20 minutes. This solution was then added to a solution of [Ni(COD)₂] (0.06 g, 0.20 mmol, 0.5 eq) and [Ni(PPh₃)₂Cl₂] (0.13 g, 0.20 mmol, 0.5 eq) in

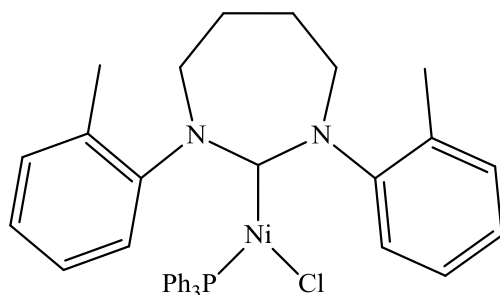
toluene (5 ml) and stirred for a further 17 hours. The resulting solution was then

filtered, under an atmosphere of nitrogen, into an empty Schlenk. The residue was washed with THF (10 ml) and then filtered again into the same Schlenk as before. The filtrate was then reduced under vacuum to 2 ml and hexane (10 ml) was added to precipitate $[\text{Ni}(7\text{-DEP})(\text{PPh}_3)\text{Cl}]$ as a bright yellow solid, yield (0.094 g, 28.6 %). MS(ES) m/z : $[\text{M}^+ - \text{Cl} + 2\text{MeCN}]$ 765.34 ($\text{C}_{47}\text{H}_{55}\text{N}_4\text{PNi}$) requires 765.63), it was not possible to obtain HRMS data for this complex.

Synthesis of $[\text{Ni}(6\text{-}o\text{-tolyl})(\text{PPh}_3)\text{Br/Cl}]$ (3)



The free carbene of 6-*o*-tolyl was prepared using the pyrimidinium salt (6-*o*-tolyl)HBr (0.20 g, 0.58 mmol, 1 eq) with KHMDS (0.16 g, 0.81 mmol, 1.4 eq) in toluene (10 ml) for 20 minutes. This solution was then added to a solution of $[\text{Ni}(\text{COD})_2]$ (0.08 g, 0.29 mmol, 0.5 eq) and $[\text{Ni}(\text{PPh}_3)_2\text{Cl}_2]$ (0.19 g, 0.29 mmol, 0.5 eq) in toluene (5 ml) and stirred for a further 17 hours. The resulting solution was then filtered, under an atmosphere of nitrogen, into an empty Schlenk. The residue was washed with THF (10 ml) and then filtered again into the same Schlenk as before. The filtrate was then reduced under vacuum to 2 ml and hexane (10 ml) was added to precipitate $[\text{Ni}(6\text{-}o\text{-tolyl})(\text{PPh}_3)\text{Br/Cl}]$ as a bright yellow solid, yield (0.037 g, 9.8 %). MS(ES) m/z : $[\text{M}^+]$ 619.1597 ($\text{C}_{36}\text{H}_{35}\text{N}_2\text{PNiCl}$) requires 619.1580).

Synthesis of [Ni(7-*o*-tolyl)(PPh₃)Br/Cl] (4)

The free carbene of 7-*o*-tolyl was prepared using the pyrimidinium salt (7-*o*-tolylH)Br (0.20 g, 0.56 mmol, 1 eq) with KHMDS (0.16 g, 0.78 mmol, 1.4 eq) in toluene (10 ml) for 20 minutes. This solution was then added to a solution of [Ni(COD)₂] (0.08 g, 0.28 mmol, 0.5 eq) and [Ni(PPh₃)₂Cl₂] (0.18 g, 0.29 mmol, 0.5 eq) in toluene (5 ml) and stirred for a further 17 hours. The resulting solution was then filtered, under an atmosphere of nitrogen, into an empty Schlenk. The residue was washed with THF (10 ml) and then filtered again into the same Schlenk as before. The filtrate was then reduced under vacuum to 2 ml and hexane (10 ml) was added to precipitate [Ni(7-*o*-tolyl)(PPh₃)Br/Cl] as a bright yellow solid, yield (0.13 g, 35.0 %). MS(ES) *m/z*: [M⁺] 633.1752 (C₃₇H₃₇N₂PNiCl) requires 633.1736).

6.5: References

- 1 Hamilton, T. *PhD Thesis* **2010**.
- 2 Davies, C. J. E.; Page, M. J.; Ellul, C. E.; Mahon, M. F.; Whittlesey, M. K. *Chem. Comm.* **2010**, 46, 5151-5153.
- 3 Page, M. J.; Lu, W. Y.; Poulten, R. C.; Carter, E.; Algarra, A. G.; Kariuki, B. M.; Macgregor, S. A.; Mahon, M. F.; Cavell, K. J.; Murphy, D. M.; Whittlesey, M. K. *Chem. Eur. J.* **2013**, In Press.
- 4 Miyazaki, S.; Koga, Y.; Matsumoto, T.; Matsubara, K. *Chem. Comm.* **2010**, 46, 1932-1934.
- 5 Anderson, T. J.; Jones, G. D.; Vicic, D. A. *J. Am. Chem. Soc.* **2004**, 126, 26, 8100-8101.
- 6 Zhang, K.; Conda-Sheridan, M.; Cooke, S. R.; Louie, J. *Organometallics* **2011**, 30, 9, 2546-2552.
- 7 Jones, G. D.; McFarland, C.; Anderson, T. J.; Vicic, D. A. *Chem. Comm.* **2005**, 4211-4213.
- 8 Wang, H. -Y.; Meng, X.; Jin, G. -X. *Dalton Trans.* **2006**, 2579-2585.
- 9 Kogut, E.; Wiencko, H. L.; Zhang, L.; Cordeau, D. E.; Warren, T. H. *J. Am. Chem. Soc.* **2005**, 127, 32, 11248-11249.
- 10 Norman, N. C.; Orpen, A. G.; Quayle, M. J.; Whittell, G. R. *Acta Cryst. Sect. C* **2002**, 58, m160-m161.
- 11 Ingleson, M. J.; Fullmer, B. C.; Buschhorn, D. T.; Fan, H.; Pink, M.; Huffman, J. C.; Caulton, K. G. *Inorg. Chem.* **2008**, 47, 2, 407-409.
- 12 Kraikivskii, P.B.; Frey, M.; Bennour, H. A.; Gembus, A.; Hauptmann, R.; Svoboda, I.; Fuess, H.; Saraev, V. V.; Klein, H. -F. *J. Organomet. Chem.* **2009**, 694, 12, 1869-1876.
- 13 Xiong, Y.; Yao, S.; Bill, E.; Driess, M. *Inorg. Chem.* **2009**, 48, 16, 7522-7524.
- 14 Lee, E. Y.; Hong, D.; Park, H. W.; Suh, M. P. *Eur. J. Inorg. Chem.* **2003**, 17, 3242-3249.
- 15 Gosden, C.; Healy, K. P.; Pletcher, D. *Dalton Trans.* **1978**, 972-976.
- 16 Dunsford, J. J.; Cavell, K. J.; Kariuki, B. M. *Organometallics* **2012**, 31, 4118-4121.

- 17 Van Doorslaer, S.; Vinck, E. *Phys. Chem. Chem. Phys.* **2007**, 9, 4620-4638.
- 18 Chang, R. *Physical Chemistry for the Chemical and Biological Sciences*, University Science Books, **2000**, 741.
- 19 Van Doorslaer, S.; Caretti, I.; Fallis, I. A.; Murphy, D. M. *Coordination Chem. Revs.* **2009**, 253, 2116-2130.
- 20 Kitiachvili, K. D.; Mindiola, D. J.; Hillhouse, G. L. *J. Am. Chem. Soc.* **2004**, 126, 34, 10554-10555.
- 21 Bai, G.; Wei, P.; Stephen, D. W. *Organometallics*, **2005**, 24, 24, 5901-5908.
- 22 Nilges, M. J.; Barefield, E. K.; Belford, R. L.; Davis, P. H. *J. Am. Chem. Soc.* **1977**, 99, 3, 755-760.
- 23 Saraev, V. V.; Kraikivskii, P. B.; Lazarev, P. G.; Myagmarsuren, G.; Tkach, V. S.; Schmidt, F. K. *Russ. J. Coord. Chem.* **1996**, 22, 615-621.
- 24 Saraev, V. V.; Kraikivskii, P. B.; Svoboda, I.; Kuzakov, A. S.; Jordan, R. F.; *J. Phys. Chem. A* **2008**, 112, 12449-12455.
- 25 Pietrzyk, P.; Podolask, K.; Sojka, Z. *J. Phys. Chem. A* **2008**, 112, 12208-12219.
- 26 COLLECT; Nonius BV: Delft, The Netherlands, **1998**.
- 27 Otwinowski, Z.; Minor, W. *Methods Enzymol.* **1997**, 276, 307-326.
- 28 Altomare, A.; Cascarano, G.; Giacovazzo, C.; Guagliardi, A. *J. Appl. Crystallogr.* **1993**, 26, 343-350.
- 29 Sheldrick, G. M. *Acta Crystallogra. Sect. A* **2008**, A64, 112-122.
- 30 Blessing, R. H. *Acta Crystallogra. Sect. A* **1995**, 51, 33-38.
- 31 www.molnac.unisa.it/OMtools/sambvca.php
- 32 Stoll, S.; Schweiger, A. *J. Magn. Reson.* **2006**, 178, 42-55.
- 33 Dunsford, J. J.; Cavell, K. J.; Kariuki, B. *J. Organomet. Chem.* **2011**, 696, 188-194.
- 34 Iglesias, M.; Beetstra, D. J.; Kariuki, B.; Cavell, K. J.; Dervisi, A.; Fallis, I. A. *Eur. J. Inorg. Chem.* **2009**, 1913-1919.